



## Durham E-Theses

---

### *Synthesis and complexation chemistry of new n-functionalised tetra-arzamacrocycles*

Maffeo, Davide

#### How to cite:

---

Maffeo, Davide (2001) *Synthesis and complexation chemistry of new n-functionalised tetra-arzamacrocycles*, Durham theses, Durham University. Available at Durham E-Theses Online: <http://etheses.dur.ac.uk/2002/>

#### Use policy

---

The full-text may be used and/or reproduced, and given to third parties in any format or medium, without prior permission or charge, for personal research or study, educational, or not-for-profit purposes provided that:

- a full bibliographic reference is made to the original source
- a [link](#) is made to the metadata record in Durham E-Theses
- the full-text is not changed in any way

The full-text must not be sold in any format or medium without the formal permission of the copyright holders.

Please consult the [full Durham E-Theses policy](#) for further details.

# Synthesis and Complexation Chemistry of New N-Functionalised Tetra-azamacrocycles

Davide Maffeo

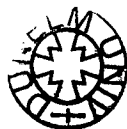
The copyright of this thesis rests with the author. No quotation from it should be published in any form, including Electronic and the Internet, without the author's prior written consent. All information derived from this thesis must be acknowledged appropriately.

A thesis submitted in part-fulfilment of the Degree of Doctor of Philosophy  
of the University of Durham

October 2001

Research carried out at the Department of Chemistry

1998-2001



22 MAR 2002

## **ABSTRACT: Synthesis and Complexation Chemistry of New N-Functionalised Tetra-azamacrocycles**

Davide Maffeo

Tetraazamacrocycles occupy a unique position in coordination chemistry, owing to their ability to form very stable complexes with a large range of metal ions. The inclusion of additional pendent coordinating groups is of particular interest, due to the effect on the properties of these compounds as ligands.

The regioselective synthesis of N,N'-dialkylated-1,4,8,11-tetraazacyclotetradecane in positions 1,5-, 1,8- and 1,11- has been accomplished using different substituents, including the potentially coordinating 2-pyridylmethyl group. A number of synthetic strategies have been investigated. The functionalisation of the related, cyclic dioxotetramines, 1,4,8,11-tetraazacyclotetradecane-*a,b*-diones ( $a,b = 2,3, 5,7$  and  $5,12$ ) at the amino nitrogens has also been carried out. The nickel, copper and chromium complexes of some of these ligands have been prepared and characterised. In several cases, solid state structures have been elucidated by X-ray crystallography, and have revealed a number of distinct and intriguing structural types and macrocycle conformations. UV-Visible absorption spectroscopy, cyclic voltammetry and (for chromium) luminescence spectroscopy have been used to investigate the properties in solution.

New octadentate ligands based on the 1,4,7,10-tetraazacyclododecane ring, *tris*-N-functionalised with acetate groups, have been synthesised, for preparation of water-soluble lanthanide complexes of high thermodynamic and kinetic stability. In one class of ligand, the eighth donor atom is the carbonyl oxygen of a covalently-linked *para*-substituted acetophenone  $\{-\text{CH}_2\text{C}(\text{O})\text{C}_6\text{H}_4\text{-X}$ , where  $\text{X} = \text{H}, \text{OMe}, \text{NMe}_2\}$ . Efficient sensitisation of europium(III) luminescence is observed following excitation of the acetophenone, with the *para*-substituent exerting a significant effect on the photophysical properties. In the second class, the macrocycle is connected through a three- or four-atom linker, containing a coordinating amide group, to a benzophenone moiety, found to act as an efficient sensitiser of both europium(III) and terbium(III) bound to the macrocycle. In both classes, lifetime measurements in  $\text{H}_2\text{O}$  and  $\text{D}_2\text{O}$  reveal the presence of a water molecule occupying the ninth coordination site of the metal ion. In the third class, 8-benzyloxyquinoline has been linked to the macrocycle, through a single 2-methylene unit. In this system, the nitrogen of the aromatic group is appropriately positioned to bind to the coordinated metal ion. No additional water molecule is observed in this case, and it is proposed that this is due to the benzyloxy group successfully occupying the site normally taken by the water molecule.

*University of Durham, October 2001.*

## **DECLARATION**

The research described in this thesis was undertaken at the Department of Chemistry of the University of Durham between October 1998 and September 2001. All of the work is my own, except where specifically stated otherwise. No part of it has been submitted previously for a degree at this or any other University.

## **STATEMENT OF COPYRIGHT**

The copyright of this thesis rests with the author. No quotation from it should be published without his prior written consent and information derived from it should be acknowledged.

## ACKNOWLEDGEMENTS

It is not possible to express all the gratitude that I have for all the people whom I have worked with during my Ph.D. in Durham.

Starting with my supervisor, Dr. J.A.G. Williams who was definitely more than a supervisor, always ready to help, extraordinary in explaining when I had any doubts, and constantly encouraging me through all the three years.

The technical staff at Durham who are really unique, from the people in the different services (NMR, Mass spectra, Elemental analysis and Crystallography department) to all the staff (stores, glass-blowing, etc.).

Dr. A. Beeby and Miss L. Bushby helped me a lot in understanding the fascinating world of luminescence, Dr. P. Low did the same for the cyclic voltammetry and Dr. A. Whitwood of the University of York for ESR.

The colleagues in the lab made this university a second house for me, and particular thanks go to B. Dutton and D. Orton who helped me a lot in improving my English.

Finally I would like to thank all the friends who have helped me in the work and in everyday situations, especially Hadjar and Alessia (and not just for their strong coffees which were the only way for me to wake up), Effie, who helped me with the thesis and was always ready to be the subject of my stress, and my parents, who always supported me in everything I decided to do.

# Contents

## Chapter 1 - Introduction

1.1	Introduction .....	2
1.2	Cyclam.....	3
1.2.1	<i>Mono-substitution of cyclam using a Michael acceptor</i> .....	5
1.2.2	<i>Direct alkylation of the metal complex</i> .....	6
1.2.3	<i>pH-Controlled selective protection of macrocycles</i> .....	7
1.2.4	<i>Synthesis of substituted derivatives of cyclam using N-tosyl intermediates</i> .....	9
1.2.5	<i>Synthesis of di-substituted cyclam using dioxoamines</i> .....	11
1.2.6	<i>Formation of 1,11-bis-(pendant donor)-cyclam derivatives via the formamidinium salt</i> .....	14
1.2.7	<i>Synthesis of di-substituted cyclams using a tricyclic system</i> .....	15
1.2.8	<i>Template reaction</i> .....	16
1.3	Metal complexes.....	18
1.4	Factors affecting the metal-binding properties of macrocycles .....	19
1.5	Photochemistry.....	21
1.6	Chromium.....	24
1.7	Copper .....	28
1.8	Nickel .....	31
1.9	Lanthanides .....	33
1.9.1	<i>Introduction</i> .....	33
1.9.2	<i>Cyclen and lanthanide complexation</i> .....	34
1.9.3	<i>Lanthanide excited states and luminescence</i> .....	35
1.9.4	<i>Photo-excitation of lanthanide ions</i> .....	39
1.9.5	<i>Applications of lanthanide luminescence</i> .....	41
1.10	References .....	46
1.10.1	<i>Books</i> .....	46
1.10.2	<i>Articles</i> .....	47

## Chapter 2 - Cyclam

2.1	Introduction .....	52
2.2	Synthesis of di-substituted cyclam using dioxotetraamines.....	53
2.3	Synthesis of 1,11-isomer, L <sup>2</sup> , and analogues using the formamidinium salt .....	58
2.4	Synthesis of 1,8-isomer, L <sup>1</sup> , using a tricyclic intermediate.....	60
2.5	Attempted synthesis of the 1,4-isomer, L <sup>3</sup> , using a template reaction .....	61
2.6	Synthesis of the 1,4-isomer, L <sup>3</sup> , using an oxamide intermediate .....	65
2.7	Mono-substitution of cyclam.....	66
2.7.1	<i>Mono-substitution of cyclam using a Michael acceptor</i> .....	67
2.7.2	<i>Mono-functionalisation of cyclam with a quinaldine-containing pendant (Method A)</i> .....	68
2.7.3	<i>Mono-functionalisation of cyclam with a quinaldine-containing pendant (Method B)</i> .....	72
2.8	References .....	74
2.8.1	<i>Articles</i> .....	74

## Chapter 3 – Copper, nickel and chromium complexes

3.1	Introduction .....	77
3.2	Nickel and copper complexes of 1,4,8,11-tetrazacyclotetradecane-5,12-dione, L <sup>4</sup> ..	78
3.3	Copper complexes of 1,8-bis(2-pyridylmethyl)-1,4,8,11-tetrazacyclotetradecane- 5,12-dione, L <sup>5</sup> .....	83
3.4	Nickel and copper complexes with the three isomeric bis(2-pyridylmethyl) substituted cyclams, L <sup>1</sup> , L <sup>2</sup> and L <sup>3</sup> .....	88
3.5	Chromium complexes.....	102
3.6	References .....	110
3.6.1	<i>Books</i> .....	110
3.6.2	<i>Articles</i> .....	110

## Chapter 4 - Cyclen

4.1	Introduction .....	114
4.2	Synthesis of the “antenna” groups.....	115
4.2.1	<i>4-Methoxy-2-bromoacetophenone</i> .....	116
4.2.2	<i>Antenna group containing the 8-hydroxyquinoline unit</i> .....	117
4.2.2.1	<i>N-(8-benzyloxy-quinolin-2-ylmethyl)-2-vinyl-N-methyl-acetamide</i> .....	118
4.2.2.2	<i>N-(8-benzyloxy-quinolin-2-ylmethyl)-2-chloro-N-methyl-acetamide</i> .....	119
4.3	Synthesis of the N-substituted cyclen ligands .....	123
4.4	Synthesis of the metal complexes .....	125
4.5	Alternative synthetic route to DOTA-type ligands with amide-linked chromophores .....	128
4.6	References .....	130
4.6.1	<i>Articles</i> .....	130

## Chapter 5 – Luminescence properties of lanthanide complexes

5.1	Sensitisation of lanthanide(III) excited states .....	132
5.2	Desired properties of the ligands.....	134
5.3	Ligands based on acetophenone .....	135
5.3.1	<i>Absorption spectra</i> .....	136
5.3.2	<i>Phosphorescence of gadolinium complexes</i> .....	137
5.3.3	<i>Emission spectra and lifetimes of europium complexes</i> .....	138
5.3.4	<i>Emission spectra and lifetimes of terbium complexes</i> .....	145
5.4	Ligands based on benzophenone .....	146
5.4.1	<i>Absorption spectra</i> .....	147
5.4.2	<i>Phosphorescence of lanthanum complex</i> .....	147
5.4.3	<i>Emission spectra and lifetimes of terbium complexes</i> .....	148
5.4.4	<i>Emission spectra and lifetimes of ytterbium complexes</i> .....	150
5.4.5	<i>Emission spectra and lifetimes of europium complexes</i> .....	152



5.5 Ligands based on quinaldine .....	156
5.5.1 Absorption spectra .....	157
5.5.2 Phosphorescence of gadolinium complexes .....	158
5.5.3 Emission spectra and lifetimes of europium complexes .....	158
5.6 Conclusions .....	161
5.7 References .....	162
5.7.1 Articles .....	162

## Chapter 6 – Experimental

6.1 Experimental Procedures: General .....	165
6.2 Luminescence Measurements .....	168
6.3 Synthetic Procedures for Chapter 2 .....	172
6.3.1 1,8-Bis(2-methylthiophene)-1,4,8,11-tetraazacyclotetradecane .....	172
6.3.2 1,8-Dimethyl-1,4,8,11-tetraazacyclotetradecane .....	174
6.3.3 1,8-Bis(2-pyridylmethyl)-1,4,8,11-tetraazacyclotetradecane-5,12-dione .....	175
6.3.4 1,8-Bis(2-pyridylmethyl)-1,4,8,11-tetraazacyclotetradecane .....	176
6.3.5 1,11-Bis(2-methylthiophene)-1,4,8,11-tetraazacyclotetradecane .....	177
6.3.6 1,11-Bis(2-pyridylmethyl)-1,4,8,11-tetraazacyclotetradecane-5,7-dione .....	178
6.3.7 1,11-Bis(2-pyridylmethyl)-1,4,8,11-tetraazacyclotetradecane .....	179
6.3.8 1,11-Dimethyl-1,4,8,11-tetraazacyclotetradecane .....	181
6.3.9 1,4-Bis(2-pyridylmethyl)-1,4,8,11-tetraazacyclotetradecane-9,10-dione .....	182
6.3.10 Chloromethylpyrene .....	184
6.3.11 5,8-Bis(2-pyridylmethyl)-1,5,8,12-tetraazadodecane .....	185
6.3.12 1,4-Bis(2-pyridylmethyl)-1,4,8,11-tetraazacyclotetradecane .....	187
6.3.13 N-(4-benzoyl-phenyl)-3-(1,4,8,11-tetraazacyclotetradec-1-yl)-propionamide .....	188
6.3.14 2-(Mesyloxy)methyl-8-benzyloxyquinoline .....	189
6.3.15 1-(2-Methyl-8-hydroxyquinoline)-1,4,8,11-tetraazacyclotetradecane .....	192
6.3.16 1-(2-methyl-8-benzyloxyquinoline)-1,4,8,11-tetraazacyclotetradecane .....	194

6.4 Synthetic Procedures for Chapter 3 - Metal Complexes .....	195
6.4.1 <i>Copper complexes</i> .....	195
6.4.2 <i>Nickel complexes</i> .....	197
6.4.3 <i>Chromium complexes</i> .....	198
6.5 Synthetic Procedures for Chapter 4.....	199
6.5.1 <i>Lanthanide complexes of L<sup>7</sup></i> .....	199
6.5.2 <i>Lanthanide complexes of L<sup>8</sup></i> .....	201
6.5.3 <i>Lanthanide complexes of L<sup>9</sup></i> .....	203
6.5.4 <i>Lanthanide complexes of L<sup>10</sup></i> .....	205
6.5.5 <i>Lanthanide complexes of L<sup>11</sup></i> .....	206
6.5.6 <i>Lanthanide complexes of L<sup>12</sup></i> .....	207
6.5.7 <i>N-(8-benzyloxy-quinolin-2-ylmethyl)-2-chloro-N-methyl-acetamide</i> .....	209
6.5.8 <i>Lanthanide complexes of L<sup>13</sup></i> .....	211
6.6 References .....	213
6.6.1 <i>Articles</i> .....	213

<b>Appendix A</b>	216
-------------------	-----

<b>Appendix B</b>	221
-------------------	-----

## ABBREVIATIONS

### *Compounds*

Cyclam – 1,4,8,11-tetraazacyclotetradecane

Cyclen – 1,4,7,10-tetraazacyclododecane

EDTA – ethylenediamine-N,N,N',N'-tetraacetic acid

DOTA - 1,4,7,10-tetraazacyclododecane-1,4,7,10-tetraacetic acid

DO3A – 1,4,7-tetraazacyclododecane-1,4,7-triacetic acid

Ln – generic symbol for a lanthanide ion

EDC - 1-(3-dimethylaminopropyl)-3-ethyl-carbodiimide hydrochloride

Ms – mesyl

Ts – tosyl

TFA – trifluoroacetic acid

Bipy – bipyridine

Terpy – terpyridine

Phen – 1,10-phenanthroline

Am – ammonia or general amines

X – acido ligand such as halide, nitro or sulfate ion

DMFDMA – dimethyl acetal of DMF

DMSO – dimethyl sulfoxide

THF - tetrahydrofuran

EtOH - ethanol

MeOH – methanol

EtOAc – ethyl acetate

DMF – dimethyl formamide

CH<sub>3</sub>CN - acetonitrile

CH<sub>3</sub>Cl - chloroform

CH<sub>2</sub>Cl<sub>2</sub> – dichloromethane

EPA – ethanol/isopentane/diethyl ether in the ratio 2/5/5 by volume

### *Photophysical processes*

S – singlet

T – triplet

IC – internal conversion  
ISC – intersystem crossing  
vc – vibrational cascade or relaxation  
F – fluorescence  
P – phosphorescence  
 $\tau$  – lifetime  
 $\Phi$  – quantum yield

### *Geometry*

$O_h$  - octahedral  
*tbp* - trigonal bipyramidal  
*sp* – square planar

### *Techniques and spectroscopy*

IR – infra red spectroscopy  
MS – mass spectrometry  
ES+ - electrospray ionisation using positive mode  
ES- - electrospray ionisation using negative mode  
 $M^+$  – molecular ion  
NMR – nuclear magnetic resonance  
ESR – electron spin resonance  
UV-Vis – ultraviolet-visible absorbance spectroscopy  
TLC – thin layer chromatography

# **CHAPTER 1**

## **INTRODUCTION**



## 1.1 Introduction

The coordination chemistry of macrocyclic ligands has been a fascinating area of interest to inorganic chemists all over the world for over 30 years. The continued interest in designing new macrocyclic ligands stems mainly from their use in a diverse range of applications: for example, as models for protein-metal binding sites in a range of metalloproteins, as synthetic ionophores, as models to study magnetic exchange phenomena, as therapeutic reagents in chelation therapy for treatment of metal intoxication, as cyclic antibiotics that owe their antibiotic actions to specific metal complexation, in studying host-guest interactions and in catalysis.<sup>(VI, XI)</sup>

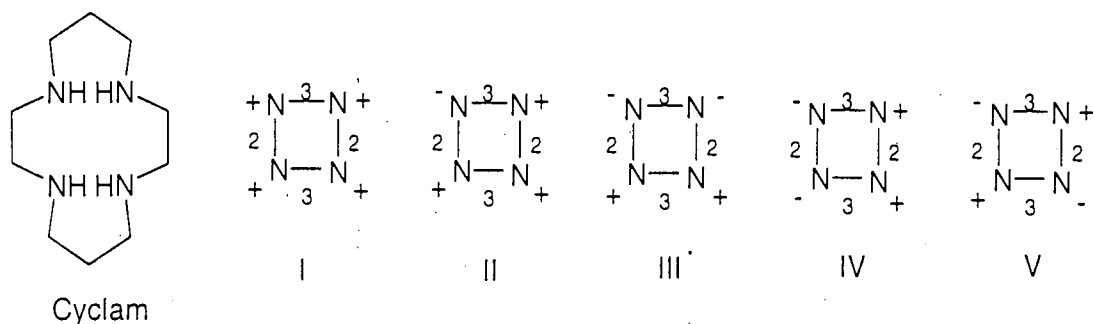
Within this large group of compounds, tetraazamacrocycles attract a great deal of research interest, owing to their ability to form complexes with a large range of metal ions, often with very high *thermodynamic* and *kinetic* stability with respect to metal ion dissociation. Moreover, those which bear additional pendant coordinating groups have been found to be particularly valuable, as their properties and selectivity for certain metal ions over others may be quite different from those of the unsubstituted parent macrocycles.<sup>(VI, XI)</sup>

The work described in this thesis is focused on ligands based on one of the two azamacrocycles:

1. Cyclam, and complexes with some metals of the *d*-block.
2. Cyclen, and complexes with lanthanide(III) ions.

## 1.2 Cyclam

The cyclic tetraamine 1,4,8,11-tetraazacyclotetradecane, commonly known as cyclam, is a particularly important and versatile ligand as it forms complexes with such a large variety of metal ions<sup>(1,2,3,4,5,6)</sup>. Moreover the ligand can be found in “flat” or “folded” configurations, leading to a range of conformations in the complexes<sup>(6)</sup> (figure 1.1).



Configuration of ligand	I	II	III	IV	V
Trans	XX	XX	XX	XX	Y
Cis	X	XX	YY	Y	XX

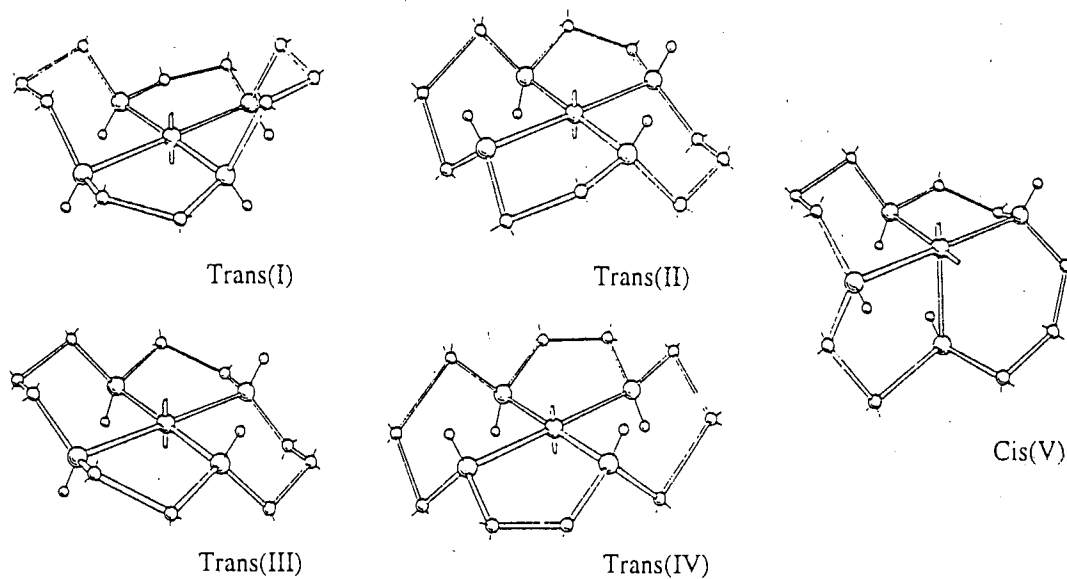


Fig. 1.1 – Qualitative estimation of feasibility of the various isomers of the octahedral complexes of cyclam. In the diagrams the plus refers to N-H bonds that point above the plane formed by the four nitrogen atoms and a minus to ones that point below. XX= strain free with no repulsion between atoms; X= strain-free with possible interatomic repulsion; Y= strained with distorted bond angles; YY= not possible.<sup>(6)</sup>

In the *trans* conformation the four nitrogens of the cyclam are coplanar; it is possible in principle to turn each of these *trans* forms into a *cis* analogue by a simple displacement of nitrogen along the edge of the octahedron.

The chemistry of both N- and C-functionalized cyclam ligands has received much attention in recent years with more and more resources being directed towards the rational design and efficient synthesis of new functionalised ligands.<sup>(2,5,7,8,9,10,11,12)</sup> The main reason for this is due to their ability to coordinate different metal cations. Great effort has been devoted to the incorporation of introducing pendent groups into a saturated macrocyclic tetraamine structure to produce ligands ranging from tetra- through to octadentate and where the preferred conformations and the nature of the additional coordinating groups can profoundly influence the properties of the resulting metal complexes.<sup>(1,2,5,7,8,9,10)</sup>

In fact, the functionalization of cyclam has provided coordination chemists with many new and interesting ligands. C-functionalization is in general more difficult to achieve than N-functionalization, as the substituents must be incorporated into the carbon backbone prior to cyclization. During this work, we have been interested primarily in preparing new pentadentate and hexadentate ligands by selective mono-substitution and di-substitution of cyclam in the 1,4-, 1,8- and 1,11- positions with a range of pendant coordinating groups (figure 1.2).

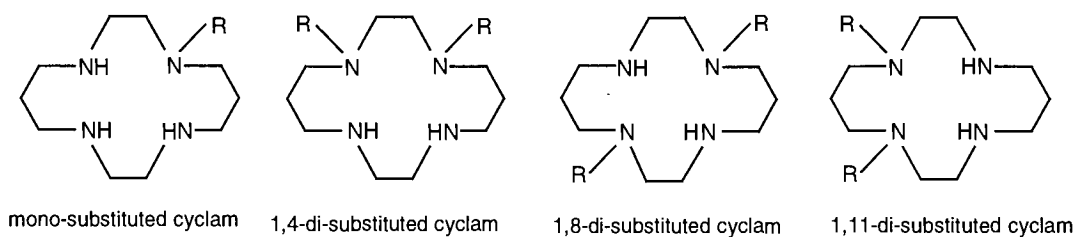


Fig 1.2 – Mono- and di-substituted cyclams.



In order to achieve the desired selectivity in extent and relative position of N-substitution, several different pathways may be considered, many for cyclen as well as cyclam, and involving:

1. Reaction with a Michael acceptor.
2. Direct alkylation of the metal complex.
3. pH-controlled selective protection.
4. N-tosyl intermediates.
5. Dioxocyclams.
6. Formamidinium salt.
7. Tricyclic system.
8. Template reaction.

### 1.2.1 Mono-substitution of cyclam using a Michael acceptor

Different approaches have been devised for the selective mono-N-substitution of tetraazamacrocycles. One method follows a protection-alkylation-deprotection sequence in which three of the four nitrogen atoms are reversibly protected whilst alkylation of the fourth is carried out.<sup>(7,8)</sup> A second way relies on the use of a great excess of tetraazamacrocycle over alkylating agent, thereby minimising polyalkylation.<sup>(9)</sup> In a recent development, the use of protecting groups or large excess of macrocycle is avoided through nucleophilic addition of commercially available or easily prepared Michael acceptors.<sup>(10)</sup> N-Monoalkylated derivatives are selectively obtained in one step by reacting cyclam with an equimolar amount of the Michael acceptor in chloroform in the presence of one equivalent of *p*-toluene-sulfonic acid, providing a general route to new mono-

substituted azamacrocycles with various pendant groups. The selectivity for monoaddition results from protonation of the azamacrocycle in the presence of the acid (figure 1.3).

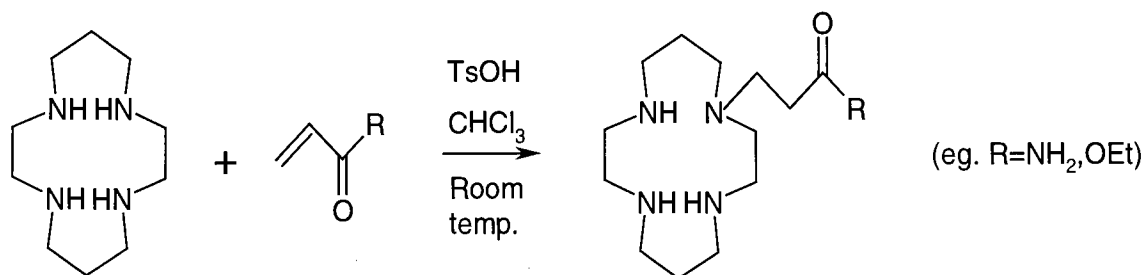


Fig. 1.3 – N-Monoalkylation of cyclam using a Michael acceptor.

## 1.2.2 Direct alkylation of the metal complex

Another approach for the alkylation of tetraazamacrocycles is the direct alkylation of the metal complexes. Coordinated amines have no nucleophilic properties; however removal of a proton generates a nucleophilic amide that may be alkylated.<sup>(11)</sup> Base-solvent systems, such as KOH-DMSO and NaCH<sub>2</sub>S(O)CH<sub>3</sub>-DMSO, are useful for generating deprotonated forms of metal complexes of tetraazamacrocycles and these deprotonated forms may be alkylated with several reagents (figure 1.4).<sup>(12)</sup>

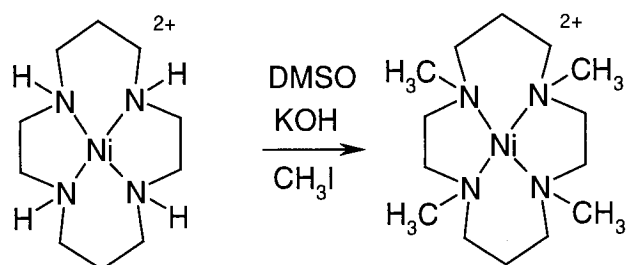
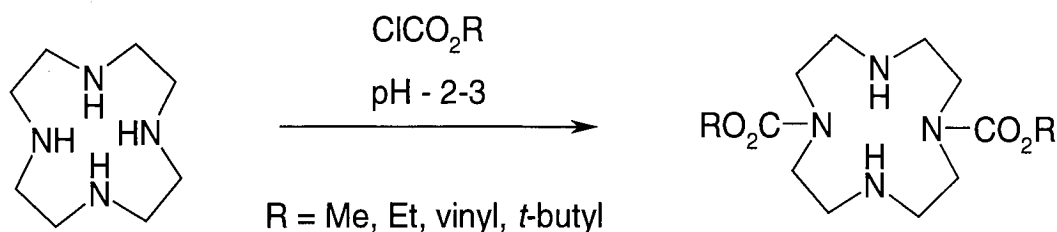


Fig. 1.4 – Alkylation of a macrocyclic amine complex of nickel(II).

This method does not offer good selectivity for mono-alkylation, but is nevertheless interesting for other reasons, as will be discussed in the next chapter.

### 1.2.3 pH-Controlled selective protection of macrocycles

This method,<sup>(13)</sup> which may lead to high yields of selectively substituted polyaza macrocycles, involves a protection-functionalization-deprotection sequence. Carbamates, widely used in peptide synthesis to protect amino groups, are used for protection of two of the ring nitrogen atoms because they are stable, easy to handle compounds and some of them (benzyl, *tert*-butyl) can be cleaved under mild conditions. The general protection reaction is shown in scheme 1.



Scheme 1.

When two equivalents of methyl, ethyl or vinyl chloroformate are added to an aqueous solution of tetraazacyclododecane (cyclen) and the pH is carefully kept just below 3, regioselective reaction occurs and the 1,7-diprotected derivatives are formed essentially in quantitative yields. After the reaction mixture is made basic with concentrated sodium hydroxide, the free base is isolated by extraction into an organic solvent. Methyl and ethyl carbamate derivatives can be difficult to cleave, since they are resistant to acid or base hydrolysis. On the other hand, benzyloxycarbonyl derivatives can be cleaved by relatively

mild acid hydrolysis or removed selectively by catalytic hydrogenation, making them more appropriate for use. They are formed upon reaction with benzyl chloroformate in much the same way as the alkyl carbamates, except that the solvent is a mixture of water and dioxane, the latter being added to increase the solubility of the acylating reagent.

The high regioselectivity observed in the cyclen reactions probably reflects the protonation state of the macrocycle at pH 3. Cyclen has two basic and two acidic nitrogens, as does cyclam<sup>(14)</sup> (table 1), so that two of the nitrogens are protonated (and hence protected) over a wide pH range.

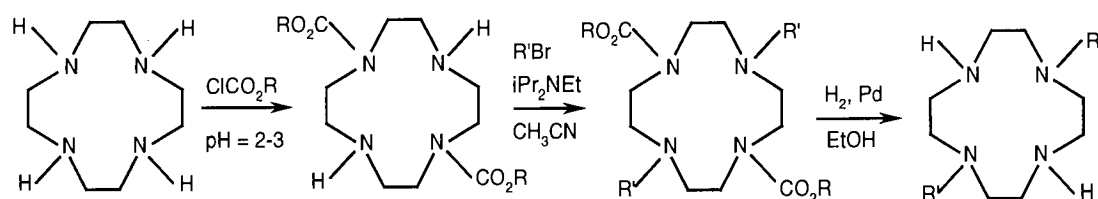
Ligand	Cyclen	Cyclam
pK <sub>1</sub>	10.6	11.02
pK <sub>2</sub>	9.6	9.96
pK <sub>3</sub>	1.5	2
pK <sub>4</sub>	0.7	0.8

Table 1. <sup>(13,14)</sup>

Electrostatic repulsions within the 12-membered ring favour protonation of nitrogens as far removed from each other as possible leaving the remaining non-protonated nitrogens available for reaction with the chloroformate. Hence, the selectivity is for the 1,7-dialkylated compound, with little or no 1,4 product. This method gives good yields for cyclen because in this system only two carbon atoms separate the nitrogens. In cyclam, 1,5-diprotonation is not as unfavourable as 1,4-diprotonation in cyclen, so that the selectivity and yield are lower in this case. The optimal pH region for the selective protection is between 2 and 3. At lower pH the reaction becomes inconveniently slow. At

higher pH, as the less protonated species react faster with the chloroformate, the reaction loses selectivity and increasing amounts of fully protected products are formed.<sup>(13)</sup>

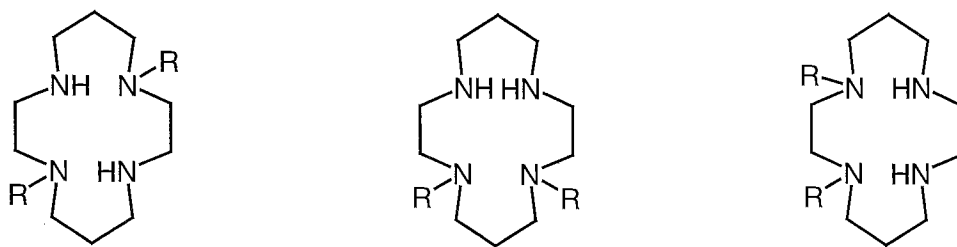
After reaction of the non-protected nitrogen atoms with the appropriate alkylating agent, removal of the benzyloxycarbonyl group may be accomplished readily by catalytic hydrogenation in ethanol solution. The ease of protection and deprotection makes this methodology very attractive for the synthesis of new di-substituted derivatives. The overall reaction sequence is summarised in scheme 2.



Scheme 2.

### 1.2.4 Synthesis of substituted derivatives of cyclam using N-tosyl intermediates

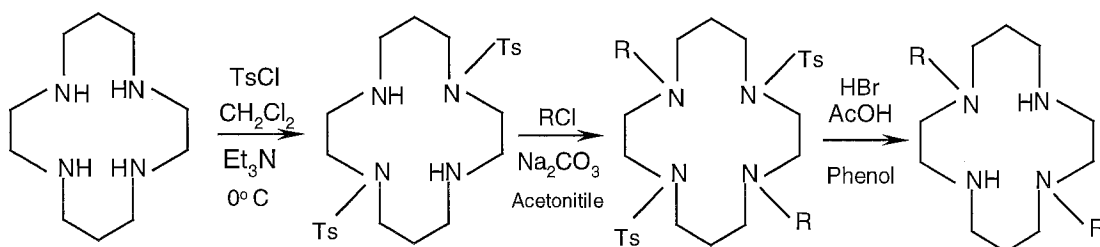
This method<sup>(15)</sup> allows the synthesis of mono, di and tri-N-substituted derivatives of cyclam. The formation of [1,n] di-substituted derivatives of cyclam is intrinsically more difficult than for cyclen as it preferably requires the selective formation of one of the three constitutional isomers: the 1,4-, 1,8- and 1,11- derivatives (figure 1.5), whereas only two are possible for cyclen, 1,4- and 1,7-.



1,8 - di-substituted cyclam      1,11 - di-substituted cyclam      1,4 - di-substituted cyclam

Fig 1.5 – Isomers of di-substituted cyclam.

Careful tosylation of cyclam with two equivalents of tosyl chloride ( $\text{CH}_2\text{Cl}_2$ ,  $\text{Et}_3\text{N}$ ,  $0^\circ\text{C}$ ) gives the two constitutional isomers 1,8- and 1,11- in reasonable yield and in the ratio 8:1. These isomers can be separated from each other by flash chromatography on silica gel. It is not possible to isolate the 1,4- isomer because it is formed in very low yield (<3.5%) under these reaction conditions. It is then possible to use the di-tosyl derivatives as diprotected cyclams similar to the dicarbamates of the previous section. Alkylation with the appropriate alkylating agent gives a tetra-substituted cyclam from which the required di-substituted compound may be obtained upon removal of the tosyl groups using hydrogen bromide in acetic acid in the presence of phenol or using  $\text{Li}/\text{l.NH}_3/\text{EtOH}/\text{THF}$  (scheme 3).



Scheme 3.

### 1.2.5 Synthesis of di-substituted cyclam using dioxoamines

The macrocyclic dioxotetraamines, shown in figure 1.6, are unique chelating ligands for some transition-metal ions. They bear the dual structural features of macrocyclic tetraamines and of peptides and their complexes have many interesting properties and potential applications.

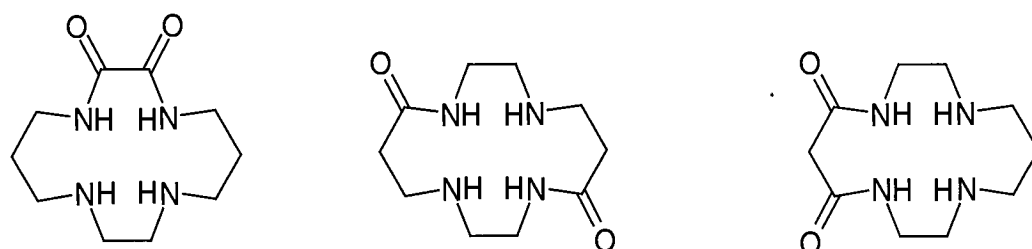


Fig 1.6 – [2,3], [5,12] and [5,7] dioxotetraamines.

The [2,3] dioxotetraamine<sup>(16)</sup>, first prepared in 1982 and then “rediscovered” in 1999, is easily prepared by dropwise addition of an ethanolic solution of dimethyloxalate and *N,N'*-bis(3-aminopropyl)ethylenediamine, to refluxing ethanol over a period of 32 hours (figure 1.7). Separation of the required product from acyclic condensation products is straightforward as the former crystallises from solution.

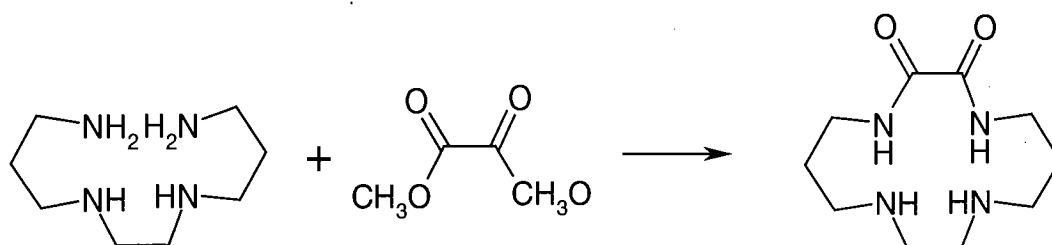


Fig. 1.7 - Synthesis of [2,3] dioxotetraamine.

The [1,8] dioxotetraamine is also prepared readily by reaction of simple acrylic esters with 1,2-ethylenediamine exemplified by the methyl ester in figure 1.8.<sup>(17)</sup>

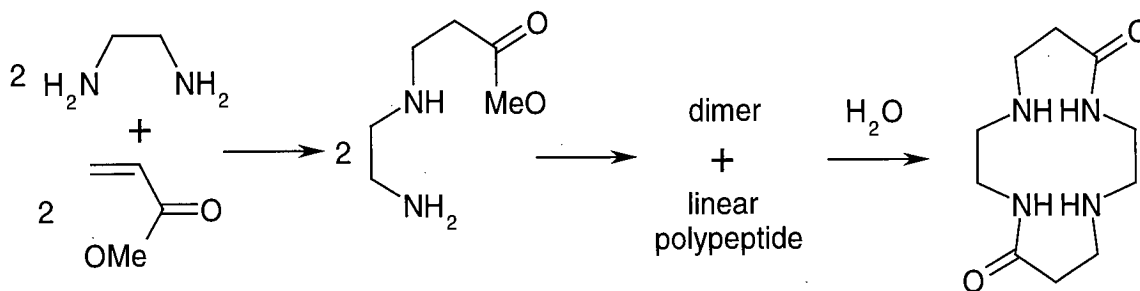


Fig 1.8 – Synthesis of [1,8] dioxotetraamine.

The Michael addition reaction is easily effected by simply mixing the two reactants, preferably without a solvent, and maintaining the temperature between 20°C and 60°C. The Michael addition product readily undergoes subsequent intermolecular and intramolecular amidation reactions to form first the dimeric reaction product, and then the linear polypeptide product. A small amount of the required cyclic dimerised product also forms, if temperatures higher than 60°C are avoided.

Reaction times of up to several weeks may be required for the cyclization process to occur. Alternatively, the Michael addition product may be dissolved in water (about 25 weight percent) for the cyclization reaction. Normally, the cyclic peptide product, being less soluble than the addition product and linear polymeric material, is readily precipitated from the reaction medium as it forms and is recovered by filtration.

The dioxotetraamines<sup>(18)</sup> of the [5,7] type are easily prepared by reaction of polyethylenepolyamines with  $\alpha,\omega$ -diesters (figure 1.9). For example, the [5,7] compound itself (figure 1.6) is obtained by refluxing a mixture of N,N-bis-(2-aminoethyl)-1,3-propanediamine with diethyl malonate for seven days.



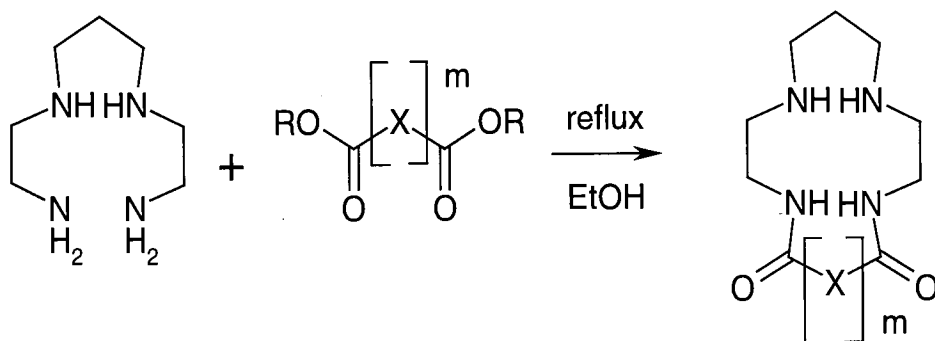


Fig 1.9 – Synthesis of [5,7] dioxocyclam ( $m=1$  and  $X=CH_2$  for the 5,7-dioxocyclam).

It is possible to obtain di-substituted dioxocyclam ligands<sup>(5,19)</sup> by reaction of a solution of the dioxotetraamine with two equivalents of an appropriate alkylating agent, in the presence of base, usually in refluxing acetonitrile (figure 1.10).

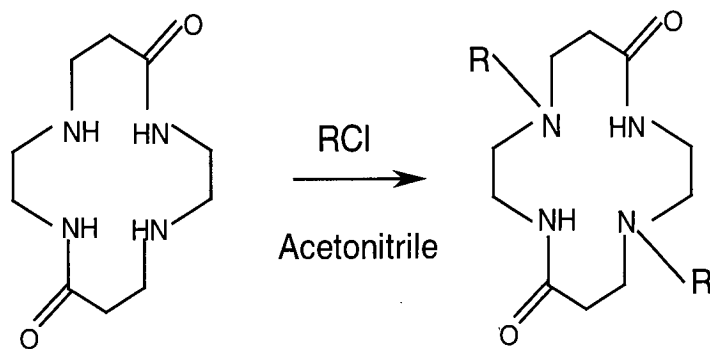
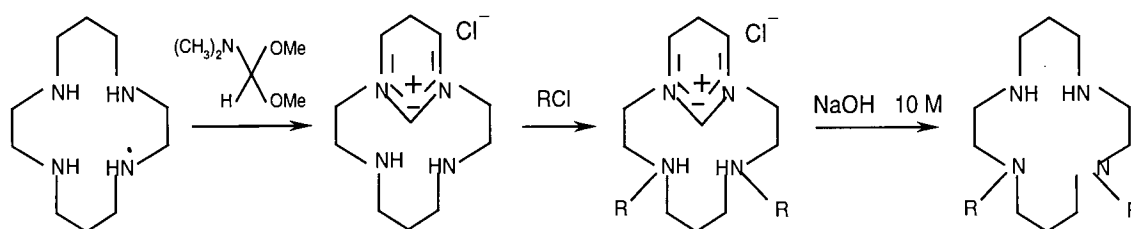


Fig. 1.10 – Synthesis of di-substituted dioxocyclam.

## 1.2.6 Formation of 1,11-bis-(pendant donor)-cyclam derivatives via the formamidinium salt

The reaction of the dimethyl acetal of N,N-dimethylformamide (dmfdma) with cyclam<sup>(20)</sup> in chloroform provides a means of selective 1,11-dialkylation of cyclam (scheme 4).



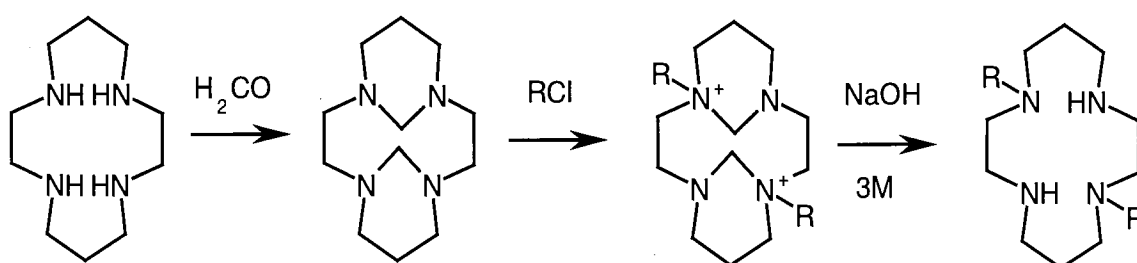
Scheme 4.

The formamidinium salt is obtained in 75% yield upon reaction of cyclam with an equimolar amount of dmfdma in refluxing chloroform for a period of 18 h. This compound offers protection of a pair of 4,8-related amine sites on the cyclam moiety whilst allowing substitution on the other two.

The formamidinium salt is then converted to the free base, in good yields, by reaction with 10 M sodium hydroxide for some hours.

### 1.2.7 Synthesis of di-substituted cyclams using a tricyclic system

The “classical” synthetic reactions for the preparation of *trans*-1,8-N,N-disubstituted cyclams discussed in the preceding section usually suffer from low yields. The new method shown in scheme 5 proceeds in three steps via the tricyclic 1,4,8,11-tetraazatricyclo[9.3.1.1<sup>4,8</sup>]hexadecane system.<sup>(21)</sup>



Scheme 5.

The synthetic route proceeds at room temperature to yield the *trans*-N,N'-disubstituted cyclam at a high rate and in good yield. The first intermediate may be obtained by reaction of cyclam with formaldehyde or by refluxing cyclam in 30% NaOH aqueous solution in the presence of dichloromethane. The pure product is easily isolated by concentration of the organic phase and recrystallisation from a THF/water mixture. The crystallographic structure shows a *trans* conformation for the two methylenic bridges. In the second step, the ligand is dissolved in acetonitrile and two equivalents of an alkyl halide (methyl iodide, picolyl chloride, etc.) are rapidly added to yield the new disubstituted macrotricyclic system having two non-adjacent quaternary nitrogen atoms. High yields are obtained and no *cis*-disubstituted macrocycle is detected. This indicates a strong selectivity for the *trans* disubstitution, thought to arise from the rigid conformation

of the intermediate. The final *trans*-disubstituted cyclam is then easily formed after basic hydrolysis in sodium hydroxide 3M at room temperature.

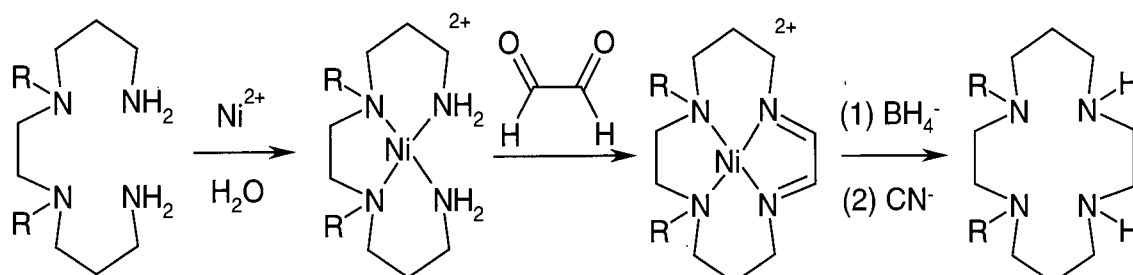
A significant advantage of this synthesis lies in the fact that, in each step, reagents and products have very different solubility and are easy to separate.

### 1.2.8 Template reaction

The macrocyclic complexes of metal ions are usually synthesized by the reaction of the required metal ion with the preformed macrocyclic ligands, but there are potential disadvantages in this method. The synthesis of a macrocycle in the free form often results in a low yield of the desired product with side reactions, such as polymerisation, predominating. In order to circumvent this problem, the ring-closure step in the synthesis may be carried out under conditions of high dilution or a rigid group may be introduced to restrict rotation in the open-chain precursor thereby facilitating cyclisation.<sup>(VII)</sup>

One effective method for the synthesis of macrocyclic complexes involves an *in situ* approach wherein the presence of a metal ion in the cyclisation reaction markedly increases the yield of the cyclic product. The metal ion plays an important role in directing the steric course of the reaction and this effect is termed “metal template effect”.<sup>(VII,22)</sup>

A classic example is the synthesis of cyclam itself (scheme 6), where the nickel ion is removed by cyanide addition.<sup>(22)</sup> In fact, this is the synthetic route used to prepare our starting compound.



R = H for cyclam

Scheme 6.

Other metal templated syntheses have now been reported, not only involving condensation reactions but also exploring the synthesis of substituted macrocyclic ligand complexes (scheme 6).<sup>(23)</sup> Following this synthetic route it is thus possible to synthesise [1,4] di-substituted cyclam derivatives.

### 1.3 Metal complexes

The main interest in the first part of the work described in this thesis is in complexes of transition metal ions, particularly chromium, copper and nickel. Their partly filled *d* shells lead to many experimental observables not possible for main group and early transition metal complexes, including paramagnetism, visible absorption spectra, and sometimes luminescence (metal-centred and/or charge transfer).

The study of the geometry and conformations of the resulting complexes is important. As stated previously, the cyclam ring adopts different conformations and the presence of different substituents in different positions may serve to determine which is the preferred conformer.

The work has been concerned, in part, with the photophysics and photochemistry of some of these macrocycle metal complexes. In this respect, chromium(III) occupies an important position, because it is one of the few transition metal ions which may display luminescence from a metal-centred excited state.<sup>(1)</sup> In fact, the understanding of the photochemical, photophysical and spectroscopic features of octahedral chromium(III) complex ions, both in solution and in the solid state, has been a challenge for experimentalists and theoreticians for many years.<sup>(28)</sup> This is partly due to the number of issues which frequently remain unclear. These include the relative chemical importance of the lowest electronically excited states, the types and the roles of non-radiative processes, particularly the possible involvement of the thermally activated back-intersystem crossing from the lowest doublet excited state to initially populated quartet excited state, and the occurrence of chemically reactive excited-state intermediates (e.g. leading to photosolvation processes).

## 1.4 Factors affecting the metal-binding properties of macrocycles

The factors which determine the binding properties of macrocycles<sup>(24)</sup> include:

1. The type of binding site in the ring, e.g., O, N, S, carbonyl oxygen.
2. The number of binding sites in the ring.
3. The relative disposition of the binding sites.
4. The relative sizes of the ion and the macrocyclic cavity.
5. Steric hindrance in the ring, including torsional strain, eclipsing or transannular interactions.
6. The solvent and the extent of solvation of the ion and the ligand.
7. The electrical charge of the ion.

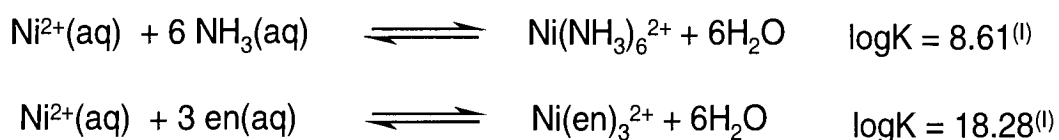
With so many variables, there is considerable scope to design macrocycles which match the requirement of individual metal ions.

Cyclic polyethers bind readily to the alkali and alkaline earth metals to form relatively stable complexes but show little tendency to bind transition metal ions. However, when the oxygen donor atoms are replaced by softer nitrogen or sulphur atoms, then more stable macrocyclic complexes with transition metal ions are readily formed.<sup>(24)</sup>

The transition metal cations generally have larger and more polarisable valence shells. They are “softer” in nature and more readily bind with “softer” donor atoms forming dative bonds, which show more covalent character in contrast to the ionic bonding, found between the alkali and alkali earth metals and “hard” oxygen donor atoms.<sup>(24)</sup>

The highest stability constants for these transition metal complexes are generally found when there is a good match between the size of the cation and the “cavity” imposed by the macrocycle, allowing optimum metal-donor bond length. A good example of this is the stability constant of the copper(II) complex of tetraazamacrocyclic ligands which reaches a maximum at [13]N<sub>4</sub> and [14]N<sub>4</sub> and falls off rapidly with smaller and larger ring size.<sup>(VI)</sup>

The term *chelate effect* refers to the enhanced thermodynamic stability of a complex system containing chelate rings compared to a similar system without such rings. An example of this is as follows:



The system Ni(en)<sub>3</sub><sup>2+</sup> in which the three chelate rings are formed is found to be nearly 10<sup>10</sup> times more stable as that in which no such ring is formed. Although the chelate effect is not usually so pronounced as this, such an effect is very general.

Macrocyclic complexes are, almost without exception, more stable *thermodynamically* and *kinetically* than their open-chain analogues. This was called the “macrocyclic effect” by its discoverers Margerum and Cabbiness,<sup>(25)</sup> and is a more profound feature of macrocyclic complexes than simply an increased “chelate effect” arising from the presence of an additional chelate ring. Much calorimetric and spectroscopic work has been carried out to investigate this phenomenon and it is thought that the enhanced stability is due to a favourable enthalpy or entropy change or a combination of both, their



relative importance being very dependent upon the particular combination of ligand and metal.<sup>(25, 25a, 25b)</sup>

Another feature of the macrocyclic effect is the *kinetic inertness* of macrocyclic complexes, particularly towards acid-catalysed dissociation. In fact, they may be so inert that decomplexation often only occurs to an appreciable extent in very strong (5-6 M) acid.<sup>(26)</sup>

Many examples have been found where there has been a reasonable correlation between cavity/cation size and the observed stability constant of the complex. It is common to ascribe the enhanced stability of the macrocyclic complexes to the fit between the metal ion diameter and the size of a relatively rigid cavity in the centre of the macrocycle. Although this may be a valid concept for explaining the selectivity of crown-ether ligands for alkali metal ions,<sup>(27)</sup> the correlation between stability and fit is less certain for tetraamine macrocycles and is metal-dependent. Moreover, macrocyclic ligands, particularly the larger rings, can be flexible and can adapt their conformations to accommodate cations of different size.

## 1.5 Photochemistry

When a molecule has been promoted to an excited state through absorption of light, it does not remain there for long. For closed-shell molecules in which all electrons are paired (e.g. almost all organic molecules), most of these light-induced transitions are from the ground state ( $S_0$ ) to excited singlet states,  $S_n$ . A singlet state is one in which all

electrons are paired ( $S_0$ ) or in which two unpaired electrons have opposite spins ( $S_n$ ) whilst a molecule in which two unpaired electrons have the same spin is called a triplet state ( $T$ ). The process by which molecules in  $S_2$  or higher  $S$  states drop to  $S_1$  is called *internal conversion* (IC) and, being an adiabatic process, leads to a vibrationally excited state of  $S_1$ . Normally, vibrational energy is lost very rapidly (*vibrational relaxation*) such that the lowest vibrational level of  $S_1$  is the only important excited singlet state. This state can undergo various physical and chemical processes. These pathways are often represented schematically using a Jablonski diagram (figure 1.11).<sup>(v)</sup>

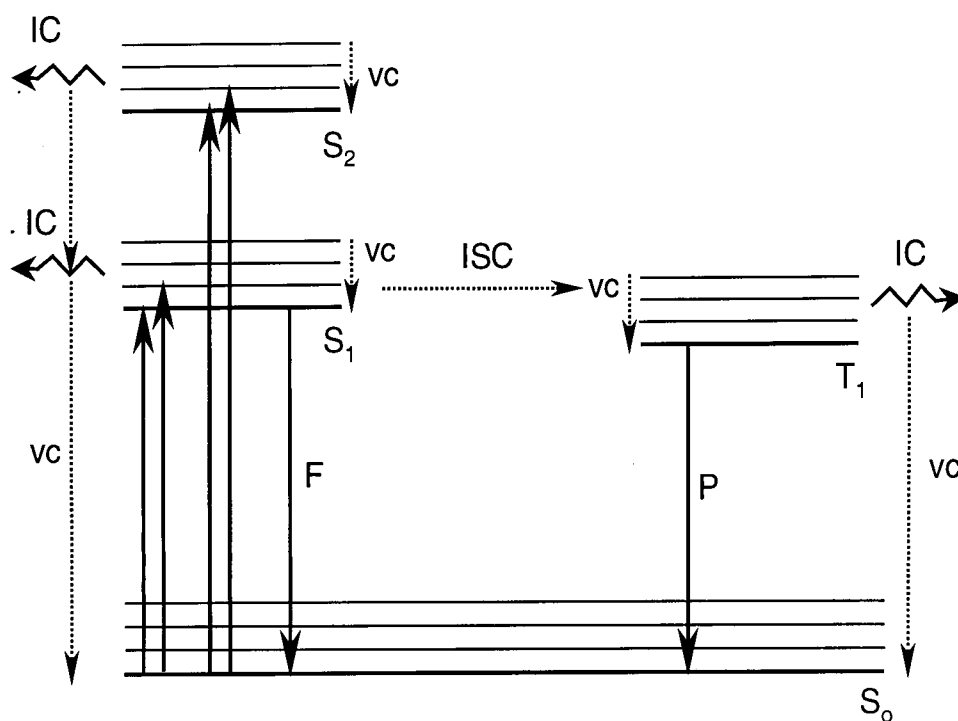


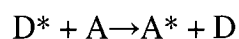
Fig 1.11 – Jablonski diagram. IC= internal conversion; ISC= intersystem crossing; vc= vibrational cascade; F= fluorescence; P= phosphorescence.

A molecule in the  $S_1$  state can undergo *internal conversion* to a vibrationally excited level of the  $S_0$  state and thence return to the ground state by giving up its energy in small increments to the environment. This process does not lead to emission of light. However, a molecule in the  $S_1$  state can sometimes drop to some low vibrational level of the  $S_0$  state

all at once by giving off the energy as a photon of light. This process is called *fluorescence*.

Molecules in the  $S_1$  state can also undergo a third process, namely *intersystem crossing* (ISC) to the lowest triplet state  $T_1$ . Intersystem crossing from singlet to triplet is, of course, a “forbidden” pathway, but this often takes place by compensations elsewhere in the system. A molecule in the  $T_1$  state may return to the  $S_0$  state by back-ISC followed by vibrational relaxation, in which case the energy is lost as thermal energy, or through emission of a photon of light. In this case, the process is termed *phosphorescence*. The spin-forbidden nature of the phosphorescent transition ( $T_1$ - $S_0$ ) gives rise to the long natural luminescence lifetime, which is often a feature of phosphorescence (emission timescales may be of the order of milliseconds to seconds in the absence of other deactivation processes). In contrast, fluorescence is a fully allowed process and decays very rapidly after excitation, typically over nanoseconds to microseconds.

If nothing else happens to it first, a molecule in an excited state ( $S_1$  or  $T_1$ ) may transfer its excess energy all at once to another molecule in the environment, in a process called *photosensitization*. The excited molecule (D for donor) thus drops to  $S_0$  while the other molecule (A for acceptor) becomes excited:



The donor D is called a *photosensitizer*. This energy transfer is usually subject to the *Wigner spin-conservation rule*, which says that the total electron spin does not change after the energy transfer.<sup>(v)</sup> Thus, a singlet donor should lead to a singlet excited state of acceptor A and so on.

## 1.6 Chromium

For chromium the highest oxidation state is that corresponding to the total number of  $3d$  and  $4s$  electrons. Chromium(VI), which exists only in the oxo species such as  $\text{CrO}_3$ ,  $[\text{CrO}_4]^{2-}$  and  $\text{CrO}_2\text{F}_2$ , is strongly oxidizing. The intermediate states  $\text{Cr}^{\text{V}}$  and  $\text{Cr}^{\text{IV}}$  have rather limited chemistry. Very low formal oxidation states are found largely in carbonyl- and organometallic-type compounds. With ligands such as aryl isocyanides, bipy, terpy and phen, it is possible to generate stable  $\text{Cr}^{\text{I}}$  compounds. With the isocyanides, electrochemical or  $\text{Ag}^+$  oxidation may be used to obtain, from  $\text{Cr}(\text{CNR})_6$ , the +1 and +2 ions, with one and two unpaired electrons, respectively. The most stable and generally important oxidation states are  $\text{Cr}^{\text{II}}$  and  $\text{Cr}^{\text{III}}$ . The oxidation states and stereochemistry are summarized in table 2.<sup>(1,II)</sup>

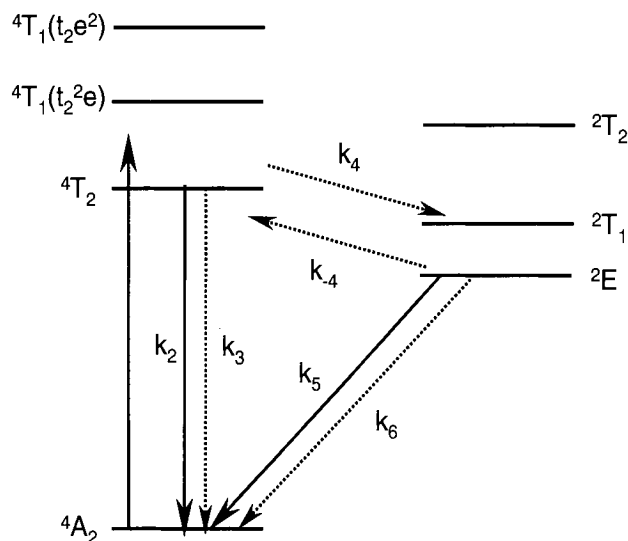
There are literally thousands of chromium(III) complexes that are, with few exceptions, all hexacoordinate. The principal characteristic of these complexes in aqueous solutions is their relative kinetic inertness reflecting the  $d^3$  electronic configuration. The ammonia and amine complexes are the most numerous chromium derivatives and the most extensively studied. They include the pure ammines  $[\text{CrAm}_6]^{3+}$ , the mixed ammine-aqua types,  $[\text{CrAm}_{6-n}(\text{H}_2\text{O})_n]^{3+}$  ( $n=0-4,6$ ), the mixed ammine-acido types,  $[\text{CrAm}_{6-n}\text{X}_n]^{(3-n)+}$  ( $n=1-4,6$ ), and the mixed ammine-aqua-acido types, for example,  $[\text{CrAm}_{6-n-m}(\text{H}_2\text{O})_n \text{X}_m]^{(3-m)+}$ . In these general formulae Am represents the monodentate ligand  $\text{NH}_3$  or  $\text{R}'\text{NH}_2$  or half of a polydentate amine such as ethylenediamine, and X represents an acido ligand such as halide, nitro, or sulfate ion.

Oxidation State	Coordination number	Geometry	Examples
Cr <sup>0</sup>	6	octahedral	Cr(CO) <sub>6</sub>
Cr <sup>I</sup> , d <sup>5</sup>	6	octahedral	[Cr(bipy) <sub>3</sub> ] <sup>+</sup>
Cr <sup>II</sup> , d <sup>4</sup>	3	T shape	Cr(OC <sub>t</sub> -Bu <sub>3</sub> ) <sub>2</sub> LiCl(THF)
	4	square	Cr(O <sub>2</sub> CCF <sub>3</sub> ) <sub>2</sub> (Me <sub>2</sub> py) <sub>2</sub>
	4	distorted tetrahedral	CrCl <sub>2</sub> (MeCN) <sub>2</sub>
	6	distorted octahedral	CrF <sub>2</sub>
Cr <sup>III</sup> , d <sup>3</sup>	3	planar	Cr(NPr <sub>2</sub> ) <sub>3</sub>
	4	distorted tetrahedral	[PCl <sub>4</sub> ] <sup>+</sup> [CrCl <sub>4</sub> ] <sup>-</sup>
	5	<i>tbp</i>	CrCl <sub>3</sub> (NMe <sub>3</sub> ) <sub>2</sub>
	6	octahedral	[Cr(NH <sub>3</sub> ) <sub>6</sub> ] <sup>3+</sup>
Cr <sup>IV</sup> , d <sup>2</sup>	4	tetrahedral	Ba <sub>2</sub> CrO <sub>4</sub>
	6	octahedral	K <sub>2</sub> CrF <sub>6</sub>
	8	dodecahedral	CrH <sub>4</sub> (dmpe) <sub>2</sub>
Cr <sup>V</sup> , d <sup>1</sup>	4	tetrahedral	CrO <sub>4</sub> <sup>3-</sup>
	5	distorted <i>tbp</i>	CrF <sub>5</sub>
	6	octahedral	K <sub>2</sub> [CrOCl <sub>5</sub> ]
	8	quasi-dodecahedral	K <sub>3</sub> Cr(O <sub>2</sub> ) <sub>4</sub>
Cr <sup>VI</sup> , d <sup>0</sup>	4	tetrahedral	CrO <sub>3</sub>
	6	octahedral	CrF <sub>6</sub> (matrix)

Table 2 - Oxidation states and stereochemistry of chromium.<sup>(1)</sup>

Cr(III) luminescence has been known for more than a century<sup>(28)</sup>. In the solid state it is exploited in, for example, the ruby laser (Cr<sup>3+</sup>:AlO<sub>3</sub>). In solution, however, the luminescence of chromium complexes is often detectable only at low temperature. At room temperature, non-radiative processes may compete efficiently, such that the excitation energy is lost as vibrational energy, unless the metal ion is bound within a very rigid complex, (for example, the *trans* cyclam complex)<sup>(1)</sup>. In fact, rigidity favours luminescence over other non-radiative processes.<sup>(v)</sup>

In order to appreciate the origin of chromium(III) luminescence, the energy level diagram of this  $d^3$  metal ion must be considered. The terms representing the 120 states of the  $d^3$  configuration of chromium are classified as quartet and doublet according to whether the three electrons have parallel spins or whether one has opposite spin. The energy levels of  $d^3$  chromium ions in octahedral symmetry are displayed in scheme 7.



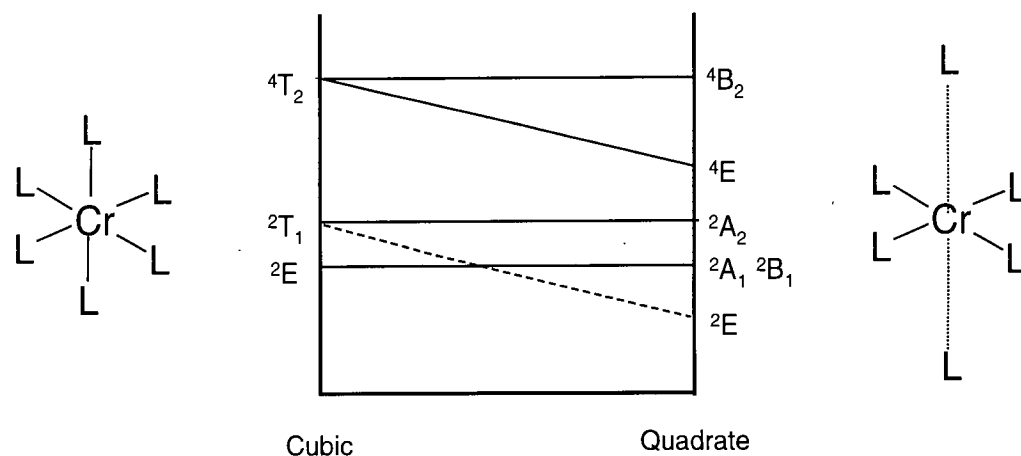
Scheme 7 – Energy levels and rate constants for chromium(III) complexes<sup>(28)</sup>.

The ground  $^4A_2$  level and the three lowest doublet levels,  $^2E$ ,  $^2T_1$ , and  $^2T_2$ , are derived from the  $t_2^3$  configuration. The lowest excited quartet states,  $^4T_2$  and  $^4T_1$  are derived from  $t_2^2e$ . Whilst the energies of the  $^4A_2$ ,  $^2E$ , and  $^2T_1$  levels are independent of the octahedral field strength,  $Dq$ , the  $^4T_2$  and  $^4T_1$  energies are proportional to  $Dq$ .

The absorption spectra typically consist of two broad spin-allowed bands,  $^4T_2 \leftarrow ^4A_2$  and  $^4T_1(t_2^2e) \leftarrow ^4A_2$ . Sometimes a third ligand field band,  $^4T_1(t_2e^2) \leftarrow ^4A_2$  is also observed at higher energy, but this transition is often obscured by much more intense charge-transfer bands. The extinction coefficients of the spin-allowed transitions are usually less than 100

$M^{-1} \text{ cm}^{-1}$ . The weaker, narrow spin-forbidden lines ( $\epsilon_{\text{max}} < 5$ ) are due to the intraconfigurational ( $t_2^3$ ) transitions,  ${}^2T_2 \leftarrow {}^4A_2$ ,  ${}^2T_1 \leftarrow {}^4A_2$ , and  ${}^2E \leftarrow {}^4A_2$ . When ligands have delocalized  $\pi$ -electron systems, relatively intense bands appear at low energies and obscure some of the metal-localized  $d-d$  absorption bands. These bands are associated with ligand-localized singlet-triplet transitions, which are intensified by coupling with the unpaired chromium(III)  $d$  electrons, rather than by spin-orbit coupling.

The environment of  $\text{Cr}^{3+}$  is strictly  $O_h$  only in a few ionic crystals. When chromium(III) is part of a  $\text{CrX}_6$  complex ion or molecule, the  $\text{Cr}^{3+}$  site symmetry can be close to  $O_h$ , but in most complexes the spectral assignments cannot be made in terms of strict  $O_h$  symmetry. For convenience, the complexes are classified as pseudo-octahedral, trigonal, or quadrate, depending upon the approximate skeletal symmetry. In  $O_h$  symmetry  ${}^2E$  is unsplit, but is split in trigonal fields. The  ${}^2T_1$  is very sensitive to deviations from cubic symmetry.  ${}^4T_2$  and  ${}^4T_1$  are also split by noncubic fields (scheme 8).



Scheme 8 – Level splitting in quadrate fields<sup>(28)</sup>.

A very useful guide to the assignment of metal complexes' emission spectra is: "emission originates from the lowest excited level or any levels in thermal equilibrium with it". This principle, sometimes known as Kasha's Rule,<sup>(V)</sup> is obeyed by chromium(III) complexes. In pseudo-octahedral and trigonal complexes the emission in the low-temperature limit will be either  ${}^4T_2 \rightarrow {}^4A_2$  fluorescence or  ${}^2E \rightarrow {}^4A_2$  phosphorescence.

From the standpoint of the work on chromium described in chapter two, the important conclusion from a large number of studies is that, for coordination by nitrogen donors,  ${}^2E$  is invariably below  ${}^4T_2$  so that *phosphorescence* is the dominant emission process in  $CrN_6$  complexes.

## 1.7 Copper

In the metal, copper has a single *s* electron outside the filled *3d* shell. The oxidation states and stereochemistry of copper are summarized in the table 3.

The dipositive state is the most important for copper. The  $d^9$  configuration makes Cu(II) complexes subject to Jahn-Teller distortion if placed in cubic or tetrahedral environments and this has a profound effect on the coordination geometry. Jahn and Teller showed that in general no nonlinear molecule can be stable in a degenerate electronic state, the molecule must become distorted in such a way as to break down the degeneracy.<sup>(1)</sup> The driving force for the distortion is the reduction in the overall energy of the occupied *d* orbitals. When six-coordinate, the "octahedron" is severely distorted. The typical distortion is an elongation along one 4-fold axis, such that there is a planar array of four



short Cu-L bonds and two *trans* long ones. In the limit, of course, the elongation leads to a situation indistinguishable from square planar coordination as found in CuO and many discrete complexes of Cu(II). Thus, the case of tetragonally distorted “octahedral” coordination and square planar co-ordination cannot always be easily differentiated.

Oxidation State	Coordination number	Geometry	Examples
Cu <sup>I</sup> , <i>d</i> <sup>10</sup>	2	linear	Cu <sub>2</sub> O
	3	planar	K[Cu(CN) <sub>2</sub> ]
	4	tetrahedral	CuI
	4	distorted planar	CuL <sup>a</sup>
	5	<i>sp</i>	[CuLCO] <sup>a</sup>
	6	octahedral	{(Ph <sub>2</sub> MeP) <sub>3</sub> ReH <sub>5</sub> } <sub>2</sub> Cu <sup>+</sup>
Cu <sup>II</sup> , <i>d</i> <sup>9</sup>	3	trigonal planar	Cu <sub>2</sub> (μ-Br) <sub>2</sub> Br <sub>2</sub>
	4	square	CuO
	6	distorted octahedral	CuCl <sub>2</sub>
	5	<i>tbp</i>	[CuCl <sub>5</sub> ] <sup>2-</sup>
	6	octahedral	K <sub>2</sub> Pb[Cu(NO <sub>2</sub> ) <sub>6</sub> ]
	7	pentagonal bipyramidal	[Cu(H <sub>2</sub> O) <sub>2</sub> (dps)] <sup>2+</sup> <sup>b</sup>
Cu <sup>III</sup> , <i>d</i> <sup>8</sup>	8	distorted dodecahedron	Ca[Cu(CO <sub>2</sub> Me) <sub>4</sub> ] <sub>6</sub> H <sub>2</sub> O
	4	square	KCuO <sub>2</sub>
	6	octahedral	K <sub>3</sub> CuF <sub>6</sub>

<sup>a</sup> L=a macrocyclic N<sub>4</sub> anionic ligand.

<sup>b</sup> dps= 2,6-diacetylpyridine bis(semicarbazone).

Table 3 - Oxidation states and stereochemistry of copper.<sup>(1)</sup>

A number of 5 coordinate species are known, both square pyramidal and trigonal bipyramidal.<sup>(11)</sup> Four coordination is exemplified by square planar and rarely tetrahedral species as well as intermediate configurations.

The correspondence between the energy level-diagrams of octahedral and square planar complexes is shown in figure 1.12.

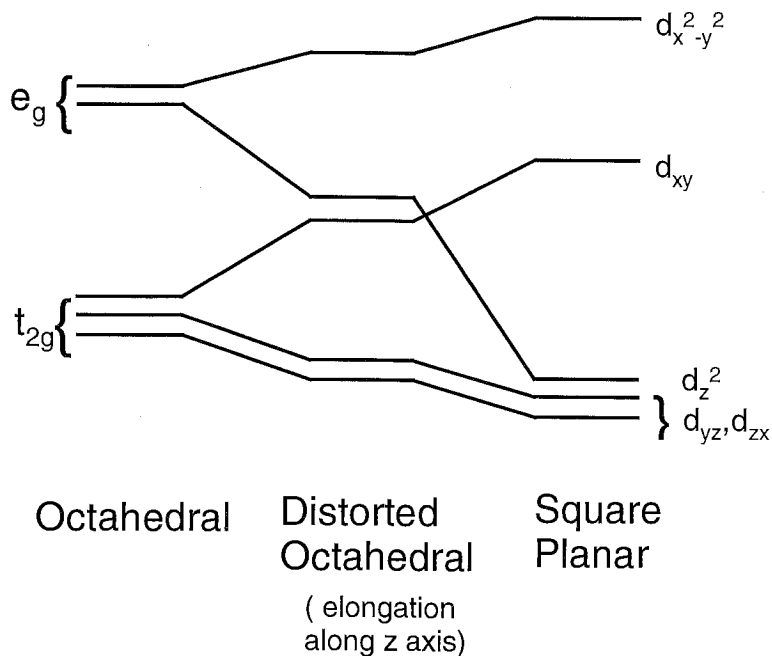


Fig 1.12 – Energy-level diagrams of octahedral and square-planar complexes.<sup>(1)</sup>

Whereas the  $\text{Cu}^{\text{II}}$  ion thus displays a preference for square planar (or at least distorted octahedral) coordination, the  $\text{Cu}^{\text{I}}$  ion, with its closed shell  $d^{10}$  configuration, prefers a coordination geometry that simply minimises the steric repulsion between the ligands, namely tetrahedral. The distorted octahedral conformation is energetically favourable for  $\text{Cu}^{\text{II}}$  ( $d^9$ ) because there are three electrons occupying the two  $e_g$  orbitals, hence two in  $d_{z^2}$  and one in  $d_{x^2-y^2}$ .

## 1.8 Nickel

The +2 is by far the most common oxidation state of this element. However, there is a diverse array of stereochemistries associated with this species. The oxidation states and stereochemistry of nickel are summarized in table 4:

Oxidation State	Coordination number	Geometry	Examples
Ni <sup>0</sup>	4	tetrahedral	Ni(CO) <sub>4</sub>
Ni <sup>I</sup> , d <sup>9</sup>	4	tetrahedral	Ni(PPh <sub>3</sub> ) <sub>3</sub> Br
Ni <sup>II</sup> , d <sup>8</sup>	3	trigonal planar	[Ni(NPh <sub>2</sub> ) <sub>3</sub> ]
	4	square	[Ni(CN) <sub>4</sub> ] <sup>2-</sup>
	4	tetrahedral	[NiCl <sub>4</sub> ] <sup>2-</sup>
	5	<i>sp</i>	BaNiS
	5	<i>tbp</i>	[Ni(CN) <sub>5</sub> ] <sup>3-</sup>
Ni <sup>III</sup> , d <sup>7</sup>	6	octahedral	NiO
	6	trigonal prism	NiAs
	6	distorted octahedral	[NiF <sub>6</sub> ] <sup>3-</sup>
Ni <sup>IV</sup> , d <sup>6</sup>	6	distorted octahedral	K <sub>2</sub> NiF <sub>6</sub>

Table 4 - Oxidation states and stereochemistry of nickel.<sup>(1)</sup>

Nickel(II) forms a large number of complexes encompassing coordination number 4,5 and 6 and all the main structural types, e.g., octahedral, trigonal bipyramidal, square pyramidal, tetrahedral and square planar. The maximum coordination number is 6. A considerable number of neutral ligands, especially amines, displace some or all of the water molecules in the octahedral [Ni(H<sub>2</sub>O)<sub>6</sub>]<sup>2+</sup> ion to form complexes such as *trans*-[Ni(H<sub>2</sub>O)<sub>2</sub>(NH<sub>3</sub>)<sub>4</sub>](NO<sub>3</sub>)<sub>2</sub>, [Ni(NH<sub>3</sub>)<sub>6</sub>](ClO)<sub>2</sub> and Ni(en)<sub>3</sub>SO<sub>4</sub> etc. Such amine complexes

characteristically have blue or purple colours in contrast to the bright green colour of the hexaquo nickel ion.

The relation between the different conformations can be explained with the Crystal Field Approach (as for copper), but in the case of nickel it is interesting to note that square planar nickel is *diamagnetic* (low spin state), whereas it is *paramagnetic* when the geometry is octahedral or tetrahedral (figure 1.13).

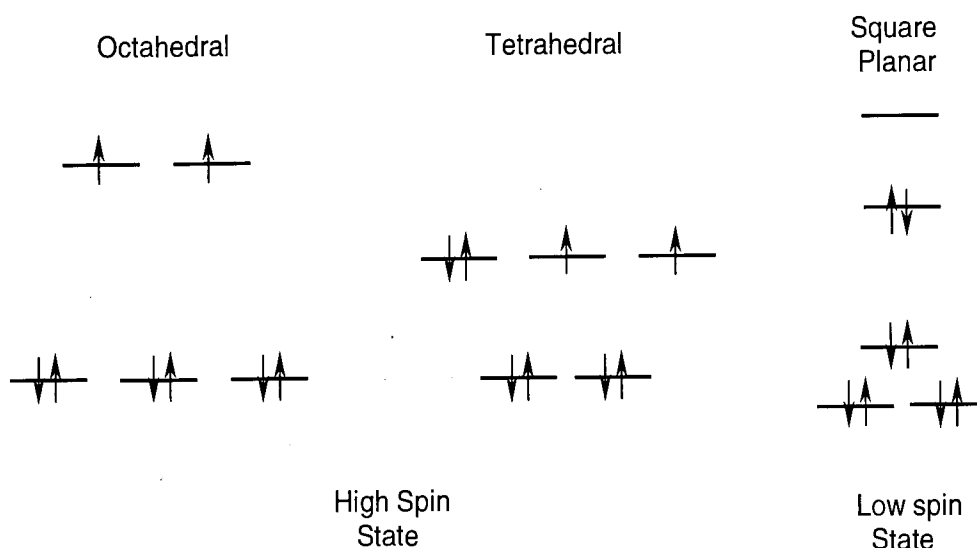


Fig. 1.13 – Diagrams showing how nickel(II) may be paramagnetic (containing unpaired electrons – octahedral and tetrahedral) or diamagnetic (all electrons paired – square planar).

## 1.9 Lanthanides

### 1.9.1 Introduction

In 1788 a new black mineral was found in an old mine pit near Ytterby (Sweden) and named “ytterbyte”. Six years later Gadolin obtained a new element, yttrium, from this mineral.<sup>(IX)</sup> Over the following 110 years, after painstaking studies, 14 other elements were eventually isolated from this material and from a second, *ceria*, discovered around the same time. In the early years of the 20<sup>th</sup> century they were shown to form the series of elements arising from the progressive filling-up of the *4f* electron sub-shell.

One element was missing until its artificial synthesis in 1947;<sup>(IX)</sup> all isotopes of promethium are unstable with short half-lives. Only with the advent of efficient separation methods towards the end of the Second World War was it possible for investigation of the chemistry of the lanthanides to begin in earnest.

There is a very strong similarity in the chemical properties of the lanthanides (which accounted for the long period of time it took for the elements to be separated and isolated). This is largely due to the fact that the main oxidation state in each case (indeed the only oxidation state for some) is the +3, and also due to the rather similar radii of the +3 ions of all the elements. The coordination number of  $\text{Ln}^{3+}$  cations has been found to have values from 3 to 12, but usually high coordination numbers are favoured (typically 8-12) and apparently limited only by steric effects. The well-defined coordination geometries typical of transition metal ions are not found, since bonding is primarily

electrostatic. The  $4f$  orbitals, with their small radial extensions, are too contracted to become significantly involved in bonding.

## 1.9.2 Cyclen and lanthanide complexation

In forming complexes, the lanthanide(III) cations behave as typical hard acids and interact preferentially with hard bases such as fluoride and oxygen rather than with softer bases such as sulphur or phosphorus. Although lanthanide interaction with softer donors can be achieved in organic solvents of low solvating power, in aqueous solutions, the soft base sites can rarely compete with water. The effect of charge is particularly important: the high charge density of the  $\text{Ln}^{3+}$  cations favours complexation by polyanionic ligands owing to a large electrostatic contribution to the binding. Interaction between  $\text{Ln}^{3+}$  and nitrogen donor sites occurs in aqueous solution when ligands such as the aminopolycarboxylates are used (for example ethylenediaminetetraacetic acid, EDTA, figure 1.14). In these complexes, it is likely that the  $\text{Ln}^{3+}$ -carboxylate interactions produce sufficient dehydration of the lanthanide cation that the amino group can interact and compete effectively with any remaining hydration water. Related to the aminopolycarboxylic acids are the macrocyclic analogues such as DOTA (1,4,7,10-tetraazacyclododecane- $\text{N}^{\text{I}}$ - $\text{N}^{\text{II}}$ - $\text{N}^{\text{III}}$ -tetraacetate, figure 1.14).<sup>(X)</sup>

Ligands such as DOTA form complexes of exceptionally high thermodynamic stability, with lanthanide(III) cations;  $K_a$  is typically in excess of  $10^{22}$ .<sup>(IX)</sup> The enhanced thermodynamic stability of these complexes may be attributed to a “macrocyclic effect”, over and above the “chelate effect” associated with the simultaneous formation of eight

chelate rings.<sup>(25,29,30,31)</sup> Moreover, the complexes also have outstanding *kinetic* stability, in contrast to those of the acyclic EDTA ligand. Kinetic inertness results from efficient shielding of the metal ion from attack by water, as hydration is usually necessary to cause decomplexation. This protection from hydration is closely related to the cavity size and rigidity of the aza ring. From both points of view, cyclen-based systems such as DOTA seem to offer optimal stability.

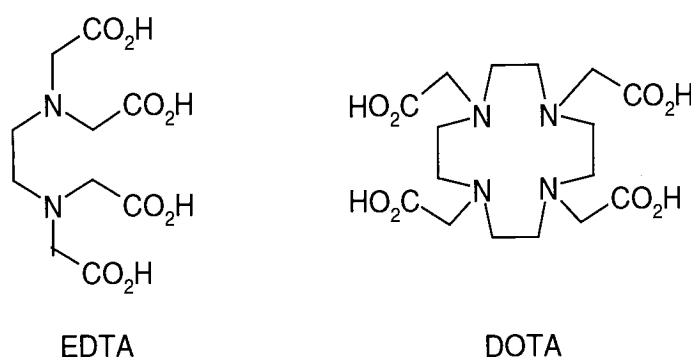


Figure 1.14 – EDTA and DOTA.

### 1.9.3 Lanthanide excited states and luminescence

The  $4f^N$  configuration of a lanthanide ion gives rise to a large number of states, whose energies are determined by a combination of interelectronic repulsions, spin orbit coupling and the ligand field. Owing to the small radial extensions of the  $4f$  orbitals, the ligand field is very small. This has three important implications for the spectra of lanthanide ions in solution. Firstly, in contrast to the broad  $d-d$  absorption bands of the transition elements, the  $f-f$  bands of the lanthanides in solids and in solution are almost as narrow as they are for the gaseous ions. Secondly, compared to the  $d-d$  bands, the  $f-f$  bands are perturbed much less by complexation, so that ligand field splitting is very

small. This means that the energy levels of a given lanthanide are effectively independent of the identity of the ligand. This is in complete contrast to the transition metals, where the energy of absorption (e.g., the colours) is so dependent on the ligand. The third point is that transitions between levels within the  $4f$  shell are forbidden by the parity selection rule, which results in weak intensities, therefore very low extinction coefficients in the absorbance spectra.

Under favourable conditions, many of the lanthanide(III) ions are able to exhibit long-lived luminescence following excitation into higher electronic states. The long natural lifetimes are again a consequence of the spin-forbidden nature of the  $f-f$  transitions. In the solid state, the competition from other non-radiative deactivation processes is small and the phenomenon is often observed. On the other hand, in solution, and especially in water<sup>(32,33)</sup>, the presence of other highly competitive non-radiative deactivation pathways often prohibits the observation of intense, long-lived emission.

The  $\text{H}_2\text{O}$ - $\text{D}_2\text{O}$  solvent system is particularly convenient to investigate the behaviour of lanthanides in aqueous solution since the substitution of  $\text{D}_2\text{O}$  for  $\text{H}_2\text{O}$  has been shown to exert no change in the absorption spectrum of  $\text{Ln}^{3+}$  ions.<sup>(34,35,36)</sup> Thus, any changes in luminescence intensity will reflect the effect of isotopic substitution on the *emissive* state.

In the 1960s it was shown that the luminescence of  $\text{Eu}^{3+}$  and  $\text{Tb}^{3+}$  was more intense in  $\text{D}_2\text{O}$  than in  $\text{H}_2\text{O}$ .<sup>(32,33,36)</sup> Lifetimes were found to be about an order of magnitude higher in  $\text{D}_2\text{O}$ . It is now well established that weak vibronic coupling of Ln(III) ion excited states with the OH oscillators of coordinated water molecules provides a facile pathway for radiationless deactivation of Ln(III) ions. Energy transfer into O-D vibrations is less



efficient than for O-H, owing to poorer Franck-Condon overlap with the higher vibrational states, and this gives rise to the observed enhancement of the luminescence intensity in D<sub>2</sub>O.

Keeping in mind this effect of the OH oscillator on the lanthanide ions, it becomes clear that only three lanthanides are likely to have especially long lifetimes in aqueous solution, namely europium, gadolinium and terbium, as these have large energy gaps between one of their excited states and the ground state.

The flanking elements, samarium and dysprosium, suffer from much more efficient deactivation by O-H or O-D oscillators, owing to the small energy gaps between their emissive and lower states.<sup>(37)</sup> The remaining ions (Pr, Nd, Ho, Er, Yb) have energy gaps between the emitting level and the next lower level of less than 6500 cm<sup>-1</sup> resulting in only weak luminescence in H<sub>2</sub>O or D<sub>2</sub>O (figure 1.15) in the near infra-red, which may be very difficult to detect.

For gadolinium, the situation is reversed: in water, OH oscillator de-excitation does not occur because the gap between the lowest excited and ground states is too large; in fact substitution of D<sub>2</sub>O has no detectable effect.<sup>(36,37)</sup> On this basis, Gd(III) would appear to be an ideal candidate for use as a luminescent probe in aqueous solution. Unfortunately, for gadolinium the emission is in the UV region, at a wavelength unsuitable for practical applications (312 nm).

On the other hand, emission from <sup>5</sup>D<sub>0</sub> of Eu<sup>3+</sup> and from <sup>5</sup>D<sub>4</sub> of Tb<sup>3+</sup> occurs in the visible region and so these are the elements which continue to receive the most attention.



water molecules,  $n$ , is given, with an estimated uncertainty of 0.5, by equation (1) where  $\tau_{\text{H}_2\text{O}}$  and  $\tau_{\text{D}_2\text{O}}$  are the experimental excited-state lifetimes (in ms) in  $\text{H}_2\text{O}$  and  $\text{D}_2\text{O}$  solutions and  $q$  is 1.05 and 4.2 for the  $\text{Eu}^{3+}$  and  $\text{Tb}^{3+}$  compounds, respectively.

$$n = q(1/\tau_{\text{H}_2\text{O}} - 1/\tau_{\text{D}_2\text{O}}) \quad (1)$$

This expression has been modified recently to account for the smaller effect of N-H and C-H oscillators and of closely diffusing but non-coordinated water molecules.<sup>(40)</sup> Thus, lifetime measurements in  $\text{H}_2\text{O}$  and  $\text{D}_2\text{O}$  may be used to provide an estimate of the hydration state of lanthanide complexes.

#### 1.9.4 Photo-excitation of lanthanide ions

It was noted earlier that the absorption bands of lanthanide ions in the visible and UV spectral region generally have very small extinction coefficients. Consequently, the excited states are not readily populated by conventional sources of light. The advent of powerful tunable lasers operating in either a continuous or a pulsed mode has prompted new interest in luminescent probes of which the lanthanides are one class. These lasers provide a high level of spectral discrimination as they generate light with very narrow bandwidths (typically  $<0.02$  nm), making narrow-line lanthanide trivalent ions ideal candidates for use as luminescent probes in this way.

Thus, the highly luminescent  $\text{Eu(III)}$  and  $\text{Tb(III)}$  ions may be excited in the visible part of the spectrum by commercially available lasers, e.g. around 580 and 488 nm, using a

rhodamine dye laser or argon ion laser, respectively. In this way, the high selectivity of the laser light and its high intensity, coupled with the high sensitivity offered by photomultiplier tubes, may largely compensate for the disadvantage of the low extinction coefficients of the lanthanide ions.

Nevertheless, a good deal of research has been focused on means by which the “effective” absorption coefficient of the lanthanide ion may be increased through binding to a ligand incorporating an “antenna” group.<sup>(41,42,43,44,45)</sup> In this case, “photosensitised” emission may be achieved, proceeding via an absorption - energy transfer - emission sequence and involving distinct absorbing (ligand, light collector or “antenna”) and emitting (metal ion) components (figure 1.16).

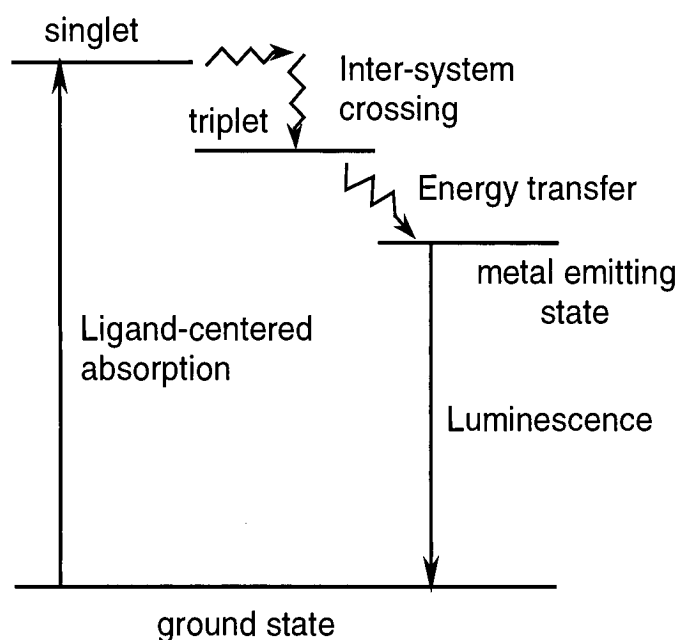


Figure 1.16 – Schematic representation of the antenna effect involving a light-absorbing or chromophore-appended ligand and the emitting metal subunits.

The “antenna” is a group (here the ligand), which absorbs strongly and transfers its excitation energy to the metal, which thereby becomes excited to its emissive state. If the

antenna has a high extinction coefficient and the energy transfer process is efficient, then the effective molar absorption coefficient of the metal is vastly increased and intense luminescence may result following excitation by conventional light sources.

Most studies have revealed that the energy transfer occurs primarily from the triplet state of the sensitiser.<sup>(VIII)</sup> In this case, the quantities that contribute to the overall quantum yield of luminescence,  $\Phi_{\text{lum}}$ , are (i) the quantum yield of triplet formation,  $\Phi_{\text{T}}$ , (ii) the efficiency of the ligand-to-metal energy transfer,  $\eta_{\text{ET}}$ , and (iii) the efficiency of the metal-centred luminescence,  $\eta_{\text{Ln}}$ . It is evident from the equation (2) that all three terms play an important role, and an important aim is to optimise each of them, as will be described in chapter 3.

$$\Phi_{\text{lum}} = \Phi_{\text{T}} \eta_{\text{ET}} \eta_{\text{Ln}} \quad (2)^{\text{(VIII)}}$$

### 1.9.5 Applications of lanthanide luminescence

Over the past 35 years, luminescent lanthanide probes have been applied in many different fields (for example, solid state chemistry, coordination chemistry in solution, biochemistry and clinical chemistry).<sup>(IX and references therein)</sup> In each of these fields, structural and analytical information may be gained on the investigated material. Moreover, the chemical flexibility of the lanthanide ions allows one to utilise them either as substitution probes or as luminescent tags able to be attached to large biological molecules.

In the solid state it is possible to obtain much information using Eu(III) and Tb(III) as substitution probes. From a group theoretical analysis of the observed splitting of the  $f-f$  transitions, the luminescence can provide information on the local site symmetry of the lanthanide ion.<sup>(46)</sup> In solution, analogous studies have included attempts to elucidate the structural features of lanthanide shift reagents<sup>(47)</sup> and the nature of adduct formation with a variety of substrates.<sup>(48,49)</sup>

Lanthanide ions have been used as luminescent chromophores for liquid chromatographic detection of aromatic aldehydes and ketones.<sup>(50)</sup> Wenzel et al. have proposed to make use of the principle of sensitized luminescence for the liquid chromatographic detection of certain nucleotides and nucleic acids.<sup>(51)</sup>

Lanthanide ions occur in only trace amounts in organisms and do not seem to play any biological role. The lanthanide ions may, however, interact with biological materials in specific ways which, along with their unique magnetic and spectroscopic properties, make them very informative substitution probes (for example, for calcium-containing biological material).<sup>(52)</sup> The biological activity of enzymes substituted by lanthanide ions has attracted a good deal of interest.<sup>(53)</sup> The lanthanides have also been employed in numerous investigations in the medicinal sciences: ultrastructure of organs, ion distribution in tissues, function of mitochondria, chemistry of blood, anti-inflammatory agents, drug metabolism, structure and function of muscle tissue, cancer and pituitary function, brain diseases and many others.<sup>(54, IX and references therein)</sup>

Estimates of the distance between energy donors and acceptors in large, complex molecules such as proteins have been made based on measurements of energy transfer

efficiency.<sup>(55,56)</sup> Such measurements assume a Förster dipole-dipole resonance mechanism of energy transfer, the efficiency of which depends on the inverse 6<sup>th</sup> power of the distance between donor and acceptor.<sup>(57)</sup> Both terbium(III) and europium(III) may act as donors to other metal ions (for example, Fe(III) and Co(III) respectively) and this has been used to estimate internal distances.<sup>(58,59)</sup>

The potential use of lanthanide complexes as luminescent labels for analyses in biological media has attracted a great deal of attention.<sup>(60,61)</sup> Many commercially available assays for important biological molecules are based on radio-labelling techniques, where the reporter group is a radioisotope, permitting detection at extremely low levels.<sup>(62)</sup> For sensitivity and specificity, radio-immunological methods for the determination of biological materials in very low concentration are far superior to any other analytical method. However, fluorescence-based methods offer an attractive alternative and a number of systems have been developed which make use of fluorescent reporter groups. The targeting part of the system may be a protein or antibody fragment, raised by immunological methods to recognise selectively and bind strongly to the target biomolecule of interest, in which case the technique is referred to as fluoroimmunoassay.

The same idea is used as well for detecting smaller molecules, for example the use of small peptides<sup>(63)</sup>, nucleic acid strands<sup>(64)</sup> or cyclodextrins.<sup>(65)</sup> In this case, the advantage is that the luminescent compounds may also be used as 'tags' to monitor the fate of molecules within cells.

For applications intended for use in biological media, the decreased intensity produced by the background makes difficult the use of fluorescent labels. Any biological sample,

including serum, contains a large number of fluorescent compounds, which will produce variable levels of background fluorescence. This interferes with the signal from the fluorescent label and cannot be properly corrected.

Luminescent lanthanide complexes may provide an attractive solution to this problem.<sup>(60)</sup> The background fluorescence of biological materials is almost invariably short-lived compared to the long luminescence lifetimes which may be observed for Eu(III) and Tb(III). Thus, a time-resolved detection procedure can be employed. In practice, between the excitation pulse and the measurement of the lanthanide luminescence is set a delay, during which the background fluorescence and scattered light have time to vanish completely (figure 1.17).

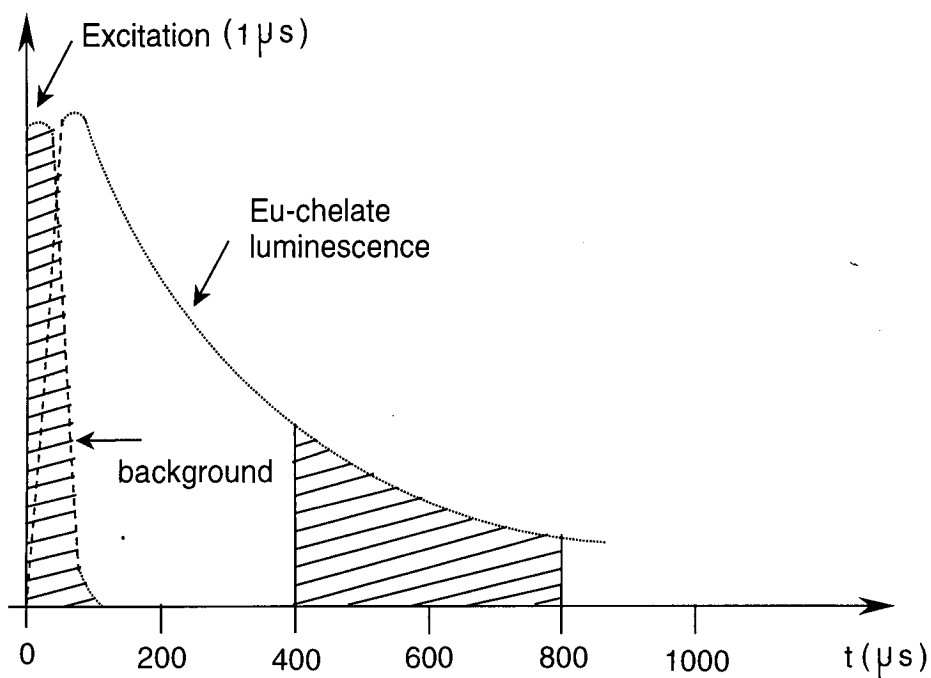


Figure 1.17 – Time resolved detection.

Provided that the luminescence decay is reproducible, then the measured luminescence over the integration time will be directly proportional to the concentration of the analyte.



Theoretically, other molecules with a sufficiently long phosphorescence lifetime could be used in this way. The outstanding advantage of using lanthanide is the possibility in their case of having a long-lived luminescence under *ambient* conditions. In contrast, in organic molecules, deoxygenated solutions and low temperatures are required in order to reduce competitive deactivation processes and allow the observation of long-lived phosphorescence.

## 1.10 References

### 1.10.1 Books

- I. F. A. Cotton, G. Wilkinson, and P. L. Gaus, "*Basic Inorganic Chemistry*", (2<sup>nd</sup> Edition), Wiley, (1987).
- II. F. A. Cotton and G. Wilkinson, "*Advanced Inorganic Chemistry*", (5<sup>th</sup> Edition), Wiley, (1988).
- III. R. T. Morrison and R. N. Boyd, "*Organic Chemistry*", (7<sup>th</sup> edition), Prentice Hall, (1998).
- IV. J. March, "*Advanced organic chemistry: reactions, mechanisms, and structure*", (4<sup>th</sup> Edition), Wiley, (1992).
- V. P. W. Atkins, "*Physical Chemistry*", (4<sup>th</sup> Edition), Oxford Univ. Press, (1990).
- VI. L. F. Lindoy, "*The Chemistry of Macrocyclic Ligand Complexes*", Cambridge University Press, (1989).
- VII. D. Parker, "*Macrocycle Synthesis: A Practical Approach*", (1<sup>st</sup> Edition), Oxford University Press, (1996).
- VIII. Open Univ. Course Team, "*Photochemistry*", The Open Univ. Press, (1982).
- IX. C. G. Bünzli and G. R. Choppin, "*Lanthanide probes in life, chemical and earth sciences*", Elsevier, (1989).
- X. J. A. G. Williams, "*Luminescence behaviour of macrocycle metal complexes*", Ph.D. Thesis, University of Durham, (1995).
- XI. J. L. Atwood, J. E. D. Davies, D. D. MacNicol, F. Vogtle and J. M. Lehn, "*Comprehensive Supramolecular Chemistry*", Pergamon Press, Oxford, 1996, vols 1 and 10.

## 1.10.2 Articles

1. N. A. P. Kane-Maguire, K. C. Wallace and D. B. Miller, *Inorg. Chem.*, **24**, 597, (1985).
2. A. Comparone and T. A. Kaden, *Helv. Chim. Acta*, **81**, 1765, (1998).
3. L. J. McClure and P. J. Ford, *J. Phys. Chem.*, **96**, 6640, (1992).
4. R. Santana da Silva and E. Tfouni, *Inorg. Chem.*, **31**, 3313, (1992).
5. L. Fabbrizzi, M. Licchelli, P. Pallavicini, A. Perotti, A. Taglietti and D. Sacchi, *Chem. Eur. J.*, **1**, 75, (1996).
6. B. Bosnich, C. K. Poon and M. L. Tobe, *Inorg. Chem.*, **4**, 1102, (1965).
7. (a) T. A. Kaden, *Topics Curr. Chem.*, **121**, 157, (1984); (b) A. Buttafava, L. Fabbrizzi, A. Perotti, A. Poggi, G. Poli and B. Seghi, *Inorg. Chem.*, **25**, 1456, (1986).
8. (a) A. Filiali, J. J. Yaouane and H. Handel, *Angew. Chem. Int. Ed. Engl.*, **30**, 560, (1991); (b) H. Bernard, J. J. Yaouane, J. C. Clement, H. des Abbayes and H. Handel, *Tetrahedron Lett.*, **32**, 639, (1991); (c) V. Patinec, J. J. Yaouane, J. C. Clement, H. Handel and H. des Abbayes, *Tetrahedron Lett.*, **36**, 79, (1995).
9. (a) I. Meunier, A. K. Mishra, B. Hanquet, P. Cocolios and R. Guillard, *Can. J. Chem.*, **73**, 685, (1995); (b) M. Studer and T. A. Kaden, *Helv. Chim. Acta*, **69**, 2081, (1986).
10. H. Fensterbank, J. Zhu, D. Riou and C. Larpent, *J. Chem. Soc., Perkin Trans. 1*, 811, (1999).
11. G. W. Watt and P. W. Alexander, *Inorg. Chem.*, **7**, 537, (1968), and references cited.
12. (a) F. Wagner, M. T. Mocella, M. J. D'Aniello, Jr., H. J. Wang and E. K. Barefield, *J. Am. Chem. Soc.*, **96**, 2625, (1974); (b) M. J. D'Aniello, Jr., M. T. Mocella, F. Wagner, E. K. Barefield and I. C. Paul, *J. Am. Chem. Soc.*, **97**, 192, (1975).
13. Z. Kovacs and A. D. Sherry, *Synthesis*, 759, (1997).

14. R. D. Hancock, R. J. Motekaitis, J. Mashishi, I. Cukrowsky, J. H. Reinspies and A. E. Martell, *J. Chem. Soc., Perkin Trans. 2*, 1925, (1996).
15. I. M. Helps, D. Parker, J. R. Morphy and J. Chapman, *Tetrahedron*, **45**, 219, (1989).
16. (a) R. W. Hay, R. Bembi and W. Sommerville, *Inorg. Chim. Acta*, **59**, 147, (1982); (b) L. Cronin, A. R. Mount, S. Parsons and N. Robertson, *J. Chem. Soc., Dalton Trans.*, 1925, (1999).
17. D. A. Tomalia and L. R. Wilson, *United States Patent*, Patent Number 4,517,122, (1985).
18. I. Tabushi, H. Okino and Y. Kuroda, *Tetrahedron Letters*, **48**, 4342, (1976).
19. (a) X. H. Bu, D. L. An, R. H. Zhang, T. Clifford and E. Kimura, *J. Chem. Soc., Dalton Trans.*, 2247, (1998); (b) S. Zhu, F. Kou, H. Lin, C. Lin, M. Lin and Y. Chen, *Inorg. Chem.*, **35**, 5851, (1996).
20. P. J. Davies, M. R. Taylor and K. P. Wainwright, *Chem. Commun.*, 827, (1998).
21. G. Royal, V. Dahaoui-Gindrey, S. Dahaoui, A. Tabard, R. Guilard, P. Pullumbi and C. Lecomte, *Eur. J. Org. Chem.*, 1971, (1998).
22. E. K. Barefield, F. Wagner, A. W. Herlinger and A. R. Dahl, *Inorg. Synth.*, **16**, 220, (1976).
23. E. K. Barefield, F. Wagner and K. D. Hodges, *Inorg. Chem.*, **15**, 1370, (1976).
24. J. J. Christensen, J. Eatough and R. M. Izatt, *Chem. Rev.*, **74**, 351, (1974).
25. D. K. Cabbiness and D. W. Margerum, *J. Am. Chem. Soc.*, **91**, 6540, (1969); (a) F. P. Hinz and D. W. Margerum, *J. Am. Chem. Soc.*, **96**, 4993, (1974); (b) E. Kimura and M. Kodama, *J. Chem. Soc., Chem. Comm.*, 326 and 891, (1974).
26. L. H. Chen and C. S. Chung, *Inorg. Chem.*, **27**, 1880, (1988).
27. R. M. Izatt, J. S. Bradshaw, S. A. Neilson, J. D. Lamb and J. J. Christensen, *Chem. Rev.*, **85**, 271, (1985).

28. L. S. Förster, *Chem. Rev.*, **90**, 331, (1990).
29. G. Schwarzenbach, *Helv. Chim. Acta*, **35**, 2344, (1952).
30. C. S. Chung, *J. Chem. Educ.*, **61**, 1062, (1984).
31. J. J. R. F. da Silva, *J. Chem. Educ.*, **60**, 390, (1983).
32. J. L. Kropp and M. W. Windsor, *J. Chem. Phys.*, **39**, 2769, (1963).
33. J. L. Kropp and M. W. Windsor, *J. Chem. Phys.*, **45**, 761, (1966).
34. P. K. Gallagher, *J. Chem. Phys.*, **43**, 1742, (1965).
35. R. Borkowski, H. Forest and D. Grafstein, *J. Chem. Phys.*, **42**, 2974, (1965).
36. J. L. Kropp and M. W. Windsor, *J. Chem. Phys.*, **42**, 1599, (1965).
37. G. Stein and E. Wurzburg, *J. Chem. Phys.*, **62**, 208, (1975).
38. W. deW. Horrocks, Jr. and D. R. Sudnick, *Science*, **206**, 1194, (1979).
39. (a) W. deW. Horrocks, Jr., G. R. Schmidt, D. R. Sudnick, C. Kittrell and R. A. Bernheim, *J. Am. Chem. Soc.*, **99**, 2378, (1977); (b) W. deW. Horrocks, Jr. and D. R. Sudnick, *Acc. Chem. Res.*, **14**, 384, (1981).
40. A. Beeby, I. M. Clarkson, R. S. Dickins, S. Faulkner, D. Parker, L. Royle, A. S. deSousa, J.A.G. Williams and M. Woods, *J. Chem. Soc., Perkin Trans. 2*, 493, (1999).
41. B. Alpha, J.-M. Lehn and G. Mathis, *Angew. Chem. Int. Ed. Engl.*, **26**, 266, (1987).
42. N. Sabbatini, S. Perathoner, V. Balzani, B. Alpha and J.-M. Lehn, in V. Balzani (Ed.), *"Supramolecular Photochemistry"*, Reidel, Dordrecht, 187, (1987).
43. J.-M. Lehn, in V. Balzani (Ed.), *"Supramolecular Photochemistry"*, Reidel, Dordrecht, 29, (1987).
44. B. Alpha, R. Ballardini, V. Balzani, J.-M. Lehn, S. Perathoner and N. Sabbatini, *Photochem. Photobiol.*, **52**, 299, (1990).
45. V. Balzani and F. Scandola, *"Supramolecular Photochemistry"*, Ellis Horwood: Chichester, 326, (1991).

46. M. C. F. Cunha, H. F. Brito, L. B. Zinner G. Vicenti and A. B. Nascimento, *Coord. Chem. Rev.*, **119**, 1, (1992).
47. C. C. Bryden and C. N. Reilley, *Anal. Chem.*, **54**, 610, (1982).
48. H. G. Brittain and F. S. Richardson, *J. Chem. Soc. Dalton Trans.*, 2253, (1976).
49. (a) H. G. Brittain and F. S. Richardson, *J. Am. Chem. Soc.*, **101**, 1733, (1979); (b) idem, *J. Chem. Soc. Dalton Trans.*, 1187, (1979); (c) idem, *Inorg. Chem.*, **19**, 640, (1980).
50. D. S. Gross and H. Simpkins, *J. Biol. Chem.*, **256**, 9593, (1981).
51. T. J. Wenzel and L. M. Collette, *J. Chromatogr.*, **436**, 299, (1988).
52. R. J. P. Williams, *Quarterly Reviews*, 351, (1970).
53. E. Nioboer, *Struct. Bonding*, **22**, 1, (1975).
54. K. J. Ellis, *Inorg. Perspect. Biol. Med. I*, 101, (1977).
55. J. Bruno, W. deW. Horrocks, Jr. and R. J. Zauhar, *Biochemistry*, **31**, 7016, (1992).
56. W. deW. Horrocks, Jr. and W. E. Collier, *J. Am. Chem. Soc.*, **103**, 2856, (1981).
57. C. R. Cantor and P. R. Schimmel, 'Biophysical Chemistry', W. H. Freeman: San Francisco, Volume 2, (1980).
58. C. F. Meares and J. E. Ledbetter, *Biochemistry*, **16**, 5178, (1977).
59. E. T. O'Keeffe, R. L. Hill and J. E. Bell, *Biochemistry*, **19**, 4954, (1980).
60. I. Hemmila, *Clin. Chem.*, **31**, 359, (review), (1985).
61. E. F. G. Dickson et al., *Photochem. Photobiol.*, **27**, 3, (review), (1995).
62. J. Klein, 'Immunology', Blackwell Scientific ; Boston, Mass., (1990).
63. P. Gottlieb, E. Hazum, E. Tzehoval, M. Feldman, S. Segal and M. Fridkin, *Biochem. Biophys. Res. Comm.*, **119**, 203, (1984).
64. A. Oser, W. K. Roth and G. Valet, *Nucleic Acid Res.*, **16**, 1181, (1988).
65. D. M. Gravett and J. E. Guillet, *J. Am. Chem. Soc.*, **115**, 5970, (1993).

# **CHAPTER 2**

## **CYCLAM**

## 2.1 Introduction

As was shown in Chapter 1 there are several different synthetic pathways to mono- or di-N-substituted cyclams. Some appear preferable, owing to higher yields or ease of handling. We have attempted a number of them, and in this chapter it will be explained which of them worked best and in which conditions. As will become clear, the identity of the pendant groups to be introduced has an important influence in determining the ease of reaction and purification.

Our interest has been focused in particular on the synthesis of hexadentate ligands based on cyclam. The original idea of a system with six nitrogen atoms available to bind a metal was developed primarily in order to have a system ideal to favour the phosphorescence of chromium. The rigidity imposed by the macrocyclic system and the ligand field originated from the six nitrogen atoms are essential characteristics required by a chromium complex in order to be able to display phosphorescence at room temperature. Furthermore, the same ligands were interesting for the complexation of metals such as nickel and copper.

At the beginning of the project very few examples of systems similar to the ones that we had in mind, had been reported in the literature. At that stage of the work, our attention was focused mostly on the synthesis of the three possible isomers of cyclam with two pyridyl units (figure 2.1). While the project was developing, however, many related articles appeared in the literature reporting new, interesting synthetic routes to ligands closely related to those of interest to us, and full advantage has been taken of these new developments during the work.



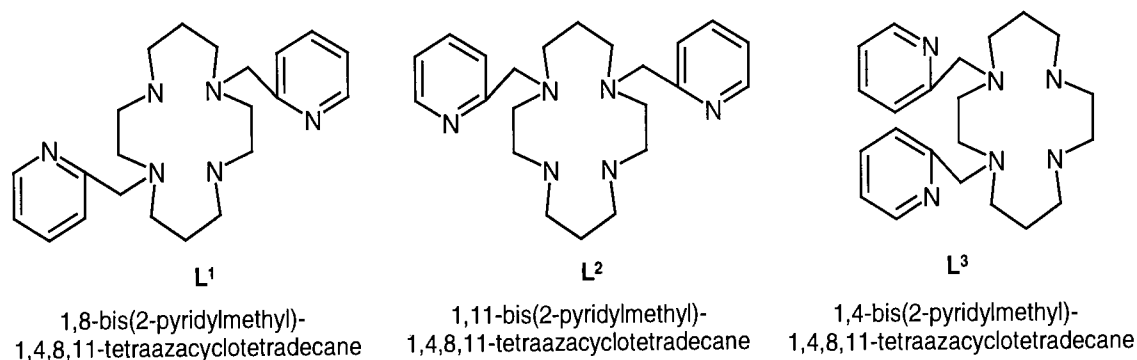


Fig. 2.1 – Ligands  $L^1$ ,  $L^2$  and  $L^3$ .

In this chapter, the synthetic part of the work will be described, and then in the next chapter the metal complexation chemistry will be the main point of discussion, with emphasis on the spectroscopic and structural features of the metal complexes.

## 2.2 Synthesis of di-substituted cyclam using dioxotetraamines

As noted in Chapter 1, [1,8] dioxotetraamine is easily prepared by reaction of an acrylic ester with 1,2-ethylenediamine. The Michael addition reaction was easily effected by mixing the two reactants, without a solvent, and maintaining the temperature between 20° C and 45°C. Reaction times of up to several weeks may be required for the cyclization process to occur, but product formation and separation may be accelerated by dissolving the mixture in water (25% by weight). Normally, the cyclic peptide product, being less soluble than other possible products, precipitates from the reaction medium as it is formed and may be recovered by filtration. However, it was sometimes observed that the compound didn't precipitate, in which case, removing a small amount of water (25%) usually induced precipitation. After washing with cold water, the compound was normally

obtained in high purity. Although the yield was always low (typically 2%), it may be noted that the starting materials are available in large quantities at low cost.

The [5,7] dioxocyclam is commercially available and was used without further purification.

The most recent report of the synthesis of [2,3] dioxotetraamine (originally prepared by Hay et al.<sup>(1)</sup>) involves the addition of a solution of dimethyloxalate and a solution of N,N'-bis(3-aminopropyl)ethylenediamine, both in ethanol, to a solution of refluxing ethanol, dropwise via two peristaltic pumps over a period of 32 hours<sup>(2)</sup>. The reaction conditions were simplified and the yield was improved taking advantage of the fact that the two starting compounds don't react at room temperature. The reaction was achieved by mixing together the two reagents in a dropping funnel to give a homogeneous solution, which was added dropwise to a large volume of refluxing ethanol. In fact, the yield of the reaction was increased by 20%, probably due to the high dilution conditions employed as well as to the fact that the equimolar stoichiometry is always maintained.

The reactions between the dioxocyclams and the following alkylating agents were attempted: 2-picolylylchloride hydrochloride, 2-(bromomethyl)thiophene, methyl iodide and 2-(chloromethyl)pyrene (figure 2.2).

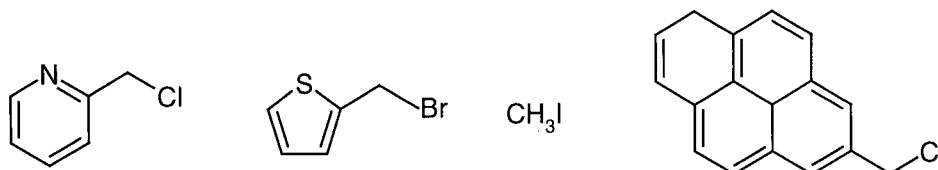


Fig 2.2 -2-Picolylylchloride hydrochloride, 2-(bromomethyl)thiophene, methyl iodide and 2-(chloromethyl)pyrene.

2-(Bromomethyl)thiophene was prepared by the action of  $\text{PBr}_3$  on 2-(hydroxymethyl)thiophene in ether solution at room temperature. The product is unstable, but can be stored for up to about two weeks in the refrigerator. 2-(Chloromethyl)pyrene was obtained in two steps from 2-pyrenecarboxaldehyde which is available commercially. After reduction to the alcohol using sodium borohydride, the alcohol was converted readily to the chloride by stirring with thionyl chloride.

It was possible to obtain di-substituted dioxocyclam ligands by reaction of a solution of the dioxocyclam with two equivalents of alkylating agent, in the presence of excess of sodium carbonate as base, in refluxing acetonitrile (figure 2.3). Sometimes a long time (3/4 weeks) was required for the reaction to occur, in which case the rate of the reaction could be increased by working with an excess of pendant (3 instead of 2 equivalents), the excess being removed during purification by chromatography on silica. Addition of a small amount of catalyst, potassium iodide, was also effective at accelerating the rate of the reaction.

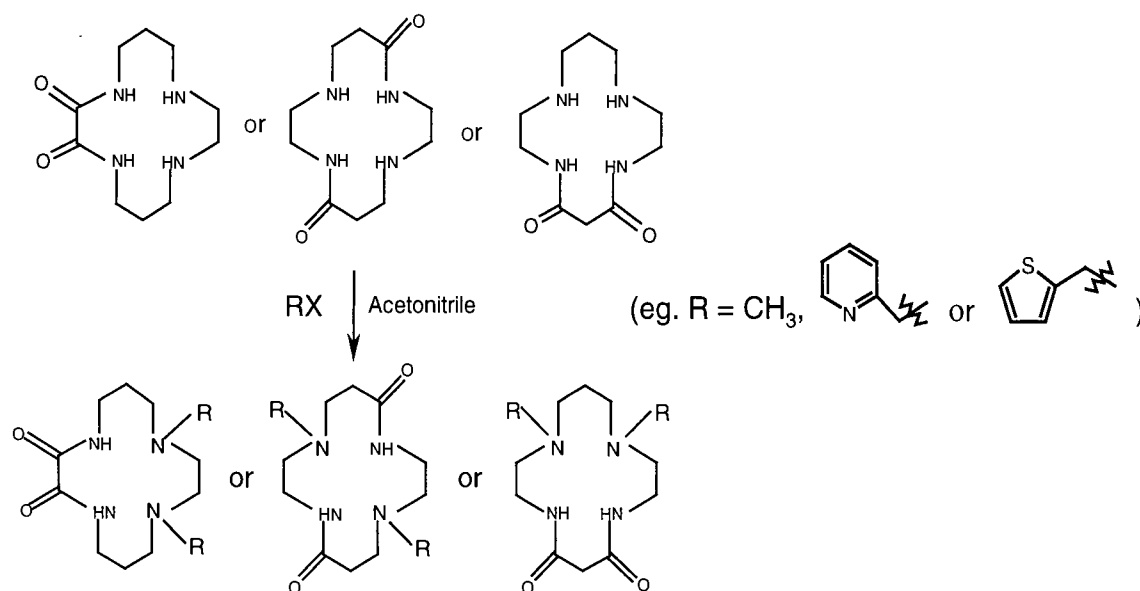


Fig. 2.3 – Synthesis of di-substituted dioxocyclams.

After the reaction, carried out with an excess of alkylating agent, a mixture was obtained, typically of mono- and di-substituted dioxocyclam, and any excess of alkylating agent that had not reacted. Nevertheless, the di-substituted compound almost always represented more than 90% of the yield.

When 2-(chloromethyl)pyrene was used as alkylating agent, the di-N-substituted compound could not be obtained. The main problem in this case was related to the solubility: a highly insoluble precipitate was always obtained. Using deuterated methanol and a small amount of trifluoroacetic acid, it was possible to solubilise the precipitate sufficiently to obtain a  $^1\text{H}$  NMR spectrum. This, together with electrospray mass spectra, showed the precipitate to consist of a mixture of the mono-substituted dioxocyclam (in low yield) and undefined side-products. Because of these problems, the synthesis of pyrene-substituted systems was not pursued further.

Otherwise, purification by column chromatography on silica was successful in each case. Subsequent reduction of the amides was accomplished by reaction with borane-THF at reflux for 4 days. The reduction worked very well and with good yield when the pendants were 2-(methyl)thiophene and methyl groups, but the necessary extraction from basic aqueous solution gave low yields (6/7% with 5,12-dioxocyclam and 1% with 5,7-dioxocyclam) when the substituent was the (2'-methylpyridyl) group.

From the IR spectrum, we were confident that in the case of the picolyl derivatives too, the compounds had indeed been reduced, because the signal of the carbonyl group had disappeared. A possible explanation for the lack of success in extracting the compound is the formation of a complex between the boron and the nitrogens (pH=14) of our ligand

(figure 2.4). There is some precedent for such an explanation from the chemistry of triazacyclononanes<sup>(3)</sup>. Thus, in order to expel the boron from the ring, an acidic pH would be required to protonate the nitrogen atoms, but the protonated compound would then not be soluble for extraction into the organic solvent.

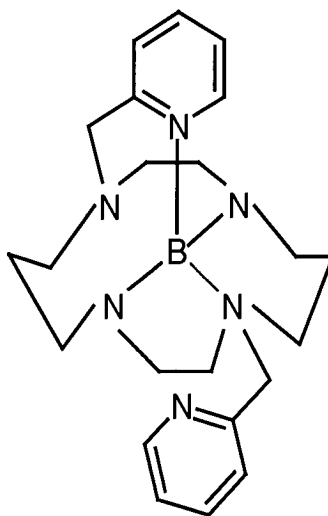


*Fig. 2.4 – Possible complex between boron and di-substituted dioxocyclam after reduction.*

Although yields were much more satisfactory in the case of the thiophene compounds, presumably because the thiophene sulfur is a very poor donor to boron, a curious side reaction occurred in the reduction of the 1,11-bis(2-methylthiophene)-1,4,8,11-tetraazacyclotetradecane-5,7-dione derivative. Whereas 1,8-bis(2-methylthiophene)-1,4,8,11-tetraazacyclotetradecane was obtained in high purity after reduction of the dioxo parent, the 1,11-bis(2-methylthiophene)-1,4,8,11-tetraazacyclotetradecane was contaminated with mono-substituted compound (10%), despite the fact that the material employed in the reduction was exclusively the di-substituted compound.

This point will be returned to in the next section, where the preparation of the same compound is reported using a different synthetic pathway. An alternative reduction of the amides using  $\text{LiAlH}_4$  proved unsuccessful.

### 2.3 Synthesis of 1,11-isomer, L<sup>2</sup>, and analogues using the formamidineium salt

The use of the formamidineium salt of cyclam for the simultaneous protection of 1,5 related nitrogens was discussed in Chapter 1.

Reaction of cyclam with an equimolar amount of the dimethyl acetal of DMF in refluxing chloroform for a period of 48 h gave an 80% yield of the formamidineium salt, in line with a recent literature report<sup>(4)</sup>. The compound was dried under vacuum and alkylated by reaction with two equivalents of the appropriate alkylating agent (2-picolychloride hydrochloride, 2-(bromomethyl)thiophene and methyl iodide have been used), in the presence of excess of sodium carbonate and some crystals of potassium iodide in refluxing acetonitrile. The use of an excess of alkylating agent led to improved yields and shorter reaction times.

Purification was effected by chromatography on silica gel, with yields of up to 80%, after which the free base could be obtained upon treatment with 10 M sodium hydroxide for some days at 80/100°C, with a yield of about 50%.

This last step worked very well when methyl iodide and picolyl chloride were the pendants, but when the 2-(bromomethyl)thiophene was used, the final compound was a mixture of the di-substituted (90%) and the mono-substituted (10%) compound (figure. 2.5).

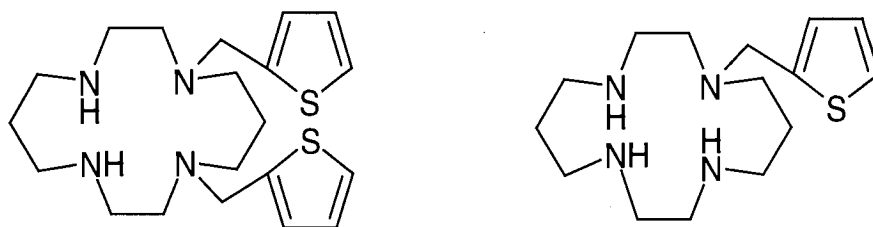


Fig 2.5 – Mono and di-substituted cyclam derivatives.

The compound prior to the hydrolysis step was pure by  $^1\text{H}$  NMR, so one of the two substituents must have been cleaved when the basic aqueous solution was used to remove the internal bridge.

One explanation could be that in this last case high temperatures were used, 140/150°C, because the removal of the internal bridge was very difficult, in fact it wasn't possible to convert all the compound to the free base.

On the other hand, we can argue that under the basic conditions employed, the di-substituted compound is not stable and undergoes degradation. This conclusion is supported by the fact that the same problem arose during the reduction of the di-substituted dioxocyclam and, notably, that, too, involved quite strongly basic conditions to allow extraction.

It is not clear why the compound degrades, but it is possible that the loss of one of the thiophene substituents is favoured by the proximity of the second, given that further decomposition to cyclam itself was not observed and also that the 1,8-disubstituted compound, in which the substituents are further apart, showed no such degradation.

## 2.4 Synthesis of 1,8-isomer, L<sup>1</sup>, using a tricyclic intermediate

During our attempts to prepare 1,8-bis(2-pyridylmethyl)-1,4,8,11-tetraazacyclotetradecane (L<sup>1</sup>), a report appeared on a facile route to 1,8-disubstituted compounds via a tricyclic intermediate, 1,4,8,11-tetraazatricyclo[9.3.1.1<sup>4,8</sup>]hexadecane<sup>(5)</sup>. This method was employed successfully for the desired compound (figure 2.6).

The first step was the reaction between cyclam and two equivalents of formaldehyde in water at 0°C. Use of an excess of formaldehyde ensures that the reaction proceeds quantitatively.

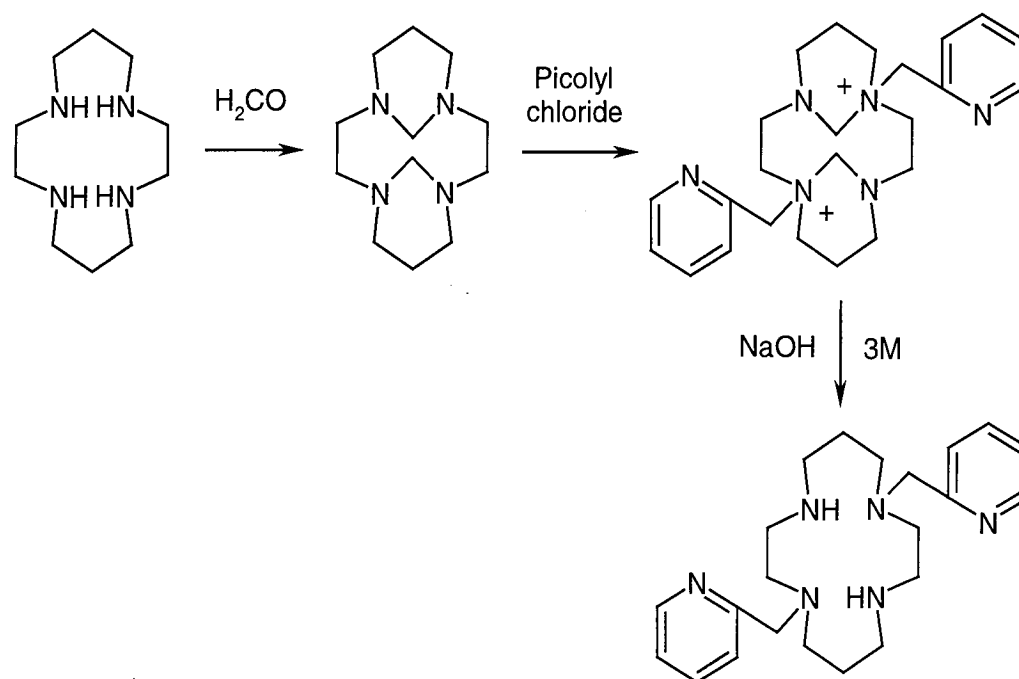


Fig 2.6 – Synthesis of 1,8-bis(picolyl)-1,4,8,11-tetraazacyclotetradecane.

The presence of the methylenic bridges was confirmed by <sup>1</sup>H NMR and the data showed a *trans* conformation for the two methylenic bridges. In the second step, the ligand was dissolved in acetonitrile and the picolyl chloride was rapidly added. The latter is available as the hydrochloride salt, and was first converted to the free amine by deprotonation in



aqueous NaOH solution, followed by extraction into  $\text{CH}_2\text{Cl}_2$ , to give an unstable red liquid. The reaction was rather slow, 3/4 weeks using 2 equivalents of alkylating agent, but the rate of the reaction was enhanced through the use of four equivalents of alkylating agent. After seven days the new compound, insoluble in acetonitrile, was easily isolated by filtration and washed with acetonitrile to remove the excess of picolyl chloride.

High yields were obtained and no *cis*-disubstituted macrocycle was detected. This indicated a strong selectivity for the *trans* disubstitution, the reasons for which have been discussed<sup>(5)</sup>.

The final *trans*-disubstituted cyclam was then easily formed after basic hydrolysis and extraction. The overall yield after all three steps was about 50%. This reaction sequence is particularly attractive, owing to the ease of separation of reagents and products at each stage, which arises from their very different solubilities.

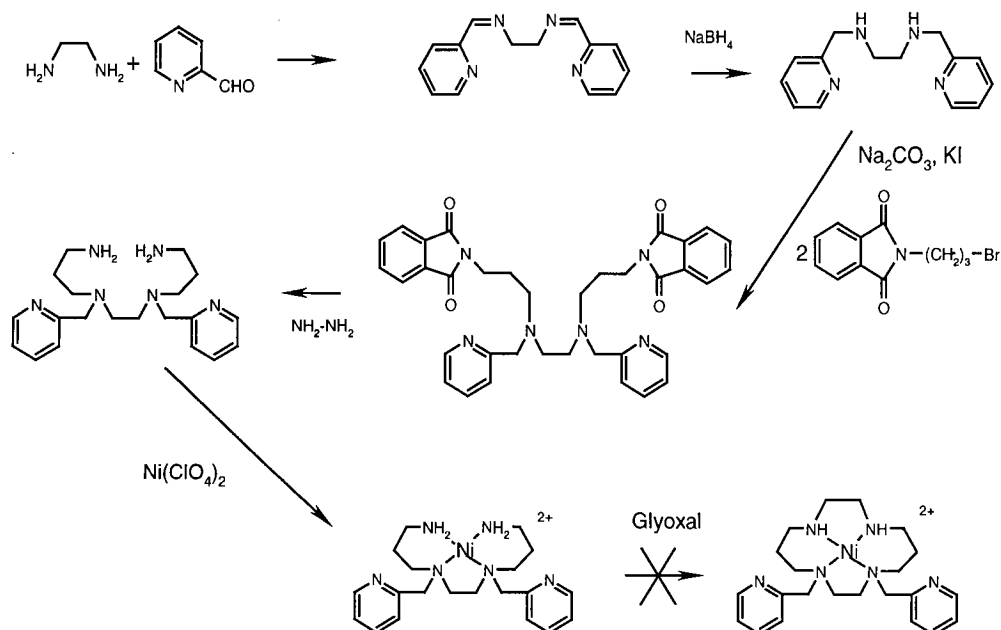
## 2.5 Attempted synthesis of the 1,4-isomer, $\text{L}^3$ , using a template reaction

The cyclisation reactions that are used to generate medium-ring and large-ring polyamines suffer from an unfavourable entropy term to the overall free energy change. Indeed, this effect often limits the temperature at which the reaction can be carried out, because heating gives rise to an even more unfavourable  $T\Delta S$  term, and competing reactions (e.g. oligomerisation) may be favoured at the expense of the desired cyclisation. Such effects may be overcome to a large extent if an ion can be used to act as a template for the cyclisation step<sup>(6,7)</sup>. In fact, the usual synthesis of cyclam itself makes use of such

a procedure<sup>(8)</sup>, where nickel is used as a templating ion in favouring cyclisation over polymerisation.

Using this metal ion assisted cyclisation procedure, it has also proved possible to synthesise some 1,4-di-substituted derivatives of cyclam in good yields<sup>(9)</sup>. Thus, the following reaction scheme (scheme 1) was planned to obtain the third of the three possible isomers of the bis-(2-pyridylmethyl) cyclam, the 1,4 derivative.

The di-imine obtained upon condensation of ethylenediamine with 2 equivalents of pyridine-2-carboxaldehyde was reduced with sodium borohydride and the amine so obtained was alkylated with N-(3-bromopropyl)phthalimide. The overall yield from the first three steps was 70%. The phthalimide protecting group was then cleaved by treatment with hydrazine<sup>(10)</sup>, in absolute ethanol.



Scheme 1.

The four steps together offered a convenient and high-yielding route to the desired open-chain ligand, 5,8-bis(2-pyridylmethyl)-1,5,8,12-tetraazadodecane ( $L^6$ ), ready for cyclisation.

The templated cyclisation was attempted by mixing an equimolar amount of nickel perchlorate with the ligand in water. As introduced in the first chapter, one of the preferred coordination geometries of nickel(II) is the square-planar. In related complexes, in fact, this is the conformation that is found, and so a complex like that shown in figure 2.7 was anticipated. By analogy with the synthetic route to cyclam<sup>(8)</sup> the nickel complex was expected to react with glyoxal in aqueous solution to give an imine which could then be reduced with sodium borohydride (figure 2.7).

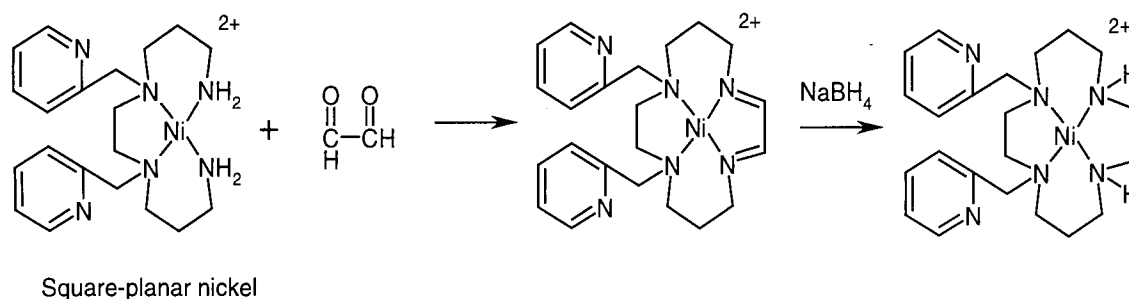


Figure 2.7 – Template reaction.

All four steps were carried out following carefully the literature procedures for non-substituted tetra-amine analogues, but mass spectra and NMR evidence indicated that only a trace of the desired compound had been formed. Repeated attempts led to the same result. Other examples of template reactions have made use of copper(II) in place of nickel(II). However, the cyclisation was equally unsatisfactory with copper(II).

The likely explanation for the lack of success of the metal-templated cyclisation became clear when crystals from the copper template reaction, suitable for X-ray analysis, were obtained (figure 2.8). It is evident from this structure that the copper does not lie in the centre of the tetraazadodecane, because of the presence of two nitrogens on the pendant arms. In this ligand there are 6 nitrogen atoms that can bind the metal and unfortunately this led to a 2:1 complex (M:L) inhibiting the formation of the required template for cyclisation. As there seemed to be no way to overcome this problem, a different synthetic route had to be considered.

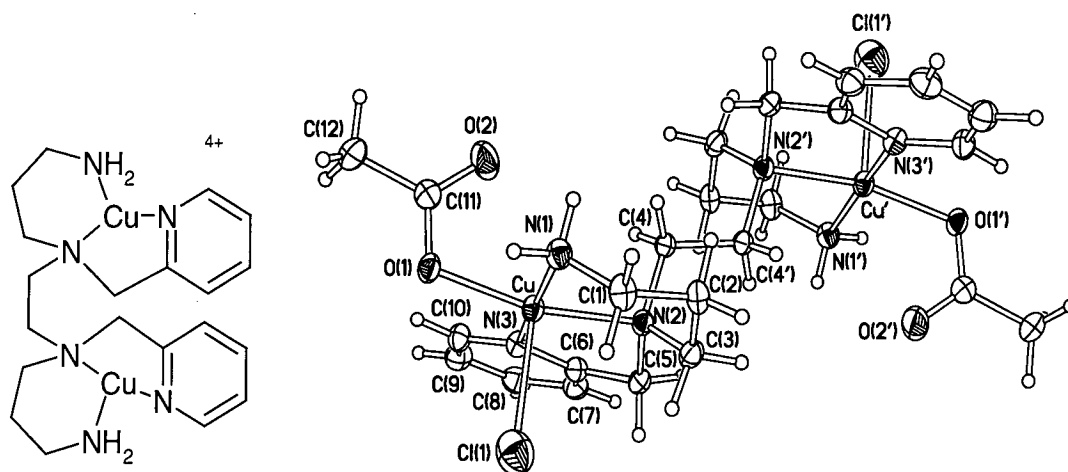


Figure 2.8 – Molecular structure of  $[L^6(CuClOAc)_2]$ .

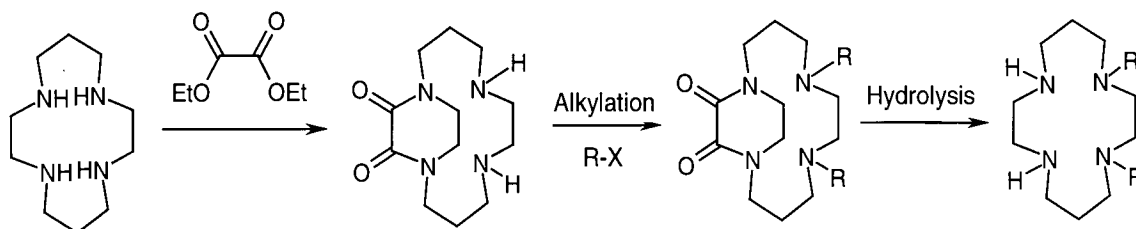
Table 1 - Selected bond lengths (Å) and angles (°) for the copper(II) complex of 5,8-bis(2-pyridylmethyl)-1,5,8,12-tetraazadodecane.

Cu–O(1)	1.985(3)	Cu–N(2)	2.090(3)
Cu–N(1)	2.005(4)	Cu–Cl(1)	2.504(2)
Cu–N(3)	2.014(3)		
O(1)–Cu–N(1)	90.17(13)	N(3)–Cu–N(2)	82.70(13)
O(1)–Cu–N(3)	91.94(13)	O(1)–Cu–Cl(1)	99.98(10)
N(1)–Cu–N(3)	170.73(14)	N(1)–Cu–Cl(1)	96.75(11)
O(1)–Cu–N(2)	163.55(13)	N(3)–Cu–Cl(1)	91.77(11)
N(1)–Cu–N(2)	92.80(14)	N(2)–Cu–Cl(1)	95.73(10)

## 2.6 Synthesis of the 1,4-isomer, L<sup>3</sup>, using an oxamide intermediate

The low yield obtained with the previous reaction necessitated the exploration of a different synthetic route. Again, an elegant solution appeared in the literature while this work was in progress: Handel et al. <sup>(11)</sup> introduced a new general strategy for the regiospecific synthesis of 1,4 disubstituted derivatives using oxamides as intermediates.

Acylation of cyclam with diethyl oxalate leads to cyclam-oxamide, which selectively converts a 1,4-related pair of amino nitrogen atoms into amide nitrogen atoms. This leaves the remaining amino nitrogen atoms free to react with an alkylating agent. Subsequently, the amide can be hydrolysed to give the desired 1,4 disubstituted compound (Scheme 2).



*Scheme 2.*

In practice, in the first step cyclam is reacted with an equimolar amount of diethyl oxalate in dry ethanol, at reflux for 12 hours. Good yields require strictly anhydrous conditions. Although a high yield is reported (82%)<sup>(11)</sup>, the maximum yield obtained in our hands was 48%, despite distillation of the starting compounds, and following carefully the suggested procedure.

In our case, the reaction was also consistently much slower than reported, but results were improved upon introducing some modifications. Firstly, a substantially longer reaction time was employed, then the diethyl oxalate was replaced with the more reactive dimethyl oxalate, and finally an excess of oxalate was used (cyclam:dimethyloxalate, 1:1.5). Eventually, the best yield obtained was 67%. Subsequent alkylation with picolyl chloride was carried out under the usual conditions, after which hydrolysis with aqueous sodium hydroxide led to the desired compound in high yield.

In this way, all three possible isomers of cyclam di-N-substituted with the 2-(pyridylmethyl) group, namely the 1,4/1,8/1,11-derivatives, were synthesised.

## 2.7 Mono-substitution of cyclam

One of the areas of interest of this work was the preparation of luminescent chromium(III) complexes of cyclam-based ligands incorporating additional pendants to act as sensitisers of the metal excited state, or as functionality for targeting other ionic species in solution.

It is well-known that efficient luminescence of Cr-cyclam at room temperature requires a *trans* conformation with the metal in the plane formed by the four nitrogen atoms.<sup>(12)</sup> However, results on some of the ligands described in the previous sections showed that the required isomerisation of the initially formed *cis* chromium complexes to the *trans* forms, was completely inhibited by the additional substituents (see section on chromium in the next chapter).

Hence, attention was turned to some selected *mono*-substituted cyclams, in the hope that they would allow the adoption of the *trans* conformation with chromium(III). The substituents investigated, containing benzophenone and 8-hydroxyquinoline functionality, were chosen owing to their potential interest with regard to the excited state properties of chromium(III) (see section on chromium in the next chapter).

### 2.7.1 Mono-substitution of cyclam using a Michael acceptor

The recently reported chemoselective addition of a Michael acceptor for the synthesis of mono-substituted azamacrocycles was described in the introduction.<sup>(13)</sup>

The possibility of applying this method to the introduction of a benzophenone substituent onto the cyclam ring was investigated, for which N-(4-benzophenone)acrylamide was required. This was prepared by the reaction of 4-aminobenzophenone with acryloyl chloride at 0°C, in the presence of triethylamine as a base (figure 2.9).

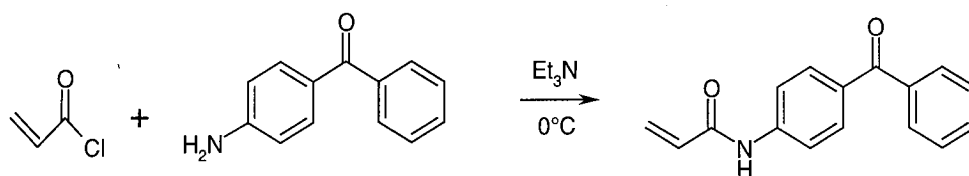


Fig. 2.9 – Synthesis of the Michael acceptor containing benzophenone moiety.

This new Michael acceptor was reacted with cyclam (figure 2.10) following the procedure described in the introduction (in chloroform, in the presence of one equivalent of toluene-*p*-sulfonic acid).

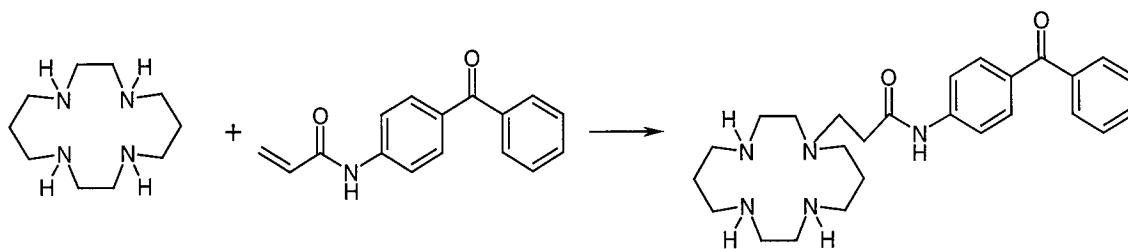


Fig. 2.10 – Synthesis of mono-substituted cyclam by reaction with a Michael acceptor.

Separation of the compound was effected by chromatography on silica gel using quite polar conditions [ $\text{CHCl}_3/\text{MeOH}/\text{NH}_3(\text{aq})$ , 10/4/1], due to the presence of three basic nitrogen atoms in the ligand. The yield was definitely satisfactory (84%).

### 2.7.2 Mono-functionalisation of cyclam with a quinaldine-containing pendant (Method A)

8-Hydroxyquinaldine represents a really interesting possible pendant group because it is able to form stable complexes with a variety of metal ions (eg.  $\text{Ni}^{2+}$ ,  $\text{Zn}^{2+}$ ,  $\text{Al}^{3+}$ ). A cyclam ligand substituted with 8-hydroxyquinaldine could, then, offer binding sites for two metal ions, one within the ring and one at the pendant. Moreover, from the view point of chromium, the triplet excited state of 8-hydroxyquinaldine is likely to be only a little higher than that of the  ${}^2\text{E}$  excited state of  $\text{Cr}(\text{III})$ , so this aromatic compound could act as an efficient sensitiser of chromium luminescence. The same unit is also of interest as a sensitiser of lanthanide excited states, as discussed in chapters 4 and 5, using similar chemistry.



8-Hydroxyquinoline was chosen as a starting compound suitable for the synthesis of an appropriate alkylating agent (figure 2.11). In the first step, the hydroxyl group was protected by reacting the starting compound with benzyl bromide in refluxing methanol, under basic conditions (KOH).<sup>(14)</sup>

In the second step, the oxidation of the methyl group to the aldehyde was accomplished by using selenium oxide in dioxane, at 80°C.<sup>(14)</sup> Separation from selenium residues proved troublesome but after several filtrations through celite and chromatography on silica gel, the aldehyde was purified successfully. Reduction to the alcohol was accomplished readily upon treatment with sodium borohydride.<sup>(15)</sup>

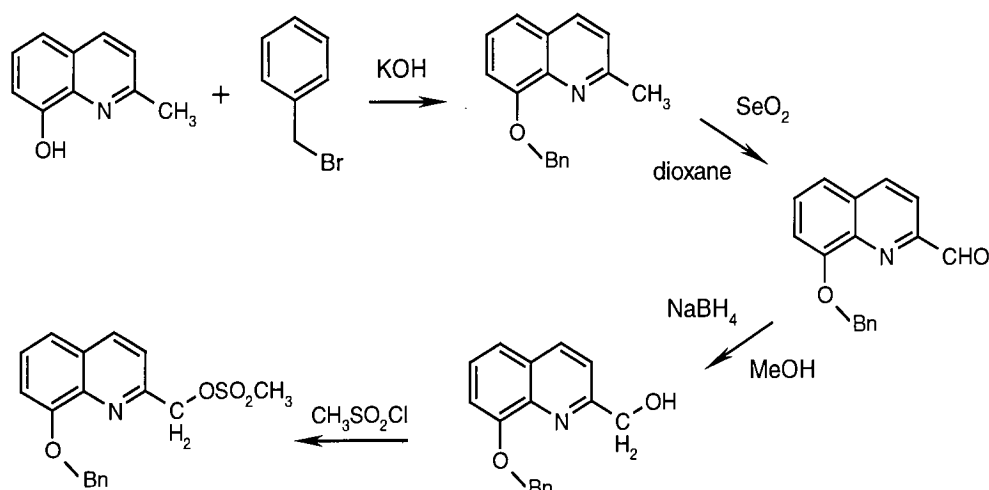


Fig. 2.11– Synthesis of 2-(mesyloxy)methyl-8-benzyloxyquinoline.

Initially, conversion of the alcohol to the alkyl chloride was attempted by treatment with thionyl chloride (alone, or in toluene solution). However, electrospray mass spectrometry and <sup>1</sup>H NMR spectroscopy revealed that a complex mixture of products had been formed, the desired one representing only a small fraction.

Attention was therefore turned to a better leaving group, namely the mesyl group. The mesylate was obtained by treatment of the alcohol with mesyl chloride at 0°C in the presence of triethylamine.<sup>(16)</sup> Because the synthesis of the alkylating agent had proved to be rather laborious, it was important to ensure selective mono-alkylation of cyclam, in order to avoid wasting any of the alkylating agent. Thus, the cyclam was protected with three BOC (*tert*-butylcarbonyl) groups.<sup>(17)</sup> Cyclam reacts with di-*tert*-butyldicarbonate (3 equiv.) in dichloromethane at room temperature to form the tris-protected compound in high yield.

The protected cyclam was then alkylated with the mesylquinaldine in refluxing acetonitrile in the presence of potassium iodide and potassium carbonate and the product purified by chromatography on silica gel (figure 2.12).

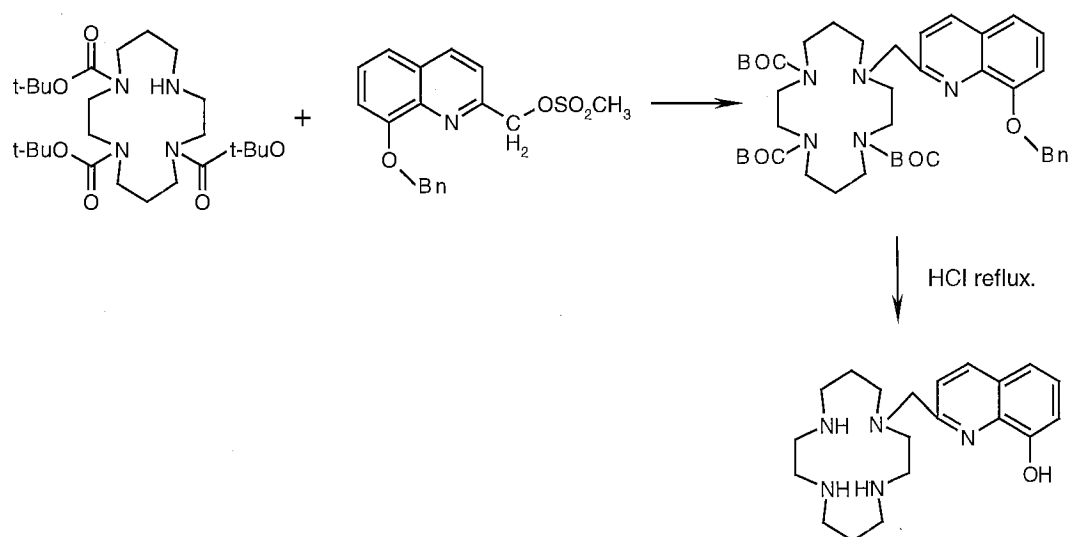


Fig. 2.12 – Synthesis of mono-substituted cyclam with a quinaldine pendant arm.

Finally, in the last step the three BOC groups were removed by heating the compound at 80°C overnight in 6M HCl. Unfortunately, after neutralisation and extraction,

spectroscopic analyses showed that, apart from cleaving the BOC groups, treating the compound with HCl had also cleaved the protective group of the hydroxyl (the benzyl ether).

This is a serious obstacle for metal complexation using this ligand, since the binding of metal ions to the di-protected 8-hydroxyquinoline unit may inhibit the entry into the ring. Furthermore, one of the starting ideas for the use of this ligand was the possibility of building a complex with different metals, hypothetically using a sequence of metal complexation, deprotection of the hydroxyl group and complexation with another metal (figure 2.13).

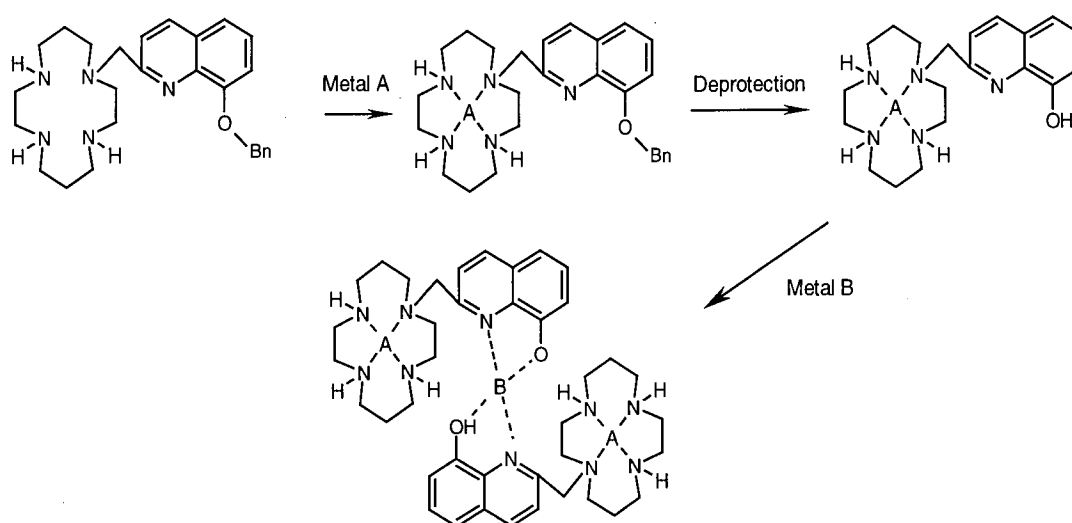


Fig. 2.13 – Supramolecular tri-metallic complex.

Clearly, an unprotected hydroxyl group is not acceptable, and a solution to overcome this problem had to be found, as discussed in the next section.

### 2.7.3 Mono-functionalisation of cyclam with a quinaldine-containing pendant (Method B)

A possible means of overcoming the previous problem was to avoid the use of protective groups altogether.

Since the 2-carboxaldehyde-8-benzyloxyquinoline (intermediate compound in the previous synthesis) was available, it was used for a direct reaction with cyclam itself, under reductive amination conditions, in the hope that only one of the four nitrogen atoms would react under equimolar conditions. Reductive amination reactions of aldehydes with sterically hindered primary amines (including amines of azacrowns) have been described,<sup>(18)</sup> and many studies have focused on the optimisation of this type of reaction.<sup>(19 and references therein)</sup> Procedures using mild and selective reagents have been developed for a wide range of substrates. Sodium triacetoxyborohydride has been shown to be a good general reducing agent for the reductive amination of aldehydes and ketones, offering high yields and few side products. However, there are apparently no reports of the use of such procedures for derivatisation of tetraazamacrocycles.

Equimolar amounts of cyclam and aldehyde were mixed in dichloromethane and then treated with sodium triacetoxyborohydride (figure 2.14). The mixture was stirred at room temperature under N<sub>2</sub> atmosphere for 12 hours. Several experiments proved that the most reliable procedure to follow was to mix the reagents initially leaving them to reach equilibrium (few minutes), and then to add the reducing agent. When the reaction was completed (monitored by TLC), 1N HCl was added to terminate it. After basicification

and extraction, the residue was purified by chromatography on silica gel leading to the required compound albeit in disappointing yield (typically 20%).

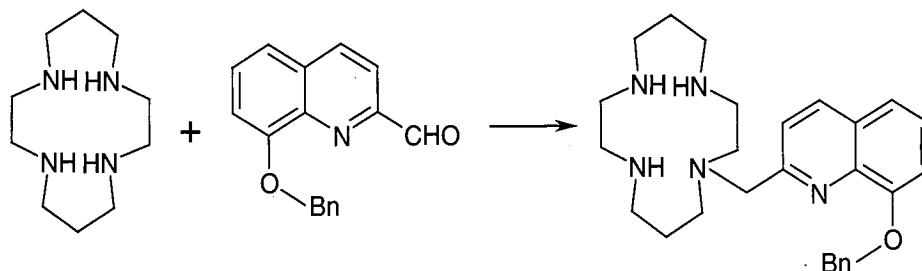


Fig. 2.14 – Synthesis of mono-functionalised cyclam.

Nevertheless, the method is quite attractive, as it involves fewer steps than the previous route and avoids the troublesome protection – alkylation – deprotection sequence usually required for this type of synthesis.

## 2.8 References

### 2.8.1 Articles

1. R. W. Hay, R. Bembi and W. Sommerville, *Inorg. Chim. Acta*, **59**, 147, (1982).
2. L. Cronin, A. R. Mount, S. Parsons and N. Robertson, *J. Chem. Soc., Dalton Trans.*, 1925, (1999).
3. J. Chapman, *Thesis for the degree of Doctor of Philosophy*, University of Durham, (1992).
4. P. J. Davies, M. R. Taylor and K. P. Wainwright, *Chem. Comm.*, 827, (1998).
5. G. Royal, V. Dahaoui-Gindrey, S. Dahaoui, A. Tabard, R. Guillard, P. Pullumbi and C. Lecomte, *Eur. J. Org. Chem.*, 1971, (1998).
6. N. F. Curtis, *J. Chem. Soc.*, 4409, (1960).
7. N. F. Curtis, Y. M. Curtis and H. J. K. Powell, *J. Chem. Soc. A*, 1015, (1966).
8. E. K. Barefield, F. Wagner, A. W. Herlinger and A. R. Dahl, *Inorg. Synth.*, **16**, 220, (1976).
9. E. K. Barefield, F. Wagner and K. D. Hodges, *Inorg. Chem.*, **15**, 1370, (1976).
10. O. Horner, J. J. Girerd, C. Philooze and L. Tchertanov, *Inorg. Chim. Acta*, **290**, 139, (1999).
11. F. Bellouard, F. Chuburu, N. Kervarec, L. Toupet, S. Triki, Y. Le Mest and H. Handel, *J. Chem. Soc., Dalton Trans.*, 3499, (1999).
12. L. S. Förster, *Chem. Rev.*, **90**, 331, (1990).
13. H. Fensterbank, J. Zhu, D. Riou and C. Larpent, *J. Chem. Soc., Perkin Trans. 1*, 811, (1999).

14. C. Caris, P. Baret, J. L. Pierre and G. Serratrice, *Tetrahedron*, **52**, 4659, (1996).
15. J. Buchi, A. Aebi, A. Deflorin and H. Hurni, *Helv. Chim. Acta*, **39**, 1677, (1956).
16. M. W. Hosseini, J. Comarmond and J. -M. Lehn, *Helv. Chim. Acta*, **72**, 1066, (1989).
17. S. Brandes, C. Gros, F. Denat, P. Pullumbi and R. Guillard, *Bull. Soc. Chim. Fr.*, **133**, 65, (1996).
18. Z. Yang, J. S. Bradshaw, X. Z. Zhang, P. B. Savage, K. E. Krakoviak, N. K. Dalley, N. Su, R. T. Bronson and R. M. Izatt, *J. Org. Chem.*, **64**, 3162, (1999).
19. A. F. Abdel-Magid, K. G. Carson, B. D. Harris, C. A. Maryanoff and R. D. Shah, *J. Org. Chem.*, **61**, 3849, (1996).

# **CHAPTER 3**

## **COPPER, NICKEL AND CHROMIUM COMPLEXES**



### 3.1 Introduction

Macrocyclic ligands containing secondary or tertiary nitrogen donors represented a relatively unstudied class of metal complexing agent up to the 1980s.<sup>(1)</sup> Since then, the chemistry of copper and nickel complexes of macrocycles has received much attention and has been extensively studied in recent years. Great effort has also been devoted to the incorporation of functionalised pendant groups into a saturated macrocyclic tetraamine structure to modify the conformational and redox properties of the metal complex.<sup>(1,2,3,4)</sup>

Quite interesting is the investigation of the behaviour of the dioxocyclams.<sup>(5,6,7,8)</sup> Typically, the 14-membered tetraamine macrocycles cyclam, monooxocyclam, and dioxocyclam, like porphyrins and corrin, incorporate metal ions into their cavities to form stable complexes.<sup>(9,10,11)</sup>

The synthesis of the copper and nickel complexes of our ligands was accomplished readily upon mixing the appropriate ligand with copper or nickel perchlorate in ethanol, or with copper or nickel acetate in deoxygenated methanol, followed by gentle heating under nitrogen atmosphere.

The formation of the complexes was confirmed by electrospray mass spectroscopy in each case, and UV-visible absorption spectroscopy has also proved useful in studying the complexes in solution, particularly with regard to the conformation adopted by the metal. In the solid state, measurements of magnetic susceptibility, using a JME balance, were informative, as were ESR measurements on some of the copper complexes. Ultimately, however, it is only X-ray crystallography that can provide a truly unambiguous picture of

the coordination geometry. In several cases, this has proved possible after sustained attempts to prepare suitable single crystals.

The ESR measurements were carried out in the University of York with the kind and essential assistance of Prof. B. Gilbert and Dr. A. Whitwood.

### **3.2 Nickel and copper complexes of 1,4,8,11-tetrazacyclotetradecane-5,12-dione, L<sup>4</sup>.**

#### (a) Nickel complex

As discussed in the introduction, macrocyclic dioxotetraamines are a unique class of chelating ligands for some transition metal ions, as they bear the structural features of macrocyclic tetraamines and of oligopeptides. They are often able to stabilise the higher oxidation states of transition metals with the result that several have been investigated for catalytic and biomimetic functions<sup>(12,13,14)</sup>. Metal binding by these ligands is almost invariably accompanied by the simultaneous deprotonation of the amide groups.

Although a great deal of work has been carried out with the 5,7-isomer of L<sup>4</sup> and its N-functionalised derivatives<sup>(5,6,7,8)</sup>, there has been far less investigation of the other isomers. In particular, the metal complexation properties of the 5,12-isomer have not been investigated, despite the fact that this compound has been known since the mid 1980s.<sup>(1)</sup> Owing to an unprecedented result (discussed in the next section, 3.3) on an N,N'-difunctionalised derivative of this compound, it was of interest to consider just how the parent ligand itself binds to copper and nickel.

Crystallographic analysis of the nickel(II) complex reveals that the metal ion is coordinated by four nitrogen atoms of the macrocycle in a square planar geometry (figure 3.1) as also suggested by the effective magnetic moment in the solid state, found to be close to zero. Selected bond lengths and angles are given in table 1, and data has been deposited<sup>(15)</sup>.

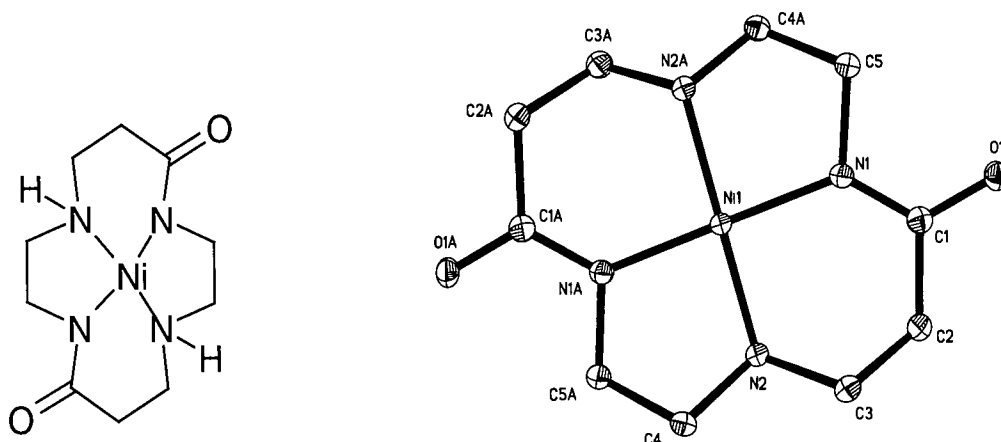


Fig. 3.1 – Molecular structure of  $\text{NiL}^4 \cdot \text{H}_2\text{O}$ .

Table 1 - Selected bond lengths (Å) and angles (°) for  $\text{NiL}^4 \cdot \text{H}_2\text{O}$ .

Ni-N(1)	1.901(1)	N(1)-N-N(1A)	180.00(10)
Ni-N(2)	1.916(1)	N(1)-N-N(2)	86.15(5)
N(1)-C(1)	1.324(2)	N(1)-N-N(2A)	93.85(5)
O(1)-C(1)	1.271(2)		

Adoption of a square planar geometry is predictable here, because the two amino nitrogen atoms, together with the two deprotonated amides, will provide a strong in-plane ligand field (so that the ligand field stabilisation is sufficient to overcome the additional pairing energy). The deprotonation of the two amides, which is expected to accompany metal binding, should lead to a shortening of the C(O)-N bond and a lengthening of the C=O, through delocalisation of the negative charge into the carbonyl group. Such an effect is

observed, although the differences in the bond lengths compared to those in the ligand [C(O)-N = 1.342(2)] itself are small<sup>(16)</sup>.

As expected, the Ni-N bond lengths are shorter for the amide nitrogens than the amino nitrogens [1.901(1) and 1.916(1) Å respectively], owing to the stronger ligand field strength of the deprotonated amide compared to an amine. It is notable, however, that the difference,  $\Delta$ , is very small ( $\Delta = 0.015$  Å), particularly compared to the nickel complex of 1,4,8,11-tetraazacyclotetradecane-5,7-dione<sup>(17)</sup>, where the corresponding bond lengths are 1.878 and 1.933 Å respectively ( $\Delta = 0.055$  Å). Presumably in that case, the ligand offers no conformational barrier to displacement of the metal ion towards the amide nitrogens disposed on the same side of the ring, whereas in our case, the simultaneous closer approach of the amide nitrogens towards the metal is disfavoured by conformational constraints of the ligand.

Upon dissolution of the nickel(II) complex in neutral aqueous solution, the lowest energy absorption band observed in the UV-visible was centred at 496 nm ( $\epsilon=55$ ). This is typical of square planar nickel complexes, indicating that the solid state coordination geometry persists in solution; the absence of any longer wavelength bands rules out any significant equilibration with a tetragonally distorted octahedral species, even in the presence of potentially coordinating water molecules.

Upon acidification, the orange solution became colourless over the pH range 4.5-3.5, consistent with re-protonation of the amide nitrogens and concomitant expulsion of the metal ion from the macrocycle cavity. Such pH-induced reversibility of metal binding is fully consistent with the well-established coordination properties of 5,7-dioxocyclam.

(b) Copper complex

Whilst the structure of the nickel complex was predictable, a fascinating unprecedented geometry was found for the copper(II) complex of  $L^4$  (figure 3.2). Unfortunately, it has not proved possible to obtain the definitive structure of the crystals formed from an aqueous solution of the complex. Frustratingly, several different attempts, using different solvents and different pH values, failed to provide a crystal good enough for a full structural analysis. The problem in solving the structure may be exacerbated by the low symmetry and the numerous conformations which can be adopted by the ligand. Nevertheless, isotropic refinement is itself sufficient to reveal an unusual polymeric structure, which is much more complicated than that of the nickel complex.

As in the nickel complex, a copper ion is located in the centre of each macrocycle, coordinated by the two amino and two amide nitrogen atoms in a square planar geometry. However, the macrocycles are themselves bridged by further pairs of copper ions, coordinated via the carbonyl oxygens which are disposed away from the ring at  $180^\circ$  to one another, leading to parallel sheets. In addition, the sheets are themselves bridged by equivalent sheets at  $60^\circ$  and  $120^\circ$ , leading to a hexagonal arrangement of macrocycles around each pair of bridging copper ions. A perchlorate ion is located within the triangular cavity formed by three macrocycles in the three planes. Perchlorate counter ions and water molecules of solvation are situated between the layers. There is little precedent for such a structure, although it is pertinent to note that the copper(II) complex of the 1,4-isomer forms a crystal in which two metal-bound macrocycles are dimerised by a bridging copper ion coordinated to the amide oxygen atoms.

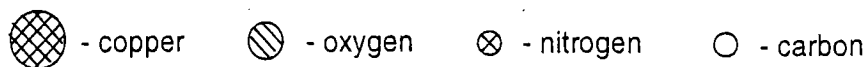
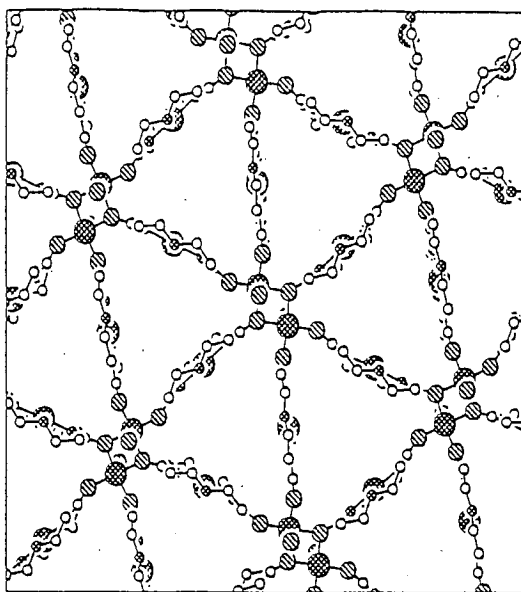
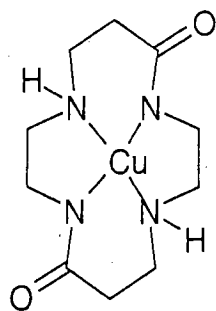


Fig. 3.2 – Isotropic refinement of  $[\text{CuL}^4]_3(\text{Cu}^{2+})_2(\text{ClO}_4)_4 \cdot 8\text{H}_2\text{O}$ .

The UV-Visible absorption spectrum of the copper complex in neutral aqueous solution shows a single band centred at 490 nm ( $\epsilon = 77$ ). Compared to square-planar complexes of tetraazacycloalkanes such as cyclam and its derivatives, where absorption is typically observed around 540-550 nm, the band is clearly shifted to higher energy. This is consistent with the rather stronger field exerted by the two deprotonated amides compared to the two amine nitrogens. Upon acidification, the blue solution became almost colourless, with the loss of the 490 nm band over the pH range 5.0-4.0 being accompanied by the appearance of a new band at 810 nm attributable to decomplexed aquated copper(II) ions.

Although not yet investigated, the magnetic properties associated with a structure of this type may prove to be very interesting, owing to the direct communication which may be possible through the bridging, deprotonated amide units.

### 3.3 Copper complexes of 1,8-bis(2-pyridylmethyl)-1,4,8,11-tetraazacyclo tetradecane-5,12-dione, L<sup>5</sup>.

Although prepared using a stoichiometric amount of copper(II), the crystals which were obtained from a solution of the copper complex of this ligand were found to have a copper:ligand ratio of 4:3 (figure 3.3). Selected bond lengths and angles are given in table 2. The structure shows two distinct units containing copper ions. In the first a single copper centre is penta-coordinate, with distorted trigonal bipyramidal geometry. The axial sites are occupied by the deprotonated nitrogen of one of the amide groups and the nitrogen of one of the pyridyl arms, with short bond lengths of 1.969(3) and 1.997(3) Å respectively. The amino nitrogens of the macrocycle and the nitrogen of the second pyridine group occupy the equatorial positions, with rather longer bonds to the copper.

A striking feature of the structure of this unit, and in which it differs from the majority of structurally characterised *cis*-dioxocyclam metal complexes,<sup>(5,8)</sup> is the fact that the other amide group is not deprotonated and is not involved in coordination to the metal, neither through the amide nitrogen nor through the carbonyl oxygen. This is probably the first crystallographically characterised example of partial deprotonation in such ligands, even though coordination in this way has been postulated several times<sup>(7,8)</sup> as an intermediate in the formation of the doubly deprotonated complexes.

The second macrocyclic unit in the structure has 2:1 metal:ligand stoichiometry and bridges two complexes of the first type through binding of the oxygens of their deprotonated amides to the two copper centres in this central macrocycle. Each copper is also coordinated by an amino nitrogen of the macrocycle, one of the amide oxygens and

the nitrogen of one of the pyridyl arms, which together form the base of a distorted square pyramid, with a water molecule occupying the fifth apical position. Neither amide group in this unit is deprotonated.

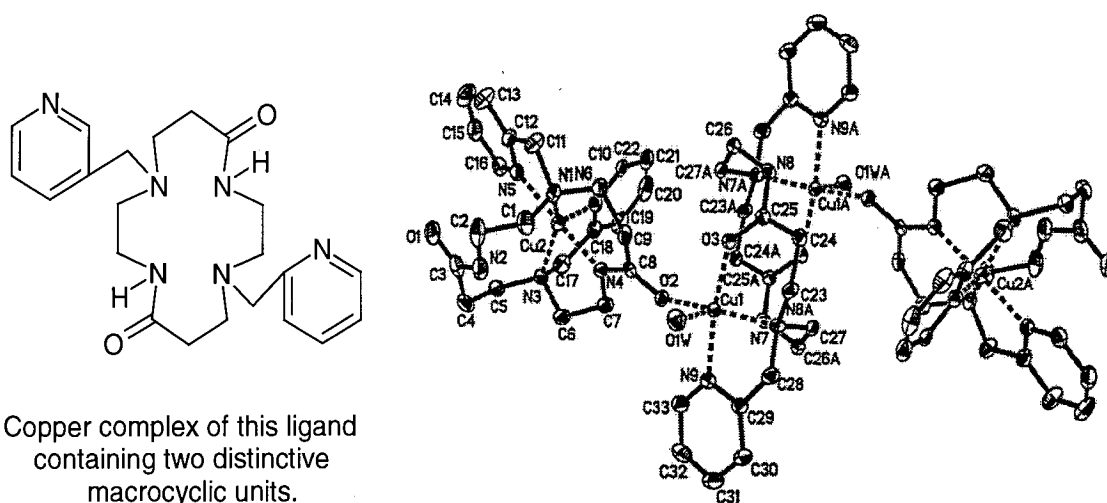


Fig. 3.3 – Molecular structure of  $[(CuHL^5)_2]^{2+}[Cu_2H_2L^5]^{4+}(Cl)_6 \cdot 15H_2O$ .

Table 2 - Selected bond lengths (Å) and angles (°) for the copper(II) complex of  $L^5$ .

Cu(1)–O(2)	1.947(3)	Cu(2)–N(6)	2.134(3)
Cu(1)–O(3)	1.956(3)	Cu(2)–N(3)	2.316(3)
Cu(1)–N(9)	1.991(3)	O(1)–C(3)	1.239(5)
Cu(1)–N(7)	2.050(3)	O(2)–C(8)	1.292(4)
Cu(1)–O(1W)	2.385(3)	O(3)–C(25)	1.260(4)
Cu(2)–N(4)	1.969(3)	N(2)–C(3)	1.354(6)
Cu(2)–N(5)	1.997(3)	N(4)–C(8)	1.308(5)
Cu(2)–N(1)	2.080(3)	N(8)–C(25)	1.333(5)
O(2)–Cu(1)–O(3)	92.01(11)	N(4)–Cu(2)–N(1)	92.89(13)
O(2)–Cu(1)–N(9)	92.95(12)	N(5)–Cu(2)–N(1)	83.52(13)
O(3)–Cu(1)–N(9)	171.74(12)	N(4)–Cu(2)–N(6)	91.12(12)
O(2)–Cu(1)–N(7)	168.39(12)	N(5)–Cu(2)–N(6)	89.16(13)
O(3)–Cu(1)–N(7)	90.09(11)	N(1)–Cu(2)–N(6)	130.52(13)
N(9)–Cu(1)–N(7)	83.76(12)	N(4)–Cu(2)–N(3)	83.31(12)
O(2)–Cu(1)–O(1W)	98.60(11)	N(5)–Cu(2)–N(3)	101.16(12)
O(3)–Cu(1)–O(1W)	99.87(11)	N(1)–Cu(2)–N(3)	151.09(13)
N(9)–Cu(1)–O(1W)	85.92(12)	N(6)–Cu(2)–N(3)	78.32(12)
N(7)–Cu(1)–O(1W)	92.29(12)	C(8)–O(2)–Cu(1)	135.1(2)
N(4)–Cu(2)–N(5)	175.48(13)	C(25)–O(3)–Cu(1)	133.5(2)



The observation that only one of the two amides in one of the macrocyclic units was deprotonated prompted an attempt to prepare and crystallise the copper complex of the ligand in basic conditions. Deprotonation of both of the amide groups within the macrocycle should then be favoured. Suitable crystals were obtained from a solution of the complex basicified to pH 12 with potassium hydroxide (Figure 3.4). Selected bond lengths and angles are given table 3.

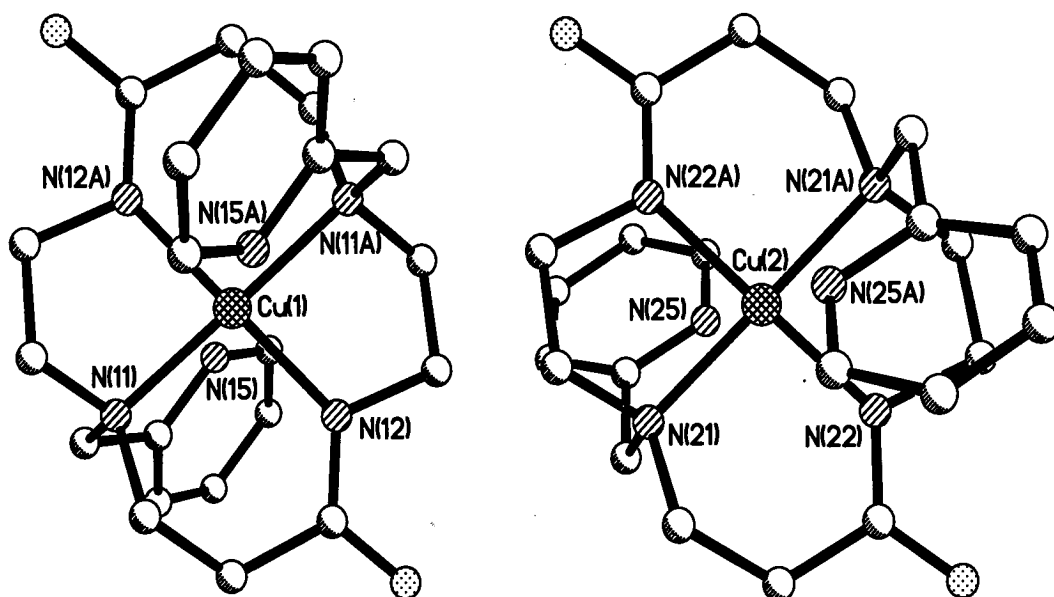


Fig. 3.4 – Molecular structure of  $[\text{CuL}^5].2\text{H}_2\text{O}$  obtained under basic conditions. Right: conformer 1. Left: conformer 2.

Table 3 - Selected bond lengths (Å) and angles ( $^\circ$ ) for the copper(II) complex of ligand  $\text{L}^5$  crystallised at basic pH.

Conformer 1		Conformer 2	
Cu(1)–N(11)	2.062(3)	Cu(2)–N(21)	2.046(3)
Cu(1)–N(12)	1.961(4)	Cu(2)–N(22)	1.962(4)
Cu(1)–N(15)	2.632(6)	Cu(2)–N(25)	2.809(6)
N(11)–Cu(1)–N(12)	95.6(2)	N(21)–Cu(2)–N(22)	95.3(2)
N(11)–Cu(1)–N(12A)	84.5(2)	N(21)–Cu(2)–N(22A)	84.7(2)

The structure confirmed the previous predictions, revealing that the copper ion is now bound within the N<sub>4</sub> plane by all four macrocycle nitrogens, with both amides deprotonated to give a stronger in-plane ligand field. The two pyridyl nitrogen atoms also coordinate to the copper ion in mutually *trans* positions, albeit weakly, as evidenced by the rather long pyridyl N-copper distances. In fact, there are two independent molecules in the unit cell, which are conformationally different. In one of them the pyridyl ring is situated above the six-membered chelate ring formed by the macrocycle and metal, while in the other it lies above the 5-membered ring. The distances between the pyridyl nitrogen and the copper are significantly different in the two cases: 2.632(6) and 2.809(6) Å respectively. The structure is further complicated by the occurrence in each conformer site of a small proportion (ca. 15%) of the other conformer.

A deep blue solution was obtained upon dissolution in water of the crystals obtained from the neutral solution. The electronic absorbance spectrum showed two bands in the visible region, with absorbance maxima at 602 and 798 nm.

The profile and the position of the longer wavelength band resembles that of simple aqueous copper(II) salts, whilst the other, rather more intense band is more similar to that observed for related complexes.<sup>(5,8)</sup> Since the molecular structure reveals an excess of copper over the ligand, it is likely that upon dissolution the additional copper ion is expelled from the bimetallic central unit in the structure to allow formation of a further equivalent of the copper penta-coordinate by the macrocyclic unit. This would account for the appearance of free copper in the absorbance spectrum, as well as the higher energy absorbance band arising from the copper coordinated by the stronger-field, mono-deprotonated macrocyclic ligand.

Support for the proposal that the ligand remains mono-deprotonated at neutral pH comes from observations of the effect of pH on the spectrum. Upon increasing the pH, the higher energy band shifts to shorter wavelengths, with a limiting absorbance maximum of 519 nm at  $\text{pH} > 11.2$ , and an observed  $\text{pK}_a$  of approximately 9.8. Clearly, this must be due to deprotonation of the second amide group, resulting in an increase in the ligand field strength, and formation of the structure shown in figure 3.4.

On the other hand, decreasing the pH to below 7 by addition of acid also resulted in a marked change in the spectrum. In this case, the two bands observed at neutral pH collapse to a single band centered at 705 nm. Although substantially longer than the wavelengths of the bands for typical azamacrocyclic-bound copper, this value is nevertheless shorter than that of aqueous copper(II). Decreasing the pH will result in protonation of the amide group, such that the copper will be coordinated only weakly, presumably by a mixture of the pyridine nitrogen atoms, the amino nitrogens of the macrocycle and water molecules. The presence of at least some nitrogen atoms in the coordination sphere of the metal ensures that the ligand field is rather stronger than in aqueous copper(II) leading to shorter wavelength absorbance.

### 3.4 Nickel and copper complexes with the three isomeric bis(2-pyridylmethyl) substituted cyclams, L<sup>1</sup>, L<sup>2</sup> and L<sup>3</sup>.

#### (a) Nickel complex of L<sup>1</sup>

Crystallographic analysis of the nickel(II) complex of L<sup>1</sup> reveals that the metal ion has a distorted octahedral coordination with four nitrogen atoms of the macrocycle and two of the pyridine rings (figure 3.5). Selected bond lengths and angles are given in table 4, and data has been deposited<sup>(18)</sup>.

The coordination of the pyridyl groups in mutually *cis* positions, with the macrocycle adopting the folded, *cis*-V configuration, is surprising. The 1,8 disubstitution of cyclam with coordinating arms should allow the cyclam ring to adopt its generally preferred *trans*-III conformation (in which the two six-membered chelate rings are in the *chair* form and the two five-membered rings are in the *gauche* form and with the four nitrogen atoms binding to the metal in a plane), whilst allowing the pendent groups to occupy axial positions (see figure 1.1).

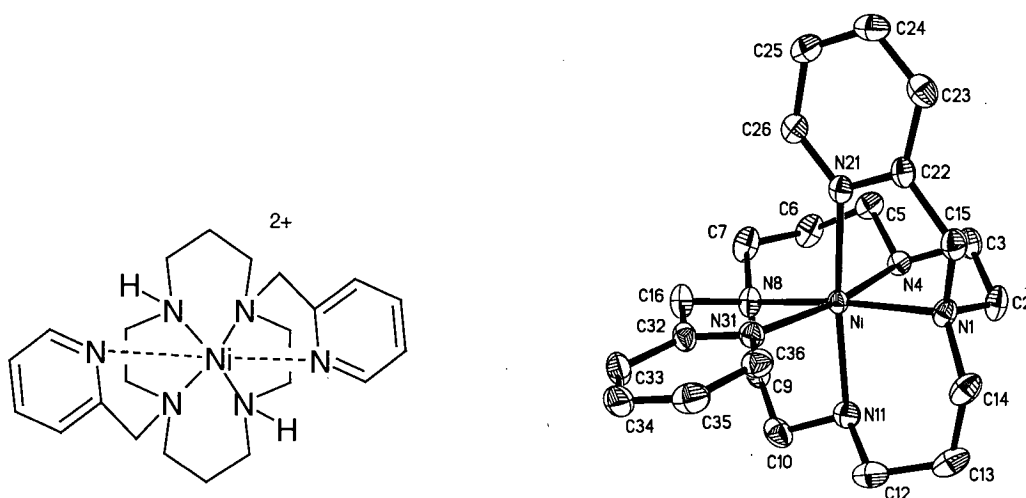


Fig. 3.5 – Molecular structure of  $[\text{NiL}^1](\text{Cl})_x(\text{C}_2\text{H}_3\text{O}_2)_{2-x}(4+x)\text{H}_2\text{O}$  [ $x = 0.428(3)$ ] (with non-stoichiometric proportion of anions and crystallisation water).

Table 4 - Selected bond lengths (Å) and angles (°) for the nickel(II) complex of *L*<sup>1</sup>.

Ni-N(1)	2.159(2)	N(8)-Ni-N(21)	106.21(7)
Ni-N(4)	2.101(2)	N(8)-Ni-N(31)	80.85(7)
Ni-N(8)	2.164(2)	N(11)-Ni-N(21)	168.93(8)
Ni-N(21)	2.096(2)	N(1)-Ni-N(4)	83.69(7)
Ni-N(31)	2.111(2)	N(8)-Ni-N(4)	89.00(7)
Ni-N(11)	2.117(2)	N(11)-Ni-N(4)	95.25(8)
N(1)-Ni-N(8)	169.13(7)	N(21)-Ni-N(4)	89.09(7)
N(1)-Ni-N(11)	88.57(8)	N(31)-Ni-N(4)	168.83(7)
N(1)-Ni-N(21)	81.78(7)	N(11)-Ni-N(31)	88.37(8)
N(1)-Ni-N(31)	107.00(7)	N(21)-Ni-N(31)	89.29(7)
N(8)-Ni-N(11)	84.09(8)		

The packing of cations leaves infinite channels, parallel to the crystallographic *x* axis, filled with anions and crystallisation water, hydrogen-bonded with one another with the cation. The asymmetric unit comprises one acetate anion and two water molecules ordered in fully occupied positions, another water molecule disordered between three positions, one site shared between a chloride anion (42.8(3)%) and a water molecule (52.2(3)%) and a cavity shared between two water molecules (42.8(3)%) and one acetate anion (57.2(3)%).

This binding mode is indeed the one found for the analogous copper(II) complex discussed below and also in those nickel(II) complexes of 1,8-disubstituted cyclam derivatives which have been reported<sup>(19)</sup>. The adoption of the *cis-V* configuration, observed in our case, is much less common. It is usually confined to those complexes in which the macrocycle-bound nickel is also coordinated by a bidentate anion (in addition to the four macrocyclic nitrogens), where coordination in mutually *cis* positions of the two ligating atoms of the anion is enforced<sup>(20)</sup>. From a search of the Cambridge Crystallographic Database, only three examples were found in which the nickel(II) complexes of 1,8-disubstituted cyclam adopt the *cis-V* configuration<sup>(2,21)</sup> and in fact, two of these have additional substituents at carbons 5,7,12 and 14. In those cases, avoidance

of non-bonding repulsive interactions probably has a major influence on the structure adopted.

The factors influencing the adoption of a given macrocycle configuration in the nickel(II) complexes of cyclam-based ligands have been reviewed recently<sup>(22)</sup>, but it is clear that in the case of N-functionalised derivatives of cyclam itself (as opposed to those incorporating C-substituents), the adoption of a given structural configuration is not readily predicted or accounted for.

#### (b) Nickel complex of L<sup>2</sup> and its parent L<sup>6</sup>

Attempts to crystallise the nickel(II) complex of the ligand L<sup>2</sup>, (which had been prepared via the formamidinium salt of cyclam, as described in section 2.3), led to two different crystal types, one red and the other blue. Only the blue crystals were of a quality appropriate for crystallographic structure determination. Given the unexpected structure elucidated (figure 3.6) with a methylene bridge present between a 1,5-related pair of nitrogen atoms, it is evident that the blue crystals had formed from a small amount of dialkylated formamidinium salt intermediate (L<sup>6</sup>) in the sample of L<sup>2</sup> used, i.e. that the bridge had not been fully cleaved.

In this ligand, the additional methylene bridge, between the non-pyridylmethyl-substituted nitrogens, prohibits the simultaneous binding of these two atoms to the metal. Thus the nickel atom has a distorted octahedral coordination involving three macrocyclic nitrogen atoms, two pyridine nitrogen atoms (in *cis*-position, as in the previous crystal) and a chloride ion. Selected bond lengths and angles are given in table 5.

This coordination probably persists in solution, since the UV-visible absorbance spectrum shows bands at wavelengths typical of nickel(II) in an octahedral environment [ $\lambda_{\text{max}}$  809 ( $\epsilon= 18$ ) and 529 nm ( $\epsilon= 28$ )]. A number of related ligands have been synthesised before with additional alkyl bridges between one or more pairs of nitrogen atoms, introduced to increase structural rigidity<sup>(23)</sup>. However, these bridges were long enough to allow both bridged nitrogen atoms to coordinate to the metal simultaneously. Thus, an ethylene bridge between the N<sup>1</sup> and N<sup>4</sup> atoms in 1,4,7,10-tetraazacyclododecane does not prevent all four N atoms from binding to nickel in a square planar fashion, even though the geometry is substantially distorted from true square planarity<sup>(24)</sup>.

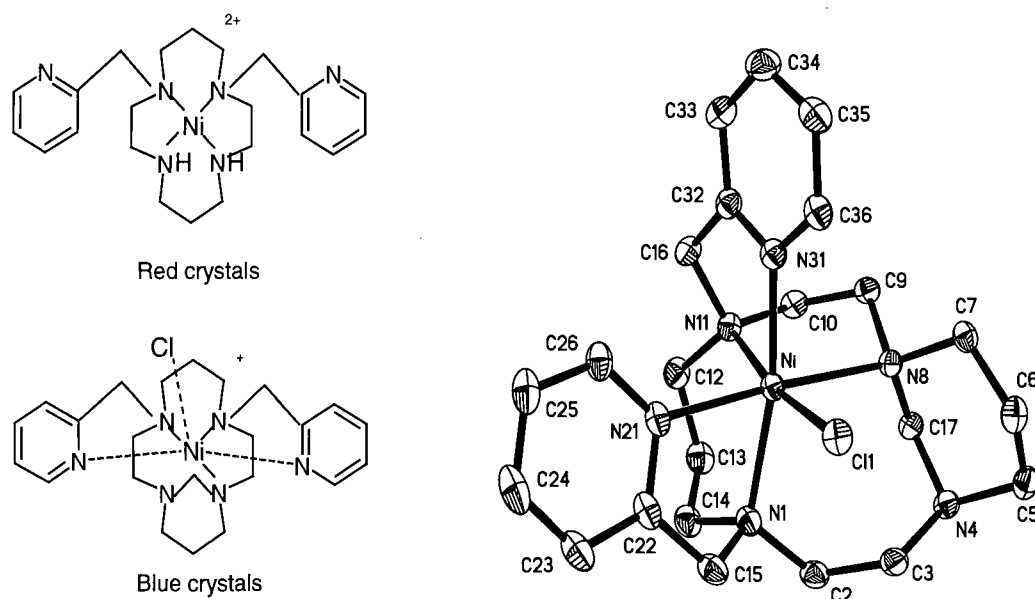


Fig. 3.6 – Molecular structure  $[Ni(4,8\text{-methylen-}L^2)](ClO_4^-)_2(Cl^-)(1/4).H_2O$ .

A possible explanation for the fact that only the impurities underwent good crystallization is that the internal bridge of the macrocycles increased the rigidity of the system which favoured the crystallization process.

Table 5 - Selected bond lengths (Å) and angles (°) for the nickel(II) complex of  $L^2$  with a methylene bridge between the two non-pyridylmethylated nitrogen atoms.

Ni-N(1)	2.240(2)	N(8)-Ni-N(21)	176.43(6)
Ni-Cl(1)	2.445(1)	N(8)-Ni-N(31)	88.90(6)
Ni-N(8)	2.278(2)	N(11)-Ni-N(21)	98.27(6)
Ni-N(21)	2.104(2)	N(1)-Ni-Cl(1)	95.08(4)
Ni-N(31)	2.107(2)	N(8)-Ni-Cl(1)	94.07(4)
Ni-N(11)	2.143(2)	N(11)-Ni-Cl(1)	169.48(4)
N(1)-Ni-N(8)	99.57(6)	N(21)-Ni-Cl(1)	85.03(5)
N(1)-Ni-N(11)	95.39(6)	N(31)-Ni-Cl(1)	89.69(5)
N(1)-Ni-N(21)	77.10(6)	N(11)-Ni-N(31)	80.16(6)
N(1)-Ni-N(31)	169.96(6)	N(21)-Ni-N(31)	94.55(6)
N(8)-Ni-N(11)	83.22(6)		

Unfortunately, further attempts to crystallise the nickel(II) complex of  $L^2$ , including the use of different solvents, failed. The same problem occurred with the 1,4 isomer  $L^3$ .

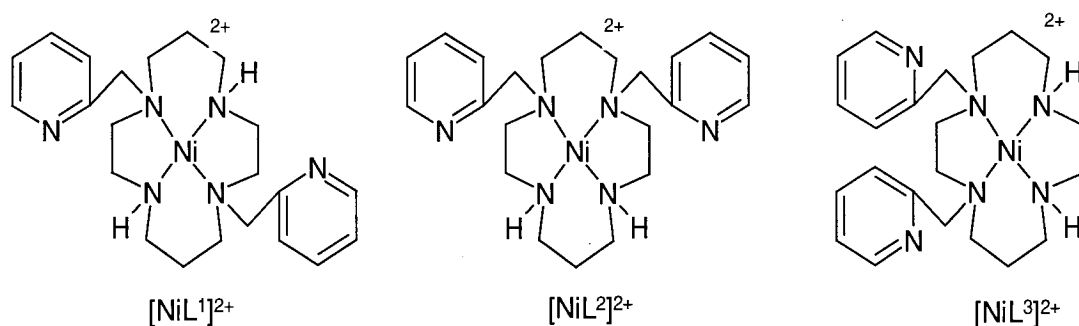
### (c) Physical properties of the nickel complexes of $L^1$ , $L^2$ and $L^3$

The spectroscopic and electrochemical data for the nickel complexes of  $L^1$ ,  $L^2$  and  $L^3$  in solution, together with the effective magnetic moments measured in the solid state, are listed in table 6. Such data are useful in elucidating the likely coordination geometry at the metal in the absence of a definitive crystal structure.

In each case, the effective magnetic moments are in line with the spin-only value of 2.83 BM expected for nickel in an octahedral environment; square planar complexes of nickel(II), in contrast, are almost always diamagnetic. The UV-Visible absorbance spectra are also indicative of octahedral coordination of the nickel in solution. The observed absorbance maxima are close to those of  $[\text{Ni}(\text{en})_3]^{2+}$  ( $\lambda_{\text{max}} = 892$  and  $544$  nm), a reasonable model for the present complexes in which the metal is coordinated by six nitrogen donors. Thus, it is very likely that in  $\text{NiL}^2$  and  $\text{NiL}^3$  as in  $\text{NiL}^1$ , the pyridyl groups are coordinated to the metal.



For all the complexes, no significant change in the spectra was observed upon changing the pH over a wide range (0.5-13.5), indicating that the pyridyl groups remain coordinated to the metal ion, even under quite strongly acidic conditions where protonation could promote dissociation.



	[NiL <sup>1</sup> ] <sup>2+</sup>	[NiL <sup>2</sup> ] <sup>2+</sup>	[NiL <sup>3</sup> ] <sup>2+</sup>
$\lambda_{\max}$ (nm) ( $\epsilon$ ) <sup>a</sup>	863 (13) 531 (11)	857 (14) 529 (12)	956 (11) 542 (12)
$E^{\circ}_{\text{Ni(III)/Ni(II)}} \text{ (V)}$ <sup>b</sup>	+ 1.54 <sup>c</sup>	+ 1.42 <sup>c</sup>	/
$\mu_{\text{eff}}$ (BM) <sup>d</sup>	2.30	2.73	2.57

<sup>a</sup> In acetonitrile. <sup>b</sup> At 293 K in acetonitrile solution, 0.1 M [NBu<sub>4</sub>][PF<sub>6</sub>], using ferrocene as an internal standard, values relative to SCE. <sup>c</sup> Quasi-reversible. <sup>d</sup> In solid state, using (NH<sub>4</sub>)<sub>2</sub>Fe(SO<sub>4</sub>)<sub>2</sub>·6H<sub>2</sub>O as standard.

Table 6 – Physical properties of the nickel(II) complexes of 1,4-, 1,8- and 1,11-bis(2-pyridylmethyl)-1,4,8,11-tetraazacyclotetradecane.

In cyclic voltammetry, quasi-reversible redox waves corresponding to the oxidation of Ni(II) to Ni(III) were observed. The values obtained were significantly higher than those found for non-N-substituted cyclam derivatives<sup>(9)</sup>. This is consistent with the generally observed trend that substitution of secondary amino groups by tertiary ones in a 14-membered tetraazamacrocyclic complex induces a relative destabilization of the higher

oxidation state, an effect which has been attributed to a variety of factors, reviewed recently, and including the increased cavity size of N-alkylated ligands, decreased solvation caused by the hydrophobic nature of the alkyl groups and possibly poorer  $\sigma$ -donor strength of tertiary nitrogen atoms<sup>(25)</sup>.

The values observed here are higher than would be expected on the basis of the effect of di-N-alkylation only. The additional destabilization of the Ni(III) observed in the present system may be due to the  $\pi$ -acceptor nature of the coordinating pyridine ligands, conferring an effect opposite to that of electron-rich or anionic pendent coordinating groups, which stabilize the Ni(III) state<sup>(9,19)</sup>.

Although all the physical data discussed in the preceding paragraphs imply strongly that the metal ion is coordinated octahedrally in the complexes of  $L^2$  and  $L^3$  (as in  $L^1$ ), by the two pyridine nitrogens as well as the macrocyclic nitrogens, it is not possible to come to any firm conclusions regarding the conformation adopted by the macrocycle. In the case of cyclam 1,11-disubstituted with coordinating arms, adoption of the *cis*-V configuration will not allow the pendent groups to bind simultaneously the metal, being disposed on opposite sides of the macrocycle. Thus, it is possible to rule out the *cis*-V, but the *trans*-I, *trans*-II and *trans*-III configurations could each permit simultaneous coordination of the pyridine groups. These cannot, however, be distinguished from the available data. A similar argument applies to the 1,4-disubstituted derivative. Only if crystals are obtained that are suitable for X-ray diffraction study will it be possible to have a definitive solution.

(d) Copper complexes of L<sup>1</sup>, L<sup>2</sup> and L<sup>3</sup>Copper complex of L<sup>1</sup>

In contrast to the nickel complex of this ligand discussed above, the copper complex adopts the predictable coordination geometry and macrocycle conformation. The copper is coordinated by the four nitrogen atoms of the macrocycle and by the nitrogen atoms of the pyridine rings, which occupy axial sites at a much greater distance, leading to a severely tetragonally elongated octahedral geometry with an inversion centre at the metal (figure 3.7). Selected bond lengths and angles are given in table 7.

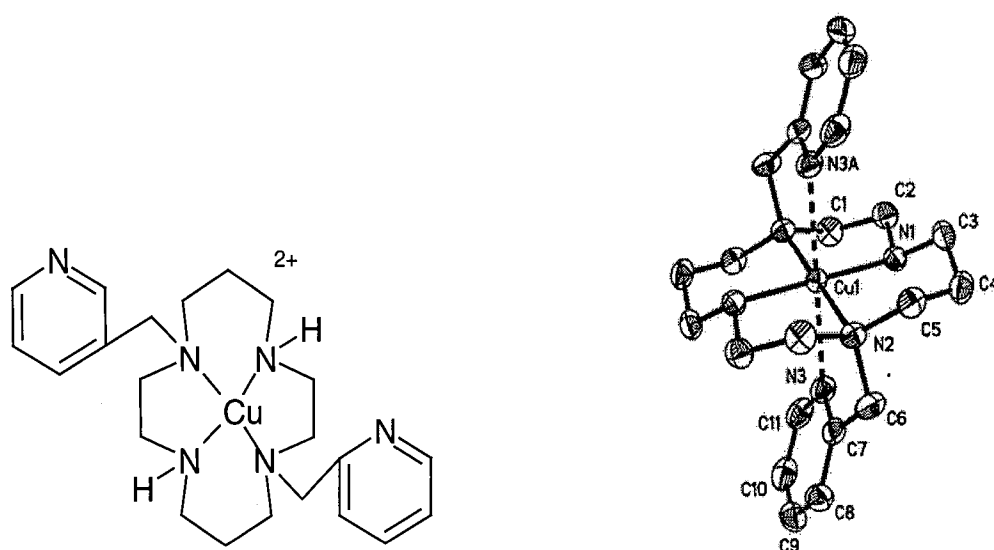


Fig. 3.7 – Molecular structure of  $[CuL^1]^{2+}(CH_3CO_2^-)_2 \cdot 6H_2O$ .

Table 7 - Selected bond lengths (Å) and angles (°) for  $[CuL^1]^{2+}(CH_3CO_2^-)_2$ .

Cu(1)–N(1)	2.015(1)	N(1)–Cu(1)–N(1)#1	180.00(6)
Cu(1)–N(2)	2.079(1)	N(1)–Cu(1)–N(2)#1	86.65(4)
Cu(1)–N(3)	2.524(1)	N(1)–Cu(1)–N(2)	93.35(4)

Symmetry operator: #1  $-x + 1, -y, -z + 1$ .

The Cu-NH bond length of 2.015(1) Å is close to that in the copper complex of cyclam itself (2.02 Å),<sup>(26a)</sup> whilst the bonds to the alkylated ring nitrogens are rather longer, at 2.079(1) Å. This is to be expected, a large number of studies having demonstrated that metal-N bond lengths are increased by N-alkyl substitution.<sup>(26b)</sup> The Cu-N (pyridyl) bond lengths of 2.524(1) Å are clearly much longer than those to the alkyl nitrogens. This large difference in bond length is, of course, consistent with a strong in-plane ligand field provided by the nitrogen atoms of the macrocycle compared to the weaker pyridine donors, notwithstanding the expected Jahn-Teller distortion. The macrocycle adopts the preferred *trans-III* conformation of cyclam.

It is interesting to compare the different behaviour of nickel and copper in the complexes with this ligand. While the copper behaves as expected, assuming a distorted octahedral conformation subject to Jahn-Teller distortion, the nickel complex adopts an unexpected and almost unique conformation. Certainly, one would expect the nickel complex to assume the same conformation as that of copper, with the macrocycle in its most stable conformation, the *trans-III*. It is possible, however, that the unexpected behaviour of the former is due to the influence of the effects of packing in the crystal structure.

### Copper complex of L<sup>2</sup>

In this case, the copper is penta-coordinate, in a distorted square pyramidal geometry, with the four nitrogen atoms of the macrocycle forming the base and with a nitrogen of one of the pyridine groups at the apical position (figure 3.8). Selected bond lengths and angles are given in table 8.

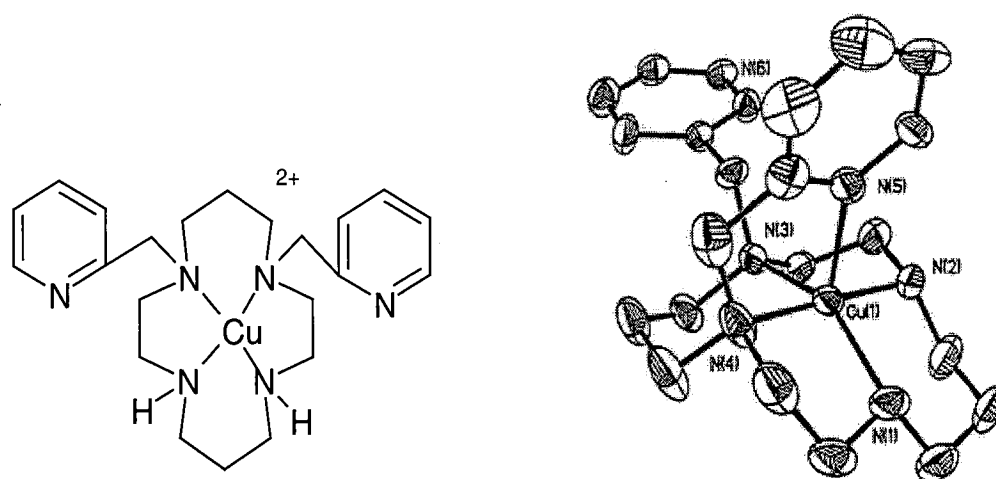


Fig. 3.8 – Molecular structure of  $[\text{CuL}^2]^{2+}(\text{ClO}_4^-)_2 \cdot \text{CH}_3\text{OH}$ .

Table 8 - Selected bond lengths (Å) and angles (°) for  $[\text{CuL}^2]^{2+}(\text{ClO}_4^-)_2$

Cu(1)–N(2)	2.030(3)	Cu(1)–N(3)	2.091(2)
Cu(1)–N(1)	2.048(3)	Cu(1)–N(5)	2.209(3)
Cu(1)–N(4)	2.059(3)		
N(2)–Cu(1)–N(1)	92.77(13)	N(4)–Cu(1)–N(3)	95.32(11)
N(2)–Cu(1)–N(4)	178.18(11)	N(2)–Cu(1)–N(5)	101.14(11)
N(1)–Cu(1)–N(4)	85.42(13)	N(1)–Cu(1)–N(5)	104.37(12)
N(2)–Cu(1)–N(3)	86.35(11)	N(4)–Cu(1)–N(5)	79.17(12)
N(1)–Cu(1)–N(3)	150.86(12)	N(3)–Cu(1)–N(5)	104.37(10)

An interesting feature of the structure is that the second pyridine group remains uncoordinated. The lengths of the Cu–N(macrocycle) bonds are in the range 2.030(3)–2.091(2) Å, with the bond to the nitrogen carrying the coordinated pyridine rather shorter than that to the nitrogen substituted by the uncoordinated pyridine [2.059(3) vs. 2.091(2) Å], presumably to allow for efficient five-membered chelate ring formation incorporating the pyridine. The macrocycle is seen to adopt the less stable *trans-I* conformation, in which the five-membered chelate rings are in the eclipsed form.

If the macrocycle were to adopt the preferred *trans*-III conformation, then octahedral coordination of the bound metal would be ruled out for such 1,11-disubstituted systems, as the additional coordinating groups would be on the same side of the nitrogens' plane (figure 3.9). On the other hand, octahedral coordination would become feasible if the macrocycle were to twist to the *trans*-II conformation, and this is indeed observed for related complexes. Adoption of the penta-coordinate, *trans*-I structure observed here is rather surprising, as it offers neither the metal the possibility of hexa-coordination nor the macrocycle its preferred conformation.

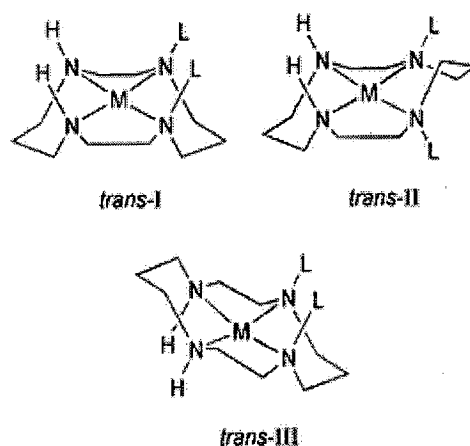


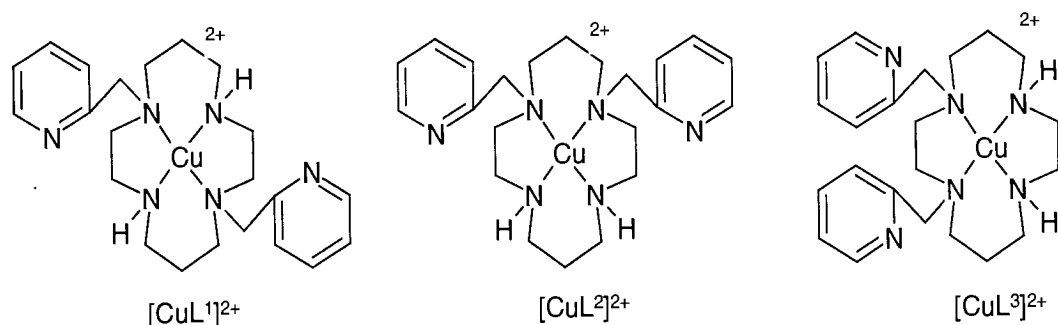
Fig. 3.9 – Three of the possible *trans* stereoisomers of cyclam-type metal complexes. *L* represents a substituent that incorporates a potentially coordinating group.

### Copper complex of $L^3$

Attempts to crystallise the copper(II) complex of 1,4-bis(2-pyridylmethyl)-1,4,8,11-tetraazacyclotetradecane have, on some occasions, led to well-formed crystals, but, unfortunately diffraction studies have shown them to be twinned.

### (e) Physical properties of the copper complexes of $L^1$ , $L^2$ and $L^3$

The physical properties of the copper complexes of 1,4-, 1,8- and 1,11-bis(2-pyridylmethyl)-1,4,8,11-tetraazacyclotetradecane ligands are listed in table 9.



	$[\text{CuL}^1]^{2+}$	$[\text{CuL}^2]^{2+}$	$[\text{CuL}^3]^{2+}$
$\lambda_{\text{max}}$ (nm) ( $\epsilon$ )	546 (69) <sup>a</sup>	578 (203) <sup>a</sup>	598 (175) <sup>b</sup>
$E^\circ_{\text{Cu(II)/Cu(I)}}$ (V) <sup>c</sup>	-0.17 <sup>d</sup>	-0.15 <sup>e</sup>	/
$g_{\text{iso}}$ (293 K) <sup>f</sup>	2.106	2.105	/
$a_{\text{Cu}}$ (293 K)/G <sup>f</sup>	71	77	/
$g_{\text{II}}$ (110 K) <sup>g</sup>	2.21	2.21	/
$A_{\text{II}}$ (110 K)/G <sup>g</sup>	173	179	/

<sup>a</sup> In aqueous solution. <sup>b</sup> In acetonitrile. <sup>c</sup> At 293 K in acetonitrile solution, 0.1 M  $[\text{NBu}_4][\text{PF}_6]$ , using ferrocene as an internal standard, values relative to SCE. <sup>d</sup> Quasi-reversible. <sup>e</sup> Irreversible. <sup>f</sup> In acetonitrile. <sup>g</sup> In 50% methanol-acetonitrile.

Table 9 – Physical properties of the copper(II) complexes of 1,4-, 1,8- and 1,11-bis(2-pyridylmethyl)-1,4,8,11-tetraazacyclotetradecane.

The cyclic voltammetry data available show, for the copper complexes of the 1,11- and 1,8-derivatives, a stabilisation of 0.7-0.8 V of the copper(I) oxidation state relative to the value in non-N-alkylated cyclam type complexes, which is in line with recently reported data on some other 1,8-dialkylated tetraazamacrocycles<sup>(27)</sup>.

A second reduction process was observed for both complexes, at -0.65 V for  $[\text{CuL}^1]^{2+}$  and -0.54 V for  $[\text{CuL}^2]^{2+}$ . This reduction, which was irreversible in both cases, led to a copper stripping peak in the subsequent oxidation cycle, indicative of decomposition of the

zerovalent complex to elemental copper at the platinum electrode. Such an effect has been described for  $[\text{Cu}(\text{cyclam})]^{2+}$ , where a stripping peak was observed following reduction at potentials  $-0.90$  V or lower<sup>(28)</sup>. In this case, as for the related nickel complexes discussed above, there is a destabilisation of the higher oxidation states for the same reasons, but in this case the +2 relative to the +1.

The ESR spectra of the complexes  $[\text{CuL}^1]^{2+}$  and  $[\text{CuL}^2]^{2+}$  (recorded at the University of York) showed four equally spaced absorptions, as expected from the coupling of the unpaired electron density to the copper nucleus ( $I=3/2$ ); the isotropic parameters are listed in table 2. The form of the low temperature spectra was typical of near axial symmetry. The  $g_{\parallel}$  values were found to be the same for both complexes, namely 2.21. This value is a little higher than that of  $[\text{Cu}(\text{cyclam})]^{2+}$  and consistent with a trend to higher  $g_{\parallel}$  values upon N-alkylation of tetraazamacrocycles, as true square planar coordination becomes disfavoured upon increasing N-substitution<sup>(29)</sup>. The hyperfine coupling constant,  $A_{\parallel}$ , is a better indicator of distortion from square planar towards pyramidal or tetrahedral coordination in copper(II) complexes. In the present instance, the values are closer to the square planar values.

No super-hyperfine coupling to the nitrogen donors was observed. In a study of the effect of aromatic nitrogen donors on the ESR spectra of copper(II) complexes of polyamines including cyclam, Siddiqui and Shepperd noted that the incorporation of aromatic N-donors into the coordination sphere of the metal activated the system such that all the nitrogen donors exhibited super-hyperfine coupling in the  $g_{\perp}$  region<sup>(30)</sup>. In the absence of such aromatic donors, such coupling was either very weak or not observed at all. Thus, the lack of super-hyperfine coupling in the present instance suggests that the pyridyl arms



are either not coordinated to the metal in aqueous solution or are coordinated only very weakly.

This conclusion is reinforced by the UV-visible absorption spectra. The spectrum of  $[\text{CuL}^1]^{2+}$  shows a maximum at 546 nm, in aqueous solution, which is typical of square planar copper complexes with a strong ligand field, rather than octahedral coordination. No significant changes in the spectrum were observed over the pH range 1.0-12.5. In contrast, the absorption maximum for the complex in solution in acetonitrile appeared at a longer wavelength of 593 nm; upon acidification with trifluoroacetic acid the band shifted to higher energy, 549 nm, similar to the value in aqueous solution (figure 3.10).

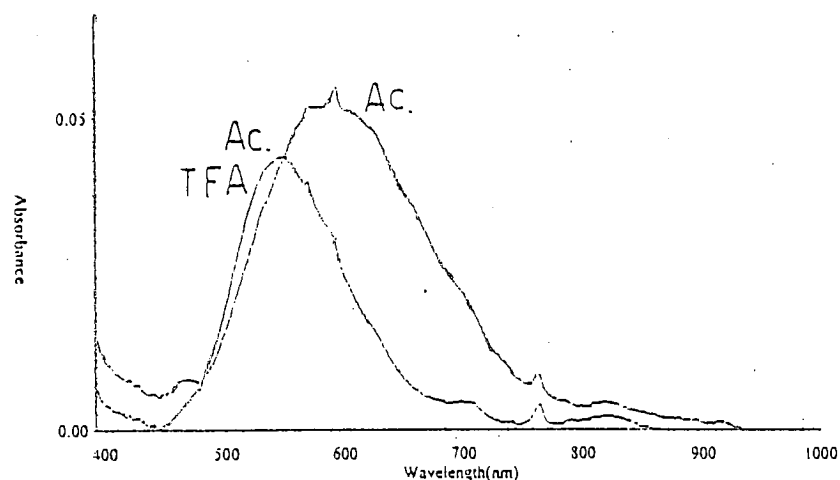
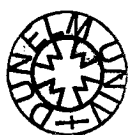


Fig 3.10 – Uv-Visible spectra of  $[\text{CuL}^1]^{2+}$  in acetonitrile with and without TFA.

This could be indicative of a rather more significant interaction of the metal with the axial pyridines when dissolved in acetonitrile (perhaps due to the poorer solvation of unbound pyridine nitrogens in this solvent), accompanied by slight elongation of the equatorial Cu-N bonds and a reduction in the in-plane ligand field strength. Protonation of the pyridyl nitrogen atoms then restores a coordination environment comparable to that found in water.



Compared to  $[\text{CuL}^1]^{2+}$ , the absorption maximum of  $[\text{CuL}^2]^{2+}$  appeared at significantly longer wavelength, 578 nm, in aqueous solution. This is consistent with the square pyramidal structure observed for this complex in the solid state, as opposed to effectively square planar coordination of the copper in  $[\text{CuL}^1]^{2+}$ , where a rather stronger ligand field would be expected. Again, no significant change in the spectrum was observed over the pH range 1.0-12.5.

Similarly, the absorbance spectrum of  $[\text{CuL}^3]^{2+}$  was independent of pH over the range 1.0-13.0 displaying an absorption maximum of 598 nm. This value is even further removed from the square planar value of  $[\text{CuL}^1]^{2+}$ , than that of  $[\text{CuL}^2]^{2+}$ , suggesting that this complex may also have a penta-coordinated (or distorted hexa-coordinated) structure, rather than a square planar geometry. Again, though, as for the nickel systems, no firm conclusions can be made in the absence of a definitive crystal structure.

### 3.5 Chromium complexes

As noted previously, the photochemistry and photophysics of octahedral chromium(III) complexes have been under active investigation from both experimental and theoretical viewpoints for many years.

This sustained interest arises in part because the photosubstitutional mechanisms and excited-state properties of chromium(III) complexes continue to pose several questions, including: the relative chemical importance of the lowest electronically excited states (spin-forbidden doublet and spin allowed quartet states), the types and the roles of non-

radiative processes such as the possible involvement of thermally activated back-intersystem crossing from the lowest doublet to a low lying quartet state, and the potential occurrence of chemically reactive intermediates.

Most chromium(III) hexamine complexes are luminescent at 77K, with long lifetimes often in the 100  $\mu$ s - 1 ms range, due to spin-forbidden transitions between the  $^2E$  excited state and  $^4A$  ground state. However, at higher temperatures, the excited state is usually deactivated efficiently by non-radiative processes, for example, by transfer of the energy into vibrations of the ligand. In order to observe room temperature luminescence, it is necessary to rigidify the complex and it has been showed that inclusion of the metal ion within a macrocycle, especially cyclam, offers just this possibility.<sup>(33)</sup> However, luminescence is favoured only when the cyclam is in a *trans* conformation, with the four nitrogen atoms coplanar with the metal ion, and with a pair of strong field ligands in the axial positions; eg.  $[\text{Cr}(\text{cyclam})(\text{NH}_3)_2]^{3+}$  has a lifetime of 0.5 ms at 77 K.<sup>(33)</sup> In contrast, in *cis* complexes of cyclam, irradiation tends to lead to quite efficient photosolvation, with displacement of the non-macrocyclic ligands, at the expense of intense luminescence. Nevertheless, this process is also potentially interesting if it can be reversed thermally, as it could then be regarded as a bistable switch (figure 3.11).

With these points in mind, it was of interest to attempt to prepare Cr(III) complexes of cyclam in which the coordinating arms (L) are covalently attached to the macrocycle, and ligands such as  $L^1$  were ideally suited as relatively simple systems to investigate this possibility.

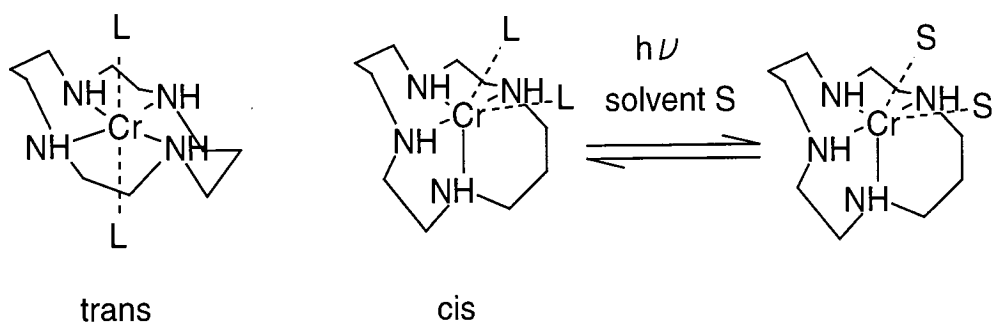


Fig 3.11 – Cis chromium complexes can undergo photosolvation.

The synthesis of  $\text{Cr}(\text{cyclam})\text{L}_2$  complexes is not, however, straightforward, owing to the *kinetic* inertness of chromium(III). Literature studies have shown that the initially formed (*kinetic*) product from reaction of cyclam with  $\text{CrCl}_3$  is always the *cis* isomer, which requires forcing conditions (high temperatures and excess of ligand) to convert it into the *trans* isomer<sup>(31)</sup>. The difficulties are exacerbated by the inertness of the chloride (=L) ligands in these products to displacement by other ligands. One method devised to assist in this is to convert  $[\text{Cr}(\text{cyclam})\text{Cl}_2]^+$  to  $[\text{Cr}(\text{cyclam})(\text{NO}_3)_2]^+$ , by reaction with  $\text{AgNO}_3$  in concentrated nitric acid at  $90^\circ\text{C}$ , the nitrate ligands of which may then be displaced readily by other ligands including amines (see figure 3.12)<sup>(32)</sup>.

The synthesis of the chromium(III) complex of  $\text{L}^1$  was attempted in this way, by reaction of the ligand with  $\text{CrCl}_3$  in DMF at high temperature. However, the procedure did not give satisfactory results, with only low yields being obtained.

The use of chromium(II) chloride proved to be a good solution to this problem. Chromium(II) ( $d^4$ ) is *kinetically* more labile than chromium(III). On the other hand, it is not very stable with respect to oxidation to the +3 state and so it had to be weighed and then rapidly added to a THF solution of the ligand, previously deoxygenated. Then the solution was stirred and gently warmed for 1 hour. Electrospray mass spectrometry

showed a signal for the dichloride complex, although the two possibilities  $[\text{CrL}^1\text{Cl}_2]^+$  (pyridyls not coordinated) and  $[\text{CrL}^1]^{3+} \cdot (\text{Cl}^-)_2$  cannot be distinguished.

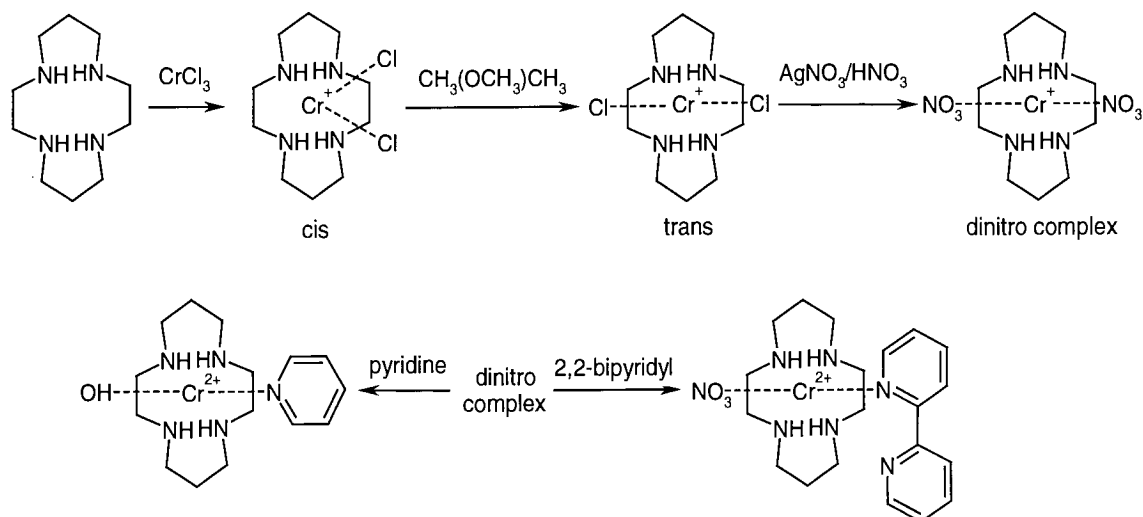


Fig 3.12 – Chromium complexes.

During attempts to crystallise the compound, it was noted that, when acetonitrile was used as the solvent, a green solid precipitated from a deep red solution. After removal of the green powder from the acetonitrile solution, leaving the solution untouched for a few more days led to more green solid, apparently showing the presence of an equilibrium between two isomers, with the green one having lower solubility in acetonitrile.

Unfortunately, it was only possible to obtain crystals suitable for X-ray analysis for the green compound. The crystals were obtained by dissolving the green powder in water and allowing the solution to evaporate slowly (figure 3.13). Selected bond lengths and angles are given in table 10.

In the crystal, the metal ion is hexa-coordinated with the four nitrogens of the macrocycle and with two chlorides. The macrocycle is in a *cis-V* conformation, and the two pyridyl

groups are not coordinated. As found in the copper complex of  $L^1$ , the metal-nitrogen distances are significantly longer for the alkylated nitrogens ( $\sim 2.2$  Å) than for the non-alkylated nitrogens ( $\sim 2.1$  Å). For each pair, however, the bond lengths are not the same, and likewise the distances to the two chloride ligands are not equivalent: 2.325(11) and 2.338(11) Å.

The UV-visible absorbance spectrum of the green solution strongly suggested that the *cis* conformation of the macrocycle was retained in solution: the two observed absorption maxima [ $\lambda_{\text{max}} = 420(136)$  and  $584(197)$  nm] are typical of a *cis* conformation<sup>(32)</sup>.

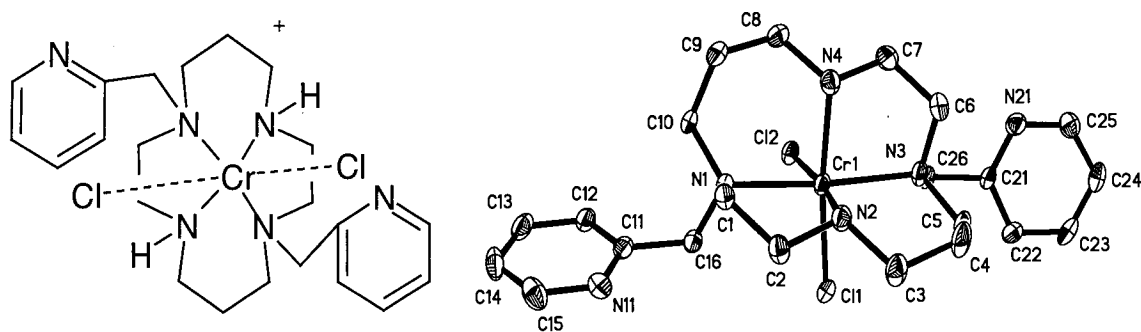


Fig. 3.13 – Molecular structure of  $[\text{Cr}L^1\text{Cl}_2]^+(\text{Cl}^-)\cdot 2\text{H}_2\text{O}$ .

Table 10 - Selected bond lengths (Å) and angles (°) for the chromium(III) complex of  $L^1$ .

Cr-N(2)	2.096(3)	N(3)-Cr-N(1)	168.93(13)
Cr-N(4)	2.109(3)	N(2)-Cr-Cl(1)	88.96(10)
Cr-N(3)	2.191(3)	N(4)-Cr-Cl(1)	172.56(9)
Cr-N(1)	2.201(3)	N(3)-Cr-Cl(1)	90.14(9)
Cr-Cl(1)	2.3252(11)	N(1)-Cr-Cl(1)	97.75(9)
Cr-Cl(2)	2.3385(11)	N(2)-Cr-Cl(2)	172.45(10)
N(2)-Cr-N(4)	92.37(13)	N(4)-Cr-Cl(2)	88.83(9)
N(2)-Cr-N(3)	90.08(12)	N(3)-Cr-Cl(2)	97.46(9)
N(4)-Cr-N(3)	82.54(12)	N(1)-Cr-Cl(2)	90.20(9)
N(2)-Cr-N(1)	82.36(12)	Cl(1)-Cr-Cl(2)	90.80(4)
N(4)-Cr-N(1)	89.68(12)		

In the absence of a crystal structure, the identity of the deep red compound was not clear, but the observation in the electrospray mass spectrum of the correct mass for  $[\text{CrL}^1\text{Cl}_2]^+$  suggests that it may be the *trans* isomer.

The luminescence properties of the two compounds were investigated at low temperature, and the results are listed in table 11. The values of emission wavelength and lifetime are in line with those found for related compounds<sup>(33)</sup>. The emission spectrum of the *cis* isomer is shown in figure 3.14.

	T	$\tau(\text{H}_2\text{O})/\text{ms}$	$\lambda_{\text{ex}}$
Cis	73K	0.30	590 nm
Trans	73 K	0.23	500 nm

Table 11 - Luminescence lifetime of the chromium(III) complex 1,8-bis(2-pyridylmethyl)-1,4,8,11-tetraazacyclotetradecane in MeOH:EtOH=1:1 glass.

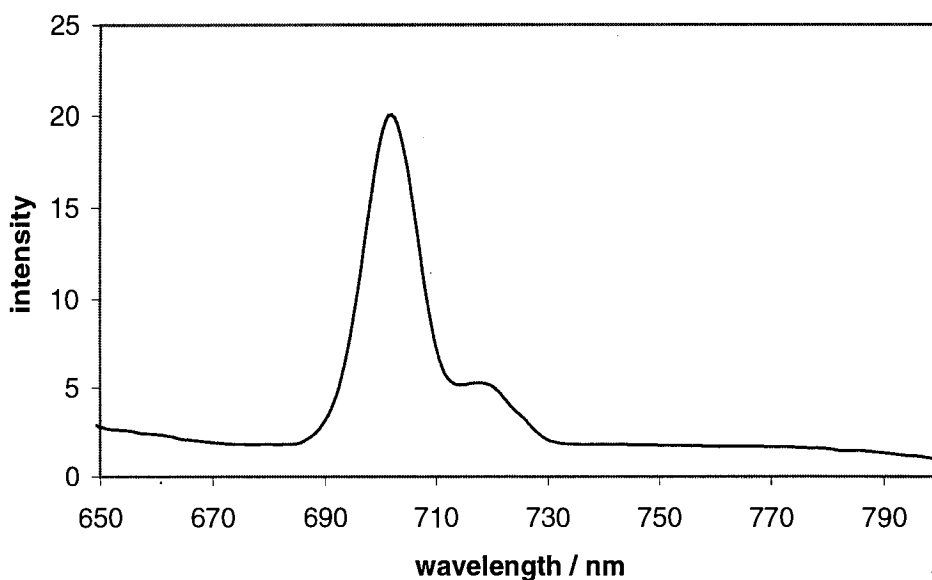


Fig. 3.14 – Emission spectrum of *cis*- $[\text{CrL}^1\text{Cl}_2]^+$ .

Neither complex was luminescent at room temperature. This, too, is predictable if the two chloride ligands are not displaced by the pyridines, based on previous results. Even for *trans*-[Cr(cyclam)Cl<sub>2</sub>]<sup>+</sup>, the chlorides are not sufficiently strong-field ligands to prevent competitive non-radiative deactivation. It is clear, then, that the two chlorides are *kinetically* too inert to be displaced by the pyridine nitrogen atoms under the conditions employed.

For this reason, the dichloro complex was converted into the dinitro, using a solution of AgNO<sub>3</sub>/HNO<sub>3</sub> at 90°C, in order to obtain a chromium complex in which the groups binding the chromium would be easily displaced, as outlined above. The problem was that in this case the complex obtained had a very high affinity for water, and nitro ligands were simply displaced by water molecules instead of by the two pyridyl nitrogen atoms. The use of more weakly coordinating solvents (eg. acetonitrile) was attempted, but was met with the same lack of success.

The solution to this problem may have been found by Sargeson<sup>(34)</sup>, who has built up a cage with six nitrogen atoms around the chromium atom, leading to a long lifetime for a chromium complex at room temperature.

The possibility of sensitising the chromium luminescence by means of the *antenna effect*, was investigated briefly, using the chromium complex of N-(4-benzoyl-phenyl)-3-(1,4,8,11-tetraazacyclotetradec-1-yl)-propionamide (figure 3.15) (made by reaction of this ligand with chromium(II) chloride). The luminescence was investigated at room and low temperature but the benzophenone chromophore didn't sensitise the metal ion. Again, the problem was probably associated with the fact that the non-macrocyclic ligands were



chloride and possibly the fact that the compound formed was the *cis* rather than the *trans* isomer. Unfortunately, time has not allowed further study on isomerisation of the complex or on the displacement of the chlorides by stronger field ligands.

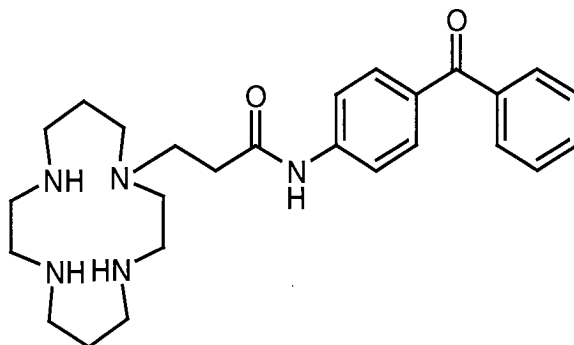


Fig. 3.15 – *N*-(4-benzoyl-phenyl)-3-(1,4,8,11-tetraazacyclotetradec-1-yl)-propionamide ligand.

## 3.6 References

### 3.6.1 Books

- I. J. L. Atwood, J. E. D. Davies, D. D. MacNicol, F. Vogtle and J. M. Lehn, “*Comprehensive Supramolecular Chemistry*”, Pergamon Press, Oxford, 1996, vols 1 and 10.
- II. S. J. Lippard and J. M. Berg, “*Principles of Bioinorganic Chemistry*”, University Science Books, Mill Valley Ca., (1994).
- III. W. Kaim and B. Schwederski, “*Inorganic Elements in the Chemistry of life*”, Wiley, Chichester, (1994).
- IV. J. J. R. F. da Silva and R. P. J. Williams, “*The Biological Chemistry of the Elements*”, OUP, Oxford, (1991).
- V. F. A Cotton and G. Wilkinson, “*Advanced Inorganic Chemistry*”, Wiley, (5<sup>th</sup> Edition), (1988).

### 3.6.2 Articles

1. R. J. Motekaitis, B. E. Rogers, D. E. Reichert, A. E. Martel, and M. J. Welch, *Inorg. Chem.*, **35**, 3821, (1996).
2. G. M. Freeman, E. K. Barefield and D. G. Van Derveer, *Inorg. Chem.*, **23**, 3092, (1984).
3. W. Nam, S. J. Baek, K. A. Lee, B. T. Ahn, J. G. Muller, C. J. Burrows and J. S. Valentine, *Inorg. Chem.*, **35**, 6632, (1996).

4. V. Bulach, D. Mandon and R. Weiss, *Angew. Chem. Int. Ed. Engl.*, **30**, 572, (1991).
5. X. H. Bu, D. L. An, R. H. Zhang, T. Clifford and E. Kimura, *J. Chem. Soc., Dalton Trans.*, 2247, (1998).
6. S. Zhu, F. Kou, C. Lin and Y. Chen, *Inorg. Chem.*, **35**, 5851, (1996).
7. L. Fabbrizzi, M. Licchelli, P. Pallavicini, A. Perrotti, A. Taglietti and D. Sacchi, *Chem. Eur. J.*, **2**, No. 1, 75, (1996).
8. X. H. Bu, X. C. Cao, D. L. An, R. H. Zhang, C. Thomas and E. Kimura, *J. Chem. Soc., Dalton Trans.*, 433, (1998).
9. R. W. Hay, M. P. Pujari, W. T. Moodie, S. Craig, D. T. Richens, A. Perotti and L. Ungaretti, *J. Chem. Soc., Dalton Trans.*, 2605, (1987).
10. L. Cronin, A. R. Mount, S. Parsons and N. Robertson, *J. Chem. Soc., Dalton Trans.*, 1925, (1999).
11. M. W. A. Steenland, A. Dierck, G. G. Herman, B. Devreese, W. Lippens, J. Van Beeumen and A. M. Goeminne, *J. Chem. Soc., Dalton Trans.*, 3637, (1997).
12. E. Kimura, *J. Coord. Chem.*, **15**, 1, (1986).
13. M. Modama and E. Kimura, *J. Chem. Soc., Dalton Trans.*, 325, (1979).
14. L. Fabbrizzi and A. Poggi, *J. Chem. Soc., Chem. Comm.*, 646, (1980).
15. D. Maffeo, H. Puschmann, J. A. K. Howard and J. A. G. Williams, *J. Chem. Soc., Dalton Trans.*, (Submitted).
16. L. Frémond, E. Espinosa, M. Meyer, F. Denat, R. Guillard, V. Huch and M. Veith, *New J. Chem.*, **24**, 959, (2000).
17. M. Chin, D. Wone, Q. Nguyen, L. C. Nathan and P. S. Wagenknecht, *Inorg. Chim. Acta*, **292**, 254, (1999).
18. A. S. Batsanov, A. E. Goeta, J. A. K. Howard, D. Maffeo, H. Puschmann and J. A. G. Williams, *Polyhedron*, **20**, 981, (2001).

19. S. G. Kang, M. S. Kim, J. S. Choi, D. Whang and K. Kim, *J. Chem. Soc., Dalton Trans.*, 363, (1995).
20. C. Benelli, A. Dei, D. Gatteschi and L. Pardi, *Inorg. Chem.*, **27**, 2831, (1988).
21. (a) L. Yu-Juan, C. Li-Qin, N. Shi-Sheng, X. Ji-De and J. Huaxue, *J. Struc. Chem.*, **14**, 44, (1995); (b) idem, *J. Struc. Chem.*, **4**, 42, (1985); (c) X. Ji-De, N. Shi-Sheng and L. Yu-Juan, *Inorg. Chim. Acta*, **61**, 111, (1986).
22. M. A. Donnelly and M. Zimmer, *Inorg. Chem.*, **38**, 1650, (1999).
23. R. D. Hancock et al., *Pure Appl. Chem.*, **65**, 473, (1993).
24. R. D. Hancock, S. M. Dobson, A. Evers, P. W. Wade, M. P. Ngwenya, J. C. A. Boeyens and K. P. Wainwright, *J. Am. Chem. Soc.*, **110**, 2788, (1988).
25. D. Meyerstein, *Coord. Chem. Rev.*, **186**, 141, (1999).
26. (a) M. Studer, A. Raisen and T. A. Kaden, *Helv. Chim. Acta*, **72**, 1253, (1989); (b) for example: V. J. Thorn, C. C. Fox, J. C. A. Boeyens and R. D. Hancock, *J. Am. Chem. Soc.*, **106**, 3198, (1984).
27. H. Aneetha, Y. H. Lai, S. C. Lin, K. Panneerselvam, T. H. Lu and S. C. Chung, *J. Chem. Soc., Dalton Trans.*, 2885, (1999).
28. A. M. Bond and M. A. Khalifa, *Inorg. Chem.*, **26**, 413, (1987).
29. F. E. Mabbs and D. Collison, *Electron paramagnetic resonance of d transition metal compounds*, Elsevier, Amsterdam, (1992).
30. S. Siddiqui and R. E. Sheperd, *Inorg. Chem.*, **25**, 3869, (1986).
31. A. Bakac and J. H. Espenson, *Inorg. Chem.*, **31**, 1108, (1992).
32. J. Ferguson and M. L. Tobe, *Inorg. Chim. Acta*, **4**, 109, (1970).
33. L. S. Forster, *Chem. Rev.*, **90**, 331, (1990).
34. K. N. Brown, R. J. Geue, G. Moran, S. F. Ralph and A. M. Sargeson, *Chem. Comm.*, 2291, (1998).

# **CHAPTER 4**

## **CYCLEN**

## 4.1 Introduction

Luminescent lanthanide(III) complexes are of growing interest owing to their application in solid and solution states from phosphors in television screens to luminescent labels for marking molecules in fluoroimmunoassays and in fluorescence microscopy, or to probes in biological systems<sup>(1,2,3)</sup>.

The design of complexes of lanthanide ions with encapsulating ligands is an important theme in the field of supramolecular chemistry because it offers the possibility to obtain luminescent lanthanide compounds, which are stable in solution. An important aspect of this research is concerned with the optimisation of the luminescence properties of the metal ion by a suitable choice of ligands.

As introduced in the first chapter, an intense luminescence of the lanthanide ion may be obtained by the “antenna effect”. In this process, the chromophore, which has to work as a light collector and then sensitise the lanthanide ion, plays a key role. A more detailed discussion of the criteria behind the choice of the “antenna group” will be presented in the next chapter. As part of the work carried out towards this thesis, some new octadentate ligands based on cyclen have been prepared, suitable for binding lanthanide ions strongly, and incorporating organic chromophores chosen to act as sensitisers of the metal excited state.

In this chapter, the synthetic part of the work will be discussed, while, in the next one, the attention will focus on the analysis of the spectroscopic and luminescent properties of the metal complexes.

## 4.2 Synthesis of the “antenna” groups

Our attention has focused on the investigation of three classes of chromophore as sensitising, or “antenna” groups, namely benzophenone, *para*-substituted acetophenones and hydroxyquinoline. With simple modifications, eight different “antenna” groups were studied, namely the conjugated aromatic parts of the eight alkylating agents A-H in figure 4.1.

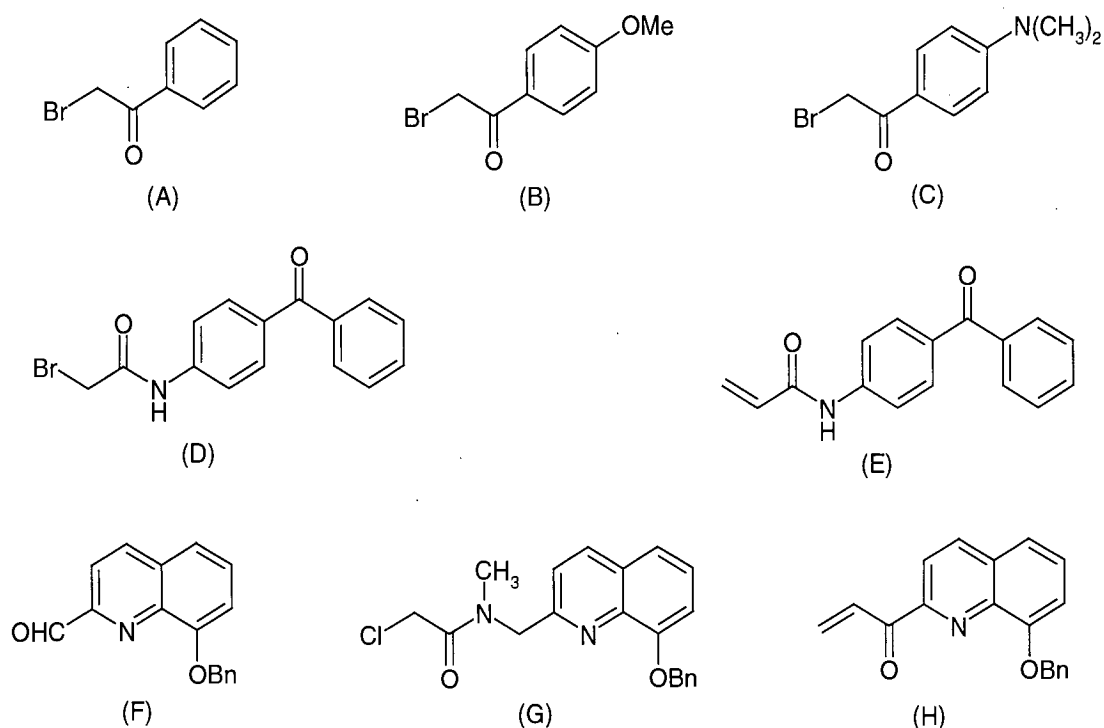


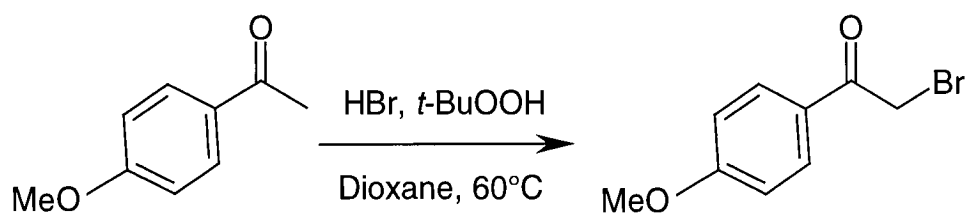
Fig. 4.1 – Compounds used to introduce antenna chromophores onto cyclen.

$\alpha$ -Bromoacetophenone (A) is commercially available. *para*-Dimethylamino- $\alpha$ -bromoacetophenone (C) and the benzophenone-containing  $\alpha$ -bromoamide (D) were provided by Dr. J.A.G. Williams and Dr. A. Beeby, having been prepared according to the published procedure<sup>(4)</sup> starting from 4-aminoacetophenone, and by reaction of 4-aminobenzo

phenone with bromoacetyl bromide, respectively. The syntheses of N-(4-benzophenone) acrylamide (E) and 2-carboxyaldehyde-8-benzyloxyquinoline (F) were described in chapter 2. The synthesis of the remaining alkylating agents, 4'-methoxy-2-bromoacetophenone (B), N-(8-benzyloxy-quinolin-2-ylmethyl)-2-chloro-N-methyl-acetamide (G) and N-(8-benzyloxy-quinolin-2-ylmethyl)-2-vinyl-N-methyl-acetamide (H) will be described in the following sections.

#### 4.2.1 4-Methoxy-2-bromoacetophenone

Bromination of arylmethylketones often leads to a mixture of products, because aromatic ring substitution and bromine addition to the enol often compete with radical side-chain bromination. The former may be particularly troublesome in the presence of activating, electron-donating substituents of which the methoxy group is one. Bedekar et al.<sup>(5)</sup> have found serendipitously that the combination of aqueous *tert*-butyl hydroperoxide and hydrohalic acid, for *in situ* generation of positive halogen species, allows the specific side-chain bromination of acetophenone, with no competitive ring bromination. Hence this methodology was adopted in order to synthesise 4-methoxy-2-bromoacetophenone (scheme 1).



Scheme 1.



A solution of *tert*-butylhydroperoxide (70% aq.) was added to a cooled mixture of hydrobromic acid (48% aq.) in dioxane and the mixture was stirred for a few minutes. 4-Methoxyacetophenone was then added, stirred for half an hour and then heated at 60°C. Work-up led to an excellent yield (85%) of the desired compound, of purity sufficient for continuation in the next step of the synthesis.

### 4.2.2 Antenna group containing the 8-hydroxyquinoline unit

The 8-hydroxyquinoline unit is of particular interest as a potential sensitising group for lanthanide excited states. With a short linker between the chromophore and cyclen ring, we can envisage that the nitrogen and the oxygen atoms could coordinate directly to the cyclen-bound metal ion. The alkylating agent F offers the possibility of achieving such a single carbon linkage, in which the chromophore is brought into very close proximity to the metal (figure 4.2).

On the other hand, if a longer linking group is employed, the nitrogen and oxygen atoms of the chromophore will not be in a position to bind to the metal ion bound within the macrocycle. On the contrary, they will be free to bind to other metal ions or to protons, in which case the sensitising properties of the chromophore will be perturbed, possibly leading to functioning as a sensor. Moreover, the ability to change the linker length offers the opportunity to investigate the effect of distance between energy donor and acceptor on the efficiency of energy transfer. Alkylating agents G and H were proposed in order to provide linker groups of four and three atoms respectively (figure 4.2). The Michael

acceptor functionality of the latter also lends itself to the methodology described in chapter 2 for selective mono-functionalisation of the cyclen ring.

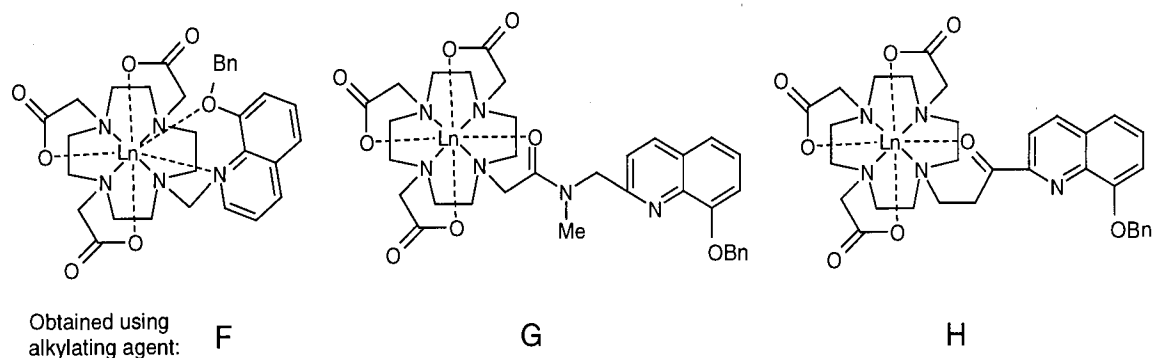


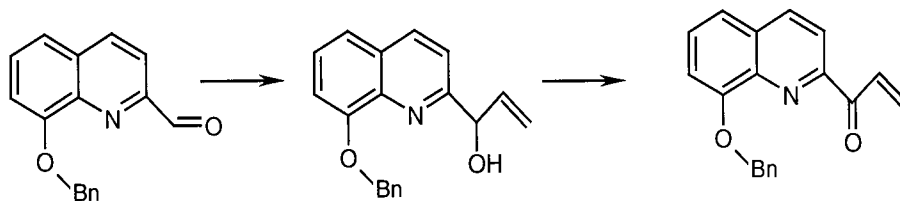
Fig. 4.2 – Complexes of ligands based on the 8-hydroxyquinoline unit.

#### 4.2.2.1 N-(8-benzyloxy-quinolin-2-ylmethyl)-2-vinyl-N-methyl-acetamide

Attempts to prepare this alkylating agent (H) were based on scheme 2. The first step involved the Grignard reaction of the aldehyde with vinyl magnesium bromide under standard Grignard conditions. After work-up, NMR and electrospray mass spectra of the organic layer confirmed the presence of the desired compound.

In order to oxidise the resulting vinylic alcohol to the desired ketone, manganese dioxide was added to the compound in chloroform solution and the mixture refluxed overnight. Electrospray mass spectra showed a mixture of the starting and the final compound. The manganese residues were removed by filtration through celite, the solvent was removed under vacuum and the compound was purified by chromatography on silica gel.

Spectroscopic analyses confirmed the purity of the desired compound but, unfortunately, the yield was very low (3.5%).

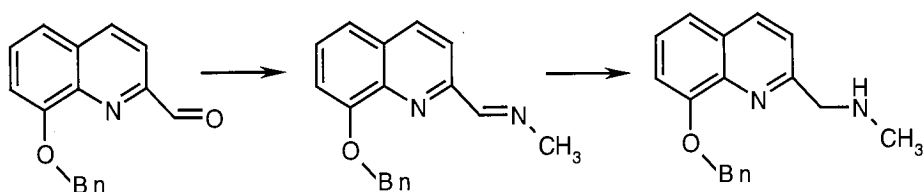


*Scheme 2.*

Repeated attempts gave the same poor result, with the loss of the compound apparently occurring during the chromatographic purification. The separation between the compound and the impurities on alumina TLC was not adequate for alumina chromatography to be employed, and recrystallisation and extraction in different solvents were equally unsuccessful. Hence, it was decided to abandon attempts to prepare this compound and to focus attention on the synthesis of the compound G instead.

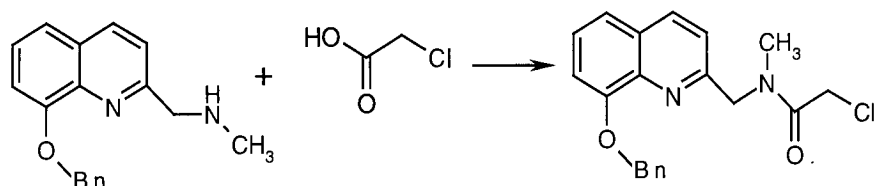
#### 4.2.2.2 N-(8-benzyloxy-quinolin-2-ylmethyl)-2-chloro-N-methylacetamide

The synthesis of the required alkylating agent G was based on the use of compound F, already available, as a starting material. In the first step (scheme 3), the aldehyde was reacted with an equimolar amount of methylamine in methanol, at room temperature, leading to a high yield of the Schiff base.



Scheme 3.

In the second step, the imine was reduced using sodium borohydride in methanol, at room temperature, giving a high yield of the amine (92%). Further derivatisation was accomplished by selective coupling of the secondary amine with chloroacetic acid, using the coupling agent 1-(3-dimethylaminopropyl)-3-ethyl-carbodiimide hydrochloride or EDC (scheme 4).



Scheme 4.

After reaction in dry THF under standard coupling conditions, electrospray mass spectrometry showed the presence of two main products, one the desired one ( $M+Na^+=377$ ), while the second corresponded to the mass of the desired compound without the chlorine atom ( $M^+=319$ ).

Sometimes, during the acquisition of an electrospray mass spectrum, the cone voltage of the instrument may be higher than is required, and may produce a bond cleavage. However, setting the cone voltage of the instrument to a lower value gave the same result and so the problem was not related to the instrument. From the analysis of the aliphatic

region of the NMR spectrum, it was evident that there were indeed two products, in a ratio 3:2 (figure 4.3).

Using the spectral data available, and based on the reactivity of some related compounds<sup>(6)</sup>, we were quite confident that the secondary, unwanted product obtained was a cyclic derivative of the desired compound (figure 4.3). In fact, observing the aliphatic region of the proton NMR spectrum, it was possible to note the complete correspondence of the 4 pairs of signals (A,B,C,D with A',B',C',D'), with just one exception, two of them are inverted, evidently due to the fact that some protons are in a different environment, hypothetically close to a positive charge (D'). Our supposition was confirmed as well by the analysis of a NOESY spectrum (figure 4.3), in which C' is too far to couple with D', instead C and D couple; moreover, B' and D' couple, while B and D do not.

Other attempts at the synthesis were made, and the conditions were changed in order to increase the proportion of the desired product, but the ratio between the two products was invariably 3:2. Since the presence of the impurity was not expected to be problematic for the subsequent alkylation reaction, the compound was used without purification in the following steps and, as will be discussed in the next section, the desired ligand has been successfully synthesised using this alkylating agent.

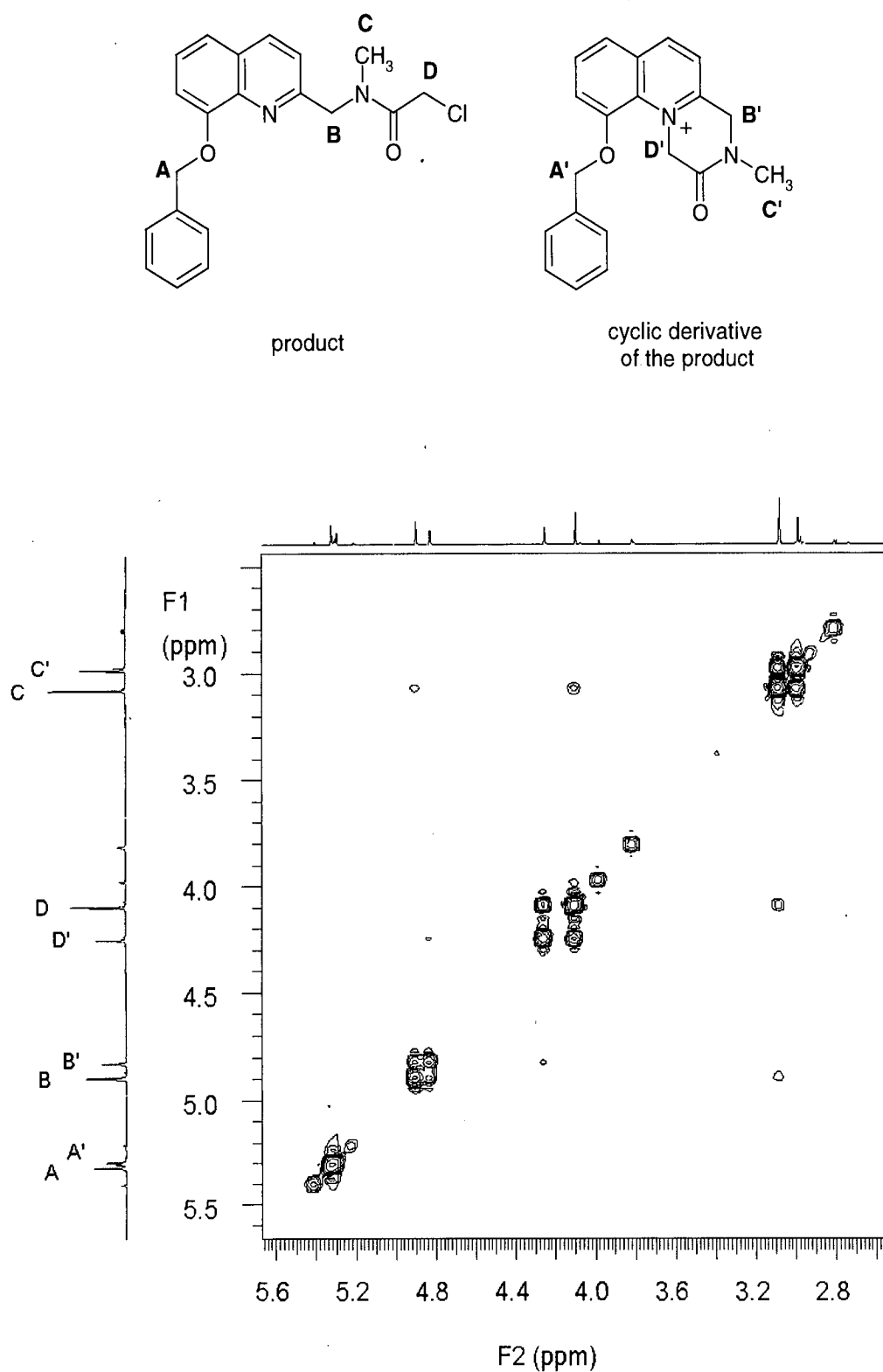
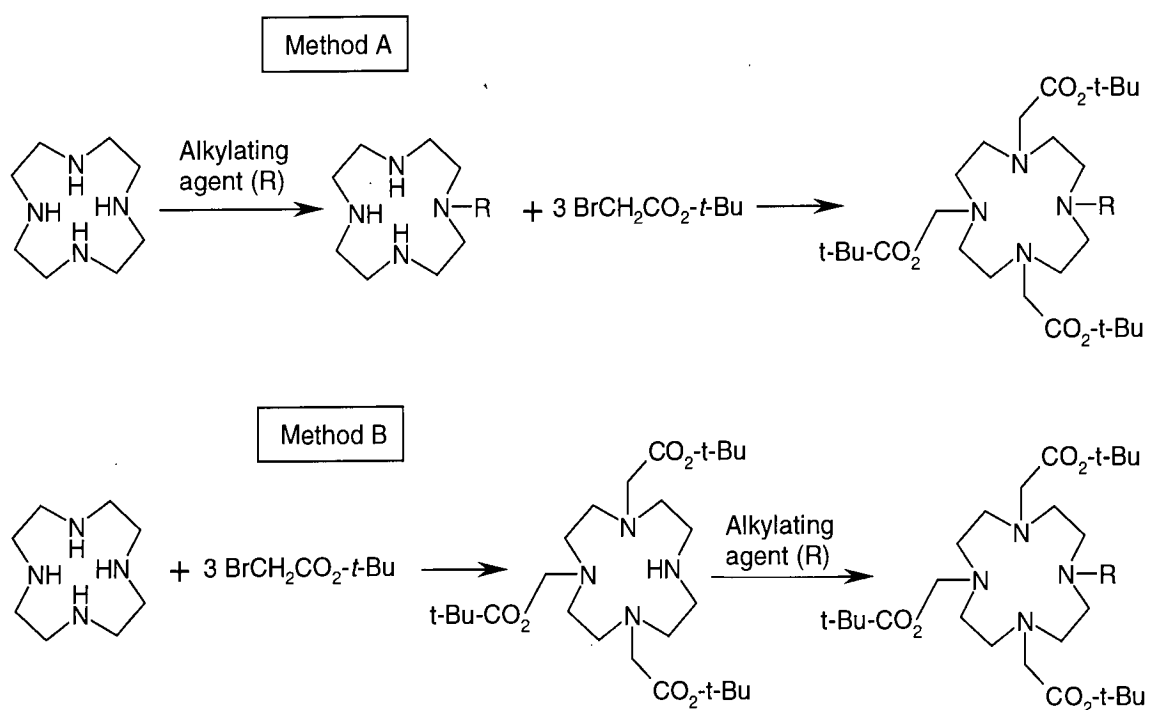


Fig. 4.3 – Aliphatic region of the proton NMR spectrum of the product and its cyclic derivative, and their NOESY spectra.

### 4.3 Synthesis of the N-substituted cyclen ligands

For the synthesis of our ligands, two synthetic strategies are available. It is possible to react the cyclen with the chromophore alkylating agents previously described, and then to react the mono-N-alkylated macrocycle with three equivalents of an ester of  $\alpha$ -bromoacetic acid (scheme 5 – Method A, where the *t*-butyl ester is used) or, on the other hand, to react cyclen with 3 equivalents of *tert*-butylbromoacetate, obtaining the tris *tert*-butyl ester of DO3A, and then in the second step react this with the alkylating agent (scheme 5 – Method B).



Scheme 5.

The issue to overcome in both cases is that of selectivity: the need to ensure *mono*-functionalisation in the first case and *tris*-functionalisation in the second. Kruper et al.<sup>(7)</sup> have shown that reaction of equivalent amounts of free base polyazamacrocycles with an alkyl halide in a nonpolar, aprotic solvent may afford the mono-N-alkylation product in

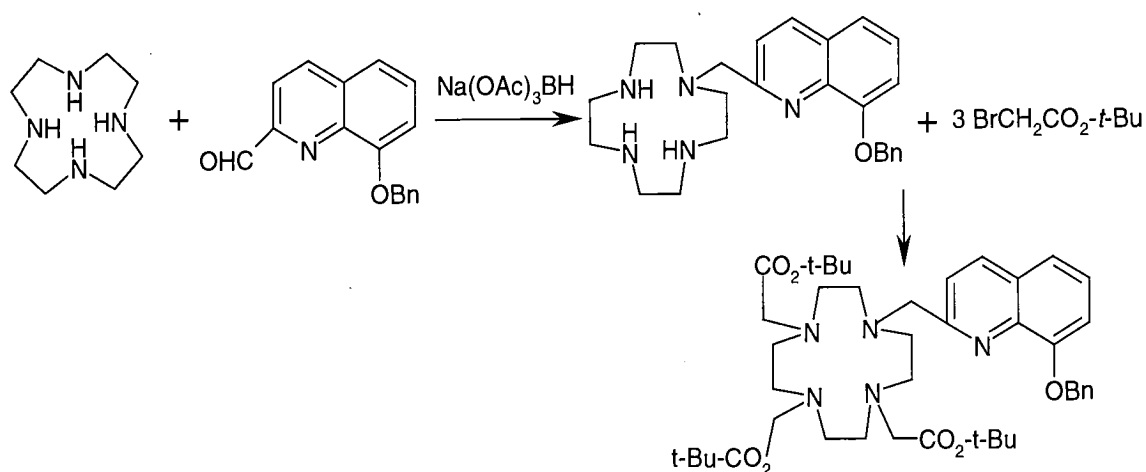
high yield with good selectivity, owing to the high affinity of the alkylated product for a single proton, which attenuates the nucleophilicity of the remaining nitrogen atoms. We decided, however, to follow the method B when possible.

The synthesis of the tris *tert*-butyl ester of DO3A represents the first step of this method, and it was carried out by mixing one equivalent of cyclen with one equivalent of potassium carbonate and 3 equivalents of *tert*-butylbromoacetate in chloroform. Use of the *tert*-butyl group offers better selectivity for tris-substitution than other alkyl groups, presumably due to the steric bulk of the *t*-butyl group inhibiting a fourth N-substitution. The reaction was carefully followed by electrospray mass spectra, adding small excesses of potassium carbonate and *tert*-butylbromoacetate to optimise the proportion of the desired product. The ending point of the reaction was determined by the appearance of the first evidence of DOTA-ester in the mass spectrum. This is because, during purification by silica gel chromatography, it was relatively straightforward to separate any di-substituted derivative from the required compound, but it was very difficult to remove the tetra-substituted (DOTA) derivative.

The DO3A ester was then reacted with the appropriate alkylating agent or Michael acceptor in refluxing acetonitrile, in the presence of potassium carbonate and a catalytic amount of potassium iodide. All the ligands obtained were then purified through chromatography on silica gel. The only exception was represented by the ligand with the benzophenone as appended arm (reaction with D and E); in fact, in this case, the amide functionality of the arm was apparently sensitive to silica, so alumina was employed.



When 8-benzyloxyquinoline-2-carboxaldehyde was used for the synthesis of the ligand, it proved easier to use method A (scheme 6). Cyclen and aldehyde were reacted in the presence of the reducing agent sodium triacetoxyborohydride, following the same procedure introduced in chapter 2 for cyclam (paragraph 2.7.3). The compound was purified by chromatography column on silica gel with a 25% yield. It was then reacted with three equivalents of *tert*-butylbromoacetate in the presence of potassium carbonate in chloroform at room temperature.

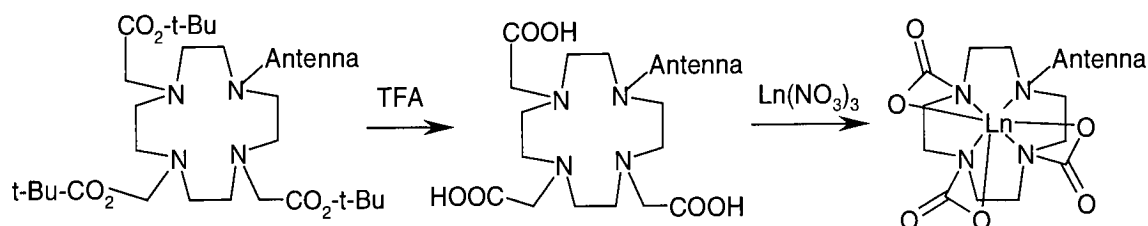


Scheme 6.

#### 4.4 Synthesis of the metal complexes

For the synthesis of the metal complexes, the following typical procedure was adopted (scheme 7). In the first step, the *tris*-acetate ligands were obtained by hydrolysis of the *tris*-butyl esters upon treatment with trifluoroacetic acid. In practice, the ligands were dissolved in the smallest necessary amount of dichloromethane and 20 equivalents of trifluoroacetic acid were added to this solution. The solution was then stirred at room temperature for 24 hours, the solvent was removed under vacuum, and the residue washed

with more dichloromethane. This step was usually repeated three or four times, to facilitate the elimination of the volatile trifluoroacetic acid.

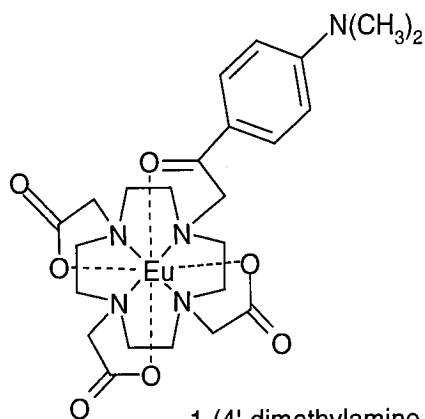


Scheme 7.

In the second step, the compound was taken into water, and the pH was adjusted to 6-7 by addition of 1M sodium hydroxide. The lanthanide(III) complexes were prepared by addition of an equimolar amount of the lanthanide(III) nitrate to the aqueous solution of the ligand. The solution was then refluxed overnight. To purify the metal complexes, alumina was added and the solvent removed under reduced pressure until the solid was dry and free flowing. The alumina with adsorbed complex was added to the top of a short column of alumina, and eluted with a solution of dichloromethane containing an increasing proportion of methanol.

Electrospray mass spectra were used to confirm the purity of the desired compounds, and for every ligand, at least one of the final metal complexes was analysed using high-resolution electrospray mass spectroscopy. This is particularly important for the complexes of terbium and, especially gadolinium, whose large paramagnetism prohibits analysis by NMR. On the other hand, the smaller shifts and narrower line-widths associated with europium(III) allow  $^1\text{H}$  NMR spectra of the europium complexes to be recorded, which often prove to be very diagnostic of the coordination geometry (figure 4.4). A full assignment of the individual resonances requires a specific dipolar shift

analysis, which is beyond the interests of our work; nevertheless the spectra showed very clearly the characteristic pattern of resonances typical of these and related complexes, in which the rigidity imposed by the metal ion leads to the inequivalence of the four protons of each ethylene unit in the macrocycle. <sup>(8,9)</sup>



Europium complex of  
1-(4'-dimethylamino-2-acetophenone)-4,7,10-tris(*tert*-butoxycarbonylmethyl)-cyclen

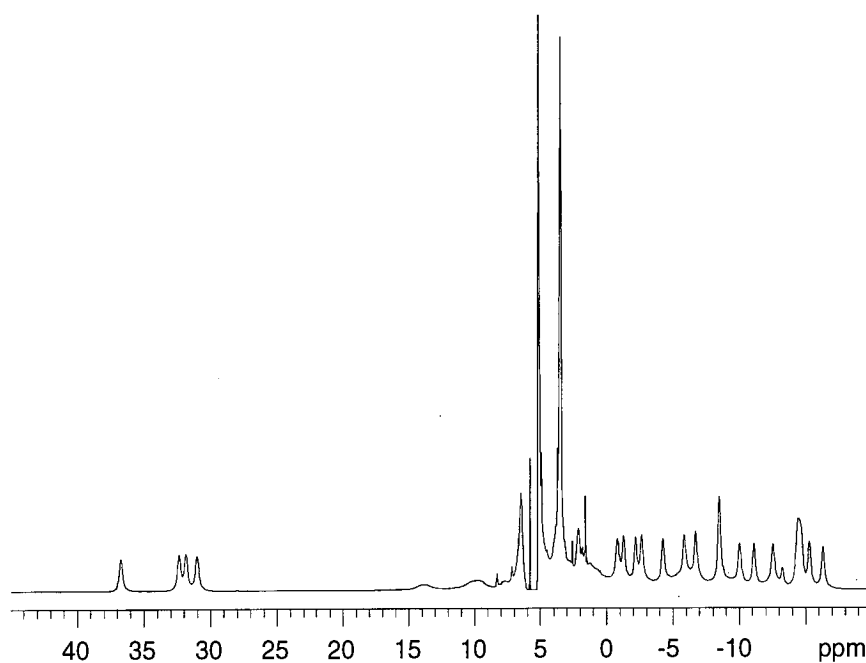
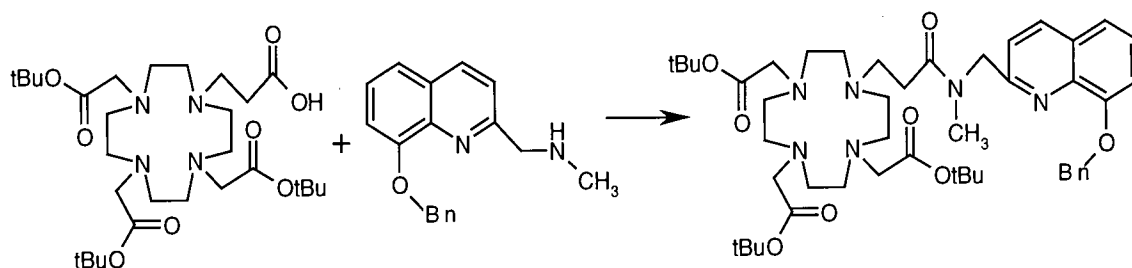


Fig. 4.4 – Example of <sup>1</sup>H NMR spectrum of one of the europium complexes.

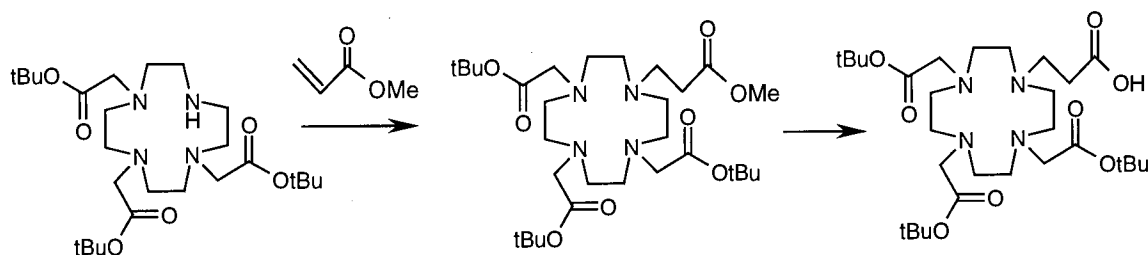
## 4.5 Alternative synthetic route to DOTA-type ligands with amide-linked chromophores

Since the synthesis of the alkylating agent G resulted in a mixture of the desired compound and impurities, a different approach was attempted. The amino derivative of the 8-benzyloxyquinoline-2-carboxaldehyde introduced in the previous paragraph was used as a starting compound to be coupled with an appropriately substituted macrocycle (scheme 8).



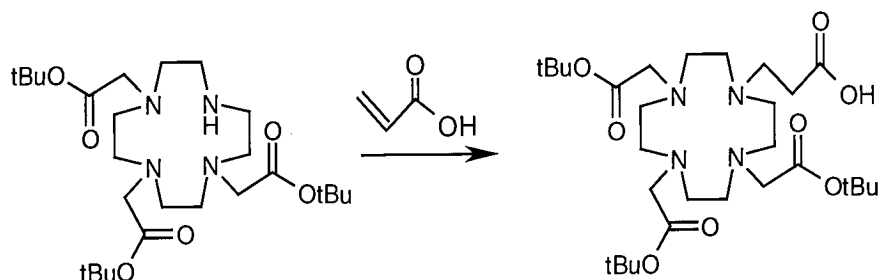
Scheme 8.

The synthesis of the DOTA system required for the coupling reaction is shown in scheme 9. The tris *tert*-butyl ester of DO3A was reacted with methyl acrylate in refluxing acetonitrile, in the presence of potassium carbonate. The reaction proceeded slowly, so an excess of methyl acrylate was added. The compound was purified by chromatography on alumina.



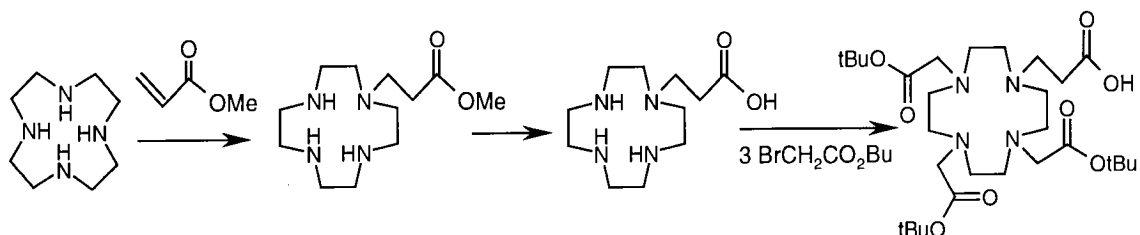
Scheme 9.

In the second step, we attempted the selective cleavage of the methyl from the carboxylic group, keeping the *tert*-butyl protection. Unfortunately, all attempts failed. Hence, a different strategy was considered, in which the DO3A was reacted with acrylic acid (scheme 10).



Scheme 10.

However, this reaction also failed. One further method was attempted, involving the reaction of cyclen with methyl acrylate, followed by cleavage of the methyl group and alkylation of the three nitrogen atoms of the cyclen (scheme 11).



Scheme 11.

However, this strategy proved equally unsuccessful and so it became clear that the method described in section 4.2, despite the presence of impurities during the reaction sequence, was eventually the best after all.

## 4.6 References

### 4.6.1 Articles

1. G. Blasse and B. C. Grabmaier, *Luminescent Materials*, Springer-Verlag, New York, (1994).
2. I. Hemmilä, V. M. Mikkala and H. Takalo, *J. Alloys Compds.*, **249**, 158, (1997).
3. M. Elbanowski and B. Makowska, *J. Photochem. Photobiol. A: Chem.*, **99**, 85, (1996).
4. Z. Diwu, C. Beachdel and D. H. Klaubert, *Tetrahedron. Lett.*, **39**, 4987, (1998).
5. N. B. Barhate, A. S. Gajare, R. D. W. Wakharkar and A. V. Bedekar, *Tetrahedron*, **55**, 11127, (1999).
6. L. J. Govenlock and D. Parker, *Unpublished Work*, University of Durham, (1999).
7. W. J. Kruper, P. R. Rudolf and C. A. Langhoff, *J. Org. Chem.*, **58**, 3869, (1993).
8. S. Aime, M. Botta, D. Parker and J. A. G. Williams, *J. Chem. Soc., Dalton Trans.*, 2259, (1995).
9. R. S. Dickins, J. A. K. Howard, C. L. Maupin, J. M. Moloney, D. Parker, J. P. Riehl, G. Siligardi and J. A. G. Williams, *Chem. Eur. J.*, **5**, 1095, (1999).

# **CHAPTER 5**

## **LUMINESCENCE PROPERTIES OF LANTHANIDE COMPLEXES**

## 5.1 Sensitisation of lanthanide(III) excited states

As introduced in the first chapter, the quantities that contribute to the overall quantum yield of luminescence,  $\Phi_{\text{lum}}$ , of a lanthanide ion excited by a sensitiser, are: (i) the quantum yield of triplet formation of the sensitiser,  $\Phi_{\text{T}}$ , (ii) the efficiency of the ligand-to-metal energy transfer,  $\eta_{\text{ET}}$ , and (iii) the efficiency of the metal-centred luminescence,  $\eta_{\text{Ln}}$ . It is evident from the equation (1) that all three terms play an equally important role.

$$\Phi_{\text{lum}} = \Phi_{\text{T}} \eta_{\text{ET}} \eta_{\text{Ln}} \quad (1)^{(1)}$$

Given this equation, it is perhaps surprising that until now the chromophores chosen for incorporation into ligands normally have triplet quantum yields considerably less than unity. Compounds suitable for this kind of application should clearly have a large triplet quantum yield and ideally have the benefit of a small singlet-triplet energy gap in order to allow long wavelength excitation. For this reason, benzophenone and acetophenones were our choices as moieties to couple with cyclen, as their  $n,\pi^*$  triplet states are populated with high efficiency.

In order to sensitise the metal ion, the energy of the excited state of the antenna group should be higher than that of the excited emissive state of the metal ion, and preferably by at least  $1500 \text{ cm}^{-1}$  in order to inhibit back energy transfer. The optimum energy for a sensitiser has been found to be  $\sim 2000 \text{ cm}^{-1}$  above the excited state of the  $\text{Ln}^{3+}$  ion.<sup>(2)</sup>

Enhanced spin-orbit coupling occurs in aromatic ketones such as benzophenone, due to the role played by the carbonyl group of the aromatic ketone, which imparts  $n\pi^*$  character



to the lowest excited state of the molecule. Therefore molecules of this type have high triplet yields and, in fact, benzophenone does not fluoresce, since intersystem crossing to the triplet state occurs so rapidly.<sup>(3)</sup> On the other hand, it is possible to observe phosphorescence from the triplet state even at room temperature, provided that the solution is deoxygenated.

Despite their potentially attractive properties, up to now, there are very few examples of the use of aromatic ketones as sensitisers of lanthanide ions. In recent work,<sup>(4)</sup> the formation of a highly luminescent bimolecular complex between europium [as the tris(6,6,7,7,8,8,8-heptafluoro-2,2-dimethyloctane-3,5-dione) complex] and Michler's ketone [4,4'-bis(dimethylamino)benzophenone], was reported with  $\Phi_{\text{lum}} = 0.20$ , demonstrating that the energy transfer process from the substituted benzophenone to the metal ion occurred readily. It was already shown that intermolecular sensitisation of  $\text{Eu}^{3+}$  and  $\text{Tb}^{3+}$  by benzophenone chromophore can occur.<sup>(5)</sup>

In another recent example,<sup>(6)</sup> it was reported that the europium and terbium complexes of a ligand containing an acetophenone group have outstandingly high luminescence quantum yields,  $\Phi_{\text{lum}} > 0.90$ . Thus, a more detailed investigation in which acetophenone or benzophenone groups would be incorporated into *kinetically* stable europium and terbium complexes, looked very promising.

The luminescence data discussed in paragraphs 5.3 and 5.4 have been obtained by L. M. Bushby, who carried out studies towards her Ph.D. over the period 1998-2001 at the University of Durham, and are more extensively presented in her Ph.D. thesis, which is focused on luminescence.

## 5.2 Desired properties of the ligands

As introduced previously, the advantage of using lanthanides is that a time-resolved detection procedure may be employed, overcoming the problem of interference from background fluorescence present in biological media, or in typical samples from the environment. Nevertheless, there are also some problems associated with the use of lanthanides, which need to be overcome.

One of these is related to the deactivation of the metal emissive state by solvent water molecules. It is important, therefore, that the ligand should be able to shield the metal from the solvent water molecules, by occupying as many of the metal coordination sites as possible. This also serves to increase the kinetic stability of the complex with respect to dissociation of the metal ion. Aminocarboxylate ligands such as DOTA and its derivatives are successful in occupying eight of the lanthanide coordination sites. However, this still leaves sufficient space for a water molecule to bind in a ninth site. One way in which binding of such a water molecule may be disfavoured appears to be the replacement of the acetate arms by larger, “harder” phosphinates.<sup>(7)</sup> However, another possibility, in the case in which the antenna group is coordinating to the metal, is the presence of a sterically encumbering moiety linked to the antenna that could effectively shield the metal from the solvent water molecules. A solution of this type will be discussed in the section later in this chapter in which the ligand based on quinaldine will be reported.

A second problem is the weakness of the bands observed in the absorption spectra of lanthanide(III) ions due to their low molar absorption coefficients. The use of sensitised

emission, as discussed in the previous paragraph, can overcome this problem, provided that the quantities  $\Phi_T$  and  $\eta_{ET}$  in equation 1 are appropriate.

The final problem linked to the use of lanthanide(III) stems from the stability of the complexes with respect to the metal ion dissociation. Lanthanides have a high affinity for water molecules as ligands, and do not form stable complexes with simple monodentate ligands. To fulfil the desired requirements, a complex should be very stable at high dilution over a wide range of pH, and the use of cyclen with acetate arms, as in DOTA and its derivatives, offers a very satisfactory solution.<sup>(8,9,10)</sup>

### 5.3 Ligands based on acetophenone

The photophysical properties of complexes of three ligands based on acetophenone,  $H_3L^7$  (acetophenone),  $H_3L^8$  (methoxy-acetophenone) and  $H_3L^9$  (dimethylamino-acetophenone), have been investigated (figure 5.1). The metal ions are chelated by a DOTA type system, in which a ketone takes the place of one of the acetates, and to which the aryl chromophore is covalently bound.

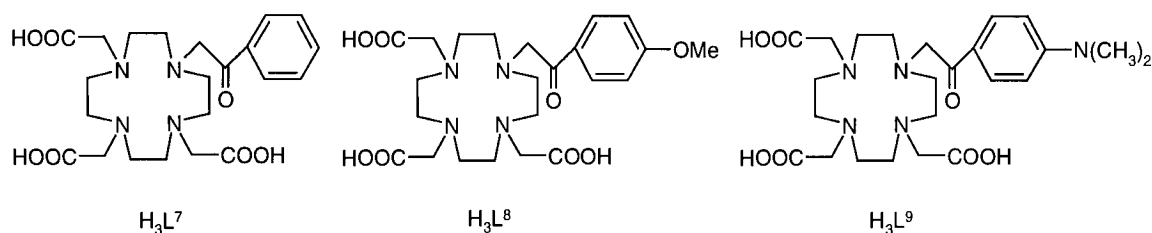


Fig. 5.1 – Ligands based on acetophenone.

### 5.3.1 Absorption spectra

The complexes of L<sup>7</sup> displayed ground-state absorbance maxima at 265 nm in aqueous solution. As expected the value was not significantly different from that of the free ligand or acetophenone itself; in fact, the phenyl ring is only a weak electron donor, and charge transfer between the chromophore and the lanthanide(III) ions does not occur to any significant extent.

When a methoxy group was introduced in the *para* position of the acetophenone, the corresponding band in the ligand was red-shifted to 305 nm as a result of the conjugation of the electron-donating methoxy group with the carbonyl acceptor of the acetophenone; again, the spectra of the complexes were not significantly different from that of the ligand.

The corresponding band in the ligand with the more strongly donating dimethylamino group in the *para* position is shifted to 339 nm, because the dimethylamino substituent has a much larger effect on the  $\pi-\pi^*$  singlet excited state of the complex. Moreover, the band is further red-shifted in the complexes by more than 30 nm, with a maximum at 372 nm, and extending to beyond 400 nm (figure 5.2). The large red-shift in the complex compared to the ligand is indicative of significant charge-transfer character, due to the stronger interaction of the carbonyl group with the metal ion, and in which the electron distribution may be thought of in terms of a resonance hybrid between the two canonical forms shown in figure 5.3.

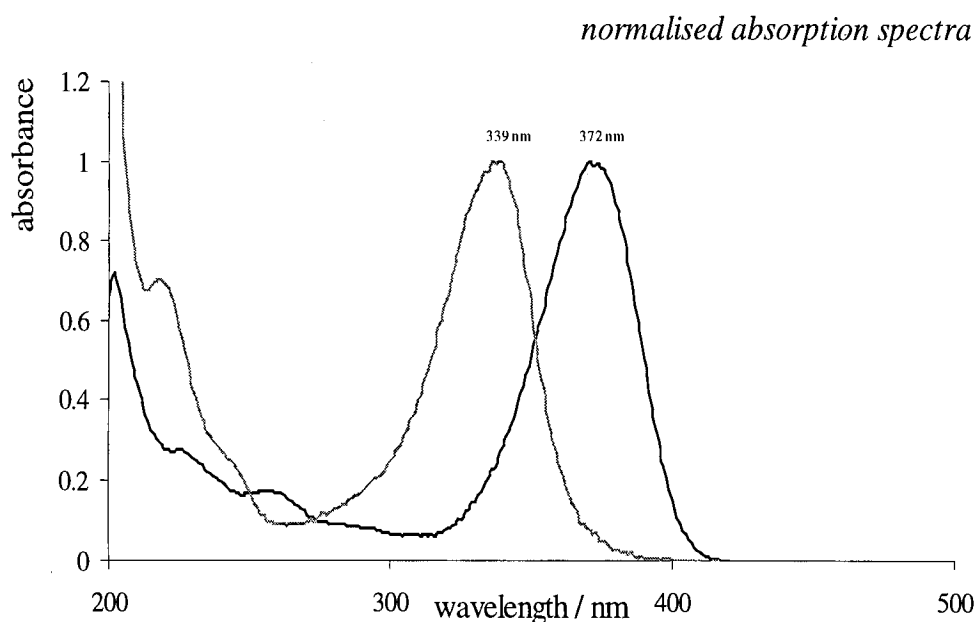


Fig. 5.2 – Absorption spectra of free ligand  $H_3L^9$  (a) and its metal complex  $LnL^9$  (b) in ethanol.

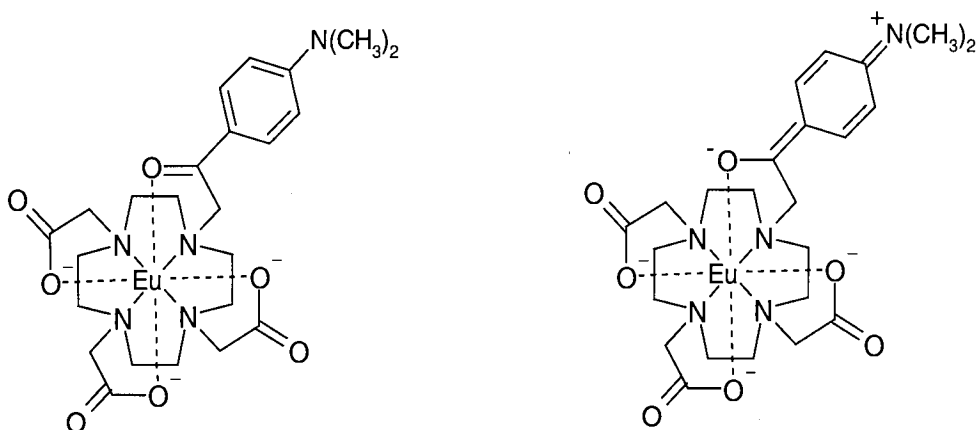


Fig. 5.3 – Two possible forms of  $[Eu^{3+}(L^9)^{3-}]$ .

### 5.3.2 Phosphorescence of gadolinium complexes

The  $Gd^{3+}$  ion does not have any excited state energy levels, which are lower in energy than the acetophenone  $S_1$  or  $T_1$  states. Not surprisingly, therefore, no metal-based emission was observed in aqueous and EPA solutions of the  $Gd^{3+}$  complexes at room

temperature. On the other hand, upon cooling to 77 K, the complexes displayed intense phosphorescence with some vibrational structure, due to emission from the  $n-\pi^*$  triplet state of the chromophore. Observation of phosphorescence requires the use of a frozen glass at low temperature because the chromophore triplet state is readily deactivated at room temperature by collisions with other species and by dissolved  $O_2$ . The values of  $25600 \pm 200 \text{ cm}^{-1}$  in EPA and  $25300 \pm 200 \text{ cm}^{-1}$  in water for the triplet energy of  $GdL^7$  were determined from the position of the highest energy band in the spectrum. As observed for the singlet excited state, (from the absorbance spectrum), introduction of the methoxy or dimethylamino substituents leads to a progressive reduction in the energy of the triplet state: a value of  $24500 \pm 200 \text{ cm}^{-1}$  was determined for  $GdL^8$  (EPA and water), and, for  $GdL^9$ , the values obtained were  $21200 \pm 200 \text{ cm}^{-1}$  in EPA, and  $20000 \pm 200 \text{ cm}^{-1}$  in water. The phosphorescence lifetimes of the complexes  $GdL^7$ ,  $GdL^8$  and  $GdL^9$  were also recorded at 77K in EPA and were determined to be respectively 10.4, 7.9 and 15.9 ms.

### 5.3.3 Emission spectra and lifetimes of europium complexes

If the energy levels of the acetophenone-based complexes are not high enough to act as sensitizers of the lowest excited state of gadolinium(III) [ $E(^6P_{7/2}) = 32000 \text{ cm}^{-1}$ ], they are, on the other hand, appropriately positioned for the sensitization of europium(III) [ $E(^5D_0) = 17300 \text{ cm}^{-1}$ ,  $E(^5D_1) = 19000 \text{ cm}^{-1}$ ] and terbium(III) [ $E(^5D_4) = 20500 \text{ cm}^{-1}$ ]. In alcohol and aqueous solution, both metal complexes  $EuL^7$  and  $EuL^8$  displayed intense metal-centred luminescence upon excitation into the  $\pi-\pi^*$  bands. That the emission was due to sensitization by the chromophore, rather than direct metal excitation, is proved by the fact

that the luminescence excitation spectra corresponded well with the ground-state absorption spectra.<sup>(11)</sup>

In table 1 are listed the lifetimes of emission. Using the Horrocks<sup>(12)</sup> equation and the values of lifetimes in water and deuterated water, it is possible to obtain the hydration number  $q$  (which provides an indication of the number of metal-bound water molecules). For the complexes EuL<sup>7</sup> and EuL<sup>8</sup>,  $q$  was found to be 1.24 and 1.20 respectively (table 1). When the weaker effect of outer-sphere water molecules is taken into account, these values are reduced to 1.10 and 1.05,<sup>(13)</sup> clearly indicating that there is one metal-bound water molecule. Observations on complexes of structurally related octadentate amide ligands, which are nine-coordinated with one metal-bound water molecule,<sup>(14)</sup> are consistent with this result, which also lends support to the assumption that the carbonyl oxygen is coordinated to the metal, shielding it from the interaction with further water molecules.

Complex	$E_T/\text{cm}^{-1}$ (a)	Absorbance $\lambda_{\text{max}}/\text{nm}$	$\tau_{\text{H}_2\text{O}}/\text{ms}$ (b)	$\tau_{\text{D}_2\text{O}}/\text{ms}$ (b)	$q$	$\Phi_{\text{H}_2\text{O}}^{(c)}$	$\Phi_{\text{D}_2\text{O}}^{(c)}$
EuL <sup>7</sup>	25600 <i>25300</i>	265	0.62	2.26	1.24	0.006	0.021
EuL <sup>8</sup>	24500 <i>24500</i>	305	0.63	2.18	1.20	0.098	0.34
EuL <sup>9</sup>	21000 <i>20000</i>	375	---	---	---	---	---

(a)  $E_T$  measured from the corresponding Gd complexes in EPA solution. Value in italic is that recorded in aqueous solution. (b) Lifetimes of the metal-centred emission monitored at 593 nm, 293K; excitation was at  $\lambda_{\text{max}}$  in the absorbance spectrum. (c) Quantum yield at 293K, measured using cresyl violet in MeOH and rhodamine 101 in acidified EtOH as standards.

Table 1.

The emission spectrum of  $\text{EuL}^7$  is shown in figure 5.4 and that of  $\text{EuL}^8$  is quite similar. A moderately intense  $^5\text{D}_0\text{-}^7\text{F}_0$  band at 579.8 nm is observed in each case; the integrated emission intensities of the  $\Delta J=1,2$  and 4 bands are approximately equal for  $\text{EuL}^7$ , in  $\text{EuL}^8$  the only difference is that the hypersensitive  $\Delta J=2$  is a little more intense. The  $\Delta J=2/\Delta J=1$  ratio can give an idea of the symmetry and polarisability of the donors around the metal ion. In symmetric sites, values are typically  $<1$ , in more asymmetric sites values are much higher, generally in the range 10-40. For the complexes  $\text{EuL}^7$  and  $\text{EuL}^8$  the values of the ratio are respectively 0.7 and 1.3, indicative in both cases of a highly centrosymmetric environment of the metal ion, with the latter being a little more distorted, probably due to the presence of the electron donating methoxy group in *para* position, which influences the polarisation of the carbonyl of the ketone and consequently the electric field around the europium(III) ion. The polarisability will be discussed more extensively when the  $\text{EuL}^9$  complex will be introduced below.

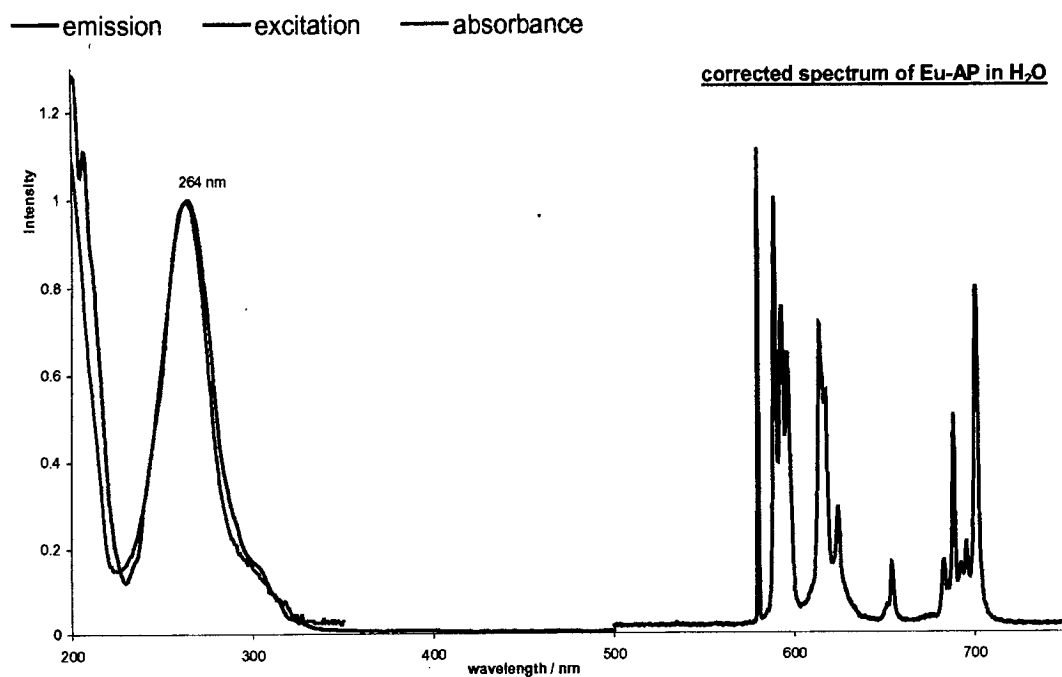


Fig. 5.4 – Emission spectrum of  $\text{EuL}^7$  in  $\text{H}_2\text{O}$ .



In table 1 are shown as well the overall quantum yields of metal-centred luminescence. Keeping in mind the equation 1 (paragraph 5.1), it would be possible to use the quantum yields to estimate the efficiency of energy transfer  $\eta_{ET}$ , but an approximate calculation of  $\Phi_T$  and  $\eta_{Ln}$  is necessary. Due to the fact that the sensitizer has an  $n,\pi^*$  triplet state, and also that the lanthanide ions have high spin-orbit coupling constants, it is appropriate to assume that the quantum yield of triplet formation ( $\Phi_T$ ) is close to one. When the pure radiative lifetime  $\tau_R$  is available, and having recorded the observed emission lifetime  $\tau_{obs}$ , it is possible to calculate the efficiency of metal-centred luminescence,  $\eta_{Ln}$ , using the equation 2:

$$\eta_{Ln} = \tau_{obs} / \tau_R \quad (2)$$

It has been reported in the literature how the pure radiative lifetime of europium(III) in different environments can be estimated from the emission spectrum.<sup>(15,16,17)</sup> The total radiative relaxation rate  $k_R$  ( $=1/ \tau_R$ ) of the emissive excited state  $^5D_0$  is the sum of the spontaneous emission probabilities,  $A(0,J)$ , to the lower J levels:

$$k_R = \sum_J A(0,J) \quad (3)$$

The relative contribution of each  $^5D_0 \rightarrow ^7F_J$  transition to the spectrum, the branching ratio  $\beta$ , is the ratio of the intensity of the band to the total intensity in the *corrected* emission spectrum, and is determined by the spontaneous emission probability:

$$\beta(0,J) = A(0,J) / \sum_J A(0,J) = A(0,J) / k_R = A(0,J) \cdot \tau_R \quad (4)$$

The forbidden lanthanide(III) *f-f* emission bands normally consist of magnetic dipole (MD) and induced electric dipole (ED) transitions. The former are virtually independent of the ion's surroundings, in contrast to the latter where the geometry and ligating atoms

have a significant effect on the transition probabilities. The  ${}^5D_0 \rightarrow {}^7F_1$  (J1) band of  $\text{Eu}^{3+}$  centred at 593 nm is entirely MD and consequently has an oscillator strength that is independent of the ligand field and complex symmetry.<sup>(18)</sup> Thus, given a value for the spontaneous emission probability  $A(0,1)$  of the  ${}^5D_0 \rightarrow {}^7F_1$  transition and using the previous equation, it is possible to estimate  $\tau_R$  from the relative contribution of this band to the experimentally determined emission spectrum:

$$1/\tau_R = A(0,1) / \beta(0,1) = A(0,1) \cdot [I_{\text{tot}} / I(0,1)] \quad (5)$$

where  $[I_{\text{tot}}/I(0,1)]$  is the ratio of the total integrated intensity of the corrected europium(III) emission spectrum to the intensity of the  ${}^5D_0 \rightarrow {}^7F_1$  band. The spontaneous emission probability,  $A(0,1)$ , can be determined directly from the theoretically calculated dipole strength of this transition, leading to a value of  $32.4 \text{ s}^{-1}$  in aqueous solution.<sup>(19)</sup>

For complexes  $\text{EuL}^7$  and  $\text{EuL}^8$ , the results of these calculations using the relative contribution of the J1 band in the corrected emission spectrum together with the experimentally determined values of  $\tau_{\text{obs}}$  and  $\Phi_{\text{lum}}$  in conjunction with the equations 1,2 and 3, leads to the values of  $\tau_R$ ,  $\eta_{\text{Ln}}$ ,  $\eta_{\text{ET}}$  and  $\Sigma k_{\text{nr}}$  given in table 2.

	$\text{EuL}^7$		$\text{EuL}^8$	
	$\text{H}_2\text{O}$	$\text{D}_2\text{O}$	$\text{H}_2\text{O}$	$\text{D}_2\text{O}$
$[I_{\text{tot}} / I(0,1)]$	0.24	0.25	0.22	0.21
$\tau_R / \text{ms}$	7.37	7.74	6.65	6.62
$k_R / \text{s}^{-1}$	136	129	150	151
$\tau_{\text{obs}} / \text{ms}$	0.62	2.26	0.63	2.18
$\eta_{\text{Ln}}$	0.084	0.29	0.094	0.33
$\Phi_{\text{tot}}$	0.058	0.21	0.093	0.34
$\eta_{\text{ET}}$	0.071	0.72	0.99	1.04
$\Sigma k_{\text{nr}} / \text{s}^{-1}$	1480	313	1440	308

Table 2.

It can be seen that the energy transfer efficiencies are high in each case and especially so for the methoxy-substituted system. The introduction of the methoxy substituent lowers the triplet energy by about  $1000\text{ cm}^{-1}$  (table 1), leading to a better match with the acceptor states,  $^5D_1$  and  $^5D_0$  of the europium ion. As expected,  $\eta_{ET}$  does not change significantly on going from  $H_2O$  to  $D_2O$ , and the main factor that limits the observed luminescence quantum yield of these complexes is the rather low efficiency of metal-centred luminescence, even in  $D_2O$ .

The complex  $EuL^9$  behaves in a different way from its parent complexes. The emission spectra recorded upon excitation of the dimethylaminobenzene group in a number of non-aqueous solvents show that the hypersensitive  $\Delta J=2$  transition is considerably more intense in the spectra, relative to the  $\Delta J=1$  band. The ratio of the integrated intensity of each of the  $^5D_0 \rightarrow ^7F_J$  bands to the  $^5D_0 \rightarrow ^7F_1$  intensity for the three complexes, shows that the relative intensity of the  $\Delta J=2$  transition increases progressively upon going from the unsubstituted to the methoxy- and subsequently dimethylamino-substituted complexes (figure 5.5).

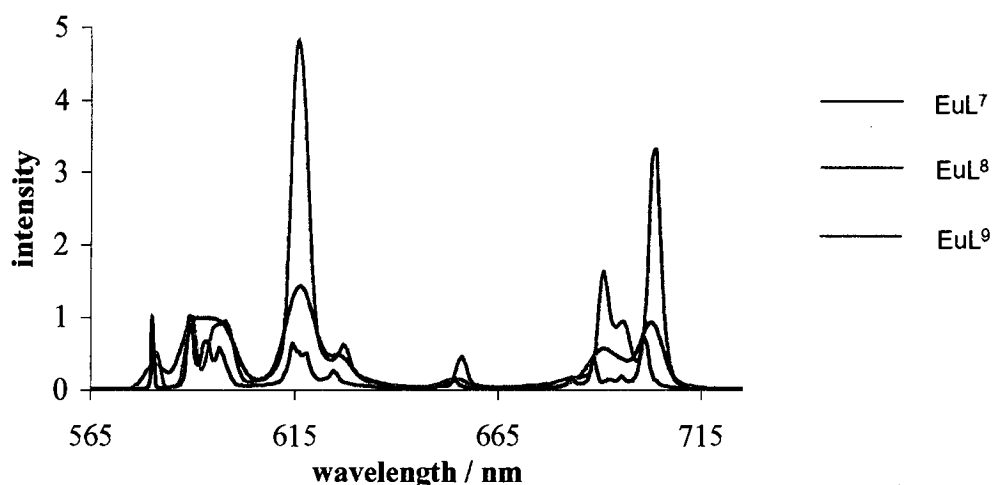


Fig. 5.5 – Emission spectra of the  $EuL^7$ ,  $EuL^8$  and  $EuL^9$  in ethanol.

As introduced before, the *f-f* emission bands normally consist of magnetic dipole and induced electric dipole transitions. The  $\Delta J=2$  transition in europium is induced electric dipole and is hypersensitive: its intensity is highly dependent on both the coordinating geometry and identity of the coordinating atoms. An attempt to explain hypersensitivity has been based on dynamic coupling (or ligand polarisation) mechanisms, relating the intensity of the hypersensitive transitions to the dipolar polarisabilities of the ligand atoms or groups, as well as to the geometry of the complex.<sup>(20)</sup> It is, therefore, possible to explain the evident increase in the intensity of the  $\Delta J=2$  band because of the more polarised Ar=C-O<sup>-</sup> character of the ketone carbonyl group upon introduction of the increasingly electro-donating methoxy and dimethylamino substituents. The observed trend thus also provides further support that the ketone group is coordinated to the metal ion in each of the three complexes.

No emission was detectable for EuL<sup>9</sup> in aqueous solution (H<sub>2</sub>O or D<sub>2</sub>O). For the other solvents examined, luminescence was observed in each case, although the intensity varied erratically, showing no correlation with the dielectric constant, or with other solvent parameters such as that of Reichardt. The measured lifetime also varied substantially with solvent. Monoexponential decay of the emission was observed in DMSO and alcohol solutions. Emission in acetonitrile, dichloromethane and chloroform displayed non-exponential decay kinetics, possibly due to the slow exchange between two species with and without a metal-bound water molecule.

The very sensitive dependence of the emission intensity and lifetime on solvent is probably a combination of effects, as revealed by applying the analysis of spectra and lifetimes, used above for the other complexes, to EuL<sup>9</sup>. The results of this treatment are

summarised in table 3, which show that the solvent has not only an expected effect on the non-radiative decay pathways, but also a profound influence on both the pure radiative lifetime and the efficiency of energy transfer. The pure radiative lifetime is significantly shorter in DMSO than in alcohols, whilst the non-radiative decays pathways ( $\Sigma k_{nr}$ ) are less significant, which together account for the much longer lifetime observed in DMSO. The efficiency of energy transfer is close to unity.

	MeOH	EtOH	iPrOH	DMSO
$[I_{tot} / I(0,1)]$	0.14	0.15	0.15	0.12
$\tau_R / ms$	4.31	4.27	0.26	2.79
$k_R / s^{-1}$	232	234	235	359
$\tau_{obs} / ms$	0.12	0.35	0.69	1.29
$\eta_{Ln}$	0.029	0.082	0.16	0.46
$\Phi_{tot}$	0.014	0.086	0.10	0.35
$\eta_{ET}$	0.48	1.05	0.62	0.96
$\Sigma k_{nr} / s^{-1}$	1220	2630	7900	418

Table 3.

Comparing the quantum yields of the  $EuL^7$ ,  $EuL^8$  and  $EuL^9$  complexes in the strongly coordinating solvent DMSO (respectively 0.026, 0.257 and 0.351), it is possible to observe the expected trend in metal centred luminescence namely the efficiency of sensitisation increasing with the electron donating ability of the *para* substituent on the acetophenone group.

### 5.3.4 Emission spectra and lifetimes of terbium complexes

The terbium(III) complex of  $L^7$  was also prepared. In the absorption spectrum, there is a maximum at 265 nm, similar to the value obtained for europium(III). The luminescence

quantum yields in H<sub>2</sub>O and D<sub>2</sub>O are respectively 0.12 and 0.23, the lifetimes 1.6 and 2.6 ms. The number of water molecules bound to the metal ion,  $q$ , was calculated from the lifetime data to be 0.98. For the europium analogue, the value of  $q$  was 1.24; in the past, smaller  $q$  values of terbium complexes compared to their europium analogues have been noted<sup>(21)</sup> and have been explained in terms of the difference in the ionic radii of the two metal ions. In fact, while europium(III) has an ionic radius of 0.950 Å, terbium(III) has a smaller ionic radius of 0.923 Å, which allows a more compact conformation of the metal-ligand complex, leaving less space for interaction with the solvent.

#### 5.4 Ligands based on benzophenone

The photophysical properties of two ligands based on benzophenone, H<sub>3</sub>L<sup>10</sup> (benzophenone) and H<sub>3</sub>L<sup>11</sup> (long arm-benzophenone), and their metal complexes have been investigated (figure 5.6). As in the previous system, the metal ions are chelated by a DOTA type system, in this case with one of the acetates replaced by an amide, to which the chromophore is covalently bound.

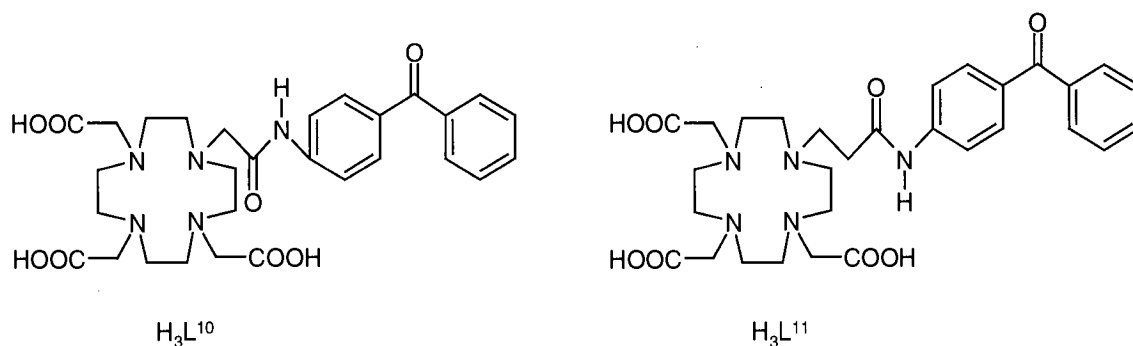


Fig. 5.6 – Ligands based on benzophenone.

### 5.4.1 Absorption spectra

All the complexes displayed ground-state absorbance maxima at ~300 nm (broad band), attributed to benzophenone. The energy of the  $S_1$  state was calculated, from the absorption spectrum, to be  $320 \text{ kJ mol}^{-1} \pm 5 \text{ kJ mol}^{-1}$ . The absorption spectra of the free ligands and the excitation spectra of the europium and terbium complexes were found to have similar profiles, proving that the lanthanide(III) ions were excited via the benzophenone group by energy transfer.

### 5.4.2 Phosphorescence of lanthanum complex of $L^{10}$

The lanthanum(III) complex  $LaL^{10}$  was prepared in order to study the triplet state properties of the chromophore. In fact, as in the case discussed before with gadolinium, the  $La^{3+}$  ion, which has no  $f$  electrons, does not have any accessible excited state energy levels. Thus, energy transfer does not occur in this case and in methanol:ethanol (1:1) solution the  $La^{3+}$  complex showed no luminescence at room temperature. Upon cooling to 77 K, intense phosphorescence was observed, due to the  $T_1 \rightarrow S_0$  transition in benzophenone. The spectra of the free ligand and metal complex were again very similar.

From the position of the highest energy band in the spectrum, the excited state energy of  $LaL^{10}$  was determined to be  $23600 \pm 400 \text{ cm}^{-1}$ . The phosphorescence lifetime of the benzophenone in the complex in methanol:ethanol at 77 K was determined to be 20 ms.

### 5.4.3 Emission spectra and lifetimes of terbium complexes of L<sup>10</sup> and L<sup>11</sup>

The complexes TbL<sup>10</sup> and TbL<sup>11</sup> were studied in aqueous solution. Upon excitation, the complexes displayed intense metal-centred green luminescence and showed the typical lanthanide(III) narrow bands due to *f-f* transitions, which in the case of terbium(III) are  $^5D_4 \rightarrow ^7F_J$  ( $J = 6-3$ ). The hypersensitive  $^5D_4 \rightarrow ^7F_5$  transition represents the strongest emission and is centred at 545 nm. Degassing the solution did not influence the intensity of the emission indicating that the rate of energy transfer to the metal is high compared to the rate of quenching of the triplet state by oxygen and also demonstrating that back energy transfer is negligible. As expected, since it is well established that the O-H bonds of bound water molecules quench the excited states of the metal ion, deuteration of the solvent increased the emission intensity. The terbium(III) does not have a transition that is pure magnetic dipole in nature and that can be used as an internal reference, thus it is not possible to calculate the pure radiative lifetime from the corrected emission spectrum using the treatment introduced for europium in the previous part of the chapter.

The emission quantum yields of TbL<sup>10</sup> and TbL<sup>11</sup> are shown in table 4. They are indicative of an efficient sensitisation of the metal ion, but the difference between the two is rather surprising. In the two complexes, the only structural difference is expected to stem from the distance between the chromophore and the terbium(III) due to the addition of a CH<sub>2</sub> group in the chain that links the chromophore to the DOTA. It is well known that the efficiency of energy transfer is expected, from theory, to decrease rapidly with distance between the donor and the acceptor, either exponentially (Dexter theory)<sup>(22)</sup> or to the inverse sixth power of the distance (Förster). So, a lower quantum yield would be



expected for TbL<sup>11</sup>. However, the increase in intensity of the hypersensitive transitions in TbL<sup>11</sup> is an indication of a different symmetry around the metal ion. The presence of an extra CH<sub>2</sub> group apparently alters the position of the carbonyl group, which is binding the terbium(III) ion, and as a result there is an enhancement of the asymmetry around the metal ion. A low temperature (77 K) experiment showed an insignificant emission from the benzophenone group, indicative of a very efficient transfer from the chromophore to the metal ion.

To determine the lifetime of the terbium(III) complexes, the metal emission was monitored at 545 nm, and the benzophenone was excited at 266 nm. In solution, a single exponential decay confirmed the presence of just one emitting species. The values obtained are in line with values obtained in related compounds.<sup>(13,19)</sup> As expected, longer lifetimes were recorded in D<sub>2</sub>O, although, the difference between H<sub>2</sub>O and D<sub>2</sub>O was not as large as for europium, owing to the weaker effect of O-H oscillators in quenching the terbium excited state. All the results are shown in table 4.

Complex	$\tau_{\text{H}_2\text{O}}/ \text{ms}$ (a)	$\tau_{\text{D}_2\text{O}}/ \text{ms}$ (a)	q	$\Phi_{\text{H}_2\text{O}}$ (b)	$\Phi_{\text{D}_2\text{O}}$ (b)
TbL <sup>10</sup>	1.14	1.74	1.27	0.27	0.41
TbL <sup>11</sup>	1.577	2.477	0.97	0.41	0.63

(a) Lifetimes of the metal-centred emission monitored at 545 nm, 293K; excitation was at  $\lambda_{\text{max}}$  in the absorbance spectrum (266 nm) (b) Quantum yield at 293K, measured using cresyl violet in MeOH and rhodamine 101 in acidified EtOH as standards.

Table 4.

From the lifetime data it was possible to estimate the number of bound water molecules,  $q$ , and the results are shown in table 4. The values 1.27 and 0.97 obtained respectively for  $\text{TbL}^{10}$  and  $\text{TbL}^{11}$  are quite different. As discussed previously, values close to 1 are typical in such kinds of complex. The lower values observed in  $\text{TbL}^{11}$  may indicate that the 6-membered chelate ring involving the amide group is more effective at sterically inhibiting the approach of a water molecule.

#### 5.4.4 Emission spectra and lifetimes of ytterbium complexes

It was decided to investigate ytterbium as it has the interesting property of emitting in the near IR, a region to which biological tissue is relatively transparent, making it of particular interest for biosensors. The ytterbium(III) complex of  $\text{L}^{10}$  displayed an emission maximum at 980 nm (broad band), corresponding to the transition  ${}^2\text{F}_{5/2} \rightarrow {}^2\text{F}_{7/2}$ . Unlike the analogous terbium(III) and europium(III) complexes, in the  $\text{YbL}^{10}$  complex the energy transfer process is slow, such that quenching by dissolved molecular oxygen competes effectively as a deactivation pathway for the triplet state of the chromophore (figure 5.7). This is clear from the substantial increase in emission intensity observed upon de-oxygenation of the solution.

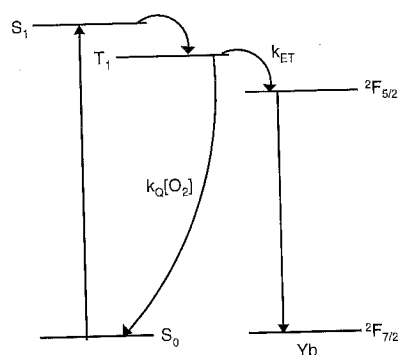


Fig. 5.7 – Dissolved molecular oxygen reduces the intensity of metal-based emission if  $k_{ET}$  is comparable to  $k_Q[\text{O}_2]$ .

The emission intensity in H<sub>2</sub>O and D<sub>2</sub>O showed a very profound effect of deuteration, with a 15 fold increase of the emission, owing to the small energy gap between the excited and ground states of ytterbium(III), favouring energy transfer into the O-H vibrations.

The quantum yield of the YbL<sup>10</sup> complex was not measured, firstly because of the lack of standards suitable for measurements in this wavelength range and secondly because related ytterbium(III) complexes are known to have very low quantum yields,<sup>(23)</sup> the ytterbium ion being very sensitive to non radiative deactivation processes. The lifetime data are shown in table 5.

	H <sub>2</sub> O aerated	H <sub>2</sub> O degassed	D <sub>2</sub> O aerated	D <sub>2</sub> O degassed
$\tau_1$ (rise time) $\mu\text{s}$	0.521	0.567	0.944	1.79
$\tau_2$ (decay) $\mu\text{s}$	1.23	1.88	7.65	8.90

Table 5.

In each case, monoexponential decay was observed, indicative of a single emitting species. It may be noted that, compared to europium(III) and terbium(III), the ytterbium(III) excited state is considerably shorter lived. Unlike the other lanthanide ions investigated, an increase in the lifetime was obtained by degassing the solution, indicative of a slower, less efficient energy transfer step. This probably reflects the very large energy gap between the triplet excited state of the chromophore and the acceptor <sup>2</sup>F<sub>5/2</sub> excited state of the metal ion. According to Förster theory, rapid energy transfer requires a good overlap between the emission spectrum of the donor and the absorbance spectrum of the acceptor, which is clearly not the case in this system.

### 5.4.5 Emission spectra and lifetimes of europium complexes

The band due to the hypersensitive transition  ${}^5D_0 \rightarrow {}^7F_2$  is the strongest among the typical narrow bands due to the  ${}^5D_0 \rightarrow {}^7F_J$  transitions in the emission spectrum of the  $\text{EuL}^{10}$  and  $\text{EuL}^{11}$  complexes. The energy transfer from the chromophore is a fast and one-way process; in fact degassing the solution did not affect the intensity of the emission. As introduced in previous sections, the ratio  $\Delta J=2/\Delta J=1$  depends on the symmetry of the complex and on the polarisability of the coordinating groups. The ratios are fairly similar to those of complexes discussed earlier in the chapter, as expected, given that the basic structure of the ligands is similar, with the same tris-acetate motif.

The emission quantum yields of  $\text{EuL}^{10}$  and  $\text{EuL}^{11}$  are shown in table 6 and indicate efficient sensitisation of the europium in aqueous solution. The addition of an extra  $\text{CH}_2$  group in the arm does not affect the quantum yields, which were very similar for the two complexes, in contrast to the trend observed with terbium.

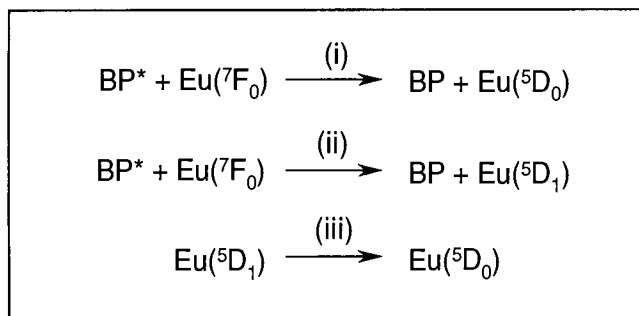
The lifetime data for  $\text{EuL}^{10}$  and  $\text{EuL}^{11}$  are also shown in table 6. The single exponential decays confirm the presence of a single emitting species in solution. As expected, the use of  $\text{D}_2\text{O}$  as a solvent gave a much longer lifetime. In order to investigate the energy transfer in the complexes, detailed kinetic measurements were carried out over short and long timescales, and a complex kinetic profile was found. Monitoring the  ${}^5D_0 \rightarrow {}^7F_0$  band at 595 nm revealed two components to the rising edge of the signal. The first component corresponding to 1/5 of the signal was very fast (in the order of nanoseconds), whilst the rise time of the second one was 1.45  $\mu\text{s}$ . The lifetime of the  ${}^5D_1$  state was found to be 1.45  $\mu\text{s}$  by monitoring the intensity of the  ${}^5D_1 \rightarrow {}^7F_1$  band at 583 nm. These results suggested

that, in the europium complexes, the processes shown in scheme 1 were occurring, with the emissive  $^5D_0$  state being populated both directly from the chromophore and indirectly via the  $^5D_1$  state.

Complex	$\tau_{H_2O}/ms$ (a)	$\tau_{D_2O}/ms$ (a)	q	$\Phi_{H_2O}$ (b)	$\Phi_{D_2O}$ (b)
EuL <sup>10</sup>	0.613	2.263	1.25	0.093	0.38
EuL <sup>11</sup>	0.607	2.034	1.20	0.097	0.35

(a) Lifetimes of the metal-centred emission monitored at 595 nm, 293K; excitation was at  $\lambda_{max}$  in the absorbance spectrum, (266 nm). (b) Quantum yield at 293K, measured using cresyl violet in MeOH and rhodamine 101 in acidified EtOH as standards.

Table 6.



BP\* = excited triplet state of benzophenone

Scheme 1.

The energy levels  $^5D_1$  and  $^5D_0$  of the europium(III) ion are both below the triplet state of the benzophenone (figure 5.8), therefore energy transfer occurs via the steps (i) and (ii) shown in scheme 1. The steps (i) and (ii) occur very rapidly unlike the relaxation step (iii), which is slower.

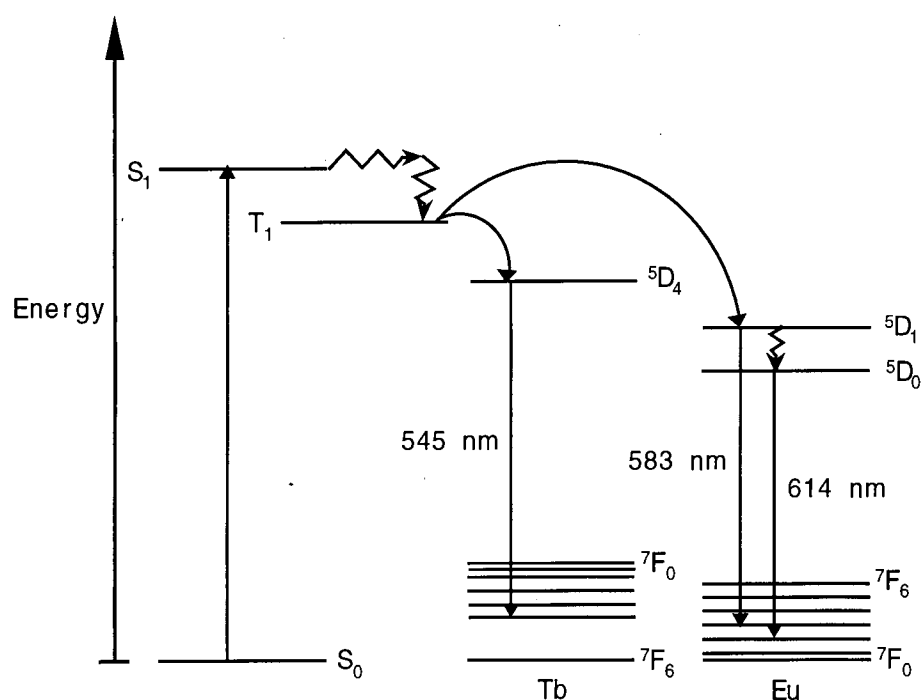


Fig. 5.8 – Energy level diagram showing the energy levels of the chromophore and the lanthanide(III) ions.

By applying the same treatment introduced in the paragraph 5.3.3, it is possible to obtain more information about the energy transfer process in the europium(III) complexes. The results are shown in table 7. From these results it is evident that the relative intensity of the bands does not change upon deuteration of the solvent. The efficiency of the energy transfer from the benzophenone group in the complex  $\text{EuL}^{10}$  is close to one, showing that all the energy absorbed by the chromophore group is transferred to the metal ion. However, non-radiative decay is occurring from the europium(III) excited states because not all the energy is seen as europium(III) emission.

In the  $\text{EuL}^{11}$  complex the presence in the arm of an extra  $\text{CH}_2$  group affects the relative intensity of the bands, with the hypersensitive  $\Delta J=2$  transition increased, modifying: the efficiency of the europium(III) emission, the radiative rate constant ( $k_R$ ) and hence the

pure radiative lifetime ( $\tau_R$ ). However, in the two complexes the lifetimes are rather similar implying a difference in the efficiency of energy transfer ( $\eta_{ET}$ ). In fact, looking at the table, the EuL<sup>11</sup> complex displays a less efficient energy transfer in comparison to the EuL<sup>10</sup> complex. This is in line with expectations based on theories of energy transfer, which predict a falling-off with distance as discussed above. On the other hand, it contrasts with the unexpected behaviour of the terbium complexes.

	EuL <sup>10</sup>		EuL <sup>11</sup>	
	H <sub>2</sub> O	D <sub>2</sub> O	H <sub>2</sub> O	D <sub>2</sub> O
$[I_{tot} / I(0,1)]$	0.206	0.207	0.16	0.166
$k_R / s^{-1}$	156.8	156.1	201.9	194.6
$\tau_R / ms$	6.38	6.41	4.95	5.14
$\Phi_{tot}$	0.097	0.38	0.095	0.35
$\tau_{obs} / ms$	0.61	2.26	0.61	2.03
$\eta_{Ln}$	0.096	0.351	0.123	0.395
$\eta_{ET}$	1.01	1.08	0.77	0.89
$\Sigma k_{nr} / s^{-1}$	1482.5	286.4	1437.4	298

Table 7.

The very similar non-radiative rate constants, ( $\Sigma k_{nr}$ ), measured for the two complexes, indicate that the extra C-H oscillators introduced into the EuL<sup>11</sup> complex do not act as efficient quenchers of the europium(III) <sup>5</sup>D<sub>0</sub> excited state.

## 5.5 Ligands based on quinaldine

The photophysical properties of two ligands based on hydroxyquinaldine,  $H_3L^{12}$  (hydroxy quinaldine) and  $H_3L^{13}$  (long arm-hydroxyquinaldine) and their metal complexes have been investigated (figure 5.9). The ligand  $H_3L^{13}$  is reminiscent of the system described in the previous section, with the metal ion chelated by a DOTA type system, with the chromophore covalently bound via an amide unit to one of the arms of the DOTA ring. In contrast, the ligand  $H_3L^{12}$  is novel, having one of the arms replaced by the quinaldine chromophore, in which the nitrogen atom may be suitably positioned to bind the lanthanide(III) ion in a 5-membered chelate ring. In this sense, it may play the same role as the fourth carboxylate oxygen in DOTA itself, or the amide oxygen of the ligands of the previous section, or, indeed, as the ketone oxygen in the acetophenone ligands discussed at the beginning of the chapter.

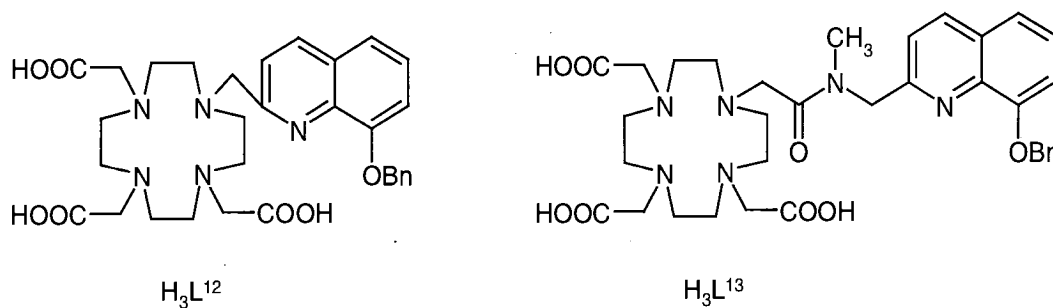


Fig. 5.9 – Ligands based on quinaldine.



### 5.5.1 Absorption spectra

All the complexes displayed intense ground-state absorbance maxima around 245 nm (broad band), due to quinaldine absorbance. The precise values were 243 nm for the free ligands  $H_3L^{12}$  and  $H_3L^{13}$ , 245 nm for the  $EuL^{13}$  and  $GdL^{13}$  complexes and 251 nm and 253 nm for  $EuL^{12}$  and  $GdL^{12}$ , respectively. The slight red-shift observed for the complexes of  $L^{12}$  compared to  $L^{13}$  suggests that there is, indeed, a direct interaction between the nitrogen atom of the quinaldine and the europium(III) and gadolinium(III) ions (figure 5.10). The  $S_1$  energy levels, calculated from the absorption spectra, were in the range  $39400-37200 \pm 300 \text{ cm}^{-1}$ . The excitation spectra of the europium complexes corresponded well with the absorption profiles, proving that the lanthanide(III) ions were being excited via the quinaldine group and hence that energy transfer was occurring.

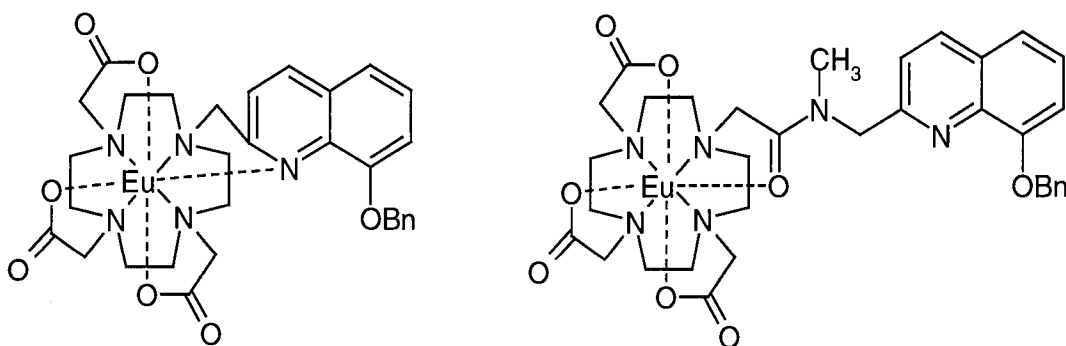


Fig. 5.10 –  $EuL^{12}$  and  $EuL^{13}$  complexes.

### 5.5.2 Phosphorescence of gadolinium complexes

As usual, the gadolinium complex is a useful model compound for measuring the triplet energy of the chromophore, as the  $Gd^{3+}$  ion does not have any excited states sufficiently low in energy to be populated. Phosphorescence with some vibrational structure was observed at 77 K, due to emission from the triplet state, and the triplet energy level of  $GdL^{12}$  was determined in this way to be at  $28100 \pm 300 \text{ cm}^{-1}$  in  $H_2O$ . As observed for the singlet excited state, this is rather lower than the triplet energy of the complex  $GdL^{13}$ , where a value of  $29400 \text{ cm}^{-1}$  was recorded under the same conditions. The phosphorescence lifetimes of the complexes  $GdL^{12}$ ,  $GdL^{13}$  were too short to be recorded, even at 77 K.

### 5.5.3 Emission spectra and lifetimes of europium complexes

The complexes  $EuL^{12}$  and  $EuL^{13}$  were studied in aqueous solution. Upon excitation, the emission spectra displayed intense metal-centred red luminescence and showed the typical lanthanide(III) narrow bands due to  $f-f$  transitions. Again, deuteration of the solvent increased the emission intensity.

The emission quantum yields of  $EuL^{12}$  and  $EuL^{13}$  are shown in table 8. They are indicative of an efficient sensitisation of the metal ion, and are rather intriguing. In the two complexes, there are two differences, firstly the distance between the chromophore and the europium(III) due to the longer chain that links the chromophore to the macrocycle in  $EuL^{13}$  and, secondly, in  $EuL^{12}$  the chromophore binds directly to the

europium via the quinoline nitrogen atom. As discussed previously, the efficiency of energy transfer is expected to decrease rapidly as the distance between the donor and the acceptor increases, and the results obtained confirm these expectations. However, the 30-fold difference between the two complexes is probably too big to be attributed just to the distance between the antenna group and the metal ion. Furthermore, upon deuteration it may be noted that a large increase in the emission intensity is observed for EuL<sup>13</sup>, but only a rather small increase is found for EuL<sup>12</sup>.

Complex	$\tau_{\text{H}_2\text{O}}/\text{ms}$ (a)	$\tau_{\text{D}_2\text{O}}/\text{ms}$ (a)	$q$	$\Phi_{\text{H}_2\text{O}}$ (b)
EuL <sup>12</sup>	0.37	0.44	0.44	0.059
EuL <sup>13</sup>	0.73	2.6	1.05	0.0021

(a) Lifetimes of the metal-centred emission monitored at 701 nm, 293K; excitation was at  $\lambda_{\text{max}}$  in the absorbance spectrum (245 nm) (b) Quantum yield at 293K, measured using cresyl violet in MeOH and rhodamine 101 in acidified EtOH as standards.

Table 8.

From the lifetime data, the number of metal-bound water molecules,  $q$ , was calculated to be 0.44 and 1.05 respectively for EuL<sup>12</sup> and EuL<sup>13</sup>. These values are clearly quite different. As discussed previously, values close to 1 are typical in such kinds of complexes with octadentate ligands. Therefore, while the value obtained for EuL<sup>13</sup> is in line with such results, the value obtained for EuL<sup>12</sup> is seen to be outstandingly low. The explanation for the anomalous behaviour of EuL<sup>12</sup> may lie in the fact that, in this complex, the nitrogen atom of the chromophore is directly bound to the metal ion. This will force the benzyloxy group attached to the phenyl ring of the quinoline to occupy the position immediately below the metal, the position normally occupied by the water

molecule in 9-coordinate DOTA-type complexes. Thus, it seems likely that the steric encumbrance associated with the chromophore simply leaves no space for coordination of a molecule of water. This would also explain why the lifetime is so little affected by deuteration of the solvent.

By applying the same treatment introduced in the paragraph 5.3.3, it is possible to obtain more information about the rate constants of the various processes involved in the europium(III) complexes, in aqueous solution. The results are shown in table 9.

	EuL <sup>12</sup>	EuL <sup>13</sup>
$[I_{\text{tot}} / I(0,1)]$	0.227	0.192
$\tau_R / \text{ms}$	7.0	5.88
$k_R / \text{s}^{-1}$	142	170
$\tau_{\text{obs}} / \text{ms}$	0.371	0.726
$\eta_{\text{Ln}}$	0.053	0.123
$\Phi_{\text{tot}}$	0.058	0.0021
$\eta_{\text{ET}}\Phi_{\text{T}}$	1.09	0.172

Table 9.

In this case, the triplet yield of the chromophore is unknown, but the value obtained for the product  $\eta_{\text{ET}}\Phi_{\text{T}}$  clearly indicates that the efficiency of the energy transfer from the quinaldine group in the complex EuL<sup>12</sup> is close to one showing that all the energy absorbed by the chromophore group is transferred to the metal ion. In contrast, the value for the complex EuL<sup>13</sup> is quite low, due probably to non-radiative decay competing efficiently with the slower, energy transfer step.

## 5.6 Conclusions

In this chapter, some new lanthanide(III) complexes have been discussed, representing new classes of compounds incorporating covalently-linked acetophenone, benzophenone or hydroxyquinoline groups as sensitisers of the lanthanide(III) ion excited states.

In the case of the acetophenone-based ligands, it has been shown that the efficiency of europium(III) sensitisation is highly dependent upon the substituent in the *para* position of the chromophore. Introduction of a methoxy substituent into the *para* position of acetophenone increased the efficiency of energy transfer, whilst the dimethylamino substituent led to high emission in non-aqueous solvents only, showing an extreme sensitivity to the solvent.

In the case of the benzophenone-based ligands, the addition of an extra CH<sub>2</sub> group in the arm apparently lowered the symmetry of the environment of the coordinated lanthanide(III) ion and, surprisingly, led to an increase in the quantum yield of the terbium(III) complex.

The interesting feature of the hydroxyquinoline-containing complexes is the particularly low hydration state (*q*) of the europium ion in the system in which the nitrogen of the quinaldine is directly bound to the metal ion. This probably arises from the positioning of the benzyloxy group in such a way that the approach of a water molecule is inhibited.

## 5.7 References

### 5.7.1 Articles

1. Open University Course Team, "*Photochemistry*", The Open University Press, (1982).
2. S. Sato and M. Wada, *Bull. Chem. Soc. Jpn.*, **43**, 1955, (1970).
3. F. Wilkinson, *Organic Molecular Photophysics*, Wiley, New York, (1975).
4. M. H. V. Werts, M. A. Duin, J. W. Hofstraat and J. W. Verhoeven, *Chem. Comm.*, 799, (1999).
5. W. J. McCarthy and J. D. Winefordner, *Anal. Chem.*, **38**, 848, (1997).
6. J. C. Rodriguez-Ubis, M. T. Alonso, O. Juanes, R. Sedano and E. Brunet, *J. Lumin.*, **79**, 121, (1998).
7. S. Aime, A. S. Batsanov, M. Botta, R. S. Dickins, S. Faulkner, C. E. Foster, A. Harrison, J. A. K. Howard, J. M. Moloney, T. J. Norman, D. Parker, L. Royle and J. A. G. Williams, *J. Chem. Soc., Dalton Trans.*, 3623, (1997).
8. D. Parker and J. A. G. Williams, *J. Chem. Soc., Dalton Trans.*, 3613, (1996).
9. V. Alexander, *Chem. Rev.*, **95**, 273, (1995).
10. P. Caravan, J. J. Ellison, T. J. McMurry and R. B. Lauffer, *Chem. Rev.*, **99**, 2293, (1999).
11. A. Beeby, L. M. Bushby, D. Maffeo and J. A. G. Williams, *J. Chem. Soc., Perkin Trans. 2*, 1281, (2000).
12. W. DeW. Horrocks and D. R. Sudnick, *Acc. Chem. Res.*, **14**, 384, (1981).

13. A. Beeby, I. M. Clarkson, R. S. Dickins, S. Faulkner, D. Parker, L. Royle, A. S. de Sousa, J. A. G. Williams and M. Woods, *J. Chem. Soc., Perkin Trans. 2*, 493, (1999).
14. R. S. Dickins, J. A. K. Howard, C. L. Maupin, J. M. Moloney, D. Parker, J. P. Riehl, G. Siligardi and J. A. G. Williams, *Chem. Eur. J.*, **5**, 1095, (1999).
15. L. D. Carlos, Y. Messaddeq, H. F. Brito, R. A. Sa' Ferreira, V. De Zea Bermudez, S. J. L. Ribeiro, *Adv. Mater.*, **12**, 594, (2000).
16. M. H. V. Werts, *Ph. D. Thesis*, University of Amsterdam, (2000).
17. M. F. Hazenkamp and G. Blasse, *Chem. Mat.*, **2**, 105, (1990).
18. (a) R. D. Peacock, *Struct. Bonding*, **22**, 83, (1975); (b) A. F. Kirby, D. Foster and F. S. Richardson, *Chem. Phys. Lett.*, **95**, 507, (1983).
19. A. Beeby, L. M. Bushby, D. Maffeo and J. A. G. Williams, *J. Chem. Soc., Dalton Trans.*, (accepted for publication).
20. S. F. Mason, R. D. Peacock and B. Stewart, *Mol. Phys.*, **30**, 1829, (1975).
21. M. P. O. Wolbers, F. C. J. M. van Veggel, B. H. M. Snellink-Ruël, J. W. Hofstraat, F. A. Guerts and D. N. Reinhoudt, *J. Chem. Soc., Perkin Trans. 2*, 2141, (1998).
22. D. L. Dexter, *J. Chem. Phys.*, **21**, 836, (1953).
23. S. I. Klink, G. A. Hebbink, L. Grave, F. C. J. M. van Veggel, D. N. Reinhoudt, L. H. Sloof, A. Polman and J. W. Hofstraat, *J. Appl. Phys.*, **86**, 1181, (1999).

# **CHAPTER 6**

## **EXPERIMENTAL**



## 6.1 Experimental Procedures: General

### *Reaction conditions*

The synthetic procedures for the compounds used in this work are described in this chapter. Air sensitive reactions were carried out under an atmosphere of dry, oxygen-free nitrogen or argon using standard Schlenk-line techniques. Reactions were carried out at room temperature unless otherwise stated. All solvents used were reagent grade, except acetonitrile (HPLC grade, Aldrich), anhydrous DMF (99%, Aldrich), methanol (Analar) and absolute ethanol (Analar). When required anhydrous, tetrahydrofuran and ether were distilled over sodium. Water was purified using the 'Purite<sub>STILL</sub> plus' system.

### *Purification procedures*

Preparative column chromatography employed silica gel (60, 40-63 $\mu$ , Fluorochem), alumina (Activated, Neutral, Brockman I, STD Grade, CA 150), ion-exchange resin (Dowex 50X8-200, Acros) pre-washed in refluxing methanol, or octadecyl-functionalised silica gel (reversed-phase silica gel, Aldrich). Thin layer chromatography was carried out using aluminium oxide sheets (60 F<sub>254</sub>, Merck) and silica gel sheets (60 F<sub>254</sub>, Merck).

### *Characterisations*

Infra red spectra were recorded on a Perkin Elmer FT 1600 spectrometer either as a thin film or Nujol mulls on NaCl plates or as a KBr disc.

Elemental Analyses were collected on a CE-440 Elemental Analyser (Exeter Analytical Inc.) by the laboratory service of the University of Durham. Where values are omitted, this usually indicates that satisfactory correlation between experimental and predicted

values was not obtained. The normal problem was that the percentage of hydrogen recorded was too high, even after taking in account the presence of water molecules.

Standard  $^1\text{H}$  and  $^{13}\text{C}$  NMR spectra were recorded on Varian 200 MHz or 300 MHz instruments. Two-dimensional spectra (HETCOR, COSY and NOESY) were acquired on a 500 MHz Varian by the NMR service of the University of Durham.  $^1\text{H}$  NMR spectra recorded in  $\text{CDCl}_3$  were referenced to  $\text{CHCl}_3$  at  $\delta=7.26$  ppm or, when ambiguous, to  $\text{CH}_2\text{Cl}_2$  at  $\delta=5.30$  ppm, and in  $\text{D}_2\text{O}$  were referenced to HOD at  $\delta=4.79$ .  $^{13}\text{C}$  spectra recorded in  $\text{CDCl}_3$  were referenced to  $\text{CDCl}_3$  at  $\delta=77.2$ , and in  $\text{D}_2\text{O}$  to TMS. When the resolution of the  $^1\text{H}$  NMR spectra recorded was not sufficient to determine coupling constants reliably, the J values are omitted.

Electrospray mass spectra were recorded on a Fisons Platform Electrospray Instrument, high resolution electrospray spectra were recorded on a Micromass Autospec by the Mass Spectrometry Service of the University of Durham or by the EPSRC National Mass Spectrometry Service Centre of the University of Swansea.

UV-Visible spectra were recorded on a Bio-Tek Instruments Uvikon 930 spectrometer operated using LabPower Junior software or on an ATI Unicam UV-2 using Vision 4.5 software, unless otherwise stated.

In the solid state, measurements of magnetic susceptibility were carried out using a JME balance, using  $(\text{NH}_4)_2\text{Fe}(\text{SO}_4)_2 \cdot 6\text{H}_2\text{O}$  as standard. The estimated uncertainty in measurements using this procedure is  $\pm 10\%$ .

ESR spectra were measured by Dr. A. Whitwood using a Bruker ESP300 spectrometer at the University of York.

Cyclic voltammetry was carried out on an EG&G Instruments VersaStat II, using acetonitrile or H<sub>2</sub>O solutions of the complexes (2 mM) containing, respectively, [NBu<sub>4</sub>][PF<sub>6</sub>] or [K][PF<sub>6</sub>] as the supporting electrolytes (0.1 M); solutions were purged with nitrogen gas prior to each scan. A three-electrode system was employed using platinum working, reference and counter electrodes (when H<sub>2</sub>O was the solvent, the reference electrode was a Saturated Calomel Electrode). When required, the voltammograms were referenced to the ferrocene-ferrocenium couple as an internal standard ( $E^\circ$  0.40 V vs. SCE in acetonitrile, with [NBu][PF<sub>6</sub>] as the supporting electrolyte).<sup>(1)</sup>

#### *pH measurements for pH-metric titrations*

The pH was monitored using a BDH glass combination electrode attached to a Jenway 3010 pH meter. Before each titration, the electrode system was calibrated in hydrogen ion concentration units ( $p[H] = -\log[H^+]$ ) using Buffer Reference Standard solutions (Sigma) at pH 4.00±0.01, 7.00±0.01, 10.00±0.01 (25°C). The temperature of the solution during the experiments was maintained to within 2 degrees.

#### *X-ray crystal structures*

The X-ray crystal structure determinations were carried out by Dr. A. Batsanov, Dr. A. Goeta, Dr. H. Puschmann and Dr. D. Yufit of the Chemical Crystallography Group of Prof. J.A.K. Howard of the University of Durham. Data was collected using graphite monochromated Mo-K $\alpha$  radiation on a Bruker SMART-CCD detector diffractometer

equipped with a Cryosystem N<sub>2</sub> flow-cooling device. Cell parameters were determined and refined using the SMART software.<sup>(2a)</sup> Raw frame data were integrated using the SAINT program.<sup>(2a)</sup> The structures were solved using Direct Methods and refined by full-matrix least squares on F<sup>2</sup> using SHELXTL.<sup>(2b)</sup> All non-hydrogen atoms were refined with anisotropic displacement parameters. Hydrogen atoms were located from difference Fourier maps and their coordinates and isotropic displacement parameters refined.

## 6.2 Luminescence Measurements

### *Instrumentation*

Steady state fluorescence spectra were recorded using an ISA Inc. Fluoromax-2 spectrometer equipped with a red-sensitive Hamamatsu R928 photomultiplier tube, and operated using Spectramax software. Phosphorescence spectra were acquired using a Perkin-Elmer LS 50B Luminescence Spectrometer, equipped for low temperature measurements, operated using FLWinLab software. The pulsed excitation source is a xenon flash tube and the fluorescence is detected by a Hamamatsu R928 photomultiplier tube. The excitation source produces an intense and short duration pulse of radiation, the light is focused onto the excitation monochromator, where it is diffracted by the grating. A narrow wavelength band emerges, the half-peak width of which is determined by the slit widths selected (typically 2.5-15 nm). The majority of the excitation beam is focused onto the sample, but part of the beam is diverted and channelled by a set of mirrors to a second photomultiplier tube. This serves to give a reference spectrum allowing correction for the wavelength-dependent output of the lamp. Light emitted by the sample is focused onto the emission monochromator, the resolution again being determined by the slit widths selected, and is subsequently detected by the sample photomultiplier tube.

*Lifetimes*

The lifetimes ( $\tau$ ) are the average of at least 3 separate measurements, each of which was obtained by monitoring the emission intensity at the wavelength at which was found the maximum in the fluorescence spectrum. In order for an accurate decay curve to be generated, it is important for the gate time (the duration over which the intensity is measured) to be short compared to the luminescence lifetime: it proved possible to use a gate time of 0.1 ms in most cases whilst maintaining a satisfactory signal-to-noise ratio.

Mono-exponential decay of the luminescence was observed (except otherwise stated): the phosphorescence decay curves were fitted with good residuals to an equation of the form

$$I(t) = I(0) \exp (-t/ \tau)$$

using a curve fitting program (Kaleidagraph 3.0).

{where  $I(t)$  is the intensity at the time  $t$  after the excitation flash,  $I(0)$  the initial intensity at time  $t=0$  and  $\tau$  is the phosphorescence lifetime}. The estimated uncertainty in lifetimes using this procedure is  $\pm 10\%$ . The lifetime of the metal-based emission of the lanthanides were obtained in this way, as were the phosphorescence lifetimes of the organic chromophores, the latter requiring the use of low temperatures using a liquid nitrogen cooled cryostat (see below).

*Quantum yields*

Quantum yields ( $\Phi$ ) were measured relative to appropriate standards using the equation:

$$\Phi_x = \Phi_r * (\text{gradient } x / \text{gradient } r) * (\eta_x / \eta_r)$$

{where  $\Phi$  is the quantum yield,  $\eta$  is the refractive index of the solvent in which the compound is dissolved and  $x$  and  $r$  refer to sample and standard respectively}.

The gradients referred to are those obtained from a plot of the intensity of emission as a function of absorbance. In practice, at least five solutions over a range of absorbance values were used, and the linear portion of the plot used. Prior to measurement of the sample, two standards were compared in this way, in order to define the margin of error and to check for any variations in the intensity of the instrument. Provided that the values obtained for the standards were in a reasonable range of error (10%), then the same operation was done for the compound under investigation, and the value for the quantum yield of the new compound obtained in this way.

Cresyl Violet ( $\Phi = 0.54$  in methanol<sup>(3)</sup>) and Rhodamine 101 ( $\Phi = 1.0$  in H<sup>+</sup>/ethanol<sup>(3)</sup>) were used as standards for the europium complexes. In line with literature results, a reasonable margin of error (up to 30%) was anticipated in the values for most of the europium complexes, due to the rather low emission intensity. Excitation wavelengths were chosen to correspond to reasonably 'flat' portions of the absorbance spectra, thereby minimising the uncertainty in the absorbance. The estimated uncertainty in quantum yields using this procedure is  $\pm 20\%$ .

#### *Low Temperature Luminescence Spectroscopy*

Low temperature spectra were acquired using a variable temperature liquid nitrogen cryostat, Oxford Instruments model DN1704, controlled by an Oxford Instruments ITC4 temperature controller. A schematic diagram of the cryostat is shown in Figure 6.1.

The sample cell is loaded from the top and positioned at the bottom in a chamber, which is pump-filled with dry helium prior to use. There are four quartz windows providing optical access to the sample; these are separated from the outer windows by an evacuated

chamber, thus excluding water vapour, which would otherwise condense on the inner windows on cooling. A liquid nitrogen reservoir, isolated from the surroundings by an outer vacuum chamber, surrounds the central sample access tube. The sample space is cooled by allowing a flow of liquid nitrogen from the reservoir to the sample space heat exchanger, through a capillary tube. The exhaust valve controls the flow rate. A platinum resistance thermometer and heater are fitted, heat is supplied to balance the cooling power and thus set the required temperature.

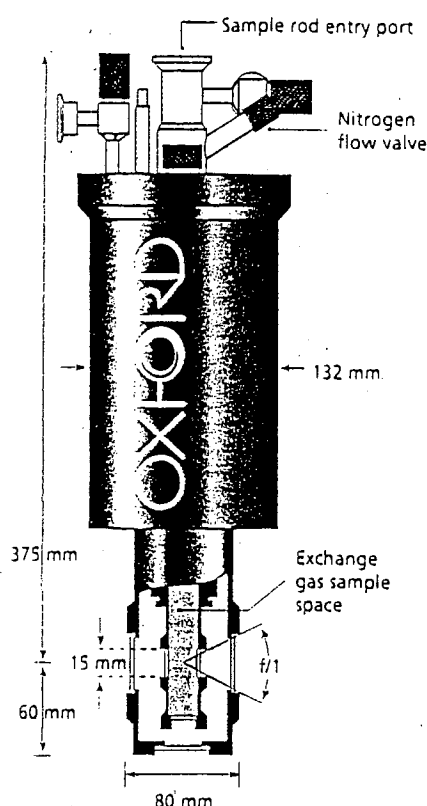
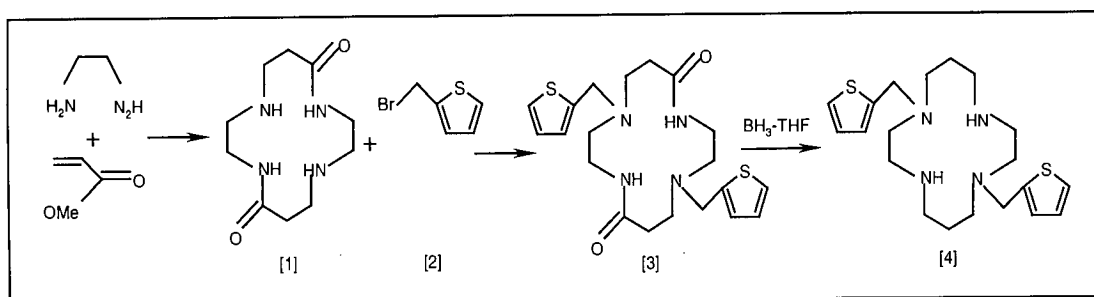


Figure 6.1 - Schematic diagram of the DN1704 variable temperature liquid nitrogen cryostat used for low temperature luminescence. (Reproduced from reference 4).

A mixture of ethanol/methanol (4/1 by volume) was chosen as the solvent for low temperature experiments for two main reasons. Firstly most of the compounds were soluble in this mixture, secondly at low temperature this mixture tends to form a transparent glass rather than the snow-like solid formed by pure ethanol, and is also less prone to fracture the costly cells used in this kind of experiments.

## 6.3 Synthetic Procedures for Chapter 2

### 6.3.1 1,8-Bis(2-methylthiophene)-1,4,8,11-tetraazacyclotetradecane



[1] – 1,4,8,11-tetraazacyclotetradecane-5,12-dione ( $H_2L^4$ )

This compound<sup>(5)</sup> was prepared by reaction of ethylenediamine (36 g, 0.6 mol) with an equimolar amount of methyl acrylate (52 g, 0.6 mol). Methyl acrylate was added dropwise into neat ethylenediamine while stirring. Addition was conducted at a rate such that the reaction temperature did not exceed 45° C, which required 1 hour. The crude colourless product, N-(2-aminoethyl)-β-alanine methyl ester, was dissolved in deionised water (90 ml). Allowing the solution to stand at room temperature for 2 weeks caused a white solid product to precipitate. On some occasions, further concentration of the solution under reduced pressure or addition of more water was required before crystallization occurred. The product was carefully washed with cold water and obtained as a fine white powder. The yield was typically 2.0±0.5%. Spectral analysis was consistent with the published data. NMR <sup>1</sup>H (D<sub>2</sub>O): δ= 3.37 (4H, t, J=5.1, CH<sub>2</sub>CO), 2.89 (4H, t, J=5.7, CH<sub>2</sub>CH<sub>2</sub>NHCO), 2.75 (4H, t, J=5.1, CH<sub>2</sub>CH<sub>2</sub>CO), 2.43 (4H, t, J=5.7, CH<sub>2</sub>CH<sub>2</sub>NHCO). IR (KBr) 1635 cm<sup>-1</sup> [ν(C=O)].



*[2] – 2-(Bromomethyl)thiophene*

This compound was prepared by following a similar method to that of Rossi et al.<sup>(6)</sup> adding a solution of PBr<sub>3</sub> (6 g, 21.5 mmol) in distilled Et<sub>2</sub>O (50 ml) to a solution of 2-hydroxymethylthiophene in distilled Et<sub>2</sub>O over a period of 2 hours. The solution was stirred for three days, and then washed four times with a similar amount of water, dried over MgSO<sub>4</sub> and the solvent removed under reduced pressure. The yield was 75%. NMR <sup>1</sup>H (CDCl<sub>3</sub>): δ= 7.33 (2H, d, J=5.7, SCH), 7.12 (2H, d, J=3, CHCHCS), 6.95 (2H, t, J=4.2, CHCHCH), 4.76 (2H, s, CH<sub>2</sub>Br). <sup>13</sup>C (CDCl<sub>3</sub>): δ= 27.0, 127.4, 128.4, 140.7.

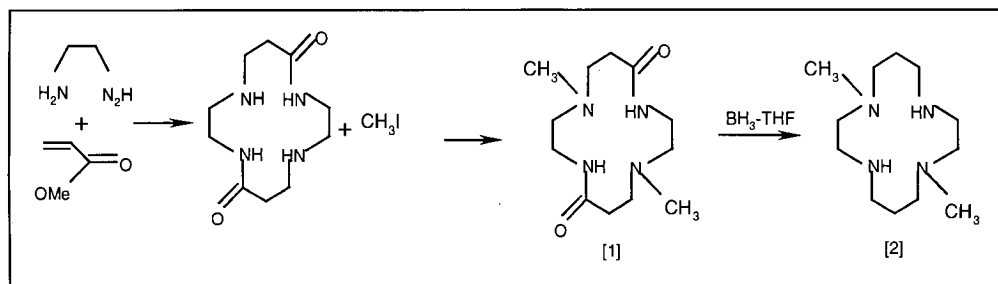
*[3] – 1,8-Bis(2-methylthiophene)-1,4,8,11-tetraazacyclotetradecane-5,12-dione*

To a solution of 1,4,8,11-tetraazacyclotetradecane-5,12-dione (0.5 g, 2.2 mmol) in acetonitrile (20 ml) was added 2-(bromomethyl)thiophene (0.79 g, 4.46 mmol, 2 equiv.), sodium carbonate (1.0 g, 9.46 mmol, 4 equiv.) and some crystals of potassium iodide. The solution was refluxed under nitrogen for 4 days. The solvent was removed under reduced pressure and the solid obtained was dissolved in an aqueous solution of NaOH (5.0 g, 50 ml) and extracted with dichloromethane (3x100 ml). The solvent was removed and the residue purified by chromatography on silica gel (CH<sub>2</sub>Cl<sub>2</sub>, MeOH from 0% to 10%, R<sub>f</sub> = 0.3 with MeOH 3%). The yield was 75% (0.69 g). Spectral analysis confirmed the product's structure. NMR <sup>1</sup>H (CDCl<sub>3</sub>): δ= 8.58 (2H, t), 7.21 (2H, d, J=5.1, SCH), 6.91 (2H, t, J=4.2, CHCHCH), 6.86 (2H, d, J=3.6, CHCHCS), 3.86 (4H, s, NCH<sub>2</sub>CS), 3.41 (4H, m, CH<sub>2</sub>CO), 2.63 (8H, m, NCH<sub>2</sub>CH<sub>2</sub>CO and CH<sub>2</sub>CH<sub>2</sub>NCO), 2.39 (4H, t, J=5.9, NCH<sub>2</sub>CH<sub>2</sub>NCO). <sup>13</sup>C (CDCl<sub>3</sub>): δ= 172.3, 138.5, 128.2, 127.2, 126.0, 52.1, 51.1, 49.5, 36.2, 32.5. IR (thin film) 1443 cm<sup>-1</sup> [ν(C=O)].

## [4] - 1,8-Bis(2-methylthiophene)-1,4,8,11-tetraazacyclotetradecane

To a solution of 1,8-bis(2-methylthiophene)-1,4,8,11-tetraazacyclotetradecane-5,12-dione (0.7 g, 1.66 mmol) in THF was added borane-THF (1.0 M, 30 ml, 30 mmol, 18 equiv.) and the mixture was refluxed for four days. Excess of borane was destroyed by careful addition of methanol, after which the solvent was removed and the residue heated to reflux in 6M HCl for 24 hours. Removal of water gave a brown residue, to which was added aqueous base (20% KOH) giving a black solid (0.6 g). The mixture was extracted with dichloromethane and the extracts dried over anhydrous sodium carbonate and evaporated to give a black solid. The yield was 90% (0.58 g). Despite the dark colour, spectral analysis confirmed the presence of the product in high purity. NMR  $^1\text{H}$  ( $\text{CDCl}_3$ ):  $\delta$ = 7.21 (2H, d,  $J=5.1$ , SCH), 6.95 (2H, t,  $J=4.2$ ,  $\text{CHCHCH}$ ), 6.91 (2H, d,  $J=3.5$ ,  $\text{CHCHCS}$ ), 3.94 (6H, s,  $\text{NCH}_2\text{CS}$ ), 2.73 (8H, m), 2.64 (4H, t,  $J=5.6$ ), 2.55 (4H, t), 1.83 (4H, q,  $\text{CH}_2\text{CH}_2\text{CH}_2$ ).  $^{13}\text{C}$  ( $\text{CDCl}_3$ ):  $\delta$ = 139.9, 127.2, 126.8, 125.2, 54.4, 51.6, 51.4, 50.2, 47.9, 26.3. MS-electrospray: 393  $[\text{M}+\text{H}]^+$ .

## 6.3.2 1,8-Dimethyl-1,4,8,11-tetraazacyclotetradecane



## [1] - 1,8-Dimethyl-1,4,8,11-tetraazacyclotetradecane-5,12-dione

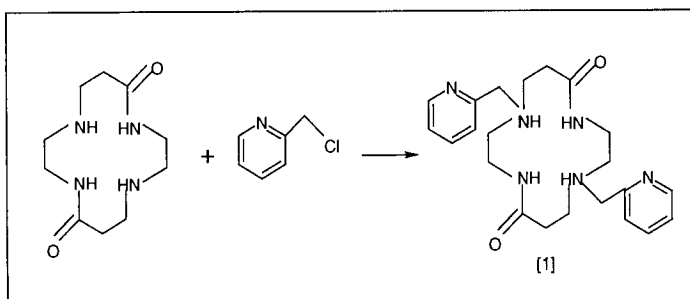
To a solution of 1,4,8,11-tetraazacyclotetradecane-5,12-dione (1.0 g, 4.4 mmol) in acetonitrile was added methyl iodide (1.9 g, 13.14 mmol, 3 equiv.) and sodium carbonate

(1.9 g, 17.5 mmol, 4 equiv.). The solution was stirred under nitrogen in a closed system for 24 hours at 45° C. The solvent was removed under reduced pressure. The yield was 60% (0.67 g). NMR  $^1\text{H}$  ( $\text{D}_2\text{O}$ ):  $\delta$ = 3.50 (4H, t,  $\text{CH}_2\text{CO}$ ), 3.13 (18H, m). IR (thin film)  $1632\text{ cm}^{-1}$  [ $\nu(\text{C}=\text{O})$ ].

[2] - 1,8-Dimethyl-1,4,8,11-tetraazacyclotetradecane

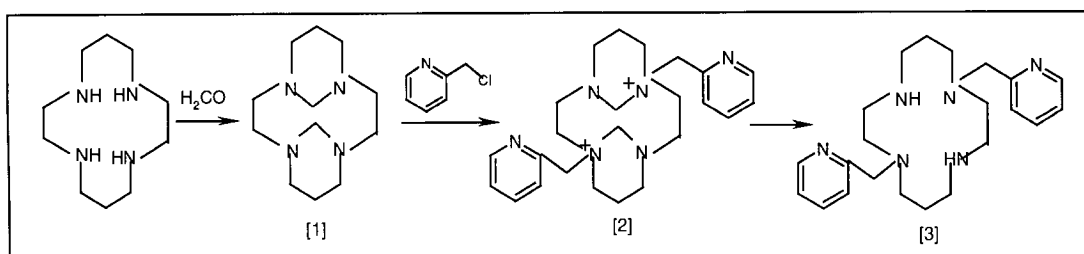
To a solution of dimethyl-1,4,8,11-tetraazacyclotetradecane-5,12-dione (1.05 g, 4.59 mmol) in THF (20 ml) was added borane-THF (1.0 M, 50 ml, 50 mmol, 19 equiv.) and the mixture was refluxed for four days. Excess of borane was destroyed with methanol after which the solvent was removed and the residue heated to reflux in 6M HCl for 24 hours. Removal of water gave a brown residue, to which was added aqueous base (20% KOH) giving a yellow solid. The mixture was extracted with dichloromethane (3x75 ml) and the extracts dried over anhydrous sodium carbonate and evaporated to give a yellow solid. The yield was 60% (0.56 g). NMR  $^1\text{H}$  ( $\text{CDCl}_3$ ):  $\delta$ = 2.68 (6H, s,  $\text{CH}_3$ ), 2.76-2.60 (12H, m), 2.42 (4H, t), 1.72 (4H, q,  $\text{CH}_2\text{CH}_2\text{CH}_2$ ). MS-electrospray: 229  $[\text{M}+\text{H}]^+$ .

**6.3.3 1,8-Bis(2-pyridylmethyl)-1,4,8,11-tetraazacyclotetradecane-5,12-dione ( $\text{H}_2\text{L}^5$ )**



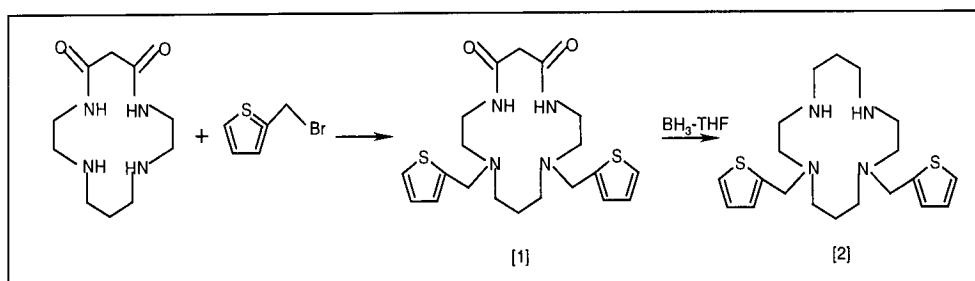
## [1] – 1,8-Bis(2-pyridylmethyl)-1,4,8,11-tetraazacyclotetradecane-5,12-dione

To a solution of 1,4,8,11-tetraazacyclotetradecane-5,12-dione (0.66 g, 2.9 mmol) in acetonitrile was added picolyl chloride (0.96 g, 5.86 mmol, 2 equiv.), sodium carbonate (1.24 g, 11.7 mmol, 4 equiv.) and some crystals of potassium iodide. The solution was refluxed under nitrogen for 5 days. The solvent was evaporated and the solid obtained was taken up into a mixture of NaOH solution (pH=14) and dichloromethane. The organic phase was separated and the aqueous extracted a further three times with dichloromethane. The organic extracts were combined and the solvent removed. Purification of the compound was effected by chromatography on silica gel (CH<sub>2</sub>Cl<sub>2</sub>, MeOH from 0% to 10%). The yield was 75% (0.91 g). NMR <sup>1</sup>H (CDCl<sub>3</sub>): δ= 9.13 (2H, t, NHCO), 8.55 (2H, d, J=4.8, NCHCH), 7.69 (2H, t, J=7.5, NCHCHCH), 7.40 (2H, d, J=7.5, NCHCHCHCH), 7.17 (2H, t, J=6.15, CHC), 3.80 (4H, s, pyCH<sub>2</sub>N), 3.41 (4H, t, CH<sub>2</sub>CO), 2.69 (8H, m, COCH<sub>2</sub>CH<sub>2</sub>, and NHCH<sub>2</sub>CH<sub>2</sub>N), 2.38 (4H, t, J=5.6, NHCH<sub>2</sub>CH<sub>2</sub>N). <sup>13</sup>C (CDCl<sub>3</sub>): δ= 172.3, 158.0, 149.5, 136.6, 124.1, 122.7, 59.6, 52.7, 50.2, 36.4, 32.8. IR (thin film) 1658 cm<sup>-1</sup> [ν(C=O)].

6.3.4 1,8-Bis(2-pyridylmethyl)-1,4,8,11-tetraazacyclotetradecane (L<sup>1</sup>)

The procedure described in literature was followed, and spectral analyses were consistent with the published data.<sup>(7)</sup>

## 6.3.5 1,11-Bis(2-methylthiophene)-1,4,8,11-tetraazacyclotetradecane

*[1] – 1,11-Bis(2-methylthiophene)-1,4,8,11-tetraazacyclotetradecane-5,7-dione*

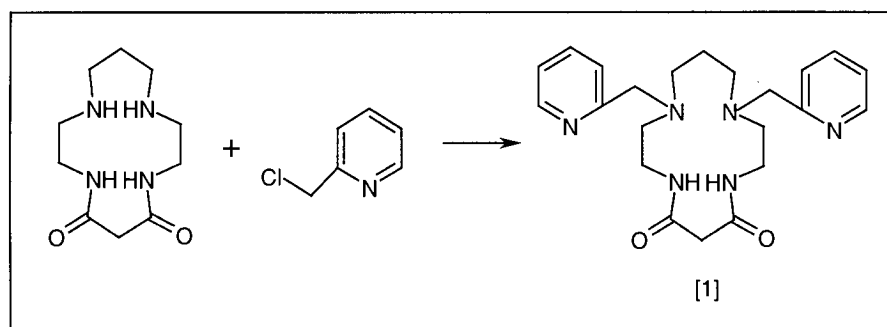
To a solution of 1,4,8,11-tetraazacyclotetradecane-5,7-dione (0.6 g, 2.7 mmol) in acetonitrile (15 ml) was added 2-(bromomethyl)thiophene (1.0 g, 5.65 mmol, 2 equiv.), sodium carbonate (1.1 g, 10.38 mmol, 4 equiv.) and some crystals of potassium iodide. The solution was refluxed under nitrogen for 10 days. The solvent was removed and the residue was dissolved in a mixture of NaOH(aq) (pH=14) and dichloromethane. The organic phase was removed, and the aqueous phase was extracted three times with dichloromethane, after which the organic extracts were combined, dried over  $\text{K}_2\text{CO}_3$  and the solvent removed. Separation of the compound was effected by chromatography on silica gel ( $\text{CH}_2\text{Cl}_2$ , MeOH from 0% to 10%,  $R_f = 0.3$  with MeOH 3%). The yield was 45% (0.66 g). Spectral analysis confirmed the product's structure. NMR  $^1\text{H}$  ( $\text{CDCl}_3$ ):  $\delta = 7.24$  (2H, d,  $J=5.1$ , SCH),  $6.94$  (2H, t,  $J=4.2$ , CHCHCH),  $6.88$  (2H, d,  $J=3.6$ , CHCHCS),  $3.78$  (4H, s,  $\text{NCH}_2\text{CS}$ ),  $3.39$  (4H, t,  $J=8.1$ ,  $\text{CONCH}_2$ ),  $3.25$  (2H, s,  $\text{CH}_2\text{CO}$ ),  $2.64$  (4H, t,  $J=5.7$ ,  $\text{CONCH}_2\text{CH}_2\text{N}$ ),  $2.47$  (4H, t,  $J=6.6$ ,  $\text{NCH}_2\text{CH}_2\text{CH}_2$ ),  $1.63$  (2H, q,  $\text{CH}_2\text{CH}_2\text{CH}_2$ ).

*[2] – 1,11-Bis(2-methylthiophene)-1,4,8,11-tetraazacyclotetradecane*

To a solution of 1,11-bis(2-methylthiophene)-1,4,8,11-tetraazacyclotetradecane-5,7-dione (0.5 g, 1.19 mmol) in THF was added borane-THF (1.0 M, 25 ml, 25 mmol, 21 equiv.)

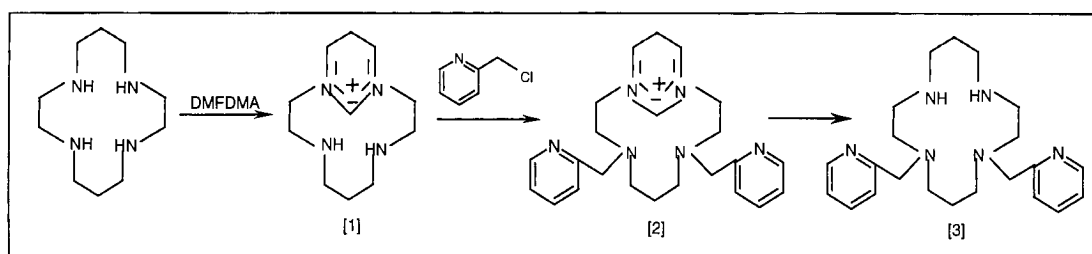
and the mixture was refluxed at 80° C for two days. Excess of borane was destroyed with methanol, after which the solvent was removed and the residue heated to reflux in 6M HCl for 24 hours. Removal of water gave a brown residue, to which was added aqueous base (20% KOH) giving a black suspension (0.5 g). The mixture was extracted with dichloromethane and the extracts dried over anhydrous sodium carbonate and evaporated to give a black solid. The yield was 90% (0.42 g). Spectral analysis confirmed the presence of the product, contaminated with a small proportion (~10%) of the mono-substituted compound [1-(methylthiophene)-1,4,8,11-tetraazacyclo tetradecane]. NMR data for the di-substituted compound:  $^1\text{H}$  ( $\text{CDCl}_3$ ):  $\delta$ = 7.20 (2H, d,  $J$ =5.1, SCH), 6.91 (2H, t,  $J$ =4.4,  $\text{CHCHCH}$ ), 6.85 (2H, d,  $J$ =2.7,  $\text{CHCHCS}$ ), 3.78 (4H, s,  $\text{NCH}_2\text{CS}$ ), 2.80-2.46 (16H, m,  $\text{tpCH}_2\text{CH}_2\text{NH}$ ,  $\text{tpCH}_2\text{CH}_2\text{NH}$ ,  $\text{tpCH}_2\text{CH}_2\text{CH}_2$ , and  $\text{NHCH}_2\text{CH}_2\text{CH}$ ), 1.84-1.66 (4H, q+q,  $\text{NHCH}_2\text{CH}_2\text{CH}_2$  and  $\text{tpCH}_2\text{CH}_2\text{CH}_2$ ). MS-electrospray: 393  $[\text{M}+\text{H}]^+$ .

### 6.3.6 1,11-Bis(2-pyridylmethyl)-1,4,8,11-tetraazacyclotetradecane- 5,7-dione



*[1] - 1,11-Bis(2-pyridylmethyl)-1,4,8,11-tetraazacyclotetradecane-5,7-dione*

To a solution of 1,4,8,11-tetraazacyclotetradecane-5,7-dione (497 mg, 2.18 mmol) in acetonitrile was added picolyl chloride (714 mg, 4.35 mmol, 2 equiv.), and sodium carbonate (930 mg, 8.77 mmol, 4 equiv.) and some crystals of potassium iodide. The solution was refluxed under nitrogen for 48 hours. The solvent was removed and the residue taken up into a mixture of aqueous NaOH (pH=14) and dichloromethane. After three extractions with dichloromethane the solution was dried and the solvent evaporated. Separation of the compound was effected by chromatography on silica gel (CH<sub>2</sub>Cl<sub>2</sub>, MeOH from 0% to 10%, R<sub>f</sub> = 0.5 with MeOH 3%). The yield was 72% (0.645 g). Spectral analysis is consistent with the published data.<sup>(8)</sup> NMR <sup>1</sup>H (CDCl<sub>3</sub>): δ= 8.53 (2H, d, arom), 7.67 (2H, t, arom), 7.28 (2H, d, arom), 7.18 (2H, t, arom), 3.70 (4H, s, CH<sub>2</sub>CH<sub>2</sub>CH<sub>2</sub>), 3.36 (4H, t, CONCH<sub>2</sub>), 3.27 (2H, s, pyCHCHCH), 2.61 (4H, t, NCH<sub>2</sub>), 2.50 (4H, t, NCH<sub>2</sub>), 1.71 (2H, m, CH<sub>2</sub>CH<sub>2</sub>CH<sub>2</sub>). MS-electrospray: 411 [M+H]<sup>+</sup>.

**6.3.7 1,11-Bis(2-pyridylmethyl)-1,4,8,11-tetraazacyclotetradecane (L<sup>2</sup>)***[1] – Formamidinium salt of 1,4,8,11-tetraazacyclotetradecane*

Reaction of 1,4,8,11-tetraazacyclotetradecane (1.1 g, 5.5 mmol) with an equimolar amount of the dimethyl acetal of dimethylformamide (0.71 g, 5.6 mmol) in refluxing chloroform (25 ml) for a period of four days gave the formamidium salt of 1,4,8,11-

tetraazacyclotetradecane in 90% yield (1.04 g). Spectral analysis is consistent with the published data<sup>(9)</sup>. NMR <sup>1</sup>H (CDCl<sub>3</sub>): δ= 9.37 (1H, s), 3.74 (4H, t), 3.35 (4H, t), 2.80-2.95 (4H, m), 2.21 (2H, q), 1.68 (2H, q).

*[2] - 1,11-Bis(2-pyridylmethyl) di-substituted derivative of the formamidinium salt of 1,4,8,11-tetraazacyclotetradecane.*

To solution of formamidinium salt (1.0 g, 5.0 mmol) was added picolyl chloride (1.8 g, 11 mmol, 2 equiv.), sodium carbonate (2.4 g, 22.6 mmol, 4 equiv.) and some crystals of potassium iodide in refluxing acetonitrile. After four days, the solvent was removed under reduced pressure. Separation of the compound was effected by chromatography on silica gel (CH<sub>2</sub>Cl<sub>2</sub>, MeOH from 0% to 10%, R<sub>f</sub> = 0.25 with MeOH 5%). The yield was 80% (1.49 g). Spectral analysis confirmed the product's structure. NMR <sup>1</sup>H (CDCl<sub>3</sub>): δ= 9.5 (1H, s, NCHN), 8.52 (2H, d, J=4.8), 7.69 (2H, t, J=7.5), 7.25 (2H, d, J=7.8), 7.19 (2H, t, J=5.4), 3.66 (4H, s, NCH<sub>2</sub>py), 3.51 (4H, t, J=5.25, NCH<sub>2</sub>CH<sub>2</sub>Npy), 3.23 (4H, t, J=5.7, NCH<sub>2</sub>CH<sub>2</sub>CH<sub>2</sub>N), 2.75 (4H, t, NCH<sub>2</sub>CH<sub>2</sub>NCH<sub>2</sub>py), 2.44 (4H, t, py CH<sub>2</sub>NCH<sub>2</sub>CH<sub>2</sub>CH<sub>2</sub>), 2.07 (2H, q, NHCH<sub>2</sub>CH<sub>2</sub>CH<sub>2</sub>), 1.65 (2H, q, pyNCH<sub>2</sub>CH<sub>2</sub>CH<sub>2</sub>). MS-electrospray: 393 [M]<sup>+</sup>.

*[3] – 1,11-Bis(2-pyridylmethyl)-1,4,8,11-tetraazacyclotetradecane*

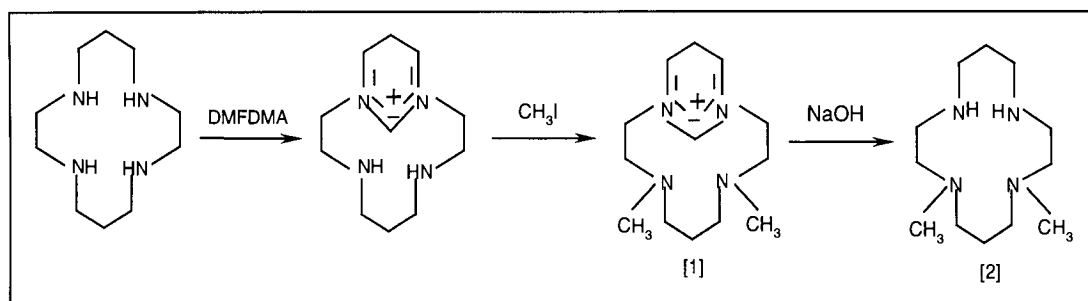
The previous compound (1.35 g, 3.44 mmol) was converted to the free base by refluxing with sodium hydroxide (10M, 20 ml) for 7 days. After extraction with dichloromethane (3x75 ml) the solution was dried over sodium carbonate, and the solvent was removed under vacuum to give the desired compound. The yield was 45% (0.59 g). Spectral analysis confirmed the product's structure. NMR <sup>1</sup>H (CDCl<sub>3</sub>): δ= 8.50 (2H, d, J=4.8), 7.64 (2H, t, J=7.5), 7.44 (2H, d, J=7.8), 7.14 (2H, t, J=5.4), 3.67 (4H, s, NCH<sub>2</sub>py), 2.80-



2.50 (16H, m), 1.79 (2H, q,  $\text{pyNCH}_2\text{CH}_2\text{CH}_2$ ), 1.69 (2H, q,  $\text{pyNCH}_2\text{CH}_2\text{CH}_2$ ).  $^{13}\text{C}$  ( $\text{CDCl}_3$ ):  $\delta$ = 160.6, 149.2, 136.7, 123.3, 122.2, 61.3, 54.6, 51.4, 48.9, 47.9, 28.6, 27.1.

MS-electrospray: 383  $[\text{M}+\text{H}]^+$ .

### 6.3.8 1,11-Dimethyl-1,4,8,11-tetraazacyclotetradecane



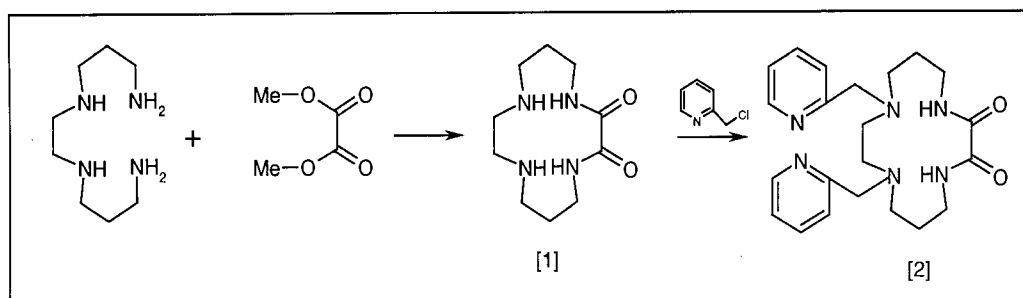
[1] - 1,11-Di-N-methylated formamidinium salt of 1,4,8,11-tetraazacyclotetradecane

To a solution of the formamidinium salt (0.5 g, 2.5 mmol) was added methyl iodide (1.5 g, 10.46 mmol, 4 equiv.), and sodium carbonate (1.1 g, 10.4 mmol, 2 equiv.) in acetonitrile and the solution was heated at 45°C. After five days the solvent was removed under reduced pressure. Separation of the compound from the residue was effected by chromatography on silica gel ( $\text{CH}_2\text{Cl}_2$ , MeOH from 0% to 10%,  $R_f$  = 0.3 with MeOH 4%). The yield was 20% (0.113 g). Spectral analysis confirmed the product's structure. NMR  $^1\text{H}$  ( $\text{CDCl}_3$ ):  $\delta$ = 8.85 (1H, s, NCHN), 3.66 (4H, t,  $J=5.25$ ,  $\text{NCH}_2\text{CH}_2\text{NCH}_3$ ), 3.37 (4H, t,  $J=5.85$ ,  $\text{NHCH}_2\text{CH}_2\text{CH}_2$ ), 2.56 (4H, t,  $\text{NCH}_2\text{CH}_2\text{NCH}_3$ ), 2.40 (2H, q,  $\text{NHCH}_2\text{CH}_2\text{CH}_2$ ), 2.25 (6H, s,  $\text{CH}_3$ ), 2.22 (4H, t,  $\text{CH}_3\text{NCH}_2\text{CH}_2\text{CH}_2$ ), 1.65 (2H, q,  $\text{NCH}_3\text{CH}_2\text{CH}_2\text{CH}_2$ ).

*[2] – 1,11-Dimethyl -1,4,8,11-tetraazacyclotetradecane*

The previous compound (250 mg, 1.04 mmol) was converted to the free base by refluxing with sodium hydroxide (10M, 10 ml) for 7 days. The compound was extracted with dichloromethane (3x100 ml) and the solvent was removed under reduced pressure. The yield was 45% (0.108 g). Spectral analysis confirmed the product's structure. NMR  $^1\text{H}$  ( $\text{CDCl}_3$ ):  $\delta$ = 2.80-2.60 (8H, m,  $\text{NHCH}_2$ ), 2.46 (4H, t,  $J=5.2$ ,  $\text{CH}_3\text{NCH}_2\text{CH}_2\text{N}$ ), 2.36 (4H, t,  $J=6.3$ ,  $\text{CH}_3\text{NCH}_2\text{CH}_2\text{CH}_2$ ), 2.15 (6H, s,  $\text{CH}_3$ ), 1.78 (2H, q,  $\text{NHCH}_2\text{CH}_2\text{CH}_2$ ), 1.63 (2H, q,  $\text{NCH}_3\text{CH}_2\text{CH}_2\text{CH}_2$ ).

### 6.3.9 1,4-Bis(2-pyridylmethyl)-1,4,8,11-tetraazacyclotetradecane-9,10-dione

*[1] – 1,4,8,11-Tetraazacyclotetradecane-2,3-dione*

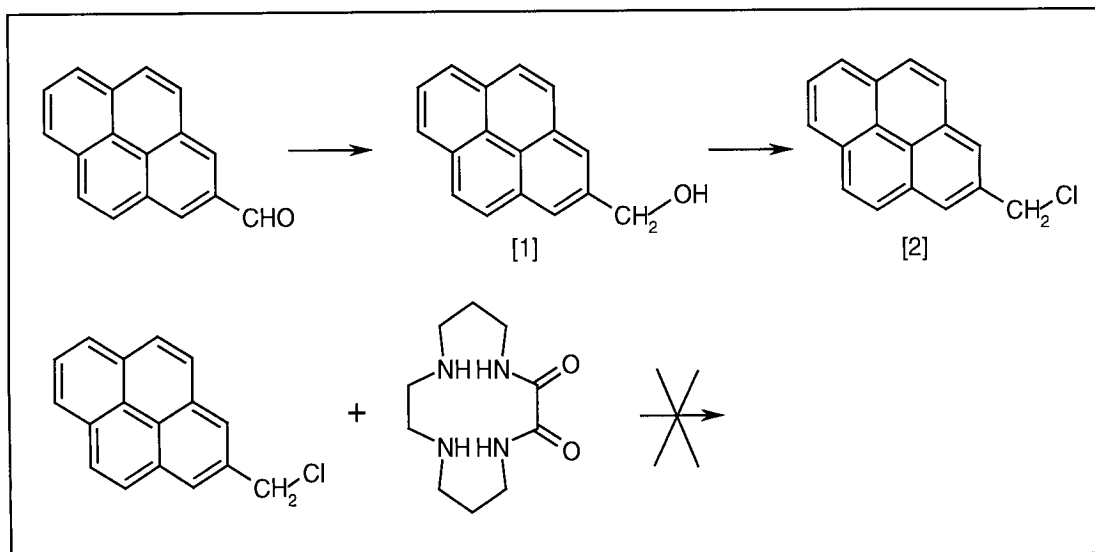
A mixture of dimethyloxalate (787 mg, 6.6 mmol) and *N,N'*-bis(3-aminopropyl) ethylenediamine, previously distilled, (1.15 g, 6.6 mmol), dissolved in ethanol (150 ml), was added to refluxing ethanol (150 ml) dropwise over a period of 18 hours. After 24 hours the solution was cooled and filtered. The solution was then reduced to dryness and the white product taken up into hot propan-2-ol (50 ml). Filtering the hot solution and then reduction to dryness gave the desired product in 71% yield (1.08 g). Spectral

analysis was consistent with the published data<sup>(10)</sup>. NMR  $^1\text{H}$  ( $\text{CDCl}_3$ ):  $\delta$ = 3.35 (4H, t,  $\text{CH}_2\text{N}$ ), 2.8-2.6 (8H, m,  $\text{CH}_2\text{N}$ ), 1.69 (4H, q,  $\text{CH}_2\text{CH}_2\text{CH}_2$ ). MS-electrospray: 229  $[\text{M}+\text{H}]^+$ .

*[2] – 1,4-Bis(2-pyridylmethyl)-1,4,8,11-tetraazacyclotetradecane-9,10-dione*

To a solution of 1,4,8,11-tetraazacyclotetradecane-2,3-dione (1.3 g, 5.69 mmol) in acetonitrile was added picolyl chloride (1.91 g, 11.39 mmol, 2 equiv.), and sodium carbonate (2.41 g, 22.78 mmol, 4 equiv.) and some crystals of potassium iodide. The solution was refluxed under nitrogen for 48 hours. The solvent was removed and the residue obtained was dissolved in a mixture of NaOH solution (pH=14) and dichloromethane. After three extractions with dichloromethane, the solution was dried and the solvent removed. Separation of the compound was effected by chromatography on silica gel ( $\text{CH}_2\text{Cl}_2$ , MeOH from 0% to 10%,  $R_f$  = 0.5 with MeOH 4%). The yield was 44% (1.03 g). Spectral analysis confirmed the product's structure. NMR  $^1\text{H}$  ( $\text{CDCl}_3$ ):  $\delta$ = 8.49 (2H, d, arom), 7.63 (2H, t, arom), 7.50 (2H, d, arom), 7.14 (2H, t, arom), 3.73 (4H, s,  $\text{NCH}_2\text{arom}$ ), 3.24 (4H, q,  $\text{NCH}_2$ ), 2.93 (4H, s,  $\text{NCH}_2$ ), 2.86 (4H, t,  $\text{NCH}_2$ ), 1.81 (4H, m,  $\text{CH}_2\text{CH}_2\text{CH}_2$ ).  $^{13}\text{C}$  ( $\text{CDCl}_3$ ):  $\delta$ = 160.1, 149.2, 136.9, 123.7, 122.4, 102.2, 62.0, 55.1, 52.1, 40.2, 25.5. MS-electrospray: 411  $[\text{M}+\text{H}]^+$ .

## 6.3.10 Chloromethylpyrene

*[1] – Hydroxymethylpyrene*

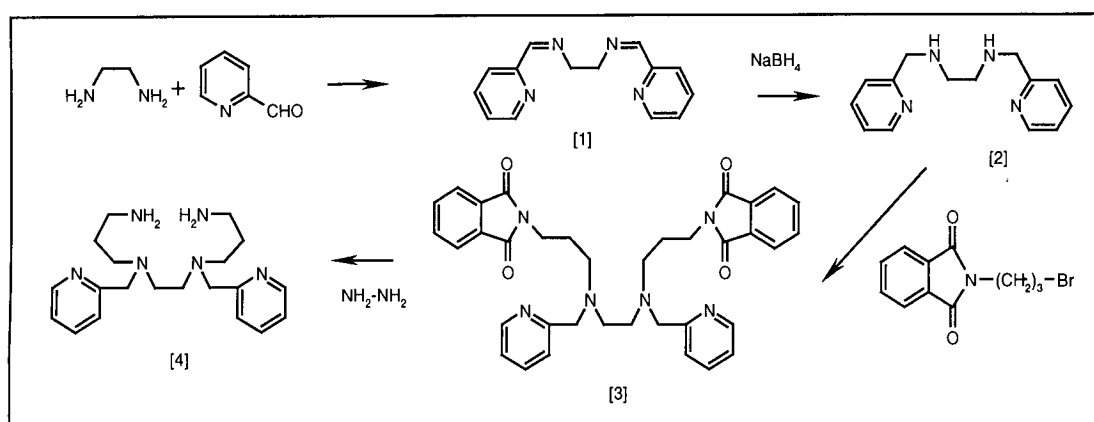
To a stirred solution of  $\text{NaBH}_4$  (166 mg, 4.3 mmol) in MeOH (40 ml), was added 1-pyrenecarboxaldehyde (1.0 g, 4.3 mmol). After stirring for an hour at room temperature, the bright yellow starting compound became soluble and pale yellow. The light yellow solution was concentrated under vacuum, and water (40 ml) was added. The mixture was neutralised with 1N HCl, extracted with EtOAc (2x 50 ml), dried over  $\text{Na}_2\text{CO}_3$ , and concentrated under vacuum, to give the desired product. The yield was 84% (0.85 g). NMR  $^1\text{H}$  ( $\text{CDCl}_3$ ):  $\delta$ = 8.37 (1H, d,  $J$ =9.3, arom), 8.25-8.0 (8H, m, arom), 5.41 (2H, s,  $\text{CH}_2\text{OH}$ ).  $^{13}\text{C}$  ( $\text{CDCl}_3$ ):  $\delta$ = 133.9, 131.4, 130.9, 129.0, 127.6, 127.5, 126.2, 126.1, 125.4, 125.4, 124.9, 123.1, 64.0. MS-electrospray: 233  $[\text{M}+\text{H}]^+$ .

*[2] – Chloromethylpyrene*

Hydroxymethylpyrene (200 mg, 0.86 mmol) was added to thionyl chloride (5 ml). After stirring for 12 hours at room temperature, water (10 ml) was added to destroy the unreacted thionyl chloride. The solution was extracted with  $\text{CH}_2\text{Cl}_2$  (3x 25 ml), dried over

$\text{Na}_2\text{CO}_3$ , and concentrated under vacuum to give the desired product. The yield was 74% (0.16 g). NMR ( $^1\text{H}$ ,  $\text{CDCl}_3$ ):  $\delta$ = 8.37 (1H, d,  $J$ =9.3, arom), 8.30-8.0 (8H, m, arom), 5.33 (2H, s,  $\text{CH}_2\text{OH}$ ).  $^{13}\text{C}$  ( $\text{CDCl}_3$ ):  $\delta$ = 132.1, 131.3, 130.4, 129.2, 128.5, 128.1, 127.8, 127.4, 126.3, 125.7, 125.2, 124.8, 124.7, 122.8, 44.9.

### 6.3.11 5,8-Bis(2-pyridylmethyl)-1,5,8,12-tetraazadodecane



#### [1] – *N,N'*-Bis-pyridin-2-ylmethylene-ethane-1,2-diamine

Ethylenediamine (1.17 g, 19.4 mmol) was dissolved in methanol, and pyridine-2-carboxaldehyde (4.17 g, 38.9 mmol) was added. The reaction mixture was refluxed for 6 hours. The solvent was rotary evaporated to give the desired compound. The yield was 95% (4.41 g). NMR  $^1\text{H}$  ( $\text{CDCl}_3$ ):  $\delta$ = 8.61 (2H, m, arom), 8.40 (2H, s, CH), 7.96 (2H, d, arom), 7.71 (2H, t, arom), 7.28 (2H, t, arom), 4.05 (4H, s,  $\text{CH}_2$ ). MS-electrospray: 239  $[\text{M}+\text{H}]^+$ .

#### [2] – *N,N'*-Bis-pyridin-2-ylmethyl-ethane-1,2-diamine

To a stirred solution of  $\text{NaBH}_4$  (2.0 g, 52.9 mmol) in MeOH (40 ml), was added *N,N'*-bis-pyridin-2-ylmethylene-ethane-1,2-diamine (4.3 g, 18.07 mmol). After stirring at room

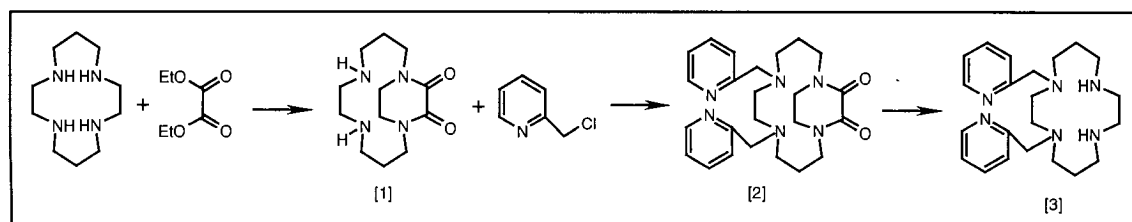
temperature for one hour, the solution was refluxed overnight. The solution was concentrated under vacuum and aqueous NaOH (40 ml) was added. The solution was extracted with dichloromethane (3x50 ml), the extracts combined and dried over Na<sub>2</sub>CO<sub>3</sub>, and the solvent removed under vacuum to give the desired product. The yield was 93% (4.07 g). NMR <sup>1</sup>H (CDCl<sub>3</sub>): δ= 8.46 (2H, d, arom), 7.54 (2H, t, arom), 7.23 (2H, d, arom), 7.06 (2H, t, arom), 3.84 (4H, s, NCH<sub>2</sub>arom), 2.74 (4H, s, NCH<sub>2</sub>CH<sub>2</sub>). MS-electrospray: 243 [M+H]<sup>+</sup>.

[3] – 5,8-Bis(2-pyridylmethyl)-1,12-di[N-(propyl)phthalamide]-1,5,8,12-tetraazadodecane

To a solution of N,N'-bis-pyridin-2-ylmethyl-ethane-1,2-diamine (4.0 g, 16.5 mmol) in acetonitrile (100 ml) was added N-(3-bromopropyl)phthalamide (8.86 g, 33.05 mmol, 2 equiv.), potassium carbonate (4.57 g, 33.05 mmol) and some crystals of potassium iodide. The solution was refluxed under nitrogen for 48 hours. The solvent was removed and the residue dissolved in a mixture of aqueous NaOH (pH=12) and dichloromethane. After three extractions with dichloromethane the combined organic extracts were dried over sodium carbonate. Separation of the compound was effected by chromatography on silica gel (CH<sub>2</sub>Cl<sub>2</sub>, MeOH from 0% to 10%, R<sub>f</sub> = 0.5 with MeOH 5%). The yield was 79% (8.04 g). Spectral analysis confirmed the product's structure. NMR <sup>1</sup>H (CDCl<sub>3</sub>): δ= 8.44 (2H, d, arom), 7.82-7.42 (12H, m, arom), 7.08 (2H, t, arom), 3.71 (4H, s, NCH<sub>2</sub>arom), 3.68 (4H, t, J=7.8, NCH<sub>2</sub>CH<sub>2</sub>), 2.64 (4H, s, NCH<sub>2</sub>CH<sub>2</sub>), 2.56 (4H, t, J=6.8, NCH<sub>2</sub>CH<sub>2</sub>), 1.84 (4H, m, CH<sub>2</sub>CH<sub>2</sub> CH<sub>2</sub>). <sup>13</sup>C (CDCl<sub>3</sub>): δ= 168.5, 160.4, 149.1, 136.6, 134.1, 132.5, 123.4, 123.2, 122.1, 61.1, 52.6, 52.5, 36.5, 26.6. MS-electrospray: 617 [M+H]<sup>+</sup>.

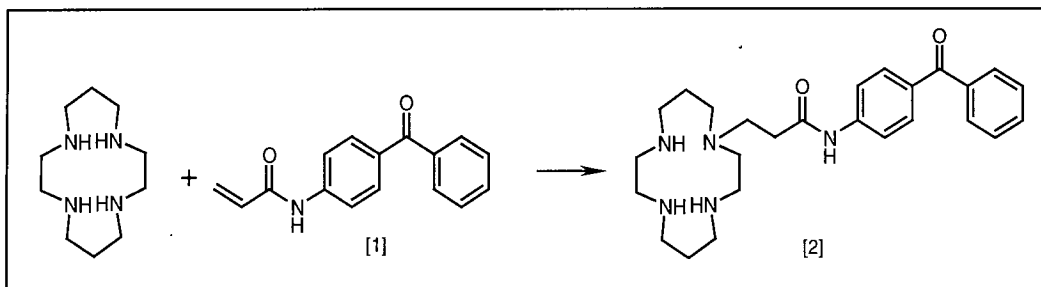
## [4] – 5,8-Bis(2-pyridylmethyl)-1,5,8,12-tetraazadodecane

5,8-Bis(2-pyridylmethyl)-1,12-di[N-(propyl)phthalamide]-1,5,8,12-tetraazadodecane (6.0 g, 9.74 mmol) was dissolved in 50 ml of absolute ethanol containing hydrazine (1.0 g, 19.5 mmol). The mixture was allowed to reflux for 18 hours. After cooling, HCl (10M, 15 ml) was added and the mixture was stirred for a further hour. The solution was then filtered to remove the white precipitate and the ethanol was removed from the filtrate under vacuum. Aqueous NaOH was added, and the aqueous solution extracted with dichloromethane (3x 40 ml). The combined dichloromethane extracts were dried over sodium carbonate, filtered and concentrated under vacuum to give a yellow oil. The yield was 58% (2.01 g). Spectral analysis confirmed the product's structure. NMR  $^1\text{H}$  ( $\text{CDCl}_3$ ):  $\delta$ = 8.50 (2H, d,  $J$ =4.5, arom), 7.61 (2H, t,  $J$ =7.6, arom), 7.41 (2H, d,  $J$ =7.8, arom), 7.13 (2H, t,  $J$ =6.8, arom), 3.72 (4H, s,  $\text{NCH}_2\text{arom}$ ), 2.67 (8H, m,  $\text{NCH}_2\text{CH}_2$ ), 2.51 (4H, t,  $J$ =7.2,  $\text{NCH}_2\text{CH}_2$ ), 1.59 (4H, m,  $\text{CH}_2\text{CH}_2\text{CH}_2$ ).  $^{13}\text{C}$  ( $\text{CDCl}_3$ ):  $\delta$ = 160.2, 148.8, 136.2, 122.7, 121.7, 60.9, 52.4, 52.3, 40.3, 30.9. MS-electrospray: 357  $[\text{M}+\text{H}]^+$ .

6.3.12 1,4-Bis(2-pyridylmethyl)-1,4,8,11-tetraazacyclotetradecane ( $\text{L}^3$ )

The procedure described in literature was followed, and spectral analyses were consistent with the published data.<sup>(11)</sup>

### 6.3.13 N-(4-benzoyl-phenyl)-3-(1,4,8,11-tetraazacyclotetradec-1-yl)-propionamide



#### [1] – N-(4-benzoylphenyl)acrylamide

A solution of triethylamine (2.015 g, 19.7 mmol) and 4-aminobenzophenone (2.645 g, 13.14 mmol) in dichloromethane (50 ml) was stirred at 0° and a solution of acryloyl chloride (1.11 ml, 13.14 mmol) in dichloromethane (25 ml) was added dropwise. After 24 hours the solution was washed twice with water (50 ml) and the solvent was removed under vacuum to give the desired compound. The yield was 92% (2.83 g).

NMR  $^1\text{H}$  ( $\text{CDCl}_3$ ):  $\delta$ = 10.48(1H, s, NH), 8.02 (2H, d,  $J$ =8.7, arom), 7.74 (4H, td,  $J$ =8.7, 7.8, arom), 7.55 (1H, t,  $J$ =7.8, arom), 7.45 (2H, t, 7.8, arom), 6.81 (1H, q,  $J$ =16.4, 10.4,  $\text{CH}_2=\underline{\text{CH}}$ ), 6.42 (1H, d,  $J$ =16.9,  $\text{HCH}=\underline{\text{CH}}$  trans), 6.68(1H, d,  $J$ =10.35,  $\text{HCH}=\underline{\text{CH}}$  cis).  $^{13}\text{C}$  ( $\text{CDCl}_3$ ):  $\delta$ = 195.5, 164.4, 143.1, 137.6, 131.9, 131.8, 131.5, 130.9, 129.4, 128.0, 127.1, 118.9. (Electrospray,  $\text{ES}^-$ ): 250 (M), 286 (M+Cl).

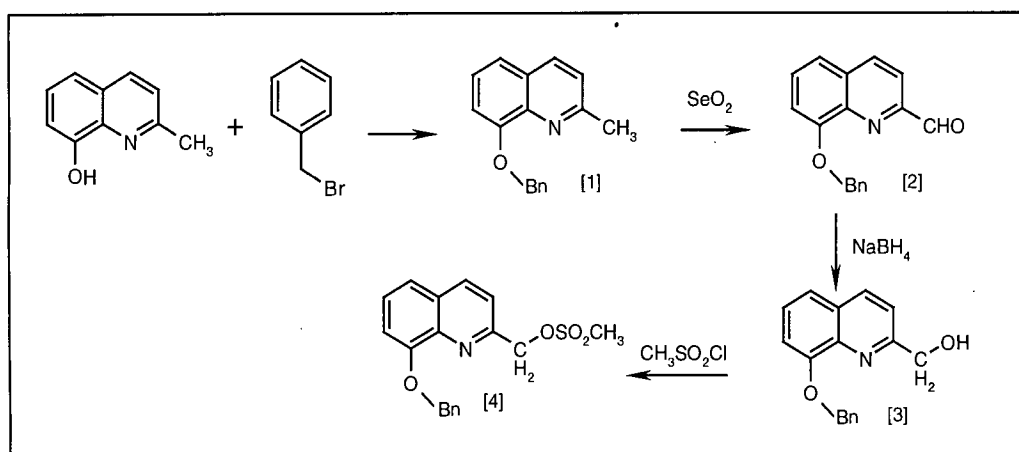
#### [2] – N-(4-benzoyl-phenyl)-3-(1,4,8,11-tetraazacyclotetradec-1-yl)-propionamide

A 25 ml round bottomed flask was charged with 1,4,8,11-tetraazacyclotetradecane (511 mg, 2.55 mmol), *p*-toluene-sulfonic acid monohydrate (500 mg, 2.55 mmol) and 10 ml of chloroform. N-(4-benzoylphenyl)acrylamide (640 mg, 2.55 mmol), dissolved in 5 ml of chloroform, was added. The resulting solution was stirred for 24 hours at room



temperature. The mixture was basicified with aqueous NaOH (pH=10) and the organic layer separated, dried over anhydrous sodium carbonate and evaporated to give a white solid. Separation of the compound was effected by chromatography on silica gel ( $R_f = 0.5$  with  $\text{CHCl}_3/\text{MeOH}/\text{NH}_4\text{OH}$ , 10/4/1). The yield was 84% (0.917 g). Spectral analysis confirmed the product's structure. NMR  $^1\text{H}$  ( $\text{CDCl}_3$ ):  $\delta = 7.84$  (2H, d,  $J=9$ , arom), 7.78 (2H, d,  $J=8.5$ , arom), 7.73 (2H, d,  $J=8$ , arom), 7.55 (1H, t,  $J=7.5$ , arom), 7.45 (2H, t,  $J=7.5$ , arom), 2.44-2.78 (20H, m,  $\text{NCH}_2$  and  $\text{NCH}_2\text{CO}$ ), 1.77 (2H, m,  $\text{CH}_2\text{CH}_2\text{CH}_2$ ), 1.64 (2H, m,  $\text{CH}_2\text{CH}_2\text{CH}_2$ ).  $^{13}\text{C}$  ( $\text{CDCl}_3$ ):  $\delta = 195.8, 171.9, 143.4, 138.1, 132.2, 131.7, 129.9, 128.3, 118.4, 77.3, 55.1, 53.1, 51.1, 50.2, 49.6, 49.2, 48.2, 47.8, 47.7, 47.3, 36.9, 28.5, 26.3, 25.9$ . MS-electrospray: 452  $[\text{M}+\text{H}]^+$ .

### 6.3.14 2-(Mesyloxy)methyl-8-benzyloxyquinoline



#### [1] – 2-Methyl-8-benzyloxyquinoline

8-Hydroxyquinoline (2.0 g, 12.3 mmol) was added to a solution of KOH (760 mg, 13.54 mmol) in ethanol (25 ml). Then benzyl bromide (2.58 g, 14.8 mmol) was added dropwise; the mixture was heated under reflux until no starting material was detectable (12 h) by

TLC ( $\text{CH}_2\text{Cl}_2/\text{MeOH}$ , 90/10). KBr was filtered off and washed with more ethanol. The solvent was evaporated and the residue was dissolved in distilled water (20 ml). The mixture was acidified with aqueous 2N HCl in order to obtain a clear solution, which was then washed with  $\text{Et}_2\text{O}$  (2x 30 ml). Addition of NaOH 5N was added to precipitate the product. The solid was filtered, dried and collected in hexane. The yield was 71% (2.24 g). Spectral analysis was consistent with the published data<sup>(11)</sup>. NMR  $^1\text{H}$  ( $\text{CDCl}_3$ ):  $\delta$ = 8.0 (1H, d,  $J$ =8.7, NCHCH), 7.54 (2H, d,  $J$ =7.2, arom), 7.41-7.26 (6H, m, arom), 7.01 (1H, d,  $J$ =6.8, arom), 5.47 (2H, s,  $\text{CH}_2$ ), 2.82 (3H, s, Me). MS-electrospray: 250  $[\text{M}+\text{H}]^+$ .

### [2] – 2-Carboxaldehyde-8-benzyloxyquinoline

Under nitrogen, 2-methyl-8-benzyloxyquinoline (1,35 g, 5.42 mmol) was added to a suspension of selenium oxide (752 mg, 6.78 mmol) in 20 ml of dioxane and the mixture was stirred at 80°C for 24 hours. The hot mixture was filtered on celite to remove black selenium. The solution was evaporated and the residue was treated with acetone, after which the precipitated red selenium was filtered off. Chromatography (silica gel,  $\text{CH}_2\text{Cl}_2/\text{MeOH}$ , 99/1) afforded the desired aldehyde as a yellow oil. The yield was 54% (0.77 g). Spectral analysis was consistent with the published data<sup>(12)</sup>. NMR  $^1\text{H}$  ( $\text{CDCl}_3$ ):  $\delta$ = 10.33 (1H, s, CHO), 8.26 (1H, d, arom), 8.08 (1H, d, arom), 7.60-7.30 (7H, m, arom), 7.17 (1H, d, arom), 5.49 (2H, s,  $\text{CH}_2\text{O}$ ). MS-electrospray: 264  $[\text{M}+\text{H}]^+$ .

### [3] – 2-Hydroxymethyl-8-benzyloxyquinoline

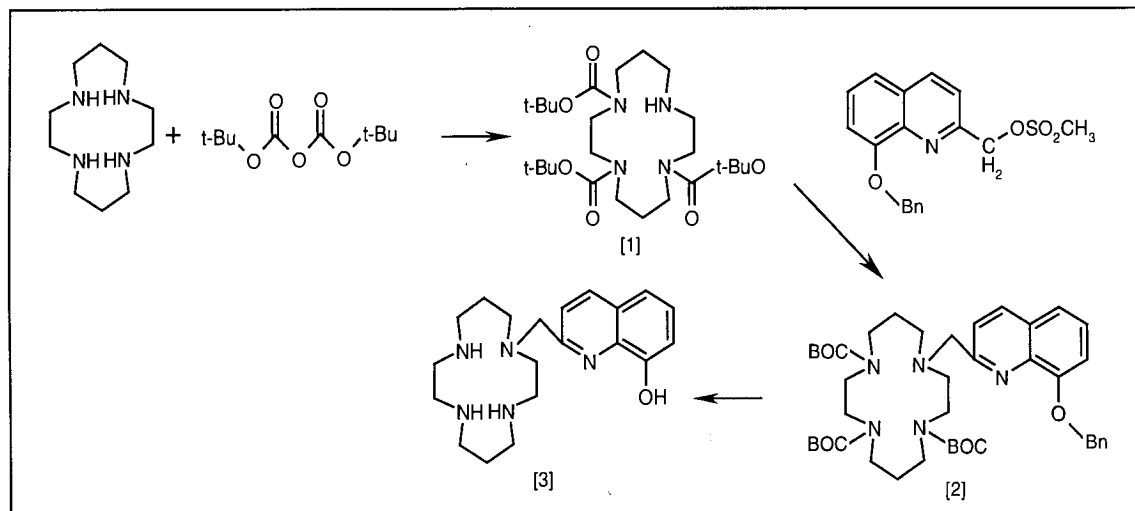
To a stirred solution of  $\text{NaBH}_4$  (144 mg, 3.8 mmol) in MeOH (30 ml), was added a solution of 2-carboxaldehyde-8-benzyloxyquinoline (986 mg, 3.75 mmol) in MeOH (15 ml) dropwise over 5 minutes at room temperature. After stirring for an additional hour, the yellow solution was concentrated under vacuum and water (50 ml) was added. The

mixture was neutralised with 1N HCl and extracted with EtOAc (2x 50 ml). The extracts were dried over Na<sub>2</sub>CO<sub>3</sub>, and concentrated under vacuum to give the desired product. The yield was 77% (0.765 g). NMR <sup>1</sup>H (CDCl<sub>3</sub>): δ= 8.14 (1H, d, J=8.7, arom), 7.56 (2H, d, J=6.9, arom), 7.45-7.20 (6H, m, arom), 7.15 (1H, t, J=4.5, arom), 5.39 (2H, s, CH<sub>2</sub>OBn), 4.97 (2H, s, CH<sub>2</sub>OH). MS-electrospray: 266 [M+H]<sup>+</sup>.

*[4] – 2-(Mesyloxy)methyl-8-benzyloxyquinoline*

To a solution of 2-hydroxymethyl-8-benzyloxyquinoline (540 mg, 2.05 mmol) dissolved in dry CH<sub>2</sub>Cl<sub>2</sub> (20 ml), Et<sub>3</sub>N (1.45 ml) was added, and the mixture was stirred and cooled in an ice bath. To this was added dropwise (over 10 min) a solution of MsCl (359 mg, 3.07 mmol) in CH<sub>2</sub>Cl<sub>2</sub> (20 ml), the mixture was further stirred for 3 hours at room temperature before it was rapidly washed with H<sub>2</sub>O/ice (20 ml), 10% HCl (20 ml), saturated solution of NaHCO<sub>3</sub> (20 ml), and brine (20 ml). The organic layer was dried (Na<sub>2</sub>CO<sub>3</sub>) and evaporated to dryness under vacuum at room temperature yielding oils (starting compound and final product), which were not further purified. The yield was 64% (0.447 g). NMR <sup>1</sup>H (CDCl<sub>3</sub>): δ= 8.18 (1H, d, J=8.7, arom), 7.55-7.30 (8H, m, arom), 7.11 (1H, d, J=4.6, arom), 5.56 (2H, s, CH<sub>2</sub>OMs), 5.35 (2H, s, CH<sub>2</sub>OBn), 3.12 (3H, s, Ms). MS-electrospray: 366 [M+Na]<sup>+</sup>.

### 6.3.15 1-(2-Methyl-8-hydroxyquinoline)-1,4,8,11-tetraazacyclotetradecane



#### [1] – 1,4,8-Tris-(2,2-dimethyl-propionyloxy)-1,4,8,11-tetraazacyclotetradecane

Di-*tert*-butyldicarbonate (1.56 g, 7.1 mmol) dissolved in dichloromethane (100 ml), was added dropwise over a period of 2 hours to a solution of 1,4,8,11-tetraazacyclotetradecane (0.475 g, 2.37 mmol) in dichloromethane (100 ml). The solution was stirred at room temperature and monitored by TLC. When the reaction was completed the solvent was removed under vacuum and the residue purified by chromatography on silica gel ( $\text{CH}_2\text{Cl}_2$ , MeOH from 0% to 10%,  $R_f = 0.5$  with MeOH 2%). Spectral analysis was consistent with the published data<sup>(13)</sup>. The yield was 91% (1.08 g). NMR  $^1\text{H}$  ( $\text{CDCl}_3$ ):  $\delta = 3.5\text{--}3.2$  (12H, m,  $\text{CH}_2\text{N}$ ), 2.75 (2H, t,  $\text{CH}_2\text{N}$ ), 2.58 (2H, t,  $\text{CH}_2\text{N}$ ), 1.88 (2H, m,  $\text{CH}_2\text{CH}_2\text{CH}_2$ ), 1.66 (2H, m,  $\text{CH}_2\text{CH}_2\text{CH}_2$ ), 1.42 (27H, s, *t*-Bu). MS-electrospray: 501  $[\text{M}+\text{H}]^+$ .

[2] – *1-(2-Methyl-8-benzyloxyquinoline)-4,8,11-tris-(2,2-dimethyl-propionyloxy)-1,4,8,11-tetraazacyclotetradecane*

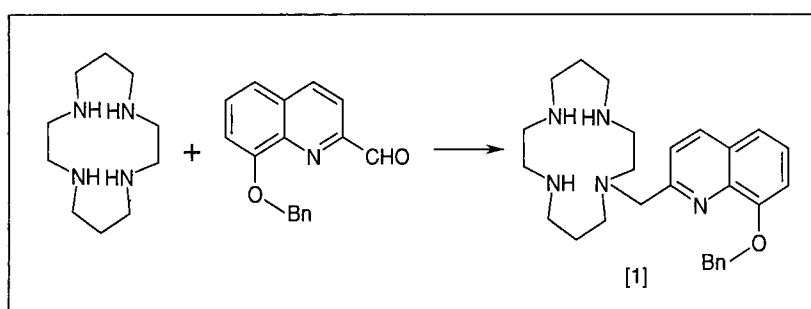
2-(Mesyloxy)methyl-8-benzyloxyquinoline (983 mg, 2.87 mmol, 1.2 equiv.) was added to a solution of 1,4,8-tris-(2,2-dimethyl-propionyloxy)-1,4,8,11-tetraazacyclotetradecane (1.2 g, 2.4 mmol) in acetonitrile, together with potassium carbonate (397 mg, 2.87 mmol, 1.2 equiv.) and some crystals of potassium iodide. The solution was refluxed under nitrogen for 10 days. The solution was dried and the solid obtained was dissolved in aqueous NaOH (pH=12) and dichloromethane. After three extractions with dichloromethane the organic solution was dried and the solvent removed. Separation of the compound was effected by chromatography on silica gel (CH<sub>2</sub>Cl<sub>2</sub>, MeOH from 0% to 10%, R<sub>f</sub> = 0.5 with MeOH 3%). The yield was 76% (1.36 g). Spectral analysis confirmed the product's structure. NMR <sup>1</sup>H (CDCl<sub>3</sub>): δ= 8.06 (1H, d, arom), 7.42-7.25 (8H, m, arom), 7.02 (1H, d, arom), 5.43 (2H, s, CH<sub>2</sub>O), 3.96 (2H, s, CH<sub>2</sub>N<sub>arom</sub>), 3.5-3.2 (12H, m, CH<sub>2</sub>N), 2.73 (2H, m, CH<sub>2</sub>N), 2.55 (2H, m, CH<sub>2</sub>N), 1.87 (2H, m, CH<sub>2</sub>CH<sub>2</sub>CH<sub>2</sub>), 1.73 (2H, m, CH<sub>2</sub>CH<sub>2</sub>CH<sub>2</sub>), 1.43 (27H, s, *t*-Bu). MS-electrospray: 770 [M+Na]<sup>+</sup>.

[3] – *1-(2-Methyl-8-hydroxyquinoline)-1,4,8,11-tetraazacyclotetradecane*

1-(2-Methyl-8-benzyloxyquinoline)-4,8,11-tris-(BOC)-1,4,8,11-tetraazacyclotetradecane (500 mg, 0.67 mmol) was added to aqueous HCl (6M, 50 ml) and the mixture was refluxed for 15 hours. The pH was then increased to 12 by careful addition of sodium hydroxide at 0° C. The solution was then extracted with chloroform (3x 50 ml), the organic layer dried over sodium carbonate, filtered and evaporated to give the product as an off-white solid. The yield was 91% (0.217 g). Spectral analysis confirmed the product's structure. NMR <sup>1</sup>H (CDCl<sub>3</sub>): δ= 8.11 (1H, d, arom), 7.5-7.1 (4H, m, arom), 3.83

(2H, s, CH<sub>2</sub>Narom), 2.9-2.6 (16H, m, CH<sub>2</sub>N), 1.9-1.8 (4H, m, CH<sub>2</sub>CH<sub>2</sub>CH<sub>2</sub>). MS-electrospray: 358 [M+H]<sup>+</sup>.

### 6.3.16 1-(2-methyl-8-benzyloxyquinoline)-1,4,8,11-tetraazacyclotetradecane



#### [1] - *N*-(2-methyl-8-benzyloxyquinoline)-1,4,8,11-tetraazacyclotetradecane

Equimolar amounts of 1,4,8,11-tetraazacyclotetradecane (460 mg, 2.3 mmol) and 2-carboxaldehyde-8-benzyloxyquinoline (636 mg, 2.3 mmol) were mixed in dichloromethane and then treated with sodium triacetoxyborohydride (767 mg, 3.45 mmol). The mixture was stirred at room temperature under N<sub>2</sub> atmosphere for 12 hours and the progress of the reaction was monitored by TLC on silica. When the reaction was completed, 1 N HCl was added to terminate the reaction. Then 1N NaOH was added to adjust the pH of the solution to 10-12. The solution was extracted several times with dichloromethane. The combined CH<sub>2</sub>Cl<sub>2</sub> extracts were dried (Na<sub>2</sub>CO<sub>3</sub>) and filtered. The solvent was removed and the residue purified by chromatography on silica gel (CHCl<sub>3</sub>/MeOH/NH<sub>4</sub>OH =10/4/1, R<sub>f</sub> = 0.5). The yield was 21% (0.221 g). Spectral analysis confirmed the product's structure. NMR <sup>1</sup>H (CDCl<sub>3</sub>): δ= 8.07 (1H, d, J=8.4,

arom), 7.77 (1H, d, J=8.7, arom), 7.50 (2H, d, J=7.2, arom), 7.33 (5H, m, arom), 7.03 (1H, d, J=7.2, arom), 5.43 (2H, s, CH<sub>2</sub>O), 3.99 (2H, s, NCH<sub>2</sub>arom), 2.5-2.8 (16H, m, NCH<sub>2</sub>CH<sub>2</sub>), 2.91 (2H, q, CH<sub>2</sub>CH<sub>2</sub>CH<sub>2</sub>), 2.70 (2H, q, CH<sub>2</sub>CH<sub>2</sub>CH<sub>2</sub>). <sup>13</sup>C (CDCl<sub>3</sub>): δ= 159.7, 154.2, 140.1, 137.5, 136.2, 128.8, 128.6, 127.8, 127.0, 126.1, 121.6, 120.1, 110.9, 71.1, 60.8, 55.8, 53.7, 50.9, 49.4, 49.2, 49.1, 48.3, 47.6, 28.9, 26.5. MS-electrospray: 460 [M]<sup>+</sup>.

## 6.4 Synthetic Procedures for Chapter 3 - Metal Complexes

### 6.4.1 Copper complexes

Two different procedures were used for the synthesis of the copper complexes:

Method A: The complex was obtained by mixing equimolar amounts of Cu(ClO<sub>4</sub>)<sub>2</sub>·6H<sub>2</sub>O and ligand in EtOH and gentle heating.

Method B: The complex was obtained by mixing a 1:1 molar ratio of Cu(O<sub>2</sub>CMe)<sub>2</sub> and ligand in deoxygenated MeOH under reflux for about 30 min.

The Method B was preferentially used for the synthesis of the complexes. Perchlorate salts of metal complexes are potentially explosive and so method A was used only when it was not possible to obtain crystals using the previous method.

#### [1] – CuL<sup>I</sup>

The complex crystallised from a solution in acetonitrile and diethyl ether (Method B).

MS-electrospray: 223 [M]<sup>2+</sup>.

*[2] – CuL<sup>2</sup>*

The complex crystallised from a solution in methanol (Method A). MS-electrospray: 223 [M]<sup>2+</sup>.

*[3] – CuL<sup>3</sup>*

It was not possible to obtain crystals suitable for the X-ray analysis (Method A and B). MS-electrospray: 222 [M]<sup>2+</sup>.

*[4] – CuL<sup>4</sup>*

The complex crystallised from a solution in water (Method A), in this case a full structural analysis was not possible. MS-electrospray: 290 [M]<sup>+</sup>.

*[5] – CuL<sup>5</sup>*

The complex crystallised from a solution in methanol (Method A). The crystals at basic pH were isolated from water basicified to pH 12 with potassium hydroxide. MS-electrospray: 472 [M]<sup>+</sup>.

*[6] – CuL<sup>6</sup>*

The complex crystallised from a solution in acetonitrile and methanol (Method B). MS-electrospray: 209 [M]<sup>2+</sup>.

*[7] – Cu complex of 1,4-bis(2-pyridylmethyl)-1,4,8,11-tetraazacyclotetradecane-9,10-dione*

It was not possible to obtain crystals suitable for the X-ray analysis (Method A). MS-electrospray: 473 [M]<sup>+</sup>.



## 6.4.2 Nickel complexes

Two different procedures were used for the synthesis of the nickel complexes:

Method A: The complex was obtained by mixing equimolar amounts of  $\text{Ni}(\text{ClO}_4)_2 \cdot 6\text{H}_2\text{O}$  and ligand in EtOH and gentle heating.

Method B: The complex was obtained by mixing a 1:1 molar ratio of  $\text{Ni}(\text{O}_2\text{CMe})_2$  and ligand in deoxygenated MeOH under reflux for about 30 min.

As for copper, the Method B was preferred, owing to the hazards associated with perchlorates.

### [1] – $\text{NiL}^1$

The complex crystallised from a solution in acetonitrile and diethyl ether (Method B).

MS-electrospray: 220  $[\text{M}]^{2+}$ .

### [2] – $\text{NiL}^2$

It was not possible to obtain crystals suitable for the X-ray analysis (Method A and B).

MS-electrospray: 221  $[\text{M}]^{2+}$ .

### [3] – $\text{Ni}^3$

It was not possible to obtain crystals suitable for the X-ray analysis (Method B). MS-

electrospray: 220  $[\text{M}]^{2+}$ .

### [4] – *Ni complex of 1,4-bis(2-pyridylmethyl)-1,4,8,11-tetraazacyclotetradecane-9,10-dione*

It was not possible to obtain crystals suitable for the X-ray analysis (Method B). MS-

electrospray: 468  $[\text{M}]^+$ .

*[5] – NiL<sup>5</sup>*

The complex crystallised from a solution in water and methanol (Method B). MS-electrospray: 285 [M]<sup>+</sup>.

*[6] – NiL<sup>6</sup>*

It was not possible to obtain crystals suitable for the X-ray analysis (Method A and B). MS-electrospray: 207 [M]<sup>2+</sup>.

### 6.4.3 Chromium complexes

*[1] – CrL<sup>1</sup>*

The complex was obtained by mixing a 1:1 molar ratio of CrCl<sub>2</sub> and ligand in deoxygenated THF under reflux for about 30 min. MS-electrospray: 504 [M+2Cl]<sup>+</sup>.

*[2] – Cr complex of 1,8-bis(methyl)-1,4,8,11-tetraazacyclotetradecane*

The complex was obtained by mixing a hot solution of ligand in DMF with an equimolar amount of CrCl<sub>3</sub>.6H<sub>2</sub>O in DMF at 100°C in the presence of 2,2-dimethoxypropane (2 ML). MS-electrospray: 350 [M+2Cl]<sup>+</sup>.

*[3] – Cr complex of 1,11-bis(methyl)-1,4,8,11-tetraazacyclotetradecane*

The complex was obtained by mixing a hot solution of ligand in DMF with an equimolar amount of CrCl<sub>3</sub>.6H<sub>2</sub>O in DMF at 100°C in the presence of 2,2-dimethoxypropane (2 ML). MS-electrospray: 350 [M+2Cl]<sup>+</sup>.

*[4] – Cr complex of 1-benzo -1,4,8,11-tetraazacyclotetradecane*

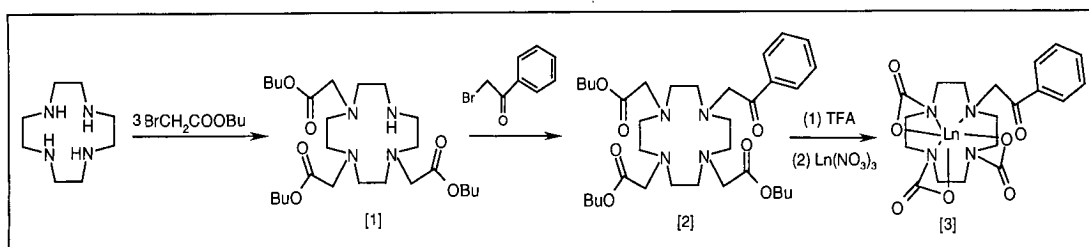
The complex was obtained by mixing a 1:1 molar ratio of  $\text{CrCl}_2$  and ligand in deoxygenated THF under reflux for about 30 min. MS-electrospray: 573  $[\text{M}+2\text{Cl}]^+$ .

*[5] – Cr complex of 1-(2-methyl-8-hydroxyquinoline)- 1,4,8,11-tetraazacyclotetra decane*

The complex was obtained by mixing a 1:1 molar ratio of  $\text{CrCl}_2$  and ligand in deoxygenated THF under reflux for about 30 min. MS-electrospray: 479  $[\text{M}+2\text{Cl}]^+$ .

## 6.5 Synthetic Procedures for Chapter 4

### 6.5.1 Lanthanide complexes of $\text{H}_3\text{L}^7$

*[1] – 1,4,7-tris(tert-butoxycarbonylmethyl)-1,4,7,10-tetraazadodecane*

Potassium carbonate (786 mg, 5.69 mmol) and 1,4,7,10-tetraazacyclododecane (1 g, 5.69 mmol) were dissolved in chloroform (50 ml). A solution of tert-butylbromoacetate (3.4 g, 17.08 mmol) was added dropwise over 4 hours. The solution was stirred at room temperature for 72 hours. The inorganic material was removed by filtration. The solvents were then removed under vacuum and the residue was purified by column chromatography over silica gel. The column was first washed with  $\text{CH}_2\text{Cl}_2$  before the title

compound was eluted using an increasing proportion of methanol. Spectral analysis was consistent with the published data<sup>(14)</sup>. The yield was 73% (2.18 g).  $R_f = 0.5$  (7% CH<sub>3</sub>OH).

NMR <sup>1</sup>H (CDCl<sub>3</sub>):  $\delta = 3.36$  (2H, s, acetate CH<sub>2</sub>), 3.27 (2H, s, acetate CH<sub>2</sub>), 3.08-2.86 (16H, m, ring), 1.44 (27H, s, t-Bu). MS-electrospray: 515 [M+H]<sup>+</sup>.

[2] – *1-(2-Acetophenone)-4,7,10-tris(tert-butoxycarbonylmethyl)-1,4,7,10-tetraaza cyclododecane*

The previous compound [1] (750 mg, 1.46 mmol), potassium carbonate (242 mg, 1.75 mmol),  $\alpha$ -bromoacetophenone, (355 mg, 1.75 mmol) and a catalytic amount of KI were dissolved in acetonitrile. The solution was stirred at reflux for 96 hours. The solvent was removed under vacuum and the residue taken up into aqueous NaOH (1M, 10 ml), from which the product was extracted into dichloromethane (3x10 ml). The residue was purified by column chromatography over alumina. The column was first washed with dichloromethane before the title compound was eluted using methanol.  $R_f = 0.5$  (2% CH<sub>3</sub>OH). The yield was 58% (0.535 g).

NMR <sup>1</sup>H (CDCl<sub>3</sub>):  $\delta = 7.89$ (2H, d, arom), 7.57(1H, t, arom), 7.45 (2H, t, arom), 3.50- 2.30 (24 H, m, cyclen/acetate), 1.45 (27 H, s, t-but). <sup>13</sup>C (CDCl<sub>3</sub>):  $\delta = 198.6, 171.8, 134.6, 133.7, 127.7, 126.6, 81.1, 81.0, 59.2, 54.6, 53$  (broad), 52.5, 49 (broad), 26.9, 26.8. MS-electrospray: 633 [M+H]<sup>+</sup>.

[3] – *Lanthanide (III) complexes*

The *tris*-acetate ligand was prepared by addition of trifluoroacetic acid (20 equiv.) to a solution of the *tris*-ester (200 mg, 0.32 mmol) in dichloromethane (5 ml), and the solution was stirred at room temperature for 24 hours. The solvent was removed under reduced pressure and the residue was washed with more dichloromethane (3x 5 ml). Water was

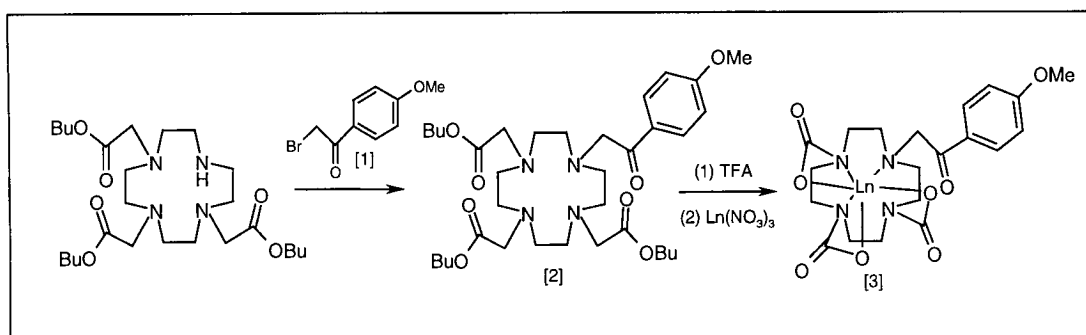
then added and the pH adjusted to 6.5-7 using NaOH (aqueous, 1M). The lanthanide (III) complexes were prepared by addition of an equimolar amount of the lanthanide (III) nitrate (Eu, Gd, Yb, La, or Tb) to an aqueous solution of the ligand (concentration ca. 40 mM). After refluxing for 24 h, alumina (2 g) was added and the solvent removed under reduced pressure until the solid was dry and free flowing. The alumina with adsorbed complex was added to the top of a short column of alumina, and eluted with  $\text{CH}_2\text{Cl}_2$  – 20% MeOH/ $\text{CH}_2\text{Cl}_2$ . The electrospray ionization mass spectrum of each complex gave, as a major peak,  $[\text{M}+\text{H}]^+$  or  $[\text{M}+\text{Na}]^+$ . Owing to the large paramagnetism associated with the gadolinium (III) and terbium (III) ions, analysis by NMR is not feasible for these complexes, but is possible for europium (III). In the last case the spectrum showed very clearly the characteristic pattern of resonances shown previously to be typical of such complexes, in which the rigidity imposed by the metal ion leads to the inequivalence of the four protons of each ethylene unit in the macrocycle.

**Eu** -  $R_f = 0.5$  (8% Methanol), (Electrospray, ES+)= 635 ( $\text{M}+\text{Na}^+$ )

**Gd** -  $R_f = 0.5$  (10% Methanol), (High resolution electrospray, ES+)= 642.1159 ( $\text{M}+\text{H}^+$ )

**Tb** -  $R_f = 0.5$  (8% Methanol), (Electrospray, ES+)= 619 ( $\text{M}+\text{H}^+$ )

### 6.5.2 Lanthanide complexes of $\text{H}_3\text{L}$ <sup>8</sup>



*[1] – 4'-Methoxy-2-bromoacetophenone*

A solution of *tert*-butylhydroperoxide (70% aq.) (0.42 ml, 3.30 mmol) was added to a cooled mixture of HBr (48% aq.) (0.56 ml, 3.30 mmol) in dioxane and the mixture was stirred for 5 minutes. To this cold solution, 4-methoxyacetophenone (500 mg, 3.30 mmol) was added, stirred for 30 minutes and then heated at 60°C. The solvent was evaporated and the residue was taken into 10 ml of water, and extracted with dichloromethane (3x20 ml). The yield was 85% (0.707 g).

NMR  $^1\text{H}$  ( $\text{CDCl}_3$ ):  $\delta$ = 7.95 (2H, d, arom), 6.94 (2H, d, arom), 4.39 (2H, s,  $\text{BrCH}_2$ ), 3.86 (3H, s,  $\text{OCH}_3$ ).  $^{13}\text{C}$  ( $\text{CDCl}_3$ ):  $\delta$ = 190.0, 164.2, 132.3, 131.4, 114.1, 55.7, 30.9. MS-electrospray: 253  $[\text{M}+\text{H}]^+$ .

*[2] – 1-(4'-Methoxy-2-acetophenone)-4,7,10-tris(tert-butoxycarboxy)-1,4,7,10-tetraazacyclododecane*

The tris-(*tert*-butyl)ester of DO3A (800 mg, 1.55 mmol), potassium carbonate (258 mg, 1.86 mmol), and *p*-methoxy- $\alpha$ -bromoacetophenone, (426 mg, 1.86 mmol) were dissolved in acetonitrile (20 ml). The solution was stirred at reflux for 96 hours. The solvent was removed under vacuum and the residue taken up into aqueous NaOH (1M, 20 ml), from which the product was extracted into dichloromethane (3x20 ml). The residue was purified by column chromatography over alumina. The column was first washed with dichloromethane before the title compound was eluted using methanol.  $R_f$ = 0.5 (2%  $\text{CH}_3\text{OH}$ ). The yield was 55% (0.602 g)

NMR  $^1\text{H}$  ( $\text{CDCl}_3$ ):  $\delta$ = 7.77 (2H, d,  $J=8.7$ , arom), 6.82 (2H, d,  $J=8.7$ , arom), 3.76 (3H, s,  $\text{OCH}_3$ ), 2.10- 3.40 (24 H, m, ring/acetate), 1.34 (27 H, s, *t*-but).  $^{13}\text{C}$  ( $\text{CDCl}_3$ ):  $\delta$ = 197.5, 172.5, 163.7, 130.4, 129.7, 128.5, 113.7, 113.5, 81.9, 81.8, 59.6, 55.5, 55.4, 53(broad), 49(broad), 27.7, 27.6. (Purification was not completely successful, the product being

contaminated with a small amount of the alkylating agent, which was readily removed after the complexation step). MS-electrospray: 685 [M+H]<sup>+</sup>.

### [3] – Lanthanide (III) complexes

The lanthanide (III) complexes were obtained according to the general procedure described in 4.5.2 part [3]. The complexes with europium (III) and gadolinium (III) were made with this ligand.

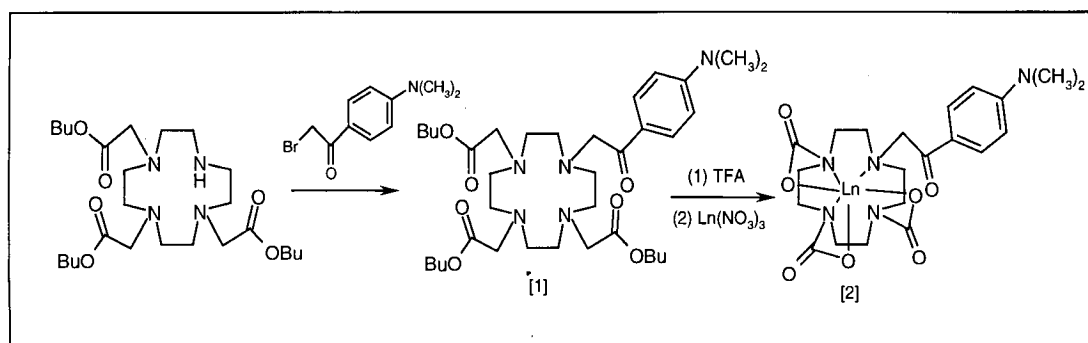
**Eu** - R<sub>f</sub> = 0.5 (8% Methanol), (High resolution electrospray, ES+)= 667.1266 (M+Na<sup>+</sup>)

Found: C 36.82, H 4.89, N 7.32 % (C<sub>23</sub>H<sub>31</sub>O<sub>8</sub>N<sub>4</sub>Eu.5H<sub>2</sub>O requires C 37.60, H 5.59, N 7.63 %).

**Gd** - R<sub>f</sub> = 0.5 (12% Methanol), (Electrospray, ES+)= 671 (M+Na<sup>+</sup>)

Found: C 36.84, H 4.82, N 7.45 % (C<sub>23</sub>H<sub>31</sub>O<sub>8</sub>N<sub>4</sub>Gd.5H<sub>2</sub>O requires C 37.35, H 5.55, N 7.58 %).

### 6.5.3 Lanthanide complexes of H<sub>3</sub>L<sup>9</sup>



[1] – 1-(4'-Dimethylamino-2-acetophenone)-4,7,10-tris(*tert*-butoxycarboxy)-1,4,7,10-tetraazacyclododecane

The tris-(*tert*-butyl)ester of DO3A (750 mg, 1,46 mmol), caesium carbonate (570 mg, 1.75 mmol), and *p*-dimethylamino- $\alpha$ -bromoacetophenone (354 mg, 1,46 mmol) (prepared according to the published procedure<sup>(15)</sup>), were dissolved in acetonitrile. The solution was stirred at reflux for 96 hours. The solvent was removed under vacuum and the residue taken up into aqueous NaOH (1M, 20 ml), from which the product was extracted into dichloromethane (3x20 ml). The residue was purified by column chromatography over alumina. The column was first washed with dichloromethane before the title compound was eluted using methanol.  $R_f = 0.5$  (4% CH<sub>3</sub>OH). The yield was 53% (0.554 g).

NMR <sup>1</sup>H (CDCl<sub>3</sub>):  $\delta = 7.70-8.10$ (4H, m, arom), 3.60-2.60 (30 H, m, ring/acetate/N(CH<sub>3</sub>)<sub>2</sub>), 1.45 (27 H, s, *t*-but). <sup>13</sup>C (CDCl<sub>3</sub>):  $\delta = 196.5, 173.0, 172.8, 153.8, 129.8, 123.7, 110.7, 82.0, 81.9, 59.4, 55.9, 55.7, 53$  (broad), 49 (broad), 40.2, 28.0. MS-electrospray: 698 [M+H]<sup>+</sup>.

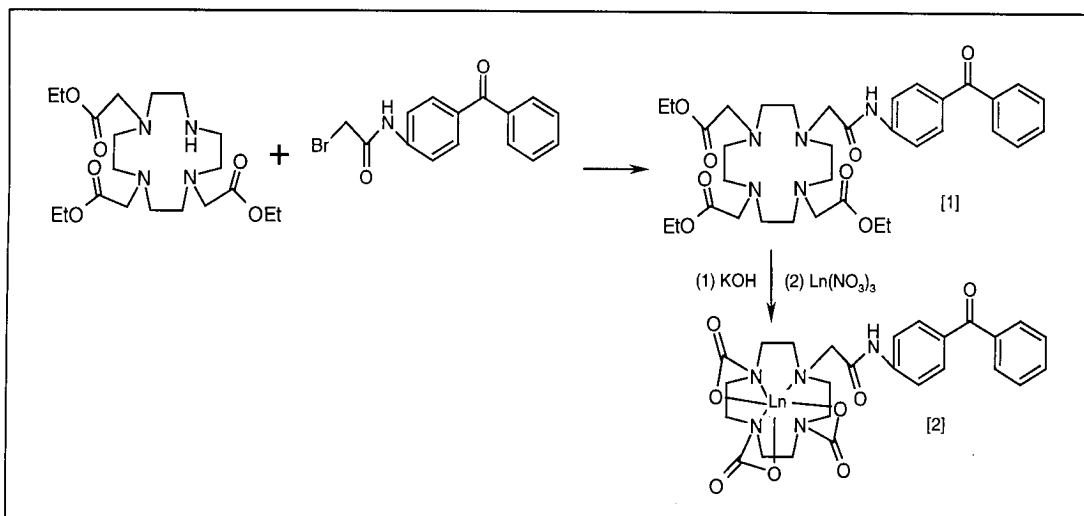
[2] – Lanthanide (III) complexes

The lanthanide (III) complexes were obtained according to the general procedure described in 4.5.2 part [3]. The complexes with europium (III) and gadolinium (III) were made with this ligand.

**Eu** -  $R_f = 0.5$  (8% Methanol), (High resolution electrospray, ES+)= 680.1612 (M+Na<sup>+</sup>)

**Gd** -  $R_f = 0.5$  (10% Methanol), (Electrospray, ES+)= 685 (M+Na<sup>+</sup>)



6.5.4 Lanthanide complexes of  $H_3L^{10}$ 

[1] – *N*-(4-benzoyl-phenyl)-2-[4,7,10-tris(ethoxycarbonylmethyl)-1,4,7,10-tetraaza cyclododecane]-acetamide

The tris-(*tert*-butyl)ester of DO3A (1.57 g, 3.58 mmol), potassium carbonate (544 mg, 3.94 mmol), benzophenone-containing  $\alpha$ -bromoamide (980 mg, 3.58 mmol) and a catalytic amount of KI were dissolved in acetonitrile. The mixture was stirred and refluxed for 48 hours. The solvent was removed under vacuum and the residue taken up into aqueous NaOH (1M, 40 ml), from which the product was extracted into dichloromethane (3x40 ml). The residue was purified by column chromatography over alumina. The column was first washed with dichloromethane before the title compound was eluted using methanol. The yield was 63% (1.32 g).  $R_f = 0.5$  (1%  $CH_3OH$ ).

NMR  $^1H$  ( $CDCl_3$ ):  $\delta = 8.1-7.4$  (9H, m, arom), 4.18 (6H, q, Et), 3.7-2.0 (24H, m, cyclen, acetate  $CH_2$ ), 1.24 (9H, t, Et).  $^{13}C$  ( $CDCl_3$ ):  $\delta = 195.8, 173.5, 173.2, 171.8, 143.3, 138.0, 132.1, 132.0, 131.0, 129.8, 128.1, 119.4, 61.4, 61.3, 55.0, 52$ (broad), 50(broad), 14.2. MS-electrospray: 690  $[M+Na]^+$ .

## [2] – Lanthanide (III) complexes

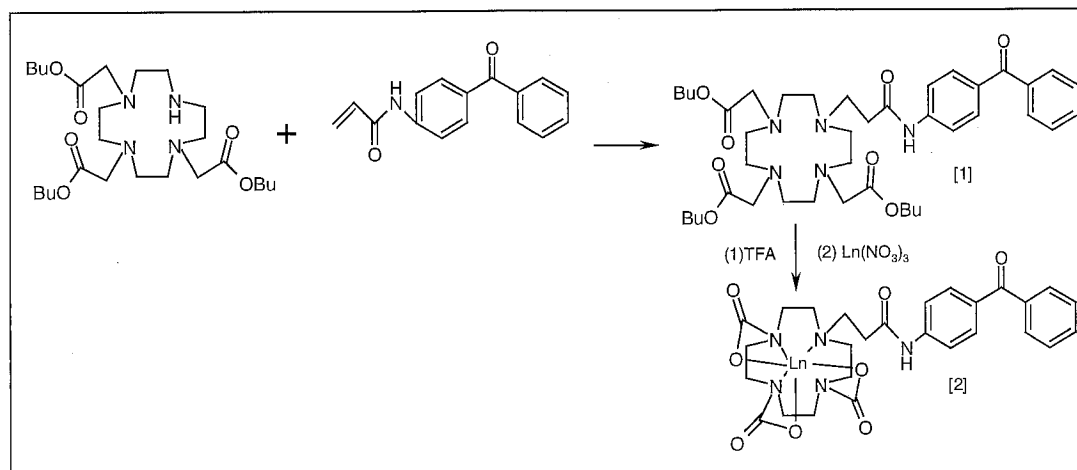
The lanthanide (III) complexes were obtained according to the general procedure described in 4.5.2 part [3], but potassium hydroxide was used instead of trifluoroacetic acid for hydrolysis of the ethyl esters. The complexes with europium (III), gadolinium (III), terbium (III) and ytterbium (III) were made with this ligand.

**Eu** -  $R_f = 0.5$  (10% Methanol), (Electrospray, ES+)= 731 ( $M+H^+$ )

**La** -  $R_f = 0.5$  (16% Methanol), (Electrospray, ES+)= 718 ( $M+H^+$ )

**Tb** -  $R_f = 0.5$  (8% Methanol), (High resolution electrospray, ES+)= 762.1559 ( $M+Na^+$ )

**Yb** -  $R_f = 0.5$  (14% Methanol), (Electrospray, ES+)= 753 ( $M+H^+$ )

6.5.5 Lanthanide complexes of  $H_3L$ <sup>11</sup>

[1] – *N*-(benzoyl-phenyl)-3-[4,7,10-tris(*tert*-butoxycarboxy)-1,4,7,10-tetraazacyclo dodecane]-propionamide

The tris-(*tert*-butyl)ester of DO3A (500 mg, 0.97 mmol), potassium carbonate (137 mg, 1.07 mmol), *N*-(4-benzophenone)acrylamide (243 mg, 0.97 mmol) and a catalytic amount

of KI were dissolved in acetonitrile (20 ml). The solution was stirred at reflux for 48 hours. The solvent was removed under vacuum and the residue taken up into aqueous NaOH (1M, 20 ml), from which the product was extracted into dichloromethane (3x20 ml). The residue was purified by column chromatography over alumina. The column was first washed with dichloromethane before the title compound was eluted using methanol. The yield was 67% (0.513 g).  $R_f = 0.5$  (2%  $\text{CH}_3\text{OH}$ ).

NMR  $^1\text{H}$  ( $\text{CDCl}_3$ ):  $\delta = 8.1-7.2$  (9H, m, arom), 3.4-2.2 (26H, m, ring, acetate  $\text{CH}_2$ ,  $\text{NCH}_2$ ), 1.45 (27H, s, t-bu). MS-electrospray: 788  $[\text{M}+\text{Na}]^+$ .

### [2] – Lanthanide (III) complexes

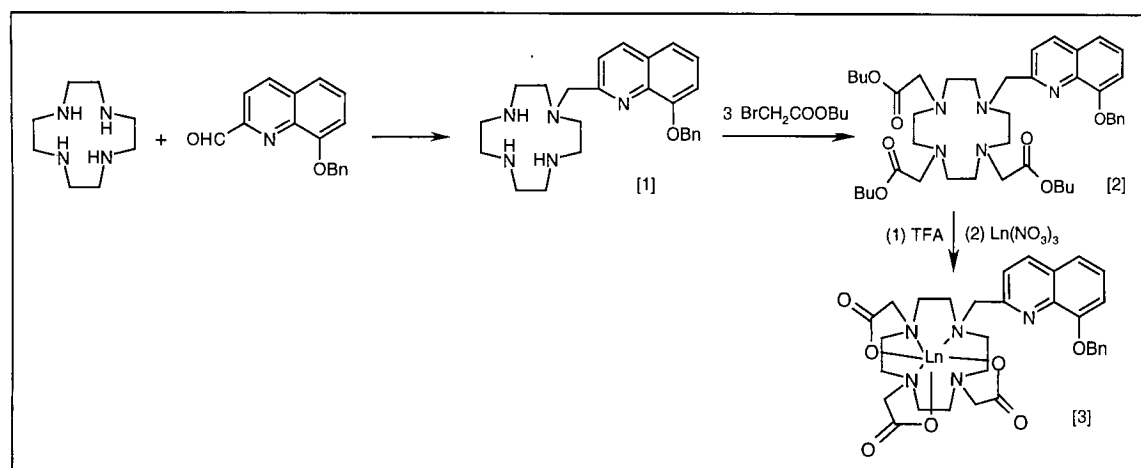
The lanthanide (III) complexes were obtained according to the general procedure described in 4.5.2 part [3]. The complexes with europium (III), terbium (III) and gadolinium (III) were made with this ligand.

**Eu** -  $R_f = 0.5$  (10% Methanol), (Electrospray, ES+)= 745 ( $\text{M}+\text{H}^+$ )

**Tb** -  $R_f = 0.5$  (8% Methanol), (High resolution electrospray, ES+)= 776.1715 ( $\text{M}+\text{Na}^+$ )

**Gd** -  $R_f = 0.5$  (6% Methanol), (Electrospray, ES+)= 750 ( $\text{M}+\text{H}^+$ )

### 6.5.6 Lanthanide complexes of $\text{H}_3\text{L}^{12}$



*[1] – 1-(2-Methyl-8-benzyloxyquinoline)-1,4,7,10-tetraazacyclododecane*

Equimolar amounts of 1,4,7,10-tetraazacyclododecane (240 mg, 1.39 mmol) and 2-carboxaldehyde-8-benzyloxyquinoline (368 mg, 1.4 mmol) were mixed in dichloromethane and then treated with sodium triacetoxyborohydride (624 mg, 2.8 mmol, 2 equiv.). The mixture was stirred at room temperature under N<sub>2</sub> atmosphere for 12 hours. The reaction was monitored by TLC. When the reaction was completed, 1N HCl was added to terminate the reaction. Then 1N NaOH was added to adjust the pH value of the solution to pH 10-12. The solution was then extracted several times with dichloromethane. The combined CH<sub>2</sub>Cl<sub>2</sub> extracts were dried (Na<sub>2</sub>CO<sub>3</sub>) and filtered. The solvent was removed and the residue purified by chromatography on silica gel (CHCl<sub>3</sub>/MeOH/NH<sub>4</sub>OH =10/4/1, R<sub>f</sub> = 0.5). The yield was 61% (0.357 g). Spectral analysis confirmed the product's structure.

NMR <sup>1</sup>H (CDCl<sub>3</sub>): δ= 8.08 (1H, d, J=8.4, arom), 7.60 (1H, d, J=8.4, arom), 7.48 (2H, d, J=6.9, arom), 7.25-7.37 (5H, m, arom), 6.98 (1H, dd, J=6.8, 2.3, arom), 5.36 (2H, s, CH<sub>2</sub>O), 3.98 (2H, s, NCH<sub>2</sub>arom), 2.76 (4H, t, ring), 2.65 (8H, s, ring), 2.53 (4H, t, ring).  
<sup>13</sup>C (CDCl<sub>3</sub>): δ=159.1, 153.9, 139.7, 137.2, 136.4, 128.5, 128.4, 127.4, 126.6, 125.8, 121.1, 119.9, 110.7, 77.4, 70.7, 61.7, 51.6, 47.0, 46.1, 45.0. MS-electrospray: 420 [M]<sup>+</sup>.

*[2] – 1-(2-Methyl-8-benzyloxyquinoline)-4,7,10-tris(tert-butoxycarboxy)-1,4,7,10-tetraazacyclododecane*

Potassium carbonate (392 mg, 2.84 mmol, 3.3 equiv.) and 1-(2-methyl-8-benzyloxyquinoline)-1,4,7,10-tetraazacyclododecane (360 mg, 0.86 mmol) were dissolved into a flask containing chloroform (50 ml). A chloroform solution of *tert*-butylbromoacetate (564 mg, 2.84 mmol, 3.3 equiv.) was added dropwise. The solution was stirred at room temperature for 72 hours. The inorganic material was removed by

filtration. The solvents were then removed under vacuum and the residue purified by column chromatography over silica gel. The column was first washed with  $\text{CH}_2\text{Cl}_2$  before the title compound was eluted using methanol. The yield was 47% (0.307 g).  $R_f = 0.5$  (3%  $\text{CH}_3\text{OH}$ ). NMR  $^1\text{H}$  ( $\text{CDCl}_3$ ):  $\delta = 8.11$  (1H, d,  $J = 8.4$ , arom), 7.58 (1H, d,  $J = 8.4$ , arom), 7.46 (2H, d,  $J = 6.6$ , arom), 7.28-7.38 (5H, m, arom), 7.02 (1H, dd,  $J = 5.4, 3.6$ , arom), 5.41 (2H, s,  $\text{CH}_2\text{O}$ ), 3.91 (2H, s,  $\text{NCH}_2\text{arom}$ ), 2.2-3.2 (22H, m, ring and  $\text{CH}_2\text{CO}$ ), 1.35 (18H, s, Bu), 1.33 (9H, s, Bu).  $^{13}\text{C}$  ( $\text{CDCl}_3$ ):  $\delta = 172.5, 172.4, 157.2, 153.5, 139.6, 136.7, 136.6, 128.4, 128.2, 127.6, 126.5, 126.5, 122.4, 199.8, 110.6, 82.7, 82.8, 70.4, 60.2, 56.2, 56.1, 53.5, 50.6, 28.0, 27.7$ . MS-electrospray: 784  $[\text{M} + \text{Na}]^+$ .

### [3] – Lanthanide (III) complexes

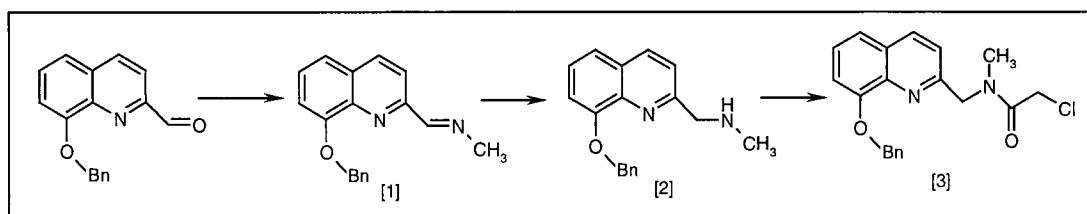
The lanthanide (III) complexes were obtained according to the general procedure described in 4.5.2 part [3]. The complexes with europium (III), terbium (III) and gadolinium (III) were made with this ligand.

**Eu** -  $R_f = 0.5$  (6% Methanol), (Electrospray, ES+) = 765 ( $\text{M} + \text{H}^+$ )

**Tb** -  $R_f = 0.5$  (10% Methanol), (Electrospray, ES+) = 772 ( $\text{M} + \text{H}^+$ )

**Gd** -  $R_f = 0.5$  (6% Methanol), (High resolution electrospray, ES+) = 771.1727 ( $\text{M} + \text{Na}^+$ )

### 6.5.7 N-(8-benzyloxy-quinolin-2-ylmethyl)-2-chloro-N-methylacetamide



*[1] – Methyl-(8-benzyloxy-quinolin-2-ylmethylene)-amine*

8-Benzyloxyquinoline-2-carboxaldehyde (525 mg, 1.99 mmol) was dissolved in methanol, and methylamine (62 mg, 1.99 mmol, water solution) was added. The reaction mixture was stirred for 24 hours at room temperature. The solvent was rotary evaporated to give the desired compound. The yield was 95% (0.525 g). NMR  $^1\text{H}$  ( $\text{CDCl}_3$ ):  $\delta$ = 8.69 (1H, d, CHN), 8.15 (2H, s, arom), 7.54 (2H, d, arom), 7.46-7.26 (5H, m, arom), 7.06 (1H, t, arom), 5.47 (2H, s,  $\text{CH}_2\text{O}$ ), 3.63 (3H, s, Me).  $^{13}\text{C}$  ( $\text{CDCl}_3$ ):  $\delta$ = 163.5, 153.5, 152.6, 138.8, 135.8, 135.4, 128.8, 127.5, 126.4, 125.9, 118.8, 117.4, 109.5, 69.8, 46.9. MS-electrospray: 278  $[\text{M}+\text{H}]^+$ .

*[2] – Methyl-(8-benzyloxy-quinolin-2-ylmethyl)-amine*

To a stirred solution of  $\text{NaBH}_4$  (1.5 g, 39.7 mmol) in MeOH (10 ml), was added methyl-(8-benzyloxy-quinolin-2-ylmethylene)-amine (524 mg, 1.89 mmol). The reaction mixture was stirred for 24 hours at room temperature. The solution was concentrated under vacuum, aqueous NaOH (20 ml) was added, extracted with dichloromethane (3x20 ml), dried over  $\text{Na}_2\text{CO}_3$ , and concentrated under vacuum to give the desired product. The yield was 92% (0.486 g).

NMR  $^1\text{H}$  ( $\text{CDCl}_3$ ):  $\delta$ = 8.11 (1H, d,  $J=8.6$ , arom), 7.64-7.32 (8H, m, arom), 7.09 (1H, d,  $J=8.3$ , arom), 5.49 (2H, s,  $\text{CH}_2\text{O}$ ), 4.17 (2H, s,  $\text{CH}_2\text{N}$ ), 2.61 (3H, s, Me).  $^{13}\text{C}$  ( $\text{CDCl}_3$ ):  $\delta$ = 158.3, 153.1, 139.0, 136.2, 135.3, 128.5, 127.5, 126.7, 126.6, 124.9, 119.9, 118.9, 109.8, 69.9, 56.9, 35.3. MS-electrospray: 280  $[\text{M}+\text{H}]^+$ .

*[3] – N-(8-benzyloxy-quinolin-2-ylmethyl)-2-chloro-N-methyl-acetamide*

To a stirred solution of methyl-(8-benzyloxy-quinolin-2-ylmethyl)-amine (503 mg, 1.81 mmol) in dry THF (10 ml) cooled at  $0^\circ\text{C}$ , was added chloroacetic acid (173 mg, 1.81

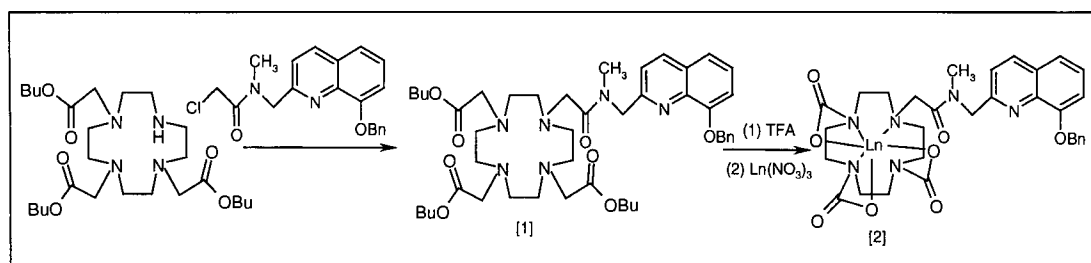
mmol) and the coupling agent 1-(3-dimethylaminopropyl)-3-ethyl-carbodiimide hydrochloride (389 mg, 1.99 mmol, 1.1 equiv.). The reaction mixture was stirred at 0°C up to the point that the lumps formed by the coupling agent became soluble. The solution was left to slowly reach room temperature and then stirred overnight. The solution was decanted, the remaining solid washed with THF (3x5 ml) and the combined organic filtrate concentrated under vacuum. Aqueous NaOH (20 ml) was added, extracted with dichloromethane (3x20 ml), dried over Na<sub>2</sub>CO<sub>3</sub>, and concentrated under vacuum to give the desired product. The yield was 59% (0.338 g). As introduced in the chapter 4, the remaining 40% was its cyclised parent compound.

NMR <sup>1</sup>H (CDCl<sub>3</sub>): δ= 8.11 (1H, d, J=8.4, arom), 7.6-7.3 (8H, m, arom), 7.08 (1H, d, arom), 5.40 (2H, s, CH<sub>2</sub>O), 4.98 (2H, s, CH<sub>2</sub>Cl), 4.17 (2H, s, CH<sub>2</sub>N), 3.16 (3H, s, Me).

MS-electrospray: 377 [M+Na]<sup>+</sup>.

Cyclised compound, NMR <sup>1</sup>H (CDCl<sub>3</sub>): δ= 8.02 (1H, d, J=8.4, arom), 7.6-7.3 (8H, m, arom), 7.03 (1H, d, arom), 5.35 (2H, s, CH<sub>2</sub>O), 4.75 (2H, s, CH<sub>2</sub>Cl), 4.55 (2H, s, CH<sub>2</sub>N), 2.94 (3H, s, Me). MS-electrospray: 319 [M]<sup>+</sup>.

### 6.5.8 Lanthanide complexes of H<sub>3</sub>L<sup>13</sup>



[1] – *N*-(8-benzyloxy-quinolin-2-ylmethyl)-2-[1,4,7-tris(*tert*-butoxycarbonylmethyl)-1,4,7,10-tetraazacyclododecane]-*N*-methyl-acetamide

The tris-(*tert*-butyl)ester of DO3A (500 mg, 0.97 mmol), potassium carbonate (148 mg, 1.07 mmol), *N*-(8-benzyloxy-quinolin-2-ylmethyl)-2-chloro-*N*-methyl-acetamide (378 mg, 1.07 mmol, 1.1 equiv.) and a catalytic amount of KI were dissolved in acetonitrile. The solution was stirred and refluxed for 48 hours. The solvent was removed under vacuum and the residue taken up into aqueous NaOH (1M, 20 ml), from which the product was extracted into dichloromethane (3x20 ml). The residue was purified by column chromatography over alumina. The column was first washed with dichloromethane before the title compound was eluted using methanol. The yield was 69% (0.574 g).  $R_f = 0.5$  (2% CH<sub>3</sub>OH).

NMR <sup>1</sup>H (CDCl<sub>3</sub>):  $\delta = 8.06$  (1H, d,  $J = 8.7$ , arom), 7.2-7.5 (8H, m, arom), 7.08 (1H, t,  $J = 4.5$ , arom), 5.43 (2H, s, CH<sub>2</sub>O), 3.06 (3H, s, Me), 2.0-3.5 (24H, m, ring and CH<sub>2</sub>CO), 1.46 (27H, s, Bu). MS-electrospray: 855 [M+Na]<sup>+</sup>.

[2] – *Lanthanide (III) complexes*

The lanthanide (III) complexes were obtained according to the general procedure described in 4.5.2 part [3]. The complexes with europium (III) and gadolinium (III) were made with this ligand.

**Eu** -  $R_f = 0.5$  (6% Methanol), (High resolution electrospray, ES<sup>+</sup>) = 837.2091 (M+Na<sup>+</sup>)

**Gd** -  $R_f = 0.5$  (8% Methanol), (High resolution electrospray, ES<sup>+</sup>) = 842.2132 (M+Na<sup>+</sup>)



## 6.6 References

### 6.6.1 Articles

1. N. G. Connelly and W. E. Geiger, *Chem. Rev.*, **96**, 877, (1996).
2. (a) SMART and SAINT, Version 6.01, Bruker Analytical X-Ray Systems, Madison, Wisconsin, USA, (1999); (b) SHELXTL, Version 5.1, Bruker Analytical X-Ray Systems, Madison, Wisconsin, USA, (1997).
3. J. R. Lakowicz, *Principles of Fluorescence Spectroscopy*, (2<sup>nd</sup> edition), Kluwer Academic, Plenum Publishers, New York, (1999).
4. *Variable Temperature Liquid Nitrogen Cryostat DNI 704 Operator's Handbook*, Oxford Instruments Ltd., Eynsham, (1993).
5. D. A. Tomalia and L. R. Wilson, *United States Patent*, Patent Number 4,517,122, (1985).
6. R. Rossi, A. Carpita, V. Lippolis and M. Beretti, *Gazz. Chim. Ital.*, **120**, 783-789, (1990).
7. G. Royal, V. Dahaoui-Gindrey, S. Dahaoui, A. Tabard, R. Guilard, P. Pullumbi and C. Lecomte, *Eur. J. Org. Chem.*, 1971, (1998).
8. X. H. Bu, D. L. An, R. H. Zhang, T. Clifford and E. Kimura, *J. Chem. Soc., Dalton Trans.*, 2247, (1998).
9. P. J. Davies, M. R. Taylor and K. P. Wainwright, *Chem. Commun.*, 827, (1998).
10. (a) R. W. Hay, R. Bembi and W. Sommerville, *Inorg. Chim. Acta*, **59**, 147, (1982); (b) L. Cronin, A. R. Mount, S. Parsons and N. Robertson, *J. Chem. Soc., Dalton Trans.*, 1925, (1999).

11. F. Bellouard, F. Chuburu, N. Kervarec, L. Toupet, S. Triki, Y. Le Mest and H. Handel, *J. Chem. Soc., Dalton Trans. 1*, 3499, (1999).
12. C. Caris, P. Baret, J. L. Pierre and G. Serratrice, *Tetrahedron*, **52**, 4659, (1996).
13. J. Chapman, *Thesis for the degree of Doctor of Philosophy*, University of Durham, (1992).
14. J. A. G. Williams, *Thesis for the degree of Doctor of Philosophy*, University of Durham, (1995).
15. Z. Diwu, C. Beachdel and D. H. Klaubert, *Tetrahedron. Lett.*, **39**, 4987, (1998).

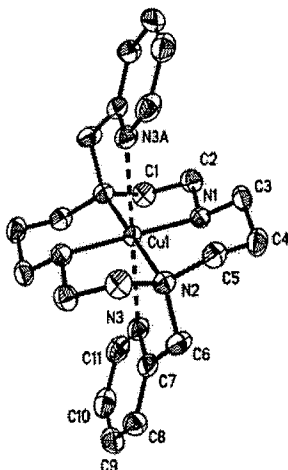
# **APPENDIX**

## **A and B**

## Appendix A

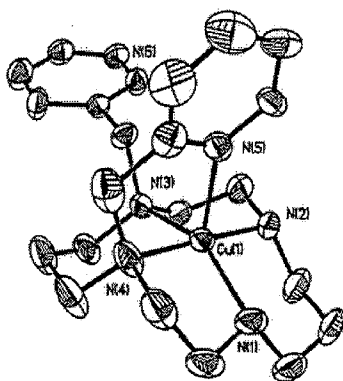
### Crystal structures

#### 1 - Copper complex of $L^1$ (A. E. Goeta)



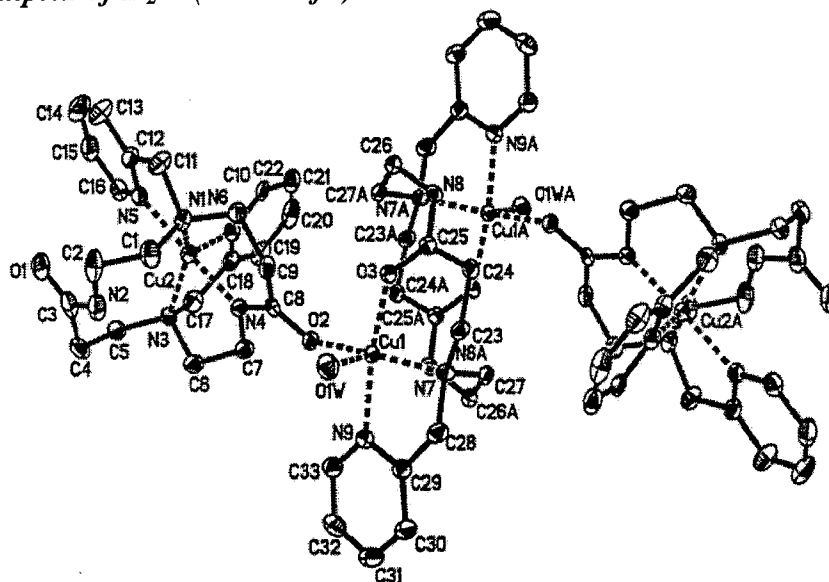
$[\text{CuL}^1]^{2+}(\text{CH}_3\text{CO}_2)_2 \cdot 6\text{H}_2\text{O}$  -  $\text{C}_{26}\text{H}_{52}\text{CuN}_6\text{O}_{10}$ ,  $M_r = 336.14$ , monoclinic, space group  $P2_1/n$  (no. 14),  $a = 8.6790(5)$ ,  $b = 15.6748(9)$ ,  $c = 11.7179(7)$  Å,  $\beta = 93.064(3)^\circ$ ,  $U = 1591.84(16)$  Å<sup>3</sup>,  $T = 150$  K,  $Z = 2$ ,  $\mu(\text{Mo-K}\alpha) = 0.748$  mm<sup>-1</sup>, 19962 reflections measured, 4454 unique ( $R_{\text{int}} = 0.027$ ) which were used in all calculations and 3863 greater than  $2\sigma(I)$ . The final  $R(F)$  was 0.028 ( $I > 2\sigma(I)$  data) and the  $wR(F^2)$  was 0.0775 (all data).

#### 2 - Copper complex of $L^2$ (A. E. Goeta)



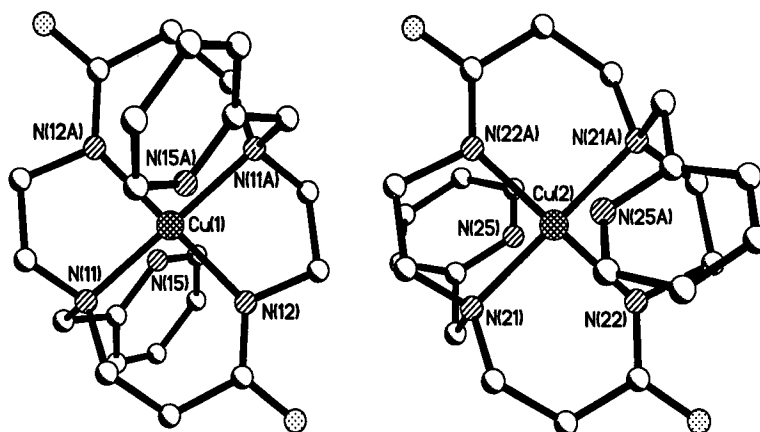
$[\text{CuL}^2]^{2+}(\text{ClO}_4)_2 \cdot \text{CH}_3\text{OH}$  -  $\text{C}_{23}\text{H}_{38}\text{Cl}_2\text{CuN}_6\text{O}_9$ ,  $M_r = 677.03$ , monoclinic, space group  $P2_1/c$  (no. 14),  $a = 8.270(1)$ ,  $b = 18.666(2)$ ,  $c = 18.717(2)$  Å,  $\beta = 97.879(3)^\circ$ ,  $U = 2862.0(6)$  Å<sup>3</sup>,  $T = 150$  K,  $Z = 4$ ,  $\mu(\text{Mo-K}\alpha) = 1.011$  mm<sup>-1</sup>, 25878 reflections measured, 8036 unique ( $R_{\text{int}} = 0.0353$ ) which were used in all calculations and 6033 greater than  $2\sigma(I)$ . The final  $R(F)$  was 0.06 ( $I > 2\sigma(I)$  data) and the  $wR(F^2)$  was 0.1479 (all data).

### 3 - Copper complex of $H_2L^5$ (D. S. Yufit)



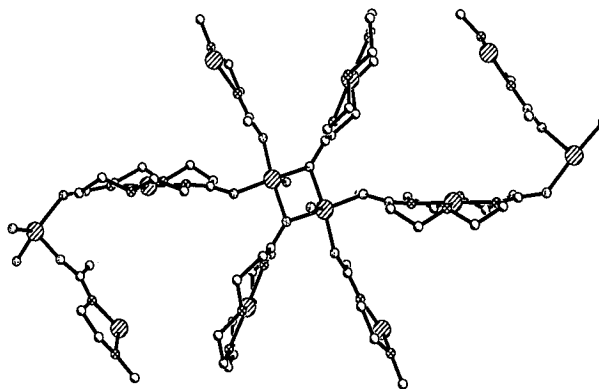
$[(CuHL^5)_2]^{2+}[Cu_2H_2L^5]^{4+}(Cl)_6 \cdot 15H_2O$  -  $C_{33}H_{63}Cl_3Cu_2N_9O_{21}$ ,  $M_r = 1155.35$ , monoclinic, space group  $P2_1/n$  (no. 14),  $a = 13.7841(4)$ ,  $b = 21.5077(6)$ ,  $c = 15.9374(4)$  Å,  $\beta = 97.544(1)^\circ$ ,  $U = 4684.0(2)$  Å<sup>3</sup>,  $T = 120$  K,  $Z = 4$ ,  $\mu(\text{Mo-K}\alpha) = 1.168$  mm<sup>-1</sup>, 31888 reflections measured, 10727 unique ( $R_{\text{int}} = 0.0498$ ) which were used in all calculations and 7383 greater than  $2\sigma(I)$ . The final  $R(F)$  was 0.0531 ( $I > 2\sigma(I)$  data) and the  $wR(F^2)$  was 0.1434 (all data).

### 4 - Copper complex of $L^5$ at basic pH (H. Puschmann)



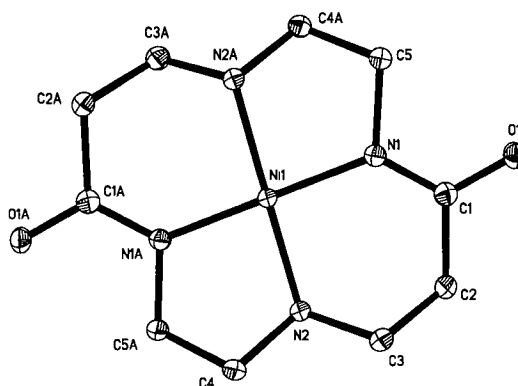
$[CuL^5] \cdot 2H_2O$  -  $C_{22}H_{32}CuN_6O_4$ ,  $M_r = 508.08$ , triclinic, space group  $P1$  (no. 2),  $a = 9.7924(3)$ ,  $b = 10.3659(3)$ ,  $c = 12.6077(3)$  Å,  $\alpha = 66.602(1)$ ,  $\beta = 81.966(1)$ ,  $\gamma = 75.804(1)^\circ$ ,  $V = 1137.37(6)$  Å<sup>3</sup>,  $T = 120$  K,  $Z = 2$ ,  $\mu(\text{Mo-K}\alpha) = 1.002$  mm<sup>-1</sup>, 11566 reflections measured, 5888 unique ( $R_{\text{int}} = 0.0719$ ) which were used in all calculations. The final  $R(F)$  was 0.0752 ( $I > 2\sigma(I)$  data) and the  $wR(F^2)$  was 0.1525 (all data). The rather large  $R(F)$  arises from a small proportion of the other conformer (*ca.* 15%) at the sites of each of the two conformers in the crystal examined.

### 5 - Copper complex of $L^4$ (H. Puschmann)



$[\text{CuL}^4]_3(\text{Cu}^{2+})_2(\text{ClO}_4)_4 \cdot 8\text{H}_2\text{O}$  -  $\text{C}_{30}\text{N}_{12}\text{O}_{30}\text{Cl}_4\text{Cu}_5$ ,  $M_r = 1528.41$ , orthorhombic, space group  $\text{Pbca}$ ;  $a = 13.8139(3)$ ,  $b = 18.7518(5)$ ,  $c = 21.0075(5)$  Å,  $\alpha=90$ ,  $\beta=90$ ,  $\gamma=90^\circ\text{C}$ ,  $V = 5441.7$  Å<sup>3</sup>;  $D_C = 3.398$  Mg m<sup>-3</sup>;  $T = 100(2)$  K,  $Z = 15$ ,  $\mu(\text{Mo-K}\alpha) = 2.219$  mm<sup>-1</sup>, 599958 reflections measured, 7447 unique ( $R_{\text{int}} = 0.0868$ ) and 6086 with  $I > 2\sigma(I)$ . The final  $R(F)$  was 0.1082 ( $I > 2\sigma(I)$  data) and the  $wR(F^2)$  was 0.2668 (all data). It was possible to arrive at the structure shown in more than one space group, although it was not possible to refine the structure anisotropically in any space group. The orthorhombic space group  $\text{Pbca}$  gave the most plausible result. Problems invariably occurred with the conformation of the macrocycles ring. Close inspection of the figure shows two of the crystallographically independent rings to be conformationally well behaved, whereas the third one appears to be almost 'flat'. This could be due to a real disorder, which could not be satisfactorily modelled, or it is possible that the material to hand did, in fact, consist of multiple crystals or exhibit unresolvable twinning.

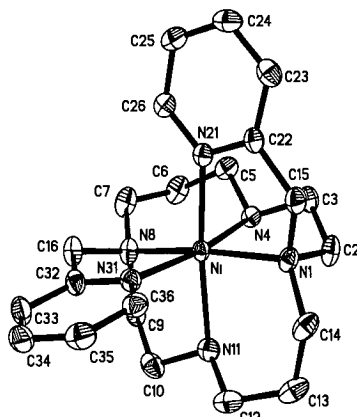
### 6 - Nickel complex of $L^4$ (H. Puschmann)



$[\text{NiL}^4] \cdot \text{H}_2\text{O}$  -  $\text{C}_{10}\text{H}_{20}\text{N}_4\text{NiO}_3$ ,  $M_r = 303.01$ , orthorhombic, space group  $\text{Pbca}$ ;  $a = 7.9298(4)$ ,  $b = 8.8809(4)$ ,  $c = 21.9353(11)$  Å,  $\alpha=90$ ,  $\beta=90$ ,  $\gamma=90^\circ\text{C}$ ,  $V = 1544.8(1)$  Å<sup>3</sup>;  $D_C = 1.629$  Mg m<sup>-3</sup>;  $T = 120(2)$  K,  $Z = 4$ ,  $\mu(\text{Mo-K}\alpha) = 0.711$  mm<sup>-1</sup>, 2040 reflections measured,

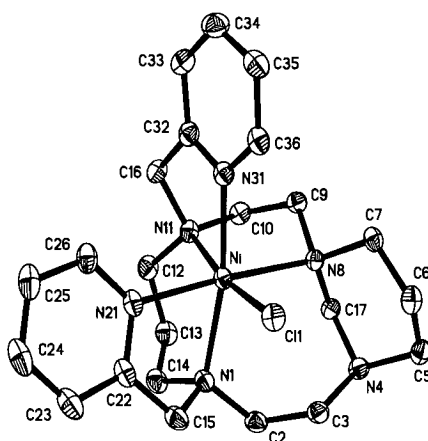
2040 unique ( $R_{\text{int}} = 0.0396$ ) and 1777 with  $I > 2\sigma(I)$ . The final  $R(F)$  was 0.0288 ( $I > 2\sigma(I)$  data) and the  $wR(F^2)$  was 0.0696 (all data).

### 7 - Nickel complex of $L^1$ (H. Puschmann)

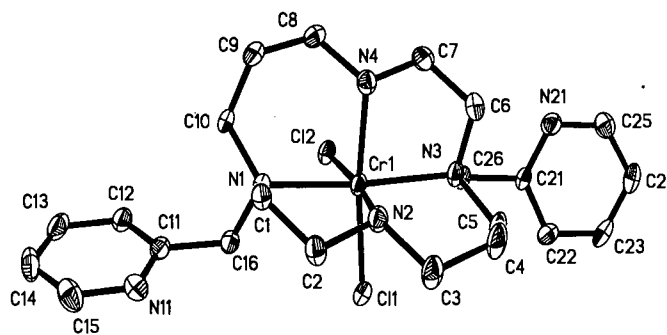


[NiL<sup>1</sup>] (with non-stoichiometric proportion of anions and crystallisation water) -  $C_{22}H_{32}N_6Ni^{2+}(Cl^-)_x(C_2H_3O_2^-)_{2-x}(4+x)H_2O$  [ $x = 0.428(3)$ ],  $M_r = 627.1$ , monoclinic, space group  $P2_1/c$ ;  $Z = 4$ ,  $a = 14.664(3)$ ,  $b = 19.785(4)$ ,  $c = 10.216(2)$  Å,  $\beta = 94.52(1)$ ,  $V = 2955(2)$  Å<sup>3</sup>;  $T = 120$  K,  $\mu(\text{Mo-K}\alpha) = 0.75$  mm<sup>-1</sup>, 22810 reflections measured, 7810 unique ( $R_{\text{int}} = 0.051$ ) and 6089 with  $I > 2\sigma(I)$ . The final  $R(F)$  was 0.0047 ( $I > 2\sigma(I)$  data) and the  $wR(F^2)$  was 0.115 (all data).

### 8 - Nickel complex of 4,8-methylen- $L^2$ (A. S. Batsanov)

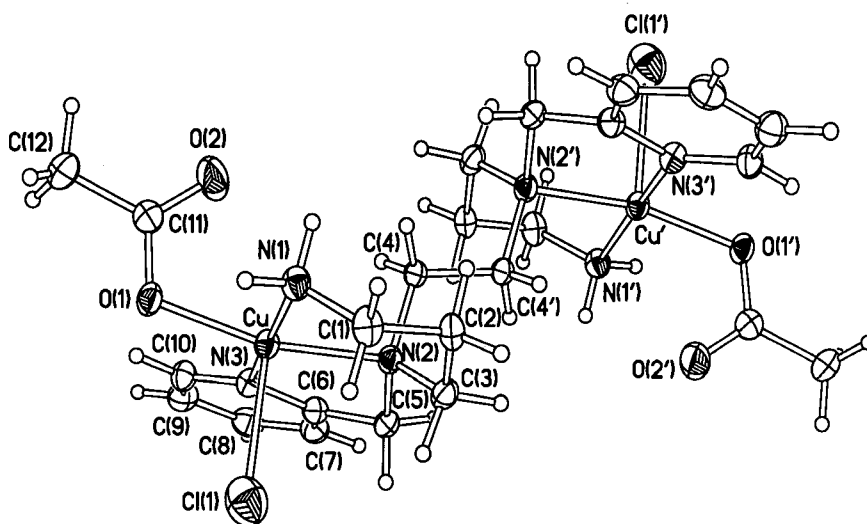


[Ni(4,8-methylen- $L^2$ )](ClO<sub>4</sub>)<sub>2</sub>(Cl)(1/4)·H<sub>2</sub>O -  $C_{23}H_{35}N_6NiCl_3O_8(1/4)H_2O$ ,  $M_r = 713.7$ , monoclinic, space group  $C2/c$ ;  $Z = 8$ ,  $a = 34.978(4)$ ,  $b = 11.956(4)$ ,  $c = 13.791(3)$  Å,  $\beta = 90.84(1)$ ,  $V = 5767(2)$  Å<sup>3</sup>;  $T = 120$  K,  $\mu(\text{Mo-K}\alpha) = 1.01$  mm<sup>-1</sup>, 34628 reflections measured, 7722 unique ( $R_{\text{int}} = 0.033$ ) and 6073 with  $I > 2\sigma(I)$ . The final  $R(F)$  was 0.0033 ( $I > 2\sigma(I)$  data) and the  $wR(F^2)$  was 0.089 (all data).

9 - Chromium complex of  $L^1$  (H. Puschmann)

$[\text{CrL}^1\text{Cl}_2]^+(\text{Cl})\cdot 2\text{H}_2\text{O}$  -  $\text{C}_{22}\text{H}_{38}\text{N}_6\text{CrCl}_3\text{O}_2$ ,  $M_r = 576.92$ , monoclinic, space group  $\text{P}2_1/c$ ;  $Z = 8$ ,  $a = 14.0373(6)$ ,  $b = 10.1737(4)$ ,  $c = 18.8463(7)$  Å,  $\alpha=90$ ,  $\beta=99.498(2)$ ,  $\gamma=90^\circ\text{C}$ ,  $V = 2654.57(18)$  Å<sup>3</sup>;  $T = 120(2)$  K,  $\mu(\text{Mo-K}\alpha) = 0.764$  mm<sup>-1</sup>, 27700 reflections measured, 6080 unique ( $R_{\text{int}} = 0.0684$ ) and 6059 with  $I > 2\sigma(I)$ . The final  $R(F)$  was 0.0556 ( $I > 2\sigma(I)$  data) and the  $wR(F^2)$  was 0.1620 (all data).

## 10 - Copper complex of 5,8-bis(2-pyridylmethyl)-1,5,8,12-tetraazadodecane (H. Puschmann - A. S. Batsanov)



$[\text{Cu}_2\text{L}^6\text{Cl}_2](\text{CH}_3\text{COO}^-)_2(\text{Cl})_2\cdot 6\text{H}_2\text{O}$  -  $\text{C}_{12}\text{H}_{25}\text{N}_3\text{Cu Cl}_2\text{O}_5$ ,  $M_r = 425.78$ , triclinic, space group  $\text{P}1$  (No. 2);  $Z = 2$ ,  $a = 10.501(4)$ ,  $b = 10.543(4)$ ,  $c = 10.718(4)$  Å,  $\alpha=62.95(1)$ ,  $\beta=88.61(2)$ ,  $\gamma=62.20(1)^\circ$ ,  $V = 907.9(6)$  Å<sup>3</sup>;  $T = 100(2)$  K,  $\mu(\text{Mo-K}\alpha) = 1.520$  mm<sup>-1</sup>, 10868 reflections measured, 4575 unique ( $R_{\text{int}} = 0.0464$ ) and 4096 with  $I > 2\sigma(I)$ . The final  $R(F)$  was 0.0768 ( $I > 2\sigma(I)$  data) and the  $wR(F^2)$  was 0.2097 (all data).

CIF files for 1,2,3 and 4 are available at <http://www.rsc.org/suppdata/dt/b0/b000739k/>

CCDC Nos. for 7 and 8 are 151638 and 151639, respectively.



## Appendix B

### Conferences Attended and Publications

#### Conferences

- **MACROCYCLES 2000** (International conference), University of St. Andrews, UK, 2-7 July 2000, Poster presented.
- **FLUORESCENCE 2001** (International conference), Amsterdam, The Netherlands, 16-19 September 2001, Poster presented.

#### Publications

- Complexation chemistry of “trans-dioxocyclam”: monomeric versus polymeric structures of the Ni(II) and Cu(II) complexes of 1,4,8,11-tetraazacyclotetradecane-5,12-dione. (Batsanov A.S., Howard J.A.K., Maffeo D., Puschmann H., Williams J.A.G.), *submitted to J. Chem. Soc., Dalton Trans., paper ref. b107931*.
- Intramolecular sensitisation of lanthanide(III) luminescence by acetophenone-containing ligands: the critical effect of para-substituents and solvent. (Beeby A., Bushby L.M., Maffeo D., Williams J.A.G.), *J. Chem. Soc., Dalton Trans.*, **1**, 2002.
- Nickel (II) complexes of the isomeric tetraazamacrocyclic ligands 1,11- and 1,8- bis (2-pyridylmethyl)-cyclam and of a structurally constrained N<sup>4</sup>, N<sup>8</sup>-methylene bridged analogue. (Batsanov A.S., Goeta A.E., Howard J.A.K., Maffeo D., Puschmann H., Williams J.A.G.), *Polyhedron*, **20**, 981-986, 2001.
- Copper (II) complexes of the isomeric tetraazamacrocyclic ligands 1,11- and 1,8-bis (2-pyridylmethyl)-1,4,8,11-tetraazacyclotetradecane and of the 1,4,8,11-tetraazacyclotetradecane-5,12-dione analogue at neutral and basic pH. (Goeta A.E., Howard J.A.K., Maffeo D., Puschmann H., Williams J.A.G., Yufit D.S.), *J. Chem. Soc., Dalton Trans.*, **12**, 1873-1880, 2000.
- The efficient intramolecular sensitisation of terbium (III) and europium (III) by benzophenone-containing ligands. (Beeby A., Bushby L.M., Maffeo D., Williams J.A.G.), *J. Chem. Soc., Perk. Trans. 2*, **7**, 1281-1283, 2000.

